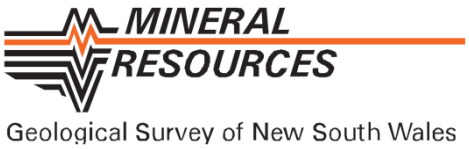

An evaluation of new mineral exploration technologies for effective mineral exploration undercover near Broken Hill.

Andrew Charles Knight

Discipline of Geology and Geophysics, School of Earth and Environmental Sciences, University of Adelaide, Adelaide, SA 5005, Australia

A Manuscript submitted for the Honours Degree of Bachelor of Science

University of Adelaide October 2010

Supervised by Dr. Steven M. Hill

External supervisor: William Reid, NSW Geological Survey

Table of Contents

Abstract:

The concealed nature of much of the Broken Hill Domain has led to a need for viable regolith sampling techniques. The Rockwell study area located 12 km south of Broken Hill, NSW, can be considered an analogy for the wider region, as it hosts multiple mineralization styles, including the Pb-Zn-Ag Broken Hill type. Surface samples were collected to assess the application of Niton field portable XRF geochemistry, soil geochemistry, biogeochemistry and regolith carbonate sampling. In order to accurately assess these methods, a 1:25000 regolith-landform map was also generated. Sampling targeted known Broken Hill (Pb-Zn-Ag), Great Eastern (Cu) and Au bearing quartz mineralization, with the aim to establish regolith geochemical characterization of each. Elevated commodity concentrations were found over Broken Hill type mineralization in all sampling media, while the Great Eastern type was identified by regolith carbonates and biogeochemistry, and Au mineralization only in regolith carbonates. The results support previous findings on the ability of biogeochemical sampling to identify mineralization, and the positive accumulation of Au in regolith carbonates. It also highlights the need for further regolith carbonate analysis in the region, as the geochemistry of regolith carbonate samples identified base metal mineralization contradicting existing literature. The exploration strategies proposed have been designed to use a composite of sampling methods to overcome limiting factors, with avenues suggested for further exploration research in the Broken Hill Domain.

KEY WORDS: Broken Hill, Regolith expression, Mineral exploration, Geochemical, Regolith carbonates, Biogeochemical, Niton FP-XRF.

1.Introduction

Australia is a continent dominated by thick and pervasive cover sequences that typically hamper the exploration for new mineral deposits. In many regions these profiles have been evolving for over 300 Ma (Smith 1996), with a variable climate causing intensive weathering, while general continental stability during the Phanerozoic has restricted overburden removal (Butt *et al.* 2005). Many profiles consist of a composite of *in-situ* and transported materials that are further subjected to alteration by surface processes such as hydrological fluctuations (Aspandiar 2006). Understanding geochemical dispersion pathways for these processes has proven critical for the effective sampling and exploration for various mineralization styles. While this overburden often obstructs traditional exploration methods such as geological mapping and hard rock geochemistry, when approached by alternative procedures it can aid exploration. Secondary dispersion halos generated during the regolith's formation and evolution are commonly of a greater spatial extent than the mineralization's primary halo, allowing for larger exploration targets. The importance of regolith and landscape processes for Australian exploration was recognised in the late 1960s (Smith 1996), leading to numerous studies on the exploration potential of various regolith components.

Exploration through the regolith is broadly divided into geophysical and geochemical processes. With the meaningful application of both subject to numerous controlling mechanisms, such as time, climate, evolution of cover and nature of the ore body (Aspandiar 2006). Geochemical exploration methods include regolith carbonate

sampling (Guedria *et al.* 1989; Lintern 2001; Witter *et al.* 2004), biogeochemical sampling (Hill *et al.* 2004; Butt *et al.* 2005; Tucker and Hill 2006) and soil geochemical sampling (Tonui *et al.* 2003; Butt *et al.* 2005; Fabris *et al.* 2009). With the applicability of each method relying heavily on the geomorphologic history and control mechanisms of an area. This results in the need for an evaluation of methods whenever a new area is explored. Initial work on the application of these sampling techniques in the Broken Hill domain has been undertaken by multiple authors (Thomas *et al.* 2002; Hill *et al.* 2004; Fabris *et al.* 2009) with many of the results suggesting viability. As part of the Broken Hill Exploration Initiative (BHEI) 2009 a substantial Niton Field Portable X-ray Fluorescence (FP-XRF) geochemical data set was released to general explorers. This data covers more than 450km^2 of dominantly outcropping terrain, with studies by Leyh and Leggo (2009) and McKinnon (2009) supporting its application for outcrop orientated Broken Hill type exploration. This study focuses on an area hosting multiple known mineralization styles, and provides further investigation into the application of biogeochemical, soil geochemical and regolith carbonate sampling within the Broken Hill domain. Due to the critical role of regolith-landform mapping in the interpretation of regolith derived data, a mapping component was included in this study.

The sample area corresponds to the Rockwell 1:25,000 geological map sheet, south east of Broken Hill, New South Wales. It represents the eastern margin of the uplifted Broken Hill Block, with the transition from exposed to concealed bedrock occurring within its extent. This transition, accompanied by the multiple mineralization styles

within the area, creates an ideal location for the evaluation of regolith sampling techniques for use in the larger Broken Hill Domain. The project aims to:

1. Characterize the regolith expression of the multiple mineralization styles, in respect to their signature in sampled media, which consists of regolith carbonates, biogeochemistry, Niton FP-XRF geochemistry and soil geochemistry.
2. Generate of a 1:25,000 scale regolith-landform map using a range of remotely sensed data sets (including hyperspectral data) to provide a framework and context for geochemical exploration.
3. Evaluate the exploration methods in respect to their use in the Broken Hill Domain.

2. Setting

2.1 Location

Broken Hill is located at 31°5S 141°2E in far western New South Wales. The Broken Hill Domain is within the south eastern portion of the Curnamona Province, which spans South Australia and New South Wales (Figure 1a), and consists of uplifted and east dipping fault bound blocks, such as the Broken Hill Block. The Broken Hill Block is constrained in the east by the Redan Fault, and the west by the Mundi Mundi Fault. Due to this tilted nature the project area focuses on the interface between exposed bedrock and sediment cover, in an area southeast of Broken Hill and corresponding to the 1:25000 Rockwell geological map sheet. The Rockwell map sheet begins approximately 12 km southeast of Broken Hill with main vehicle access along the Menindee Road. The map sheet study area covers 350 km^2.

2.2 Geology

The bedrock within the Rockwell mapping sheet includes the Willyama Supergroup. This includes the Sundown, Broken Hill and Thackaringa groups, the Mulculca Formation, Clevedale migmatite and the Thorndale composite gneiss. It has been interpreted as representing an Paleoproterozoic to Mesoprotoeozoic intracratonic rift system, with many of the mineralization zones reflecting a shallow water exhalative environment (Haydon *et al.* 1987; Walters and Bailey 1998). Multiple magmatic events have been recorded with felsic magmatism occurring at 1700-1710 Ma, and bimodal felsic-mafic magmatism at 1680-1690 Ma. The timing of the bimodal magmatism

coincides with the main Broken Hill mineralization and is thought to have been the possible heat source that drove the system. Since mineralization, many deformation events have been recorded with isoclinal and nappe-style folding, accompanied by granulite facies metamorphism at 1590-1600 Ma as part of the Olarian Orogeny (Stevens 1986). Retrogression and minor folding at 1570 Ma, dolerite dyke intrusion and retrogression at 830Ma, and retrogression, shearing and refolding during the Delamerian Orogeny 470-505 Ma (Plimer 1985)(Stevens *et al.* 1998). During the Cretaceous and Tertiary tectonic uplift, brittle deformation and extensive weathering occurred (Stevens 1986).

The multiple deformation events of different orientations have lead to a complex fold system within the mapping area. This folding played a critical role in the concentration of the main line of lode, as it increased the density of the many narrow but rich ore lenses to an economical grade. Due to this concentration factor a structure known as the Little Broken Hill anticline has been subjected to intense workings where it hosts dominantly Broken Hill Group metasediments with some areas of mineralization. Ultramafic intrusions overprint the stratigraphy and appear to have been emplaced relatively late in the geological evolution at 827±9Ma (Wingate *et al.* 1998).

A synform/antiform system occurs with a hinge line trending parallel with stratigraphy in a northeast to southwest direction. A large number of shear zones run almost perpendicular to this and have lead to varying degrees of displacement.

2.3 Mineralisation styles

The Rockwell area hosts a variety of Mineralisation styles, which can be categorised into three main groups of: strataform; shear zone related quartz veins; and, ultra basic intrusives (Burton 1994). Due to the range of mineralization styles, multiple elements have been prospected including, Pb, Zn, Ag, Fe, Cu, and Au. The three main mineralization styles sampled in this study are the Broken Hill type, Great Eastern type and Au bearing quartz. The ultra basic intrusive related deposits have not been analysed in this study due to their limited occurrences and low grade.

The location of the existing field portable XRF (Niton) data has resulted in the strataform Broken Hill-type mineralization being the dominant style analysed. For this style the elements of interest are Pb-Zn-Ag and Mn presently used for Broken Hill type exploration, as well as Sb, Cd, As, Cu and F (Walters & Bailey 1998) which are associated with Mt Isa mineralization.

The Niton survey does not cover the Great Eastern type and Au bearing quartz styles, though both of them have been investigated using biogeochemistry. The Great Eastern type mineralization is dominantly Cu mineralization with traces of (*Co&Au*), and occurs dominantly in the north of the mapping sheet. The Au bearing quartz mineralization forms the Huonville Goldfields in the southwest of the area and is associated with minor Cu mineralization.

2.3 Regolith

Due to its complex geological history the Rockwell area contains a vast array of regolith units. The area can be broadly divided into the low hill ranges in the west, gradationally changing towards sedimentary plains in the east.

The range zone includes exposures of slightly to moderately weathered bedrock on rises, with a thin sedimentary cover up to 3 m thick in valleys. The rises dominantly follow the strike of the lithological units, except for where erosion has been focused. The degree of weathering is controlled primarily by lithology with areas of ultramafic intrusion and shear zones exhibiting greater degrees of weathering.

The sedimentary plains consist predominantly of colluvial sediments with the abundance of quartz lag increasing and lithic fragments decreasing away from the ranges. Numerous low rises punctuate the plains and typically represent an increase in quartz, silcrete or ferricrete lag. These indurated rises represent paleovalleys that have been topographically inverted. Along the base of the Mulculca range-front a large quantity of hematite and maghemite pebbles form a sparse lag surface.

Ephemeral rivers up to 15 m wide flow east out of the ranges and continue south east on the flood plains. Many of the smaller tributary channels exiting the ranges interchange between confined channel flow and sheet fan flow, with the fans clearly visible on hyperspectral imagery (Figure 2).

2.4 Geomorphology

The western part of the area contains a large section of the Mulculca Fault range-front, which was subject to a study by Hill *et al.* (2003). This study included regolith-landform mapping and landscape evolution analysis. The landscape evolution model (Figure 3) proposes that during the mid-Cenozoic, multiple drainage systems flowed in a northwest to southeast direction towards and possibly into the Murray Basin. These paleo-drainage systems were both silificied and ferruginized and are now expressed by inverted topography. It is unclear how many generations are represented in these valley systems. Uplifting along the Mulculca Fault due to neotectonic activity lead to a large barrier to this palaeo-flow and pooling and sedimentation along the fault-angle depression along the range-front base. The generation of sediment accommodation space by this relative uplift provided a setting for deposition for most of the contemporary transported regolith, which is thought to reach ~20m depth along the base of the range-front.

2.5 Landuse

The current primary land use of the Rockwell area is sheep grazing, with previous high feral rabbit and goat populations leading to a significant overgrazing. This has resulted in the formation of deep erosional gullies, transecting large portions of the sedimentary plain area. Mine workings dating back to the 1800s are present in the ranges of the western and the southwestern corner of the mapsheet.

2.6 Vegetation

The area is dominated by three main vegetation communities, consisting of woodlands, chenopod shrublands and grass lands.

The ranges and other areas of local elevation host open woodlands with a sparse chenopod understorey. The woodlands are formed from black oaks on the plains, mulga within the regions of exposed bedrock, and a mix of black oak and river red gum along established creek lines.

The majority of the plains are dominated by chenopod shrubland consisting of a variation between oldman saltbush, black bluebush, and pearl bluebush, amongst various grasses.

The large alluvial and colluvial deposition fans are sparsely vegetated with grassland following wet periods.

3. Method

3.1 Regolith Landform Unit Map

Due to the large spatial extent of the area, detailed ground mapping was unfeasible in the time available. Initial landform units were selected using a base of topographical and geological maps, which were supplemented by hyperspectral satellite imagery. Mapping was carried out at 1:12,500 scale in order to achieve a presented output at 1:25,000 scale to tie in with the existing geological and neighbouring regolith maps. The initial map was then ground truthed and reviewed during the sampling stage of fieldwork. A second stage of field work was undertaken with land unit descriptions recorded as part of extensive ground truthing. This second phase of verification was limited by weather conditions preventing vehicle access to unsealed roads**.**
Each unit was described by soil composition, significant surface lag composition, landform and vegetation, with units of the same landform divided by surface lag composition. Table 1 identifies the general code used to differentiate units.

3.2 Soil sampling

In order to assess the reliability and repeatability of the large Niton dataset a small transect of 19 samples were collected (Table 2). The first 8 of these were taken at pegs remnant from the original survey, with the further samples taken as close as possible to the original surveys GPS readings. The samples were then split into two portions, with half sent for geochemical analysis, while the remainder was analysed with the Niton FP-XRF.

3.2.1 Sampling method

- Each sites location was recorded using the GPS coordinate system GDA 94 with the Universal Transverse Mercator (UTM) projection. The deviation between surveys was less than 3 m, with an unit accuracy of ± 4 m. The error range of the original survey's GPS unit is unknown, hence a maximum spatial error of ± 8m is assumed.
- Next the area was cleared of any large lithic or organic material, and the remaining soil passed through a 2 mm sieve mesh.
- The >2 mm portion was discarded while the <2 mm portion was homogenized and divided into two portions. The smaller portion was placed into a core chip tray for further laboratory based Niton analysis, while the larger portion was placed into a re-sealable plastic lunch bag.
- The samples were dried over a period of 4 days at room temperatures due to the high moisture content at the time of sampling.
- The high clay content in the majority of the samples meant that light milling was required to disrupt the clay ped integrity. An agate mortar and pestle were used with a gentle impacting motion to achieve this. Minimal force was applied in order to retain original grain sizes and avoid the generation of fines.
- When by visual analysis the sample was returned to its original state (or as close as possible), it was passed through an 80 µm mesh, with each sample was mechanically distressed for 2 minutes. This time was chosen as there was minimal increase in the <80 µm portion after 2 minutes.

Both fractions of the soil samples were sent to Genalysis Laboratories in Perth for multi-element analysis using a Aqua regia digest and B/OES/MS.

3.2.2 Data analysis

Soil geochemistry

- The returned data was manipulated using Excel to a layout acceptable to ioGas v 4.2 and Statistica 9.
- ioGas provided a platform for visualisation of the data using normal probablility plots, histograms, and XY plots. Statistica 9 was used to generate factor analysis and dendrogram plots for the identification of element clusters possibly associated with the Pb- Zn-Ag mineralization. These plots were supplemented with information obtained from literature in order to establish the presented element suites. Summary statistics, correlation matrices and principle component analysis were also generated using Statistica.
- Element concentrations for each fraction were then plotted against Northings.
- Due to the small sample size 95% confidence interval error ranges were unable to be generated for duplicated samples. Due to this QA/QC relied on the duplicate percentage difference error, 95% confidence intervals generated from standards, and detection readings of blanks.

Niton field portable XRF data

The Niton data covers much of the outcropping geology of the Rockwell sheet and consists of ~14,000 sample points. The data were collected by CBH LTD and Perilya LTD,

and was made publicly available as part of the Broken Hill Exploration Initiative 2009 conference (BHEI). The data were analysed by two methods:

- Tenement scale element concentration analysis; and,
- A single transect over known mineralization to assess prospect scale application.

Tenement scale

Tenement scale concentration analysis was undertaken using a variety of methods. To assess the effect of landform on element concentrations, the existing data set was attributed with 1:25k regolith-landform units in ArcGIS. Interrogation of the data was undertaken using ioGAS, with the normality assessed and XY plots generated. In order to establish element groupings, Statistica was used with dendrograms and factor analysis plots. Analysis was then undertaken with respect to controls on elements exhibited by location, geological unit and regolith-landform.

Prospect scale

Evaluation of the transect used data from the original survey and laboratory analysis. The FP-XRF was used in laboratory conditions due to the radioactive nature of the machine requiring licensing for use. In order to retain validity of the comparison, the samples only underwent preparation equal to that recommended for field analysis in Shefsky (2007).

Due to the common analysis method, the individual elements concentrations were plotted on a shared graph against Northings. The element distribution patterns were compared between Niton methods and soil geochemistry.

3.3 Biogeochemistry

Biogeochemical analysis was chosen as one of the exploration methods, due to the common occurrences of Bluebush *(Maireana pyramidata)* and Mulga (*Acacia aneura*), in addition to previous work in the area by Hill *et al.* (2004) and Thomas *et al.* (2002) indicating applicable characteristics and positive results using these species.

The Bluebush appears to experience a moderate landform control with common occurrences on low to medium relief areas with sand to clay substrate. Occurrences were seen around workings due to an artificial low resulting in higher moisture content. The occurrence of Bluebush was minimal in the regions of undisturbed higher elevations, leading to the majority of the samples being collected proximal to the workings.

The Mulga appeared to favour bedrock areas with well drained soils, such as those found on higher reliefs and slopes. The distribution of the trees appeared to be

unaffected between disturbed and undisturbed regions. As a result the Mulga samples were more distal to mineralization.

Sampling areas were targeted on sites of known workings with the aim to establish elemental signatures, for the Broken Hill type, Great Eastern type and Au bearing quartz mineralization styles.

3.3.1 Sampling method

Bluebush (Maireana pyramidata)

At each location a brief site description of landform and dominant vegetation was made, with the position recorded. Specimens were collected from single plants, with living twigs of a diameter of less than 8 mm targeted. Samples were collected (using cleaned hands devoid of jewellery), stripped of excess foliage, and placed into labelled unbleached brown paper bags to minimise decomposition.

Within days of collection the samples were oven dried for 48 hours at $<60^{o}$ C in order to minimise decomposition. Once dried, the specimens underwent further sorting with remnant foliage and poor quality twigs removed prior to milling. Due to the woody nature of the sample, a fine powder texture was unable to be obtained, so a consistency where the largest particles were less than 1 mm wide and 3 mm long was deemed fit for purpose. Samples were then placed into sealable bags and shipped to ACME laboratories Canada for analysis of 53 elements using acid digestion and ICP-MS.

Mulga (Acacia aneura)

The Mulga sampling was undertaken as per that of the Bluebush, with specimens consisting of foliage from single mature trees. Once dried, further sorting of the Mulga specimens removed twigs, fruit and blossoms, with the target milled product having the consistency of coarse flour.

3.3.2 Data analysis

The vegetation data was attributed with the listed mineralization styles at their respective sites prior to the application of statistics. The normal distribution and populations of each element were assessed in ioGAS. With element clusters identified in Statistica using methods common with that presented in the soil geochemistry section (3.2.2). From these groupings elements which showed association with Pb, Zn, Ag, Cu, Au were identified. IoGas was then used to generate correlation matrices and XY plots for visual interpretation. Finally the data was assessed for its possible application with each of the mineralization styles, and if applicable an expected biogeochemical signature proposed.

3.4 Regolith Carbonate sampling

Regolith carbonate samples were collected when present, though due to limited occurrences only 4 sites were recorded. In order to assess the useability of regolith carbonates, additional geochemical data was supplied by Steven Hill. The data supplied was previously unanalysed and consisted dominantly of regolith carbonates, with minor samples of sillcretes. Samples were collected from surface accumulations in the early 2000s, and analysed for 53 elements using acid digestion with ICP-MS at Amdel Laboratories, Adelaide.

From the data supplied, key mineralization elements were displayed over a true colour image to assess trends.

4. Results

4.1 Regolith-Landform Map

The mapping was carried out at 1:25,000 scale, though printable size constraints have led to a smaller scale image presented (Figure 4) with appendix I containing the 1:25,000 copy. The map is broadly includes two main landscape settings. The western section is dominated by erosional landforms and features prominent bedrock exposure, while the eastern section is dominated by transported sediments with depositional or colluvial landforms. The forty units are derived from splitting broad landforms by small but critical details, with general landforms conforming to:

- *Alluvial systems;*
    - *Incised channel confined*
    - *Complex braided flow systems*
- *Colluvial systems;*
    - *Sheet Flow*
        - *Erosion*
        - *Deposition*
- *In-Situ* Regolith;
    - *Saprock*

Alluvial systems

Due to the general east south east slope of the mapping sheet the alluvial units tend to flow eastwards out of the ranges and south east along the plains. In the ranges they are dominantly comprised of steep banked incised channels up to 3m in depth, with the

deeper channels often floored by bedrock. The trellis drainage nature is heavily controlled by lithology, as minor channels and depressions run parallel to the lithological strike, while deeper channels run perpendicular. As the incised channels exit the ranges, many form interchanging relationships with braided fan systems of various scales. Nearly all surface water exits the area along the south eastern margin. The composition of the alluvial units is highly dependent on both the scale of flow and spatial location. The larger systems display a large lithic component in the range and near range areas, with the size decreasing gradually over distance. The smaller systems are spatially controlled, with lithic fragments present within the ranges and near outcropping bedrock, rounded quartz in the central section, and frequent rounded maghemite in the eastern section. Erosional rises containing silica and iron indurated channel sediments have also been included in the alluvial systems as they are proposed to represent paleoflow.

Colluvial systems

The colluvial units are broadly broken into two main categories, erosional consisting of CHep, CHer and CHed, and depositional comprised of CHpd. With the exception of local lows, the depositional systems are focussed in the south east of the area, and have a sparse lag covering. The CHep units occupy the central portion with a quartz or maghemite surface lag, while the lithic rich CHer and CHed habit the ranges. These surface compositions mimic the alluvial systems with the exception of CHer units within the plains which show an increase in quartz lag.

In Situ Regolith

The only regolith units in the area which can be assumed to be *in-situ* are the moderately and slightly weathered bedrocks. The moderately weathered bedrock units are mainly comprised of amphibolites and/or pyroxene rich units such as the Little Broken Hill Gabbro (Bradley and Brown 1988), while slightly weathered units are comprised of assorted lithics within the ranges and quartz vein outcroppings central portion. Limited occurrences of amphibolite exposures were observed to form a floor surface within selected fluvial channels, indicating saprock within 3m of the surface.

4.2 Soil Geochemistry.

The following suites of elements were chosen for their established relationships with known Broken Hill-type mineralization within the Broken Hill and Mt Isa areas. They can be separated into two main classes:

- Primary commodity mineralization elements (Pb, Zn, Ag, Cu, Au): and,
- Possible pathfinder and mineralization accessory elements (Mn, Cd, Mg, Fe).

Where available the same set of target element suites have been presented for each sample media, though due to differing analytical processes this has not always been possible.

4.2.1 Fractionated soil geochemistry

The transect's geochemical results are divided into two main data sets of <80 µm and >80 µm fractions. The concentration against distance plots for each of Pb, Zn, Ag, Cu, Mn, Cd, As, Fe, Mg are shown in Figures 5-13.

In general, the targeted elements increase to the north, peaking around 6454350N (GDA94). The commodity elements of Pb and Zn, in addition to Cd, Co and Mg have little differentiation between the two soil fractions. Elements Ag, Sb, were concentrated in the <80 µm fraction, while As, Fe, Mn were found in higher concentration in the >80 µm fraction. Both fractions follow similar patterns across the transect with corresponding highs and lows common in most cases. Gold appears to be significantly concentrated within the <80 µm fraction with 14 readings above the lower analytical limit of detection, compared to 3 in the >80 µm fraction.

The target elements appear to consist of one population with an approximately normal distribution (Figures 14-15). Due to the small population the non linear nature of the normal probability plots could be an artefact of natural process variation as opposed to true non-normality. When viewing the data as histograms the elements have a slight to moderate right skew, excluding Cu, W with a strong right skew and Zr with a left skew.

4.2.2 Element Associations Geochemistry.

Factor analysis (Figures 16-17) shows slightly different element grouping between soil fractions. In the >80 µm fraction Zn, Cu, Mn, Mg are closely grouped with Sn, Co, Ag, Pb and Cd more distal. While the <80 µm fraction has As, Ag, Pb loosely grouped with Zn more distal. A large suite of elements are in loose association with the Broken Hill-type mineralization and include Cu, Mg, Co, Cd, and In.

The dendrogram cluster analysis method (Figures 18-19) suggests slightly different groupings to that visually interpreted from the factor analysis. For the <80 µm fraction, it places Pb, Ag and Bi in strong correlation with Cd, V and Ti loosely correlated. Zinc

occurs at a much greater distance and is tightly grouped with In and Sn. Copper is placed with Mn, Co, Sr and Fe.

The >80 µm fraction has Ag, Pb, and Cd in high correlation, with Co Cu, V, Fe, P, Mn and In nearby. Copper is closely grouped with Co and V, while Zn exhibits equal linkage distance to all of the elements listed above.

4.3 Niton analysis

The Niton results are divided into two sections with the primary focusing on the geochemical and spatial associations of the whole data set. The reliability and application of the FP-XRF was assessed along a single transect. Due to a minimal number of elements above detection limit on the laboratory tested data, a truncated set of target elements is presented.

4.3.1 Statistical interrogation of field sampled points.

When viewing the histograms (Figure 20) for the whole field Niton data set, the assumptions of normality appears fair, the exceptions being for Ag and Cr which exhibit slightly bimodal populations. Due to the large unbiasedly sampled population the histograms show only slight to moderate right skewing. The normal- normal quantile plots (Figure 21) however identify the possibility of two populations for all of the mineralization elements. The majority of the data for these elements fits the normality assumption, except at higher concentrations where a significant break in slope occurs . Since these values are of limited frequency they are hidden within the histogram plots. Cluster analysis was undertaken using dendrograms and PCA loaded factor analysis. The factor analysis method grouped Pb, Zn, Mn, Cd, As and Fe together while Ag was

loosely placed with Sb and Co (Figure 22). The Dendrogram (Figure 23), however, places Ag in close association with Cd, and loosely with Pb, As. There is minor correlation between Zn, Mn Cu and the other elements.

For X-Y plot analysis the data was separated into sediment covered and exposed bedrock classes, in order to identify possible differences (Figure 24-30). From X-Y plot and correlation matrix analysis the following groupings were identified, Pb with As, Co. Zinc with Mn and Co, and Cu with As, Co, Ni, Se. A correlation was not run for Ag due to a valid data count of only 67/10850. These correlations represent the associations between elements seen in the XY plots for both soil and bedrock sites. Pb defies this trend with a possible positive relationship with Mo in bedrock sites and a weak negative trend in sediment cover sites.

4.3.2 Spatial analysis of field sampled points.

Figures 31-37 show elements that were selected either due to previous groupings with mineralization or due to interesting spatial distribution around mineralization zones. The disparity between the northern and southern sections of the sample sites, is a product of the data being sourced from two different surveys and does not reflect a geological trend.

Tenement scale

As established in previous workings (Wolfgang et al. 2009; McKinnon 2009), the Niton data has been proven to identify regions of local exposed bedrock mineralization, hence both the Pb and Zn plots show clusters of values over 2σ in areas of known

mineralization. These two elements appear to exhibit co-central zones of very high readings (>95%).

Zinc exhibits an extensive zone of above average values (50%-70%) in a halo around the very high (>95%) readings. Lead on the other hand has a more constrained halo of above average values around a smaller group of very high readings. In areas of dense Pb and Zn highs there is some association with Cu and Ag, with the high Cu and Ag (>75%) values located along a narrow zone central to the mineralization zone. The established pathfinder for mineralization Mn appears to highlight the mineralization zone with a wide halo of values at >95% of those expected if distribution was normal. Mo exhibits an interesting trend with the mineralization sites, with many of the areas having a halo of high Mo concentrations. This halo only surrounds the mineralization zone for a short distance away from the high Pb-Zn- Ag and does not co-exist within the actual mineralization area. Furthermore, above average concentrations of Mo are only observed around mineralization in the north and south of southern Niton data set.

Prospect Scale

Figures 38-44 show a close up of one of the regions of high Pb, Zn, Ag mineralization. The initial plot shows the image over an aerial photograph, while the subsequent plots are over the 1:25k RLU map. As with the tenement scale, the elements Pb, Zn, Cu, Mn, Mo are shown.

The elements Pb, Zn and Mn all show a relationship between landform and concentration, with areas down slope from mineralization showing high concentrations. These high values correlate with the local drainage pattern. This

dispersion is most pronounced with Zn and Mn, which both show high concentrations (75%-95%) along flow paths. Copper has little to no dispersion vectors, with above average values restricted to a narrow band along the core of mineralization. Mo has a small number of above average values, though not with enough regularity to define a relationship.

4.3.3 Transect comparison

The results (Figure 45 -48) show a vast difference between the 2 mm sieved data and that of the field tested samples. This is due to the field tested data showing a wide degree of variability between neighbouring data points, while the sieved samples show a much smoother signature. Both data sets show the same general trend, with a peak concentration on the western side, a minimum central to the transect and a second high on the eastern side. It is this second peak value which is the main area of difference between the two sample sets. The sieved samples show the increase towards the edge of the transect giving a parabolic type shape to the data. This contrasts with the distinct high centred over Northings 6454350 of the field tested samples. The erratic points within the field dataset show single point increases of values greater than 6 times the average concentration, with the highs common across all elements.

4.4 Biogeochemistry

The assumption of approximate normality for both species appears reasonable for the target elements, though varying degrees of skewness towards higher values exist (Figure 49.). The elements Zn, Cu, Zn, Ag and Au all appear to have one population of data. However, within the Bluebush samples, Pb consists of two distinct populations of <5 ppm and >5 ppm Pb. The values >5 ppm correlate with the high readings of Zn and Ag which have a single population. When viewing the factor and cluster analysis plots (Figure 50-53.) there is a strong contrast between species. The bluebush samples show a distinct relationship between the mineralization suite of Pb, Zn, Ag, Cd, Mn and Sb. While the Mulga samples give a vastly different picture with Ag, Sb, Cu and Tl forming one cluster, Au, S, Pb, Se, Pt forming a second, and Zn existing a part of a larger disperse group of elements. Within both species there is a distinct group associated with Zr.

The X-Y plots (Figures 54-60) for the Bluebush samples show a strong positive relationship between the Broken Hill-type mineralization elements, a moderate positive relationship with elements in the Zr cluster : and a moderate negative relationship with P, Na, K and Rb. Of the targeted mineralization elements, Pb stands out due to changing relationships within a single X-Y plot. For the Zr cluster elements there are two contrasting correlations, with a primary strongly positive relationship for the initial Pb population of <5 ppm, and a moderately negative relationship for data points correlating to the second population of >5 ppm. The inverse of this trend occurs for P, Na, K and Rb. When viewed spatially, the second population of Pb can be linked to

areas of Broken Hill-type mineralization, with values of <5 ppm reflecting the background population. The other prospective mineralization elements of Cu and Au show less noticeable relationships. Copper exhibits a weak positive relationship with Mn, Ag, Zn, Pb, in addition to a moderate positive relationship with P, Na, K, and Rb. Gold suffers from distinct data striping due to values being very close to the LOD, however, a weak negative relationship with Pb, Zn, Ag, and Mn is able to be distinguished.

The X-Y plots of the Mulga samples (Figures 61-67) identify similar groups to those generated by factor analysis. Visual analysis associates Pb, Mg, Rb, Zn and Fe in a weak positive relationship with each other, while Zn displays a weak positive relationship with Pb, Cd and Mn. Copper forms a weak positive relationship with Ag, Ni and As, a weak negative trend with most of the other elements.

The quality of the results were assessed by the generation of percentage differences between duplicates, 95% confidence interval on the instruments accuracy, in addition to analysis of blanks (Table 4). The reliability of the statistical analysis is questionable due to the non-normality of the data. The comparison between the 95% confidence interval and the mean biogeochemical data suggests a narrow error range for Pb, Zn, Mg and Cu values, a moderate inaccuracy on Ag, and a large error range for Mn and As. The blank samples tested to be below detection limit suggesting acceptable precision, while the percentage difference values between standards were reasonable for the mineralization elements with a maximum difference below 20% in all cases except Pb. The duplicate samples showed greater variability with the Mulga samples reaching 70%

difference for Ag, Co and Cd, while Pb, Zn and Cu displayed close to 50% difference between duplicates.

4.5 Regolith Carbonates

The regolith carbonate spatial plots (Figures 68-71) show elevated readings of Pb and Zn within the ranges area, with these elevated zones present over known mineralization sites such as the Melbourne Rockwell mine. Over areas where there is no known Pb-Zn-Ag mineralization, such as on the ranges western margin and Huonville Goldfields, the readings are lower. Copper highs are in Corruga type mineralization located along the western ranges margin, with single point highs also contained within the Huonville Goldfields and flood plains. Gold appears to show highest concentration within the Huonville Goldfields with a gradational increase seen towards the north east. Plot (72) shows the concentration of Pb, Zn and Cu against Ca in order to assess the effect of $CaCO_3$ on metal concentration. Both Pb and Cu showed a weak positive relationship with Ca while Zn displayed no notable relationship.

5. Discussion.

5.1 Landscape evolution model

Along the eastern margin of the Rockwell domain is the Mulculca fault line. This fault was incorporated in an evolution model presented in Hill et al (2003) which covers the flood plain region in the east of the study area. The western ranges zone offers little additional information for the geomorphological evolution, due to it consisting mainly of weathering bedrock.

Field observations support the model presented of a eastward draining system which was disturbed by slight tectonic uplift along the Mulculca Fault. A collection of the sites presented as evidence in Hill *et al.* (2003) were visited to validate the proposed model. The key pieces of evidence observed were the eastward trending silicified and ferruginised palaeovalley sediments, which now represent inverted topography along the northern eastern section of the mapping sheet. These present day low rises, consist of a pavement surface composed of heterogeneously cemented sub-angular to rounded quartz grains ranging from coarse sands to medium pebbles, indicating both proximal and distal sediment sources. These channels line up with small valleys along the fault scarp, which were proposed to indicate a period of steady state erosion through the uplifting block. As the rate of uplift increased the fluvial system stalled, forming lakes in the fault angle depression. These lakes are thought to be the source of the well rounded hematite which steadily increases towards the base of the fault generated ranges.

The overgrazed nature of the sedimentary plains is the likely cause of reduced soil stability in the present environment, resulting in the generation of steep banked deep erosional channels. These cuttings are seen dominantly in the ranges and southern central areas. The arid climate restricts fluid flow to intermittent events; resulting in colluvial sheet flow being the main transport mechanism, with large fan systems well defined on the hyperspectral imagery. These fan systems would have existed in various locations throughout the entire sedimentation phase, with the paleo-deposition zones likely to have implications for future soil geochemical and biogeochemical sampling.

5.2 Evaluation of techniques

5.2.1 Niton FP-XRF

The aim of the Niton laboratory samples was to assess the reliability of the Niton field samples, though after interrogation the reliability of the laboratory tested samples is questionable. As when viewing the two data sets, it is evident that there is a large disparity towards the centre of the transect. The difference occurs over a section of minimal sediment cover with prominent exposed bedrock and lithic fragments. Unless care was taken for sample locations in the original survey, the relatively unweathered lithic fragments would introduce heterogeneous sampling media. This heterogeneity is one of the possible causes for the large variations in the field sampled data. However, the removal of the lithic fragments by 2 mm mesh sieving does not explain the low values seen in the laboratory tested samples. This is evident when further comparing the Niton transect with the soil geochemistry, which shows co-

central concentration highs. In addition to this the soil samples also show a moderate heterogeneity between neighbouring points, raising the possibility that not all of the variability was due to lithic fragments, and could represent differing chemistry produced by the transect running roughly perpendicular to the strike of the lithology. Because of the radioactive nature of the Niton FP-XRF machine causing the Niton laboratory data to be tested externally by the New South Wales Geological Survey, it can only be assumed that the analysis process was consistent for all the samples. When comparing the data sets, the values are similar at the beginning and end of each transect. Yet when the higher concentrations begin, the laboratory tested samples return values similar to those measured on unfertile plains. This raises issues as to whether the sample size was sufficient, as previous studies (Shefsky 1997) recommend a soil sample volume of 50 cm^3 for field measurements, with the trays used only holding 30 cm^3. Further testing of both *in-situ* and external samples would be needed to identify if this is an artefact of limited sample volume, machine error or differing of sample locations.

The application for the Niton data in areas of cover was unable to be evaluated in depth, as the original surveys focused on regions of exposed bedrock.

The spatial plots (Figures 40-44) suggest a landform control on geochemical values at the prospect scale, as the mineralization signature follows two distinct drainage depressions. The generation of detailed regolith-landform maps allows for quick identification of local depressions which act as a conduit for the fertile detritus. With mapping at 1:12500 scale suitable for prospect

evaluation. Understanding the movement of surface material in this landscape is critical for establishing the geochemical dispersion models needed for accurate drill hole placement.

The stataform nature of mineralization creates a possibility that near surface mineralization may be missed in conventional grid sampling. Initial results suggest that sampling of local drainage depressions would highlight areas of interest, even if the actual mineralization was bypassed. The continuation of the Pb-Zn-Mn signature down drainage depressions raises the possibility of using stream sediment sampling throughout the range area as an alternative to detailed grid sampling.

When looking at the element partitioning in the soil geochemistry, the main elements of Pb and Zn show no clear preference, suggesting that both proximal and distal samples should in theory, show the presence of mineralization upstream. The fact that Pb is one of the least mobile of the heavy metals (Kabata-Pendias and Pendias 2001) does not appear to affect this method, due to the source material containing the tightly bound Pb ions being the item transported. This is supported by Skey and Young (1980) who found that at Que River Tasmania, the signature of hydromorphically dispersed Zn reached over 1000m while the clastically dispersed Pb only reached 400m. The mobile nature of Mn results in partitioning towards the larger soil fraction, due to the finer fractions having undergone extensive leaching and transportation. A strong Mn signature would not be expected in samples of finer fractions distal to mineralization.

Within greenfield exploration tenements this process could be further extended to include the sampling of the large alluvial fan systems shedding material at the base of the ranges. The validity of this theory would need to be tested to determine if the mineralization signature is able to overcome the dilution factors.

5.2.2 Regolith carbonates.

Regolith carbonates show great promise for regional exploration, with samples exhibiting commodity highs proximal to mineralization, suggesting minimal transportation and either local or insitu genesis. Carbonate samples collected near Broken Hill type mineralization record high Pb and Zn, with samples collected near the Corruga (Cu-Pb-W) mineralization along the western margin of the area recording highs in Cu. The collection of additional data is needed to establish background values allowing greater accuracy of classification ranges, which would provide a basis for further trend analysis. While Pb, Zn and Cu show elevated values proximal to sites of known mineralization, the Au concentration appear to show a gradational increase towards the mineralization hosting shear zones of the Huonville Gold fields.

Though the samples were collected from sediment cover the observed landforms means it is unlikely that they represent a transported signature. While the concentration of preferential gold accumulation within regolith carbonates is well documented (e.g. Lintern 2001; Butt *et al.* 2005). The presence of base metal highs within the media contradicts previous literature,

which have found an inverse relationship between base metals and $CaCO_3$ in carbonate samples (Guedria *et al.*1989; Butt *et al.* 2005). This contrasts with the neutral or weakly positive relationships observed between Pb, Zn and Ca. The anomalies seen in this study could represent a relative increase in metal concentrations, with larger data sets needed for further investigation. The use of regolith carbonates for geochemical fertility testing is favourable over soil geochemistry due to transported sediments dominating the flood plain area, with the low energy environment greatly reducing the physical mobilization of the nodular regolith carbonates.

5.2.3 Biogeochemical

The Mulga species appears to have limited use for mineral exploration within the Broken Hill area, with the results showing minimal correlation and poor clustering between mineralization elements. However at high concentrations Pb displays a possible correlation with Zn, suggesting that while there isn't a strong association at background levels, mutual concentration occurs in zones proximal to mineralization. This can be explained by both elements having different biological roles at background concentrations, with Pb considered a passively up taken element, non-essential for plant metabolism, while Zn is considered an essential nutrient with an active uptake mechanism (Kabata-Pendias and Pendias 2001). While it appears that the Mulga can identify mineralization, the sparse coverage limits its use in regional exploration.

Bluebush displays very positive results, with a strong clustering of Broken Hill type elements. This result however needs to be treated with scepticism due to the large reading of Zr in the data set. Zirconium while often significant in soil samples has limited availability within plants, with highest concentrations within root structures suggesting low biological mobility (Kabata-Pendias and Pendias 2001; Dunn 2007). Due to this Zr readings above 0.1ppm are often associated with aeolian derived soil contamination. The Bluebush data contains values ranging up to 0.96ppm, and as a result the validity of the entire data set is questionable. The high levels of Zr and a strong correlation with Al suggest a substantial degree of contamination, while the elevated commodity concentrations over key sites suggests locally derived contamination. In order to assess the degree of Zr uptake within the Bluebush species, controlled sampling would need to be undertaken with measures taken to remove the aeolian contaminant. This would generate greater clarity on the upper limit of realistic biological Zr levels, enabling accurate assessments concerning the degree of contamination. A component of the elevated commodity concentrations could be due to biological processes, as previous studies such as Hill *et al.* (2004) have identified an increase in concentrations over buried mineralization.

5.3 Mineralization styles and effective methods.

Broken Hill type Pb-Zn-Ag (Cu-Sb-Cd-Au-Co-S)

All of the methods tested appear effective in discerning Broken Hill type mineralization. The Niton signature consists of a broad Mn/Rb halo co-central with smaller Zn and Pb halos. The mineralization hosting lithology is able to be identified by a narrow band of elevated Cu and Ag. Within the biogeochemical samples, mineralization is identified by elevated Ag, Pb, Zn, Cd and Mn in the Bluebush samples, and by Pb, Zn, Cd, Au and S in the Mulga samples. The carbonate samples exhibited elevated levels of Pb and Zn in localities proximal to mineralization, with larger data sets needed to establish a maximum spatial range for detection. Because of the similar trends observed between the Niton field data and the soil geochemistry, investigation should be undertaken into the use of soil samples collected from local drainage depressions as a low frequency sampling technique.

Great Eastern type Cu (Co,Au)

Biogeochemisty is the only data set which covers the Great Eastern type Cu mineralization. This is due to classified occurrences located on erosional rises within sediment covered regions of the ranges. A lack of carbonate material at the sites visited raises questions to the range of mineralization styles able to be identified by this method. However carbonate samples of the Corruga type (Cu-Pb-W) mineralization show distinct Cu elevations over workings, with no notable increase in other elements.

Au bearing quartz mineralization styles Au-Cu (Fe-S)

This style consists of nuggetty mineralization hosted in quartz veins, which means that untargeted point based methods such as biogeochemical sampling are un-likely to find new mineral occurrences. This is demonstrated in the biogeochemical data which lacks any increase in Au through the Huonville Goldfields area. In contrast to this, the regolith carbonates show a gradational increase in Au concentration towards the shear zone hosted mineralization, suggesting that there is great potential for regolith carbonates to assist in the identification of concealed Au mineralization within the plains zone.

5.4 Recommended exploration strategies

Exploration within the Broken Hill block has largely focussed on Broken Hill type mineralization, with the aim of either establish a new standalone mine or to supplement the existing excavations of the main line of lode. The exploration strategies proposed are applicable for all of the mineralization styles examined, and are therefore divided by landform to reflect the difference approaches between the ranges and plains.

5.4.1 Tenement – Ranges

Due to the outcrop dominated habit of the ranges, the use of detailed geological maps to identify regions hosting the Broken Hill group lithologies is a logical first step. Where present the extensive Niton FP-XRF dataset can then be used to further investigate the fertility of targeted areas. The Niton data has extensive coverage within the Rockwell area, yet it can be seen in Figure (1b) that this is not the case for much of the Broken

Hill domain. In these un-sampled areas first pass sampling of drainage depression sediments and regolith carbonates is suggested, as both of these methods appear to represent their local surroundings allowing for lower density sampling. However these methods have their limits as regolith carbonates are infrequent, and stream or depression sediment sampling requires the erosion of near surface mineralization. If an area of interest is located, the continuation of the Niton FP-XRF grid sampling with a line spacing of 100-200m and sample spacing of 25-40m is suggested. Biogeochemistry appears to have limited used within the tenement scale due to the sparse distribution of Mulga and rare occurrences of Bluebush.

5.4.2 Tenement – Plains

Due to the strong transported nature of much of the plains, the accuracy of soil geochemistry including Niton sampling is questionable. Detailed regolith mapping is critical in order to minimise the likelihood of poor sample sites, with mapping at 1:25, 000 scale providing sufficient detail to identify erosional rises which are the desired sampling landform. Where present regolith carbonates should be sampled to supplement biogeochemical data. Bluebush are the desired biogeochemical sampling species, as they are prolific across all landforms except for areas dominated by sillica or iron indurated lag. For smaller budgets, grid sampling should target erosional rises and immediate surrounding area with sample space of 25m. More extensive programs can extend the sample radius, with landform characteristics noted to allow for geochemical dispersion modelling.

5.4.3 Prospect

Detailed regolith mapping ideally at 1:12500 scale is needed to accurately understand dispersion patterns. Gridded sampling of a smaller scale would then be carried out, with the Niton FP-XRF used in areas of bedrock exposure, and biogeochemistry used in areas of cover. When Broken Hill type mineralization is targeted, transects should trend perpendicular to the geology, commonly in a NW to SE direction. Within regions covered by the Niton FP-XRF geochemistry, correction for transportation is needed to establish accurate drilling sites.

6. Conclusion

The study of the selected regolith sampling techniques within the Rockwell area, has provided insight into their exploration potential within the Broken Hill domain. This study was able to achieve this by:

1. Characterising the geochemical response of sampled media over various mineralization styles.
2. Assessing the validity and controlling factors of the sample methods, with areas for further study identified; and,
3. Proposing exploration strategies applicable to both outcropping and concealed regions.

A composite of regolith sampling methods was found to be a viable alternative to detailed Niton FP-XRF grid sampling at regional and tenement scale exploration. With the significant effect of landform type on all methods, supporting the need for continuing regolith landform mapping in the region. Key aspects of the project include:

- The identification of Cu, Pb-Zn and Au systems using regolith carbonates. Though the need for further research in the area is apparent, as the sample data presented displays a slight positive trend, when previous studies have established an inverse relationship between Pb, Zn and $CaCO_3$.
- A positive biogeochemical response for *Maireana pyramidata* and *Acacia aneura* for the Broken Hill and Great Eastern type mineralization. With the application for the Au bearing quartz mineralization questionable, as no response was

detected. Both species displayed controls on use, as *Maireana pyramidata* displayed significant aeolian contamination, while *Acacia aneura* exhibited sparse and sporadic cover.

- Niton FP-XFR sampling was able to identify the presence of mineralization and its transported signature down drainage channels. Suggesting application of the sampling of stream sediments, or using Niton geochemical sampling of depression sediments as an alternative to detailed grid sampling.
- Mineral exploration strategies using regolith sampling methods were developed to cover a range of landforms in buried and outcropping regions.
- The generation of a detailed regolith landform map to coincide with surrounding mapped areas, will enable increased accuracy in the development of regional geochemical dispersion models.

7. Acknowledgments

Firstly I would like to thank Steven Hill for his boundless enthusiasm and insight into the area, though sadly I wasn't able to show off a "big thallium" like he had hoped. I would also like to thank Bill Reid from the Geological Survey of New South Wales, for his significant help throughout the year and great tennis skills. Thanks also go to the Huonville and Farmcote property owners, in addition to Robbie Dart for the terminal use of his sieve. I am grateful of the fact of having such a diverse and entertaining cohort who provided an interesting working environment and multiple study breaks. Lastly I would like to thank my family, friends and Fiona for providing re-heatable dinners, a life outside of study and encouragement throughout the year.

References

ASPANDIAR, M.F., ANAND, R. & GRAY, D., 2006. Mechanisms of element dispersion through transported cover: A review. CRC LEME Report **230**.

BRADLEY, G.M. AND BROWN, R.E., 1982 Rockwell 1:25000 Geological sheet, *New South Wales Geological Survey, Sydney*

BURTON, G.R., 1994. Metallogenic studies of the Broken Hill and Euriowie Blocks, New South Wales. 3. Mineral deposits of the southeastern Broken Hill Block. *Geological Survey of N.S.W., Bull.* **32** 3.

BUTT, C.R.M., ROBERTSON, I.D.M., SCOTT K.M. & CORNELIUS, M. 2005. Regolith expression of Australian ore systems. *CRC LEME, Perth 431p*,

CONOR, C.H.H., PREISS, W.V. 2008, Understanding the 1720–1640Ma Palaeoproterozoic Willyama Supergroup, Curnamona Province, Southeastern Australia: Implications for tectonics, basin evolution and ore genesis. *Precambrian Research* **166**, 297–317

DUNN, C. E., 2007. Biogeochemistry in Mineral Exploration, *Handbook of Exploration and Environmental Geochemistry, Volume **9***, Pages xiii-xviii, 1-460

FABRIS, A.J., KEELING, J.L. & FIDLER, R.W., 2009, Soil geochemistry as an exploration tool in areas of thick transported cover, Curnamona Province, MESA Journal 54, 32-40

GUEDRIA, A., TRICHET, J. & WILHELM, E., 1989, Behaviour of lead and zinc in calcrete-bearing soils around Bou Grine, Tunisia - its application to geochemical exploration. *Journal of Geochemical Exploration*, **32**, 117-132

HAYDON R.C. & MCCONACHY G.W., 1987, The stratigraphic setting of the Pb-Zn-Ag mineralization at Broken Hill, *Economic Geology* **82**, 826–856.

HILL, S.M., EGGLETON, R.A. & TAYLOR, G., 2003. Neotectonic disruption of silicified palaeovalley systems in an intraplate, cratonic landscape: regolith and landscape evolution of the Mulculca range-front, Broken Hill Domain, New South Wales. *Australian Journal of Earth Sciences*, **50**, 691-707

HILL, S.M., THOMAS, M., EARL, K., FOSTER, K.A., 2004, Flying Doctor Ag-Pb-Zn prospect, Northern leases, Broken Hill, NSW. *In: Butt, C.R.M., Robertson, I.D.M., Scott, K.M. & Cornelius, M. (eds) Regolith Expression of Australian Ore Systems., 2005. 146–148 CRC LEME, Perth.*

KABATA-PENDIAS, A, PENDIAS, H., 2001, Trace Elements in Soils and Plants *CRC Press LLC.*

LEYH W.R. & LEGGO M.D. 2009 Exploration for Broken Hill type deposits combining geological mapping and Niton soil geochemistry. *Geoscience Australia, Broken Hill Exploration Initiative: Abstracts for the 2009 Conference*

LINTERN, M. J., 2001, Exploration for gold using calcrete – lessons from the Yilgarn Craton, Western Australia, *Geochemistry: Exploration, Environment, Analysis, Vol. **1**, 237–252*

MCKINNON, A.R., 2009. Application of field portable XRF geochemical data in the Broken Hill Region. *Geoscience Australia, Broken Hill Exploration Initiative: Abstracts for the 2009 Conference.*

PLIMER, I.R., 1985, Broken Hill Pb-Zn-Ag deposit a product of mantle metasomatism, *Mineralium Deposita **20*** (1985), pp. 147–153.

SHEFSKY, S. 2007, Comparing field portable X-Ray Fluorescence (XRF) to laboratory analysis of heavy metals in soil, *NITON Corporation, Billercia, MA, 1997.*

SKEY & YOUNG, 1980, Que River Zn-Pb deposit, Dundas Trough, Tas*. In: Butt C.R.M. and Smith R.E. (Editors), Conceptual Models in Exploration Geochemistry. Journal of Geochemical Exploration **12**, 284-290*

SMITH, R.E., 1996. Regolith research in support of mineral exploration in Australia. *Journal of Geochemical Exploration. **57***, 159–173

STEVENS, B. P. J., 1986, Post-depositional history of the Willyama Supergroup in the Broken Hill Block, NSW*. Australian Journal of Earth Sciences: An International Geoscience Journal of the Geological Society of Australia, 1440-0952, Vol. **33**,*
Issue 1, 73-98

STEVENS, B. P. J., BARNES, R. G., BROWN, R. E., STROUD, W. J. & WILLIS, I. L., 1988. The Willyama Supergroup in the Broken Hill and Euriowie Blocks, New South Wales. *Precambrian Research* ***40/41****, 297-327.*

THOMAS, M., EARL K.L., HILL S.M. & FOSTER K.A. 2002. A framework for regolith-landform mapping in the Flying Doctor Prospect, Broken Hill, NSW. *In: ROACH I.C. ed. Regolith and Landscapes of Eastern Australia. CRC LEME, 127-132.*

TONUI, E., DE CARITAT, P., & LEYH, W. 2003. Geochemical signatures of mineralization in weathered sediments and bedrock, Thunderdome prospect, Broken Hill, western New South Wales, Australia*: Implications for mineral exploration under cover, Geochemistry, Exploration, Environment, Analysis.* ***3*** *(2003), pp. 263–280.*

TUCKER, L.R. & HILL, S.M. 2006, Biogeochemical residence and dispersion of trace metals in the new Bendigo inlier and margins, northwest NSW. *Consolidation and Dispersion of Ideas CRC LEME (unpub.)*

WALTERS S., & BAILEY A., 1998. Geology and mineralization of the Cannington Ag-Pb-Zn deposit; an example of Broken Hill-type mineralization in the eastern succession, Mount Isa Inlier, *Australia Economic Geology; December 1998; v.* ***93****; no. 8, 1307-1329.*

WINGATE, M.T.D., CAMPBELL, I.H., COMPSTON W. & GIBSON G.M., 1998. Ion micropobe U–Pb ages for Neoproterozoic basaltic magmatism in south-central Australia and implications for the breakup of Rodinia. *Precambrian Research.* ***87*** *(1998), 135–159.*

WITTWER, P.D., BAROVICH, K.M. & HILL, S.M., 2004. Geology and geochemistry of regolith carbonate accumulations of the southwestern Curnamona Province, SA: implications for mineral exploration. *In: Roach, I.C. (ed.), Regolith 2004, CRC LEME, Perth, 402-406.*

Rockwell Regolith Landform Map
New South Wales

1:25,000

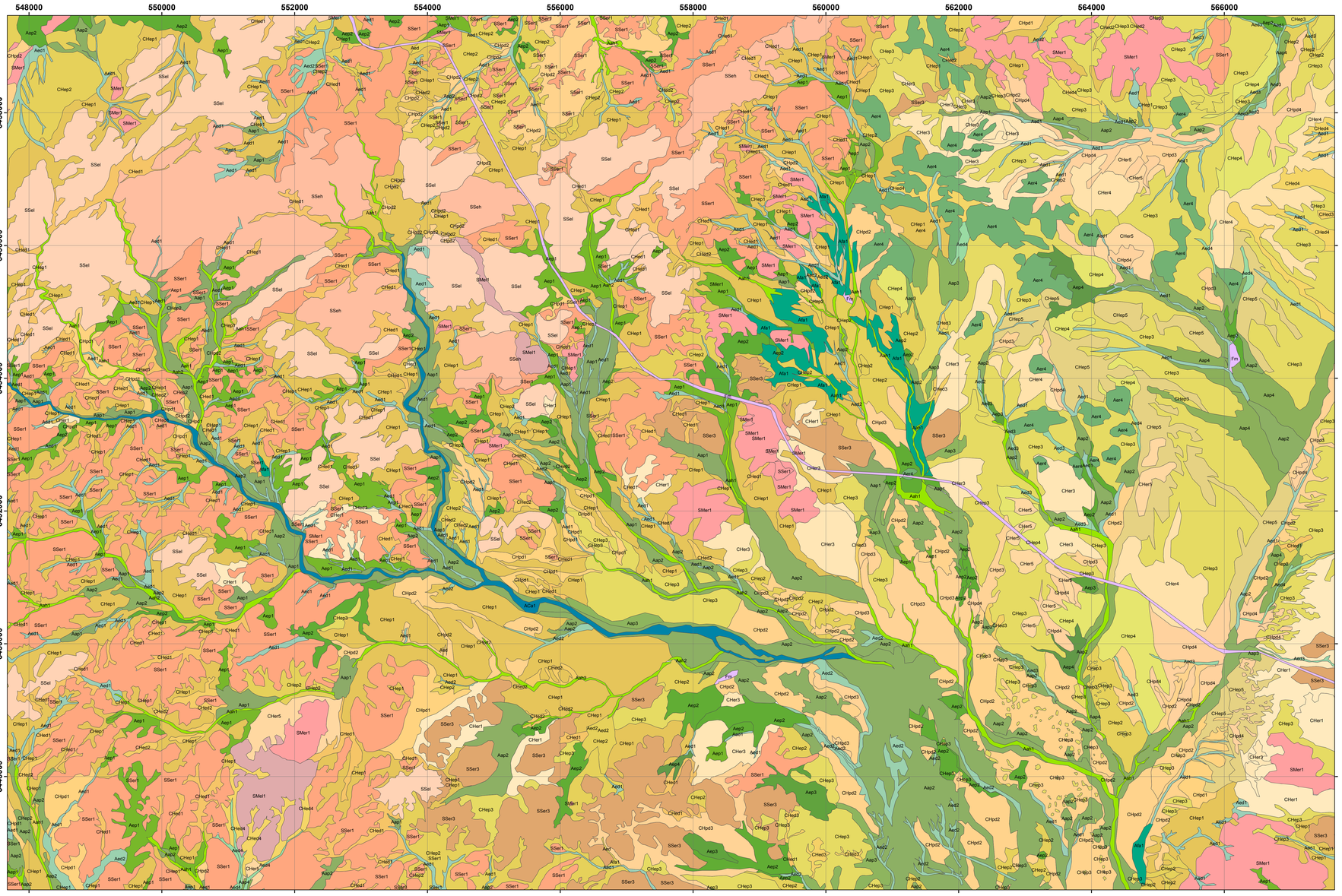

Transported Regolith

Alluvial Sediments

Alluvial Sediments

- **Aap1** — Sub-rounded to sub-angular sands, silts and gravels comprised of lithic and quartz fragments in low relief areas, with pervasive braided minor channels. Surface lag is sparse and is dominated by sub-angular lithic fragments with a minor quartz component reaching cobble size. Colonised by a sparse chenopod shrubland dominated by Maireana pyramidata, with Sida petrophila lining channels.
- **Aap2** — Sub-rounded lithic and quartzose sands and silts, with pervasive braided minor channels. Surface lag is sparse sub-rounded quartz gravels. Colonised by chenopod shrubland dominated by Maireana pyramidata, Osteocarpum dipterocarpum and Atriplex Viscaria.
- **Aap3** — Sub-rounded to sub-angular sands, silts and gravels comprised of quartz fragments in low relief areas, with pervasive braided minor channels. Surface lag dominated by sub-rounded quartz gravels. Colonised by chenopod shrubland dominated by Maireana pyramidata, Osteocarpum dipterocarpum and Sclerolaena diacantha.
- **Aap4** — Sub-rounded to sub-angular sands, silts and gravels comprised of quartz and maghemite fragments in low relief areas, with pervasive braided minor channels. Surface lag dominated by sub-rounded quartz and maghemite gravels. Colonised by chenopod shrubland dominated by Maireana pyramidata, Osteocarpum dipterocarpum and Sclerolaena diacantha.
- **Aed1** — Sub-rounded to sub-angular sands, silts and gravels comprised of lithic and quartz within depressions containing minor (<1m) incised channels. Surface lag dominated by sub-angular lithic fragments with a minor quartz component reaching cobble size. Colonised by a sparse chenopod shrubland dominated by Maireana pyramidata, with Sida petrophila lining channels
- **Aed2** — Sub-rounded sands and silts comprised of lithic and quartz within depressions containing minor (<1m) incised channels. Surface lag is sparse sub-rounded quartz gravels. Colonised by chenopod shrubland dominated by Maireana pyramidata, Osteocarpum dipterocarpum and Atriplex Viscaria.
- **Aed3** — Sub-rounded to sub-angular sands, silts and gravels comprised of quartz fragments within depressions containing minor (<1m) incised channels. Surface lag dominated by sub-rounded quartz gravels. Colonised by chenopod shrubland dominated by Maireana pyramidata, Osteocarpum dipterocarpum and Sclerolaena diacantha.
- **Aed4** — Sub-rounded to sub-angular sands, silts and gravels comprised of quartz and maghemite fragments within depressions containing minor (<1m) incised channels. Surface lag dominated by sub-rounded quartz and maghemite gravels. Colonised by chenopod shrubland dominated by Maireana pyramidata, Osteocarpum dipterocarpum and Sclerolaena diacantha.
- **Aep1** — Sub-rounded to sub-angular sands, silts and gravels comprised of lithic and quartz fragments in low relief areas, with infrequent shallow (<0.5m) incised channels . Surface lag is sparse and is dominated by sub-angular lithic fragments with a minor quartz component reaching cobble size. Colonised by a sparse chenopod shrubland dominated by Maireana pyramidata, with Sida petrophila lining channels
- **Aep2** — Sub-rounded sands and silts comprised of lithic and quartz fragments in low relief areas, with infrequent shallow (<0.5m) incised. Surface lag is sparse sub-rounded quartz gravels. Colonised by chenopod shrubland dominated by Maireana pyramidata, Osteocarpum dipterocarpum and Atriplex Viscaria.
- **Aep3** — Sub-rounded to sub-angular sands, silts and gravels comprised of quartz fragments in low relief areas, with infrequent shallow (<0.5m) incised. Surface lag dominated by sub-rounded quartz gravels. Colonised by chenopod shrubland dominated by Maireana pyramidata, Osteocarpum dipterocarpum and Sclerolaena diacantha.
- **Aep4** — Sub-rounded to sub-angular sands, silts and gravels comprised of quartz and maghemite fragments in low relief areas, with infrequent shallow (<0.5m) incised. Surface lag dominated by sub-rounded quartz and maghemite gravels. Colonised by chenopod shrubland dominated by Maireana pyramidata, Osteocarpum dipterocarpum and Sclerolaena diacantha.
- **Aer4** — Angular to sub-rounded lithic and quartz sands with minor gravels indurated by secondary silica and iron forming areas of slight relief. Surface lag is dominated by a cobble pavement of indurated material. Colonised by occasional Atriplex Viscaria
- **Afa1** — Sub-rounded lithic and quartzose sands and silts and gravels within outwash fans with braided channels. Surface lag consists of lithic and quartz gravel lag in proximal settings and coarse quartzose sands in distil settings.

Channel deposits

- **Aah1** — Sub-rounded to sub-angular sands, silts and gravels comprised of lithic and quartz fragments in low relief areas, with sub-angular lithic fragments reaching cobbles near bedrock units. Colonised by occasional open woodlands dominated by Acacia aneura and shrublands dominated by Sida petrophila.
- **Aah2** — Sub-rounded to sub-angular sands, silts and gravels comprised of lithic and quartz fragments with minor heavy minerals in low relief areas. Established channels colonised by occasional open woodlands dominated by Acacia aneura with a chenopod shurbland understory dominated by Maireana pyramidata.
- **ACa1** — Sub-rounded to sub-angular sands, silts comprised of lithic and quartz fragments, with lithics, quartzose gravels and minor heavy minerals forming minor sandy braid bars. Colonised by occasional open woodlands dominated by Eucalyptus Camaldulnesis and Acacia aneura with a chenopod shurbland understory dominated by Maireana pyramidata. Occasional Schinus Molle are present near human habitation.

Colluvial sediments

Sheet flow deposits

- **CHed1** — Sub-rounded to sub-angular sands, silts and gravels comprised of lithic and quartz within depressions. Surface lag dominated by sub-angular lithic fragments with a minor quartz component reaching cobble size. Colonised by a sparse chenopod shrubland dominated by Maireana and pyramidata Sida petrophila.
- **CHed2** — Sub-rounded sands and silts comprised of lithic and quartz within depressions. Surface lag is sparse sub-rounded quartz gravels. Colonised by chenopod shrubland dominated by Maireana pyramidata, Osteocarpum dipterocarpum and Atriplex Viscaria.
- **CHed3** — Sub-rounded to sub-angular sands, silts and gravels comprised of quartz fragments within depressions. Surface lag dominated by sub-rounded quartz gravels. Colonised by chenopod shrubland dominated by Maireana pyramidata, Osteocarpum dipterocarpum and Sclerolaena diacantha.
- **CHed4** — Sub-rounded to sub-angular sands, silts and gravels comprised of quartz and maghemite fragments within depressions. Surface lag dominated by sub-rounded quartz and maghemite gravels. Colonised by chenopod shrubland dominated by Maireana pyramidata, Osteocarpum dipterocarpum and Sclerolaena diacantha.
- **CHep1** — Sub-rounded to angular sands, silts and gravels comprised of lithic and quartz fragments. Surface lag dominated by sub-angular lithic fragments with a minor quartz component reaching cobble size. Colonised by a sparse chenopod shrubland dominated by Maireana pyramidata and Sclerolaena diacantha.
- **CHep2** — Sub-rounded lithic and quartzose sands and silts. Surface lag is sparse sub-rounded quartz and lithic gravels. Occasional nodular regolith carbonate accumulations. Colonised by chenopod shrubland dominated by Maireana pyramidata, with minor Osteocarpum dipterocarpum and Atriplex Viscaria.
- **CHep3** — Sub-rounded to sub-angular sands, silts and gravels comprised of quartz with minor lithics. Surface lag dominated by sub-rounded quartz gravels. Occasional nodular regolith carbonate accumulations. Colonised by dense chenopod shrubland dominated by Maireana pyramidata, Osteocarpum dipterocarpum and Sclerolaena diacantha.
- **CHep4** — Sub-rounded sands, silts and gravels comprised of quartz and maghemite. Surface lag dominated by sub-rounded quartz and maghemite gravels. Colonised by chenopod shrubland dominated by Maireana pyramidata, Osteocarpum dipterocarpum and Sclerolaena diacantha.
- **CHep5** — Sub-rounded sands, silts and gravels comprised of quartz and maghemite. Surface lag dominated by sub-rounded maghemite gravels. Colonised by chenopod shrubland dominated by Maireana pyramidata, Osteocarpum dipterocarpum and Sclerolaena diacantha.
- **CHer1** — Sub-rounded to angular sands, silts and gravels comprised of lithic and quartz fragments mantling areas with slight topographic relief. Surface lag is dense and dominated by sub-angular lithic fragments with a minor quartz component reaching cobble size. Colonised by open woodlands of Acacia aneura with an understory of chenopod shrubland dominated by Maireana pyramidata and Sclerolaena diacantha.
- **CHer3** — Sub-rounded to angular sands, silts and gravels comprised of quartz fragments mantling areas with slight topographic relief. Surface lag is dense and dominated by sub-rounded quartz fragments reaching cobble size. Colonised by chenopod shrubland dominated by Maireana pyramidata and Sclerolaena diacantha, with pockets of open woodlands of Casuarina pauper.
- **CHer4** — Sub-rounded to angular sands, silts and gravels comprised of quartz and quartzose fragments indurated by secondary silica and iron, mantling areas with slight topographic relief. Surface lag is dense and dominated by sub-angular indurated material reaching cobble size. Colonised by sparse chenopod shrubland dominated by Sclerolaena diacantha with minor Maireana pyramidata.
- **CHer5** — Sub-rounded to angular sands, silts and gravels comprised of quartz and quartzose fragments indurated by secondary silica and iron, mantling areas with slight topographic relief. Surface lag is dominated by a pavement of sub-angular indurated material reaching cobble size.
- **CHpd1** — Sub-rounded to sub-angular sands, silts and gravels comprised of lithic and quartz within low relief areas. Sparse sub-rounded lithic gravels with a minor quartz form a surface lag. Colonised by a sparse chenopod shrubland dominated by Maireana pyramidata and Sida petrophila.
- **CHpd2** — Sub-rounded lithic and quartzose sands and silts within low relief areas. Surface consists of sub-rounded fine lithic and quartz gravels. Minor clay pans common. Colonised by chenopod shrubland dominated by Osteocarpum dipterocarpum and Atriplex viscaria with minor Maireana pyramidata.
- **CHpd3** — Sub-rounded to sub-angular sands, silts and gravels comprised of lithic and quartz within low relief areas. Sparse sub-rounded quartz gravels form a surface lag dominantly in small clay pans. Colonised by a sparse chenopod shrubland dominated by Maireana pyramidata and Sclerolaena diacantha.
- **CHpd4** — Sub-rounded to sub-angular sands, silts and gravels comprised of lithic and quartz within low relief areas. Sparse sub-rounded quartz and maghemite gravels form a surface lag dominantly in small clay pans. Colonised by a sparse chenopod shrubland dominated by Maireana pyramidata and Sclerolaena diacantha.

In-situ Regolith

Saprolith

Saprock

- **SMel1** — Bedrock exposure with a moderate weathering surface, fracturing common in areas of moderate topographic relief. Angular lithic cobbles with a minor quartz component form a surface pavement. Colonised by sparse Ptilotus nobilis grassland with occasional Acacia aneura
- **SMer1** — Bedrock exposure with a moderate weathering surface in areas of moderate topographic relief. Angular lithic cobbles with a minor quartz component form a surface pavement. Colonised by Ptilotus nobilis with occasional Acacia aneura and Maireana pyramidata
- **SSeh1** — Bedrock exposure with a thin weathering surface, fracturing common in areas of large topographic relief. Angular lithic cobbles with a minor quartz component form a surface pavement. Colonised by sparse Ptilotus nobilis grassland with occasional Acacia aneura
- **SSel1** — Bedrock exposure with a thin weathering surface, fracturing common in areas of moderate topographic relief. Angular lithic cobbles with a minor quartz component form a surface pavement. Colonised by sparse Ptilotus nobilis grassland with occasional Acacia aneura
- **SSer1** — Bedrock exposure with a thin weathering surface in areas of moderate topographic relief. Angular lithic cobbles with a minor quartz component form a surface pavement. Colonised by Ptilotus nobilis with occasional Acacia aneura and Maireana pyramidata
- **SSer3** — Outcropping fractured quartz veins with a thin weathering surface in areas of moderate topographic relief. Angular quartz cobbles form a surface pavement. Colonised by chenopod shrubland of Maireana pyramidata with occasional Acacia aneura and Casuarina pauper

Anthropogenic

- **Fm** — Areas disrupted due to anthropogenic activity

Hyperspectral image filtered to show Mica component

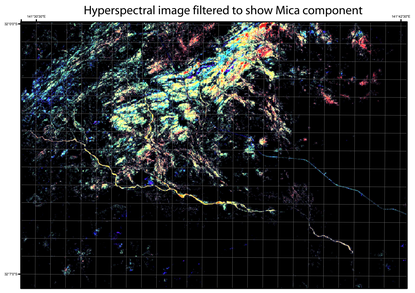

Hyperspectral image filtered to show Fe_2 component

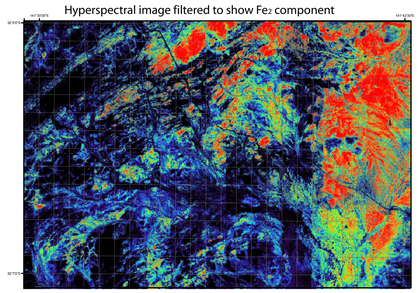

Sample Sites Locations and Confidence classes

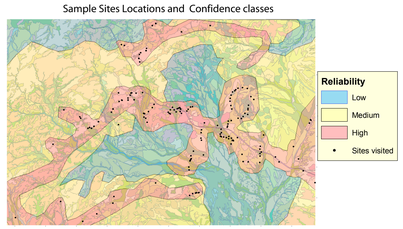

Regolith Map Compiled by Andrew Knight 2010,
Hyperspectral images sourced from Geological Survey of New South Wales

N
W E
S

0 1,000 2,000 4,000 Meters

Universal Transverse Mercator Projection
Horizontal Datum: GDA94, UTM Zone 54

Tables

Table 1. Logic process used to attribute landform units with numerical separator

Sub unit given	**Dominant lag components**
1	Lithic fragment Sub-angular to Sub-rounded up to cobbles
2	Sparse lag dominantly sub-rounded pebbles
3	Quartz dominated Sub-angular to Sub-rounded up to cobbles
4	Either contains indurated material or has a significant component of quartz and maghemite.

Table 2a. Soil geochemical data for selected elements with transect site locations shown. The plus samples represents the >80µm fraction.

			Au	Ag	Al	As	Cd	Co	Cu	Fe	Mn	Pb	Tl	W	Zn	Zr
	Eastings	Northings	ppb	ppm	ppm	ppm	ppm	ppm	ppm	%	ppm	ppm	ppm	ppm	ppm	ppm
	GDA94	GDA94	1	0.02	20	0.5	0.01	0.1	0.2	0.01	1	0.5	0.01	0.05	1	0.1
PLUS 01	554600	6454437	-	0.27	20815	4	0.52	11	29.3	3.58	727	117.6	0.22	-	225	9.2
PLUS 02	554601	6454426	-	0.21	18923	2.7	0.52	10.9	29.3	3.32	863	130.9	0.23	0.06	276	7.7
PLUS 03	554601	6454414	2	0.57	17642	4.1	0.86	14.3	78.6	3.59	1204	191.8	0.26	0.09	497	8
PLUS 04	554602	6454400	-	0.48	24195	4.4	1.75	14.9	89.9	4.76	1448	277.6	0.29	0.07	1049	7
PLUS 05	554600	6454383	4	1.32	24391	5.7	3.46	28.3	200.7	6.36	1634	675.3	0.24	0.13	1889	5.8
PLUS 06	554601	6454376	-	0.41	27583	3.5	1.02	17.8	134.6	4.86	909	215.4	0.22	-	598	6.2
PLUS 07	554600	6454362	-	0.37	33447	4.6	1.22	17.6	84.8	5.93	1697	197.4	0.19	-	794	4.8
PLUS 08	554600	6454338	-	0.86	26965	4.3	1.27	14.1	73.9	5.27	1557	559	0.28	0.05	625	6.6
PLUS 09	554600	6454319	-	0.71	28076	5.4	1.61	19.6	101.4	5.9	1995	439.2	0.3	0.09	1628	4.9
PLUS 10	554603	6454299	-	0.55	22896	3.8	1.95	13.5	64.6	4.12	1214	518	0.45	0.62	1274	8.6
PLUS 11	554599	6454285	-	0.28	20730	3.6	0.94	10.5	33.8	2.84	664	117.8	0.54	0.32	593	8.5
PLUS 12	554601	6454271	-	0.39	21427	3.6	0.91	8.4	26.5	2.88	617	153	0.3	0.05	340	8.3
PLUS 13	554600	6454319	-	0.62	28097	5.2	1.64	19.4	96.6	6.04	2048	429.4	0.3	0.26	1486	4.7
PLUS 14	554599	6454226	-	0.28	24410	3	0.56	10.3	18.9	3.57	720	141.2	0.47	0.09	289	7.1
PLUS 15	554602	6454200	-	0.68	28792	3.4	1.06	17	98.3	5.2	1871	561.3	0.45	0.21	1424	12.4
PLUS 16	554600	6454172	-	0.35	20358	2.9	1	13	63.9	3.82	1382	306.4	0.4	0.16	818	10.4
PLUS 17	554602	6454160	-	0.2	24261	3.5	0.38	11.1	26.4	3.59	856	95.7	0.52	-	237	14.4
PLUS 18	554600	6454362	-	0.37	31669	3.8	1.2	17.4	89.9	5.96	1656	192.4	0.19	-	788	7.5
PLUS 19	554605	6454254	-	0.48	26078	4.8	0.75	10.2	42.7	3.63	643	134.3	0.24	-	248	15.8

Table 2b. Soil geochemical data for selected elements with transect site locations shown. Minus represents the <80µm fraction.

			Au	Ag	Al	As	Cd	Co	Cu	Fe	Mn	Pb	Tl	W	Zn	Zr
	Eastings	Northings	ppb	ppm	ppm	ppm	ppm	ppm	ppm	%	ppm	ppm	ppm	ppm	ppm	ppm
	GDA94	GDA94	1	0.02	20	0.5	0.01	0.1	0.2	0.01	1	0.5	0.01	0.05	1	0.1
MINUS 01	554600	6454437	6	0.67	28989	3.1	0.64	10.6	28.9	3.13	634	190.4	0.25	0.09	276	13.8
MINUS 02	554601	6454426	2	0.56	29632	3.5	0.58	10.2	33.1	3.36	576	160.6	0.27	0.14	290	13.9
MINUS 03	554601	6454414	5	0.97	35328	3	1.06	13.6	104.8	3.87	865	241.5	0.34	0.07	593	15.7
MINUS 04	554602	6454400	4	0.95	30867	4.1	1.55	11.2	51.3	3.27	787	313.1	0.29	0.05	760	11.9
MINUS 05	554600	6454383	4	1.67	33457	3.8	3.44	18.5	131	4.42	1058	1036.5	0.3	0.12	1638	12.6
MINUS 06	554605	6454254	4	0.55	31194	3.8	0.68	9.1	26.6	3.16	617	187	0.25	0.07	270	13.4
MINUS 07	554600	6454362	3	0.69	44972	3.9	1.56	19.1	108.5	4.65	938	257.5	0.33	-	1094	7.2
MINUS 08	554600	6454338	2	1.35	33562	4.1	1.39	11.5	59.5	3.41	663	652.5	0.37	0.06	645	11.2
MINUS 09	554600	6454319	3	1.64	40600	3.7	1.85	17.1	97.4	4.67	1007	530.6	0.37	0.05	1691	10.5
MINUS 10	554603	6454299	-	1.23	29648	3.8	1.9	12.1	47.3	3.23	701	482.8	0.36	0.12	838	13.1
MINUS 11	554599	6454285	3	0.63	34859	3.4	1.38	13	46.1	3.69	538	166.6	0.61	0.06	701	16.4
MINUS 12	554601	6454271	-	0.71	24873	3.4	0.94	8.4	25.4	2.69	570	215.4	0.28	0.14	325	13.4
MINUS 13	554605	6454254	2	0.6	25614	3.2	0.74	9	28.8	3.03	583	185.5	0.23	0.14	271	12.8
MINUS 14	554599	6454226	-	0.63	28561	3.1	0.73	10.7	22.2	3.18	680	187.9	0.39	0.08	295	12.2
MINUS 15	554602	6454200	6	1.63	38560	3.1	1.09	17.7	118	4.45	1070	716.5	0.53	0.26	1512	12.6
MINUS 16	554600	6454172	2	0.44	24182	3.4	0.89	9.6	47.1	3.02	525	229.5	0.4	0.11	528	11.3
MINUS 17	554602	6454160	2	0.35	27132	2.4	0.47	10.4	30.1	3.19	436	120.7	0.5	0.14	242	14.2
MINUS 18	554601	6454414	3	0.98	31979	3	1.09	13	101.8	3.89	798	232.2	0.34	0.08	595	15.7
MINUS 19	554601	6454376	6	0.81	37198	3.9	1.17	16.8	137.8	3.93	764	251.3	0.3	-	731	13.2

Table 3a. Soil geochemical data summary statistics for whole data set

45 rows - Univariate	Pb	Zn	Mg	Cd	As	Fe	Mn	Ga	Cu	Ag	Co	Sb	W	Tl	Zr	Au	Sr	Ti
Count Numeric	40	40	40	40	40	40	40	40	40	40	40	40	30	40	40	18	40	40
Count Null	0	0	0	0	0	0	0	0	0	0	0	0	10	0	0	22	0	0
Minimum	14	51	0.31	0.06	2.40	2.66	290	5.50	19	0.06	8.40	0.10	0.05	0.19	4.70	2	15	287
Maximum	1037	1889	0.71	3.46	5.70	6.36	2048	13.01	201	1.67	28.30	1.44	0.62	0.61	16.40	6	85	1339
Mean	297	714	0.45	1.15	3.79	4.01	960	8.34	68	0.67	13.62	0.62	0.13	0.34	10.57	4	31	676
Median	215	597	0.44	1.04	3.75	3.66	793	7.84	55	0.59	13.00	0.51	0.09	0.30	11.25	3	28	616
Standard Deviation	217	502	0.08	0.71	0.74	1.02	457	2.02	42	0.41	4.19	0.40	0.11	0.11	3.46	1	12	248
Interquartile Range	282	717	0.13	0.82	0.85	1.46	590	2.85	69	0.48	6.65	0.55	0.07	0.15	6.07	2	11	405
Range	1023	1838	0.40	3.40	3.30	3.70	1758	7.51	182	1.61	19.90	1.34	0.57	0.42	11.70	4	70	1052
25 percentile	153	276	0.38	0.68	3.20	3.19	617	6.67	29	0.35	10.40	0.30	0.06	0.24	7.20	2	24	479
75 percentile	429	838	0.50	1.39	4.10	4.65	1204	9.51	97	0.81	17.00	0.74	0.14	0.39	13.20	4	35	855
95 percentile	675	1638	0.54	1.95	5.20	5.96	1871	12.06	135	1.63	19.40	1.35	0.26	0.53	15.70	6	45	1034

Table 3b. Soil geochemical data summary statistics for <80µm fraction

Minus	Pb	Zn	Mg	Cd	As	Fe	Mn	Ga	Cu	Ag	Co	Sb	W	Tl	Zr	Au	Sr	Ti
Count Numeric	19	19	19	19	19	19	19	19	19	19	19	19	17	19	19	16	19	19
Count Null	0	0	0	0	0	0	0	0	0	0	0	0	2	0	0	3	0	0
Minimum	121	242	0.36	0.47	2.40	2.69	436	6.59	22	0.35	8.40	0.40	0.05	0.23	7.20	2	24	381
Maximum	1037	1691	0.52	3.44	4.10	4.67	1070	13.01	138	1.67	19.10	1.44	0.26	0.61	16.40	6	45	1004
Mean	335	700	0.45	1.22	3.46	3.59	727	8.58	66	0.90	12.72	0.90	0.10	0.35	12.90	4	32	593
Median	232	595	0.44	1.09	3.40	3.36	680	8.04	47	0.71	11.50	0.90	0.09	0.34	13.10	3	30	580
Standard Deviation	241	471	0.06	0.68	0.45	0.60	188	1.74	40	0.42	3.46	0.39	0.05	0.10	2.07	2	6	152
Interquartile Range	296	548	0.10	0.82	0.70	0.77	289	2.03	76	0.63	6.60	0.79	0.08	0.11	2.00	3	11	168
Range	916	1449	0.16	2.97	1.70	1.98	634	6.42	116	1.32	10.70	1.04	0.21	0.38	9.20	4	21	623
25 percentile	187	290	0.38	0.73	3.10	3.16	576	7.23	29	0.60	10.20	0.49	0.06	0.28	11.90	2	27	479
75 percentile	313	760	0.49	1.39	3.80	3.89	798	9.22	102	0.98	13.60	1.26	0.12	0.37	13.80	4	35	636
95 percentile	717	1638	0.51	1.90	4.10	4.65	1058	11.02	131	1.64	18.50	1.43	0.14	0.53	15.70	6	41	833

Table 3c. Soil geochemical data summary statistics for <80µm fraction

Plus	Pb	Zn	Mg	Cd	As	Fe	Mn	Ga	Cu	Ag	Co	Sb	W	Tl	Zr	Au	Sr	Ti
Count Numeric	21	21	21	21	21	21	21	21	21	21	21	21	13	21	21	2	21	21
Count Null	0	0	0	0	0	0	0	0	0	0	0	0	8	0	0	19	0	0
Minimum	14	51	0.31	0.06	2.70	2.66	290	5.50	19	0.06	8.40	0.10	0.05	0.19	4.70	2	15	287
Maximum	675	1889	0.71	3.46	5.70	6.36	2048	12.50	201	1.32	28.30	0.73	0.62	0.54	15.80	4	85	1339
Mean	263	726	0.45	1.09	4.09	4.39	1171	8.12	69	0.46	14.43	0.37	0.17	0.32	8.47	3	31	751
Median	192	598	0.42	1.00	4.00	4.12	1204	7.36	65	0.39	14.10	0.32	0.09	0.29	7.70	3	26	769
Standard Deviation	191	540	0.11	0.74	0.83	1.18	527	2.27	44	0.28	4.69	0.18	0.16	0.12	3.10	1	16	295
Interquartile Range	310	900	0.15	0.90	1.25	2.01	953	3.76	64	0.32	6.80	0.33	0.17	0.22	3.40	2	14	523
Range	662	1838	0.40	3.40	3.00	3.70	1758	7.00	182	1.26	19.90	0.63	0.57	0.35	11.10	2	70	1052
25 percentile	118	248	0.36	0.52	3.50	3.57	664	6.01	29	0.27	10.50	0.22	0.06	0.23	6.20	2	20	426
75 percentile	429	1049	0.49	1.27	4.70	5.27	1634	9.55	90	0.57	17.40	0.52	0.21	0.40	9.20	2	33	993
95 percentile	561	1628	0.66	1.95	5.40	6.04	1995	12.06	135	0.86	19.60	0.66	0.32	0.52	14.40	4	61	1146

Table 4. Soil geochemical data percentage difference errors, and blank readings

Sample % Difference Error															
(Established from 3 duplicates for each fraction tested)															
Portion sampled	Au	Ag	As	Cd	Co	Cu	Fe	Mg	Mn	Pb	Sb	Tl	W	Zn	Zr
>80m	50	19.6	15.8	8.1	4.4	7.6	5.1	5.3	7.7	7	19.2	8	57.1	8.3	4.5
<80m	-	12.7	17.4	1.9	7.6	5.7	11.8	8.7	7.3	2.5	20	4.5	65.4	8.7	36

							Standard % Difference Error									
Standard	Au	Ag	As	Cd	Co	Cu	Fe	Mg	Mn	Pb	Sb	Sn	Tl	W	Zn	Zr
AE1	15.4	18.3	7.6	9.3	4.7	7.5	14.2	22.2	2.0	11.8	11.1	11.9	12.8	50.0	8.7	15.7
NGL1	10.5	13.0	3.2	12.0	8.2	2.8	3.5	9.4	5.6	10.2	6.9	7.4	0.7	47.4	13.0	16.3

BLANKS																
ELEMENTS	Au	Ag	As	Cd	Co	Cu	Fe	Mg	Mn	Pb	Sb	Sc	Tl	W	Zn	Zr
Control Blank	-	0	-	0	-	1.1	-	-	-	-	-	0.2	-	-	-	-

Table 5a. Summary statistics for the complete Niton FP-XRF field data set

Whole data	PB	ZN	CD	MN	AG	CU	AS	MO	CO	BA	FE	
Count Numeric	10454	9397	67	8567	71	457	350	510	1036	8966	10850	
Count Null	396	1453	10783	2283	10779	10393	10500	10340	9814	1884	0	
Minimum	37	62	44	257	124	82	23	8	260	25	1542	
Maximum	134152	793458	1103	267596	562	32767	18818	25	10008	10726	2556908	
Mean	300	607	86	1442	166	444	205	13	564	593	35443	
Median	190	266	59	1224	153	163	45	12	522	577	32682	
Standard Deviation	2246	9790	133	3095	56	1856	1243	3	366	192	33040	
Interquartile Range	128	205	17	707	33	118	20	4	179	169	8468	
Range	134115	793396	1059	267339	438	32685	18795	17	9748	10701	2555366	
25 percentile	136	188	51	937	140	120	35	10	445	495	29018	
75 percentile	264	392	68	1644	169	237	55	14	623	665	37484	
95 percentile	473	746	175	2588	234	1267	212	19	832	840	52266	
	CR	CS	LA	NI	SB	PD	RB	SE	SN	SR	TE	ZR
Count Numeric	791	5944	8906	347	59	44	9265	605	7	4669	185	1874
Count Null	10059	4906	1944	10503	10791	10806	1585	10245	10843	6181	10665	8976
Minimum	192	26	1944	108	46	61	14	12	100	22	57	35
Maximum	81825	421	818	3353	325	115	1146	89	165	1573	242	794
Mean	2437	48	92	453	63	77	115	29	125	71	76	281
Median	340	46	90	468	56	78	110	26	123	66	72	270
Standard Deviation	6667	14	28	218	36	10	37	10	22	38	17	74
Interquartile Range	141	18	34	119	14	10	46	15	32	22	15	84
Range	81633	395	794	3245	279	54	1132	77	65	1551	185	759
25 percentile	284	38	74	418	51	71	89	20	104	56	66	231
75 percentile	424	55	107	536	64	80	134	36	128	78	81	316
95 percentile	18599	72	138	651	79	92	179	45	165	106	99	420

Table 5b. Summary statistics for outcropping locations within the Niton FP-XRF field data

Rock Outcrop	PB	ZN	CD	MN	AG	CU	AS	MO	CO	BA	FE	
Count Numeric	5702	5229	41	4752	42	291	218	298	579	4627	5867	
Count Text	0	0	0	0	0	0	0	0	0	0	0	
Count Null	165	638	5826	1115	5825	5576	5649	5569	5288	1240	0	
Minimum	37	62	46	291	125	82	26	9	260	25	2766	
Maximum	134152	298579	1103	50687	562	32767	18818	25	10008	10726	2556908	
Mean	352	609	105	1448	170	529	290	13	573	600	36997	
Median	197	275	65	1237	154	164	47	12	512	581	33377	
Deviation	3011	6331	168	1419	69	2101	1563	3	472	223	41208	
Range	124	198	14	698	31	135	19	4	175	179	8714	
Range	134115	298517	1057	50396	437	32685	18792	16	9748	10701	2554142	
25 percentile	143	197	56	951	140	119	38	10	441	495	29843	
75 percentile	266	395	70	1648	169	254	56	14	616	674	38551	
95 percentile	452	755	246	2639	235	2095	377	19	840	868	55124	
	CR	CS	LA	NI	SB	PD	RB	SE	SN	SR	TE	ZR
Count Numeric	473	3067	4574	183	31	26	5120	372	5	2614	88	1234
Count Null	0	0	0	0	0	0	0	0	0	0	0	0
Minimum	5394	2800	1293	5684	5836	5841	747	5495	5862	3253	5779	4633
Maximum	192	26	25	108	49	63	14	15	100	22	60	35
Mean	41032	421	818	801	325	115	1146	89	165	1573	242	794
Median	2378	49	93	444	71	79	117	28	126	70	77	284
Deviation	337	46	90	475	60	78	112	24	123	64	72	271
Range	6087	15	29	159	49	12	37	10	26	47	21	75
Range	138	17	34	136	12	16	46	15	49	21	13	87
25 percentile	40840	395	793	693	276	52	1132	74	65	1551	182	759
75 percentile	282	38	74	411	54	67	91	20	100	55	67	233
95 percentile	419	56	107	546	67	82	136	35	136	77	80	320
	18567	72	139	651	82	101	182	44	165	106	102	419

Table 5c. Summary statistics for sediment covered locations within the Niton FP-XRF field data

Sediment cover	PB	ZN	CD	MN	AG	CU	AS	MO	CO	BA	FE	
Count Numeric	4752	4168	26	3815	29	166	132	212	457	4339	4983	
Count Null	231	815	4957	1168	4954	4817	4851	4771	4526	644	0	
Minimum	45	68	44	257	124	89	23	8	266	43	1542	
Maximum	17205	793458	80	267596	252	17019	2303	24	1210	4760	893829	
Mean	238	604	55	1433	160	295	66	13	553	586	33614	
Median	180	254	52	1205	153	157	41	13	533	573	31893	
Deviation	459	12877	8	4359	29	1316	199	3	150	150	19277	
Range	133	208	9	717	32	103	21	4	182	160	8017	
Range	17160	793390	36	267339	128	16930	2280	16	944	4717	892287	
25 percentile	128	178	49	922	140	121	33	11	454	496	28178	
75 percentile	261	386	58	1638	169	223	53	14	636	655	36190	
95 percentile	490	740	73	2527	228	336	74	18	826	797	47482	
	CR	CS	LA	NI	SB	PD	RB	SE	SN	SR	TE	ZR
Count Numeric	318	2877	4332	164	28	18	4145	233	2	2055	97	640
Count Null	4665	2106	651	4819	4955	4965	838	4750	4981	2928	4886	4343
Minimum	202	27	24	111	46	61	46	12	116	32	57	123
Maximum	81825	223	290	3353	72	89	619	67	128	396	105	584
Mean	2523	48	92	462	55	75	113	30	122	72	75	275
Median	344	45	89	455	53	76	107	28	122	68	71	266
Deviation	7456	14	26	269	7	8	37	10	8	21	12	72
Range	145	17	34	95	9	9	45	16	12	23	18	79
Range	81623	196	266	3242	26	28	573	55	12	364	48	461
25 percentile	288	37	73	419	49	68	86	21	116	57	65	227
75 percentile	432	55	107	514	56	78	131	37	116	80	83	306
95 percentile	19104	72	136	655	67	87	175	47	128	105	97	421

Table 6. Summary statistics for Biogeochemical results for selected elements

Total Biogeochemical	Pb ppm	Zn ppm	Mg pct	Cd ppm	As ppm	Fe pct	Mn ppm	Ga ppm	Cu ppm	Ag ppm	Co ppm	Zr ppm	Au ppm	Ti pct	Al pct
Detection limit	0.01	0.10	0.001	0.01	0.10	0.001	1.00	0.10	0.01	2.00	0.01	0.01	0.20	1.00	0.01
Count Numeric	38.00	38.00	38.000	38.00	38.00	38.000	38.00	38.00	38.00	38.00	38.00	38.00	38.00	38.00	38.00
Count Null	0.00	0.00	0.000	0.00	0.00	0.000	0.00	0.00	0.00	0.00	0.00	0.00	0.00	0.00	0.00
Minimum	0.34	7.10	0.089	0.01	0.05	0.008	12.00	0.05	2.70	4.00	0.02	0.07	0.10	4.00	0.01
Maximum	16.97	138.40	0.331	2.83	0.70	0.107	132.00	0.30	35.48	59.00	1.67	0.80	0.90	13.00	0.09
Mean	2.65	39.02	0.177	0.35	0.22	0.042	55.39	0.11	10.05	19.00	0.36	0.33	0.33	7.84	0.04
Median	1.29	25.05	0.178	0.16	0.20	0.034	48.50	0.05	8.12	14.50	0.27	0.28	0.30	7.50	0.03
Standard Deviation	3.42	32.86	0.053	0.56	0.16	0.026	31.69	0.07	6.89	13.57	0.33	0.21	0.21	2.60	0.02
Interquartile Range	2.34	28.47	0.066	0.33	0.20	0.046	48.25	0.15	5.59	19.50	0.48	0.38	0.33	4.00	0.04
Range	16.63	131.30	0.242	2.83	0.65	0.099	120.00	0.25	32.78	55.00	1.65	0.73	0.80	9.00	0.08
25 percentile	0.65	18.10	0.138	0.03	0.05	0.020	27.00	0.05	5.82	8.00	0.08	0.15	0.10	5.00	0.02
75 percentile	2.08	43.50	0.200	0.35	0.30	0.063	71.00	0.10	10.27	25.00	0.57	0.50	0.40	9.00	0.04
95 percentile	8.20	113.70	0.252	1.55	0.50	0.091	120.00	0.20	20.95	45.00	0.87	0.73	0.70	12.00	0.08
Bluebush	Pb ppm	Zn ppm	Mg pct	Cd ppm	As ppm	Fe pct	Mn ppm	Ga ppm	Cu ppm	Ag ppm	Co ppm	Zr ppm	Au ppm	Ti pct	Al pct
Count Numeric	26.00	26.00	26.000	26.00	26.00	26.000	26.00	26.00	26.00	26.00	26.00	26.00	26.00	26.00	26.00
Count Null	0.00	0.00	0.000	0.00	0.00	0.000	0.00	0.00	0.00	0.00	0.00	0.00	0.00	0.00	0.00
Minimum	0.34	7.10	0.089	0.10	0.05	0.008	12.00	0.05	5.29	4.00	0.07	0.07	0.10	4.00	0.01
Maximum	16.97	138.40	0.331	2.83	0.50	0.107	94.00	0.30	20.95	45.00	1.67	0.80	0.90	13.00	0.09
Mean	3.15	40.90	0.180	0.50	0.24	0.049	48.65	0.12	9.91	18.12	0.48	0.39	0.38	8.04	0.04
Median	1.54	28.40	0.180	0.28	0.20	0.040	45.00	0.10	8.45	14.50	0.48	0.32	0.30	7.50	0.04
Standard Deviation	3.92	35.19	0.058	0.62	0.14	0.029	22.13	0.08	4.27	11.51	0.34	0.23	0.22	3.01	0.03
Interquartile Range	3.26	31.92	0.070	0.40	0.23	0.049	38.25	0.15	4.64	17.25	0.42	0.44	0.25	6.00	0.04
Range	16.63	131.30	0.242	2.73	0.45	0.099	82.00	0.25	15.66	41.00	1.60	0.73	0.80	9.00	0.08
25 percentile	0.74	17.50	0.136	0.15	0.10	0.020	27.00	0.05	6.74	8.00	0.16	0.15	0.20	5.00	0.02
75 percentile	2.96	46.30	0.200	0.52	0.30	0.068	62.00	0.10	10.27	23.00	0.58	0.58	0.50	10.00	0.06
95 percentile	10.10	115.80	0.289	1.59	0.50	0.097	84.00	0.20	19.01	42.00	0.92	0.75	0.80	12.00	0.08
Mulga	Pb ppm	Zn ppm	Mg pct	Cd ppm	As ppm	Fe pct	Mn ppm	Ga ppm	Cu ppm	Ag ppm	Co ppm	Zr ppm	Au ppm	Ti pct	Al pct
Count Numeric	12.00	12.00	12.000	12.00	12.00	12.000	12.00	12.00	12.00	12.00	12.00	12.00	12.00	12.00	12.00
Count Null	0.00	0.00	0.000	0.00	0.00	0.000	0.00	0.00	0.00	0.00	0.00	0.00	0.00	0.00	0.00
Minimum	0.37	15.40	0.112	0.01	0.05	0.011	16.00	0.05	2.70	4.00	0.02	0.07	0.10	5.00	0.01
Maximum	5.85	113.70	0.245	0.16	0.70	0.043	132.00	0.10	35.48	59.00	0.28	0.35	0.60	10.00	0.04
Mean	1.56	34.93	0.171	0.03	0.18	0.027	70.00	0.07	10.36	20.92	0.10	0.21	0.22	7.42	0.03
Median	0.99	23.35	0.171	0.02	0.10	0.027	72.00	0.05	5.81	15.00	0.08	0.21	0.15	7.50	0.03
Standard Deviation	1.61	28.13	0.040	0.04	0.19	0.010	43.89	0.02	10.87	17.67	0.08	0.09	0.15	1.38	0.01
Interquartile Range	1.17	20.88	0.063	0.03	0.23	0.017	88.75	0.05	9.08	25.00	0.05	0.15	0.20	1.75	0.02
Range	5.48	98.30	0.133	0.16	0.65	0.032	116.00	0.05	32.78	55.00	0.26	0.28	0.50	5.00	0.03
25 percentile	0.57	15.70	0.138	0.01	0.05	0.017	26.00	0.05	3.55	7.00	0.02	0.12	0.10	6.00	0.01
75 percentile	1.29	33.80	0.197	0.03	0.20	0.034	102.00	0.05	8.39	28.00	0.09	0.28	0.20	8.00	0.03
95 percentile	3.60	61.50	0.214	0.05	0.30	0.041	127.00	0.10	29.52	47.00	0.22	0.32	0.30	9.00	0.04

Table 7 Calculated errors on biogeochemical data, including sample percentage difference error, standard percentage difference error and the 95% confidence interval for the true reading of the measured samples.

Sample % Difference Error														
(Bluebushsamplese stablished from 3 duplicates, Mulga from 2 duplicates)														
Sample	Pb	Zn	Mg	Cd	As	Fe	Mn	Ga	Cu	Ag	Co	Zr	Au	Al
Bluebush	39.8	38.2	41.5	27.5	-	47.4	35.5	50.0	21.0	27.4	41.9	53.0	-	42.9
Mulga	54.3	58.2	51.6	75.0	50.0	30.0	42.3	-	43.0	70.0	71.4	31.3	33.3	-

						95% Confidence Interval								
		Pb ppm	**Zn ppm**	**Mg pct**	**Cd ppm**	**As ppm**	**Fe pct**	**Mn ppm**	**Ga ppm**	**Cu ppm**	**Ag ppm**	**Co ppm**	**Zr ppm**	**Au ppm**	**Al pct**
Confidence interval		0.099	2.230	0.004	0.009	0.346	0.028	43.978	0.037	0.390	2.013	0.084	0.009	0.610	0.008
Sample mean		2.65	39.02	0.18	0.35	0.22	0.04	55.39	0.11	10.05	19.00	0.36	0.33	0.33	7.84
Upper mean		2.75	41.2454	0.1810	0.3615	0.5701	0.0696	99.3731	0.1426	10.4384	21.0127	0.4412	0.3401	0.9394	7.8504
Lower mean		2.55	36.79	0.17	0.34	-0.12	0.01	11.42	0.07	9.66	16.99	0.27	0.32	-0.28	7.83
Interval as a percentage of mean		3.76	5.71	2.22	2.52	154.87	66.46	79.39	35.51	3.88	10.59	23.56	2.58	185.57	0.11

Sample % Difference Error															
Reference Materials		**Cu**	**Pb**	**Zn**	**Ag**	**Co**	**Mn**	**Fe**	**As**	**Au**	**Cd**	**Mg**	**Al**	**Ga**	**Zr**
BLK	**BLK**	<0.01	<0.01	<0.1	<2	<0.01	<1	<0.001	<0.1	<0.2	<0.01	<0.001	<0.01	<0.1	<0.01
FLOUR	**BLK**	13.5	41.7	10.0	0.0	0.0	6.7	0.0	0.0	0.0	50.0	20.0	0.0	0.0	0.0
STD V14	**STD**	10.5	26.3	14.2	14.8	12.5	7.9	12.5	13.6	33.3	13.0	22.0	18.8	0.0	25.0
STD V16	**STD**	18.0	6.4	20.4	13.9	19.7	7.9	19.2	17.6	30.8	10.0	7.1	0.0	50.0	16.7
Max error		18.0	41.7	20.4	14.8	19.7	7.9	19.2	17.6	33.3	50.0	22.0	18.8	50.0	25.0

Figure captions

Figure 1a The Curnamona Province including the location of the Broken Hill Domain, and the Broken Hill township, modified from (Conor and Preiss 2008)

Figure 1b Outcropping sections of the Broken Hill Domain, overlain with the site locations for the two Niton FP-XRF surveys. The extent of the Rockwell area within the Broken Hill Domain is shown in navy.

Figure 2 This hyperspectral image has been filtered to show only the mica component, and highlights the depostional fan systems generated by confined channels exiting the ranges as they reach the plains.

Figure 3 Landscape evolution model proposed by (Hill et al., 2003), image is drawn looking south west and shows the eastwards drainage evolution of the Rockwell area.

Figure 4 Regolith-Landform map for Rockwell domain, Broken Hill.

Figure 5 Soil geochemisty concentration of Pb vs. Northing for the >80µm and <80µm soil fractions

Figure 6 Soil geochemisty concentration of Ag vs. Northing for the >80µm and <80µm soil fractions

Figure 7 Soil geochemisty concentration of Zn vs. Northing for the >80µm and <80µm soil fractions

Figure 8 Soil geochemisty concentration of Cu vs. Northing for the >80µm and <80µm soil fractions

Figure 9 Soil geochemisty concentration of Mn vs. Northing for the >80µm and <80µm soil fractions

Figure 10 Soil geochemisty concentration of Cd vs. Northing for the >80µm and <80µm soil fractions

Figure 11 Soil geochemisty concentration of As vs. Northing for the >80µm and <80µm soil fractions

Figure 12 Soil geochemisty concentration of Fe vs. Northing for the >80µm and <80µm soil fractions

Figure 13 Soil geochemisty concentration of Mg vs. Northing for the >80µm and <80µm soil fractions

Figure 14. Histogram plots of the two two soil geochemical fractions, in green is the <80µm fraction while the >80µm fraction is in blue, single yet skewed populations are common with minor bimodal populations such as Zn.

Figure 15. Normal quantile-quantile plots of the two soil geochemical fractions, in green is the <80µm fraction while the >80µm fraction is in blue, unbroken straight lines represent normally distributed single population data.

Figure 16a. PCA loaded factor analysis cluster plots of the soil geochemisty <80µm fraction, grouped of data indicates a likely association between those elements .

Figure 16b. PCA loaded factor analysis cluster plots of the soil geochemisty <80µm fraction, focussing on the Broken Hill suite elements. Grouped of data indicates a likely association between those elements .

Figure 17a. PCA loaded factor analysis cluster plots of the soil geochemisty >80µm fraction, grouped of data indicates a likely association between those elements .

Figure 17b. PCA loaded factor analysis cluster plots of the soil geochemisty >80µm fraction, focussing on the Broken Hill suite elements. Grouped of data indicates a likely association between those elements .

Figure 18. Dengrogram plot of the soil geochemisty >80µm fraction. Shorter linkage distance between elements represents higher association.

Figure 19. Dengrogram plot of the soil geochemisty <80µm fraction. Shorter linkage distance between elements represents higher association.

Figure 20 Histogram plots of the Niton FP-XRF data, green represents outcrop observed while red indicates site sediment cover.

Figure 21 Normal quantile-quantile plots of the Niton FP-XRF data, green represents outcrop observed while red indicates site sediment cover.

Figure 22. PCA loaded factor analysis cluster plots of the Niton FP-XRF field data, showing clear grouping of Zn, Mn, Pb and Cd within the soil geochemistry.

Figure 23. Dengrogram plot of the Niton FP-XRF field data.

Figure 24. Niton FP-XRF X-Y scatter plots for Pb against selected elements.

Figure 25. Niton FP-XRF X-Y scatter plots for Cu against selected elements.

Figure 26. Niton FP-XRF X-Y scatter plots for Zn against selected elements.

Figure 27. Niton FP-XRF X-Y scatter plots for Mn against selected elements .

Figure 28. Niton FP-XRF X-Y scatter plots for Mo against selected elements .

Figure 29. Niton FP-XRF X-Y scatter plots for Co against selected elements .

Figure 66. X-Y scatter plots for Zn against selected elements for biogeochemical Mulga data.

Figure 67. X-Y scatter plots for Mn against selected elements for biogeochemical Mulga data.

Figure 68. Spatial association map Au in regolith carbonate samples.

Figure 69. Spatial association map Cu in regolith carbonate samples.

Figure 70 Spatial association map Pb in regolith carbonate samples.

Figure 71. Spatial association map Zn in regolith carbonate samples.

Figure 72. Plot of Zn, Pb and Cu against Ca to assess the relationship between $CaCO_3$. It has been assumed that Ca concentration is directly proportional to $CaCO_3$ in regolith carbonate samples.

Figure 1a.

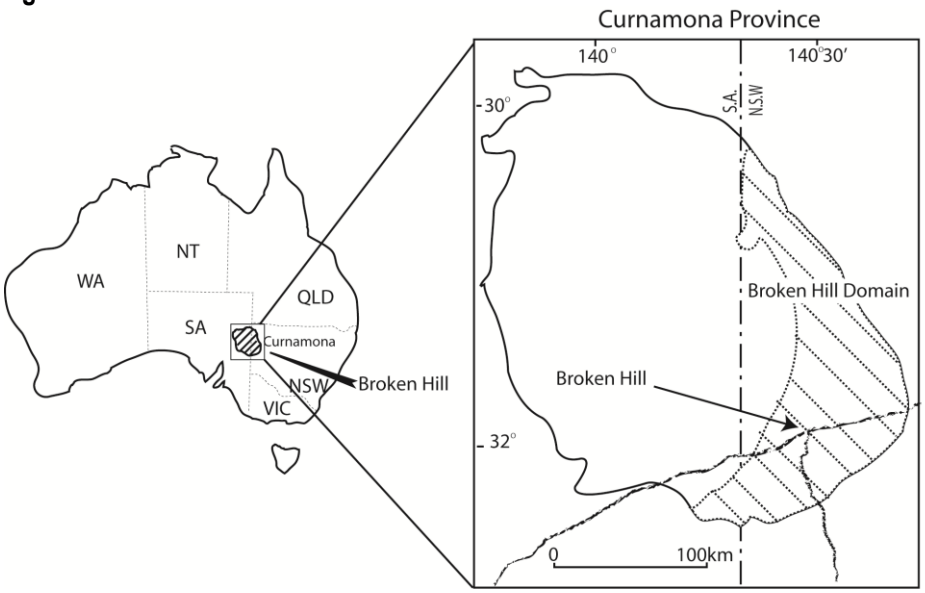
Curnamona Province
140°
140°30′
30°
32°
S.A.
N.S.W
WA
NT
QLD
SA
Curnamona
NSW
VIC
Broken Hill
Broken Hill Domain
Broken Hill
0
100km

Figure 1b.

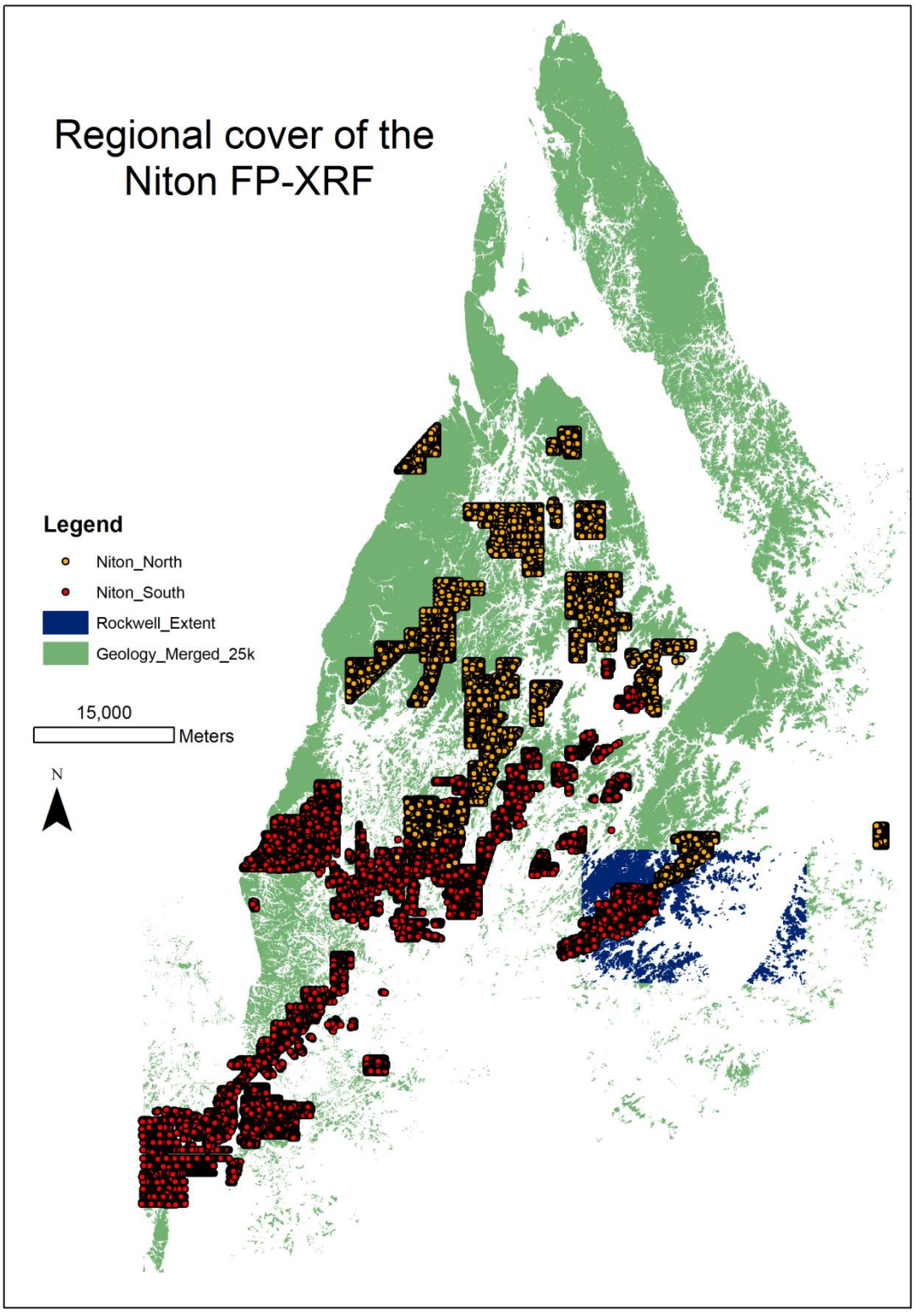
Regional cover of the
Niton FP-XRF
Legend
Niton_North
Niton_South
Rockwell_Extent
Geology_Merged_25k
15,000
Meters
N

Figure 2.

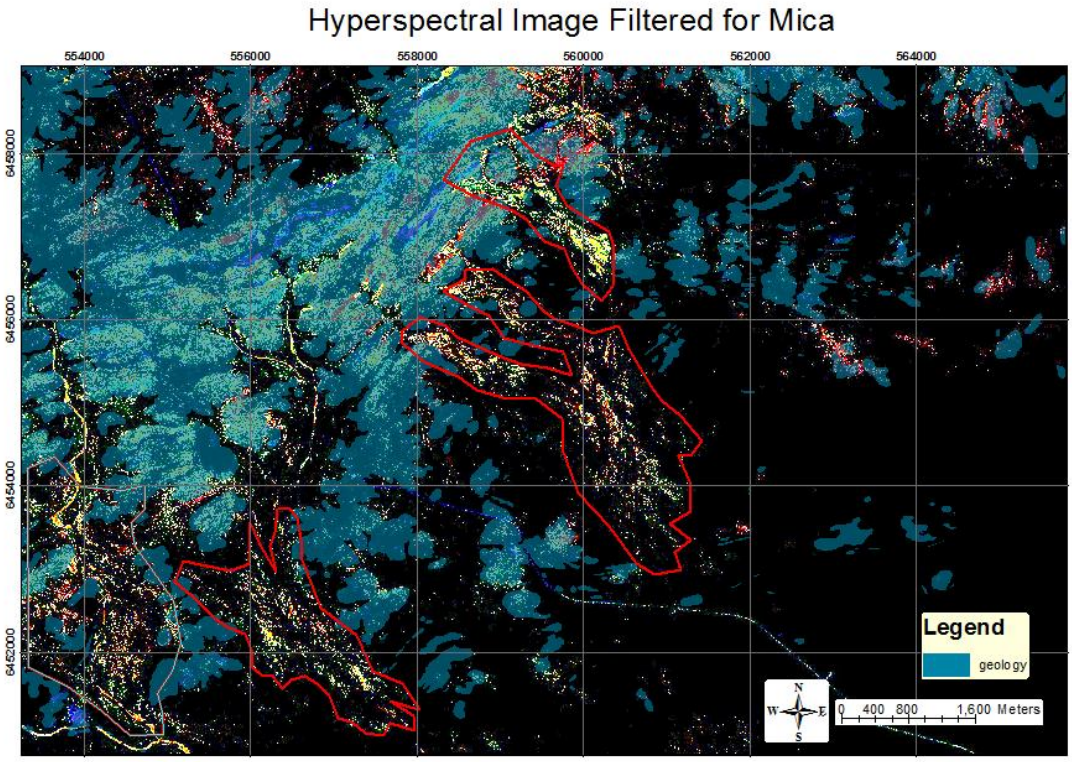
Hyperspectral Image Filtered for Mica
554000
556000
558000
560000
562000
564000
6458000
6456000
6454000
6452000
Legend
geology
N
W
E
S
0 400 800 1,600 Meters

Figure 3.

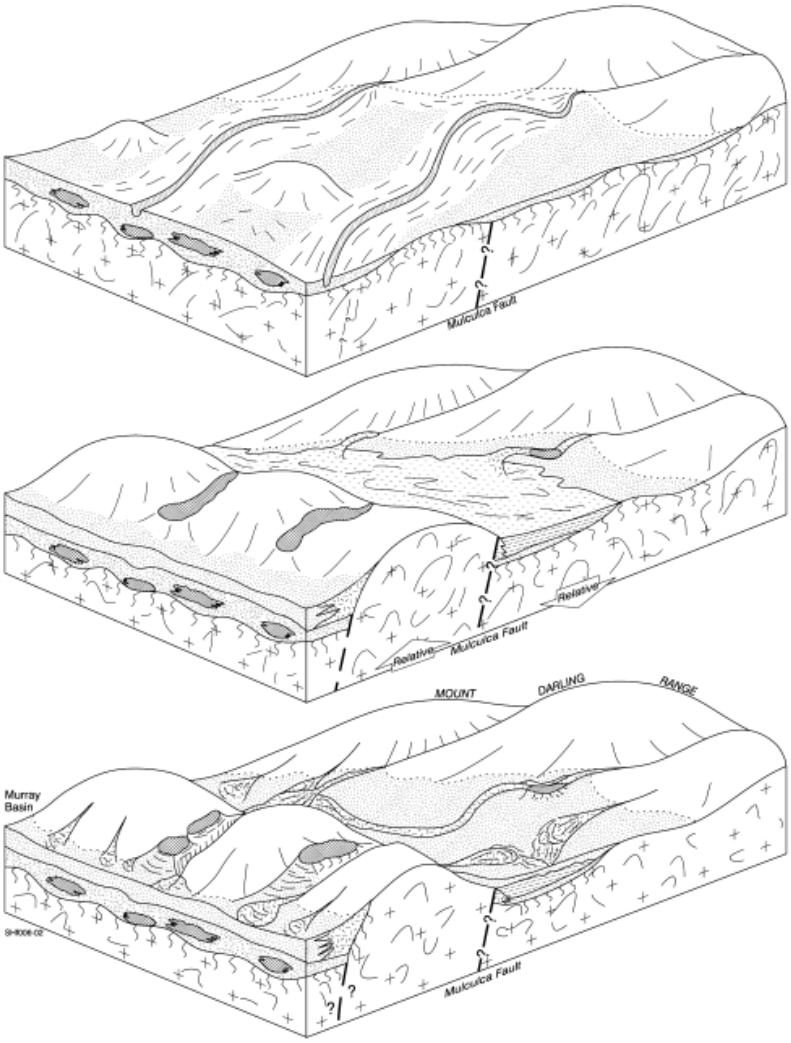
Mulculca Fault
Relative
Mulcuica Fault
Relative
MOUNT
DARLING
RANGE
Murray
Basin
Mulcuica Fault

Figure 5.

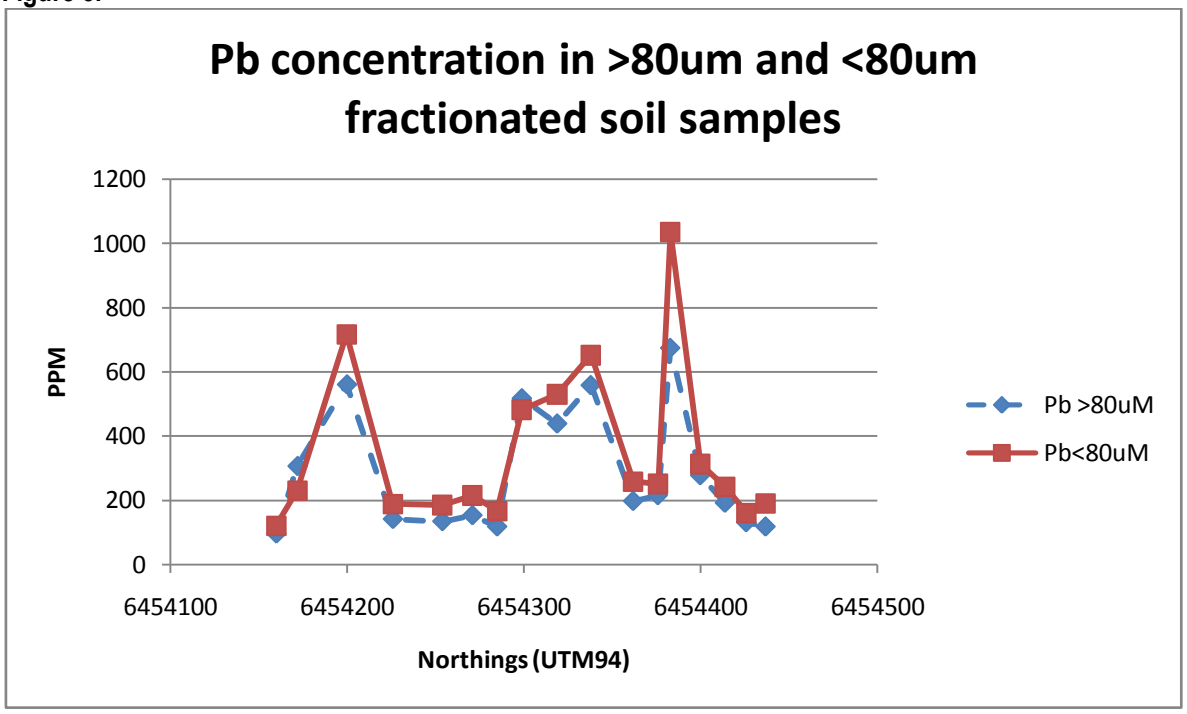
Pb concentration in >80um and <80um fractionated soil samples
1200
1000
800
600
400
200
0
PPM
6454100
6454200
6454300
6454400
6454500
Northings (UTM94)
Pb >80uM
Pb<80uM

Figure 6.

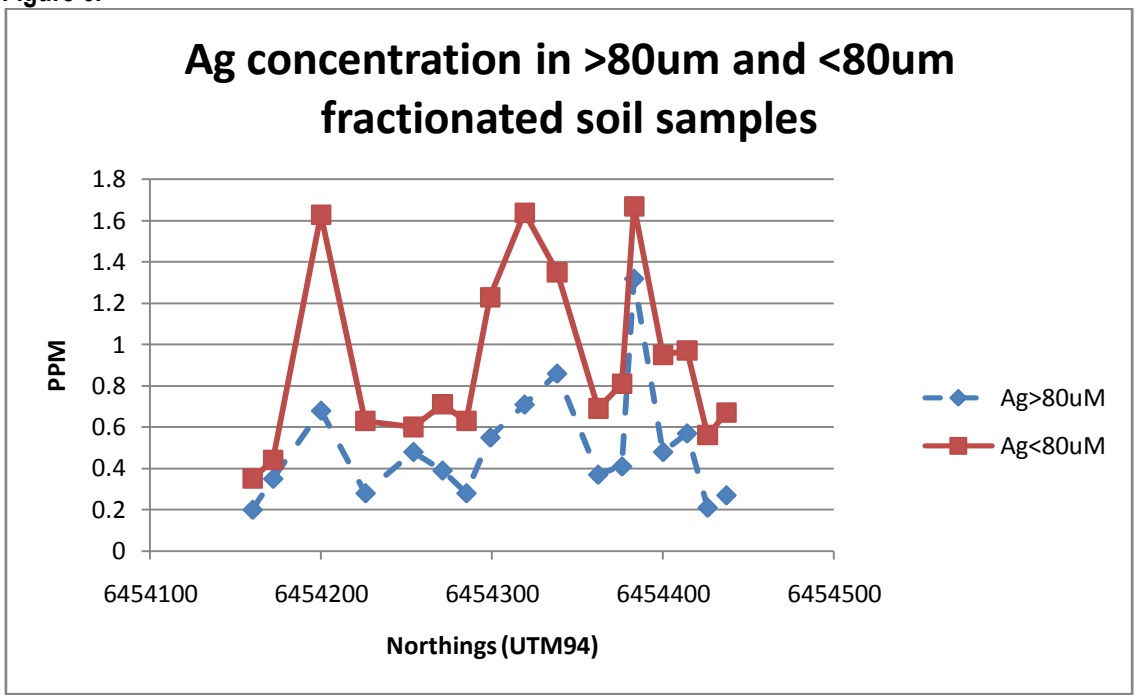
Ag concentration in >80um and <80um fractionated soil samples
PPM
1.8
1.6
1.4
1.2
1
0.8
0.6
0.4
0.2
0
6454100
6454200
6454300
6454400
6454500
Northings (UTM94)
Ag>80uM
Ag<80uM

Figure 7.

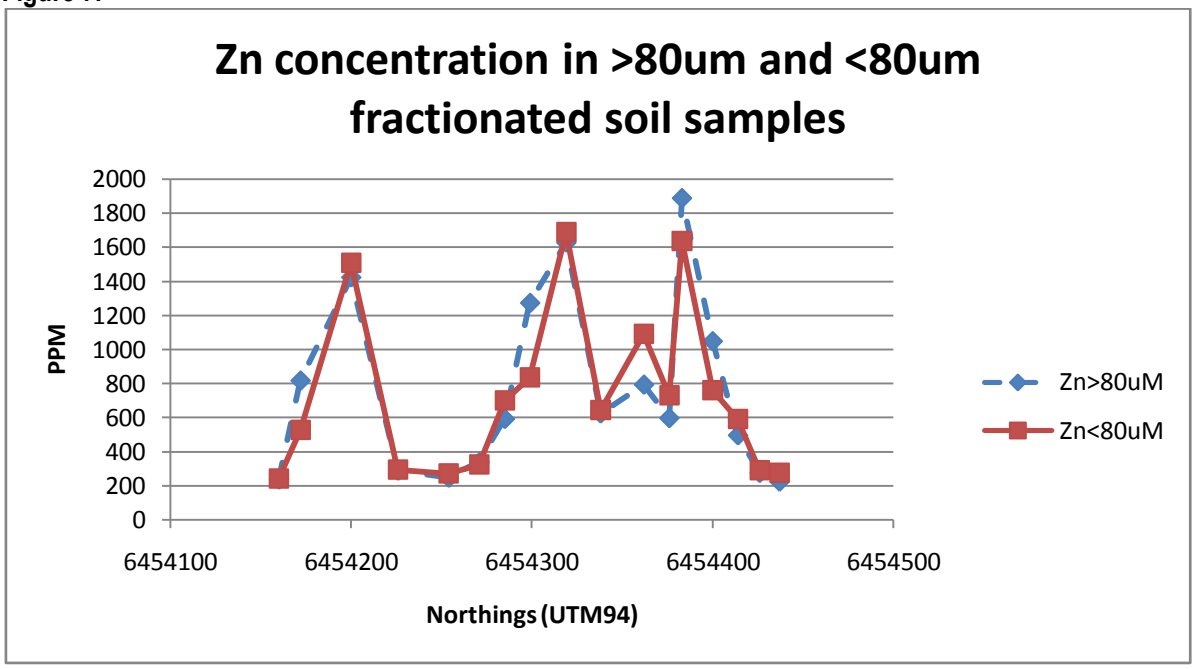
Zn concentration in >80um and <80um fractionated soil samples
PPM
2000
1800
1600
1400
1200
1000
800
600
400
200
0
6454100
6454200
6454300
6454400
6454500
Northings (UTM94)
Zn>80uM
Zn<80uM

Figure 8.

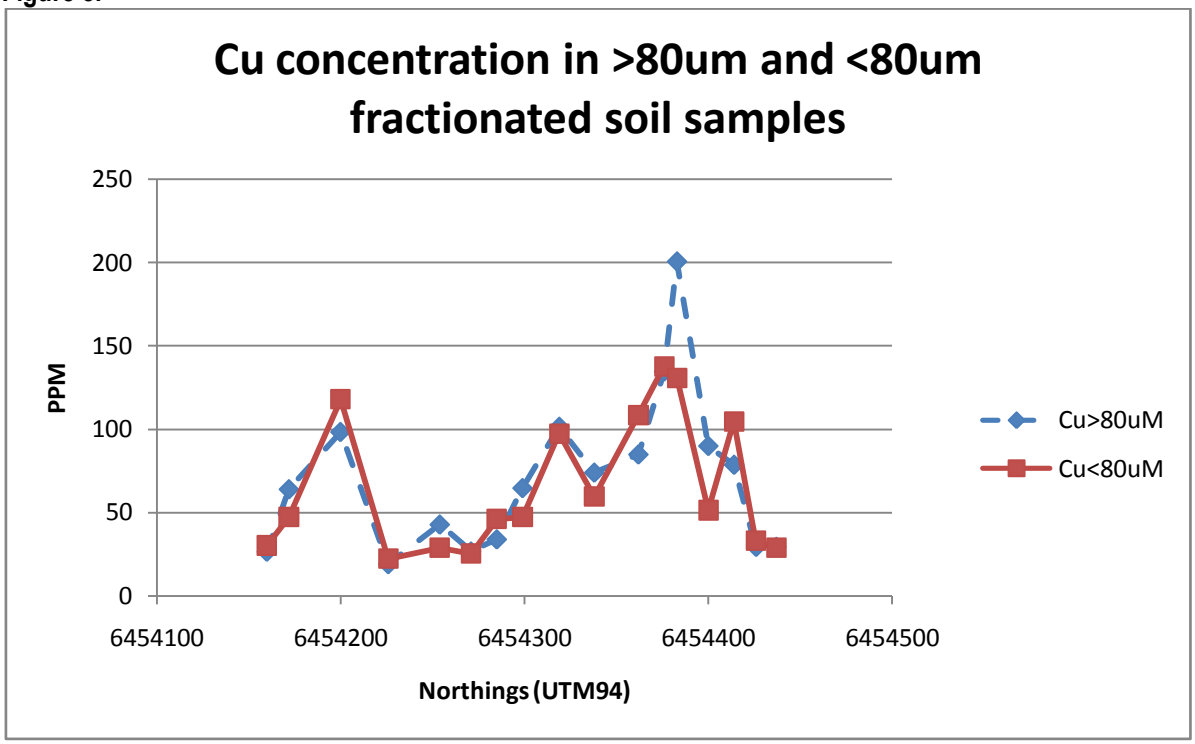
Cu concentration in >80um and <80um fractionated soil samples
250
200
150
100
50
0
PPM
6454100
6454200
6454300
6454400
6454500
Northings (UTM94)
Cu>80uM
Cu<80uM

Figure 9.

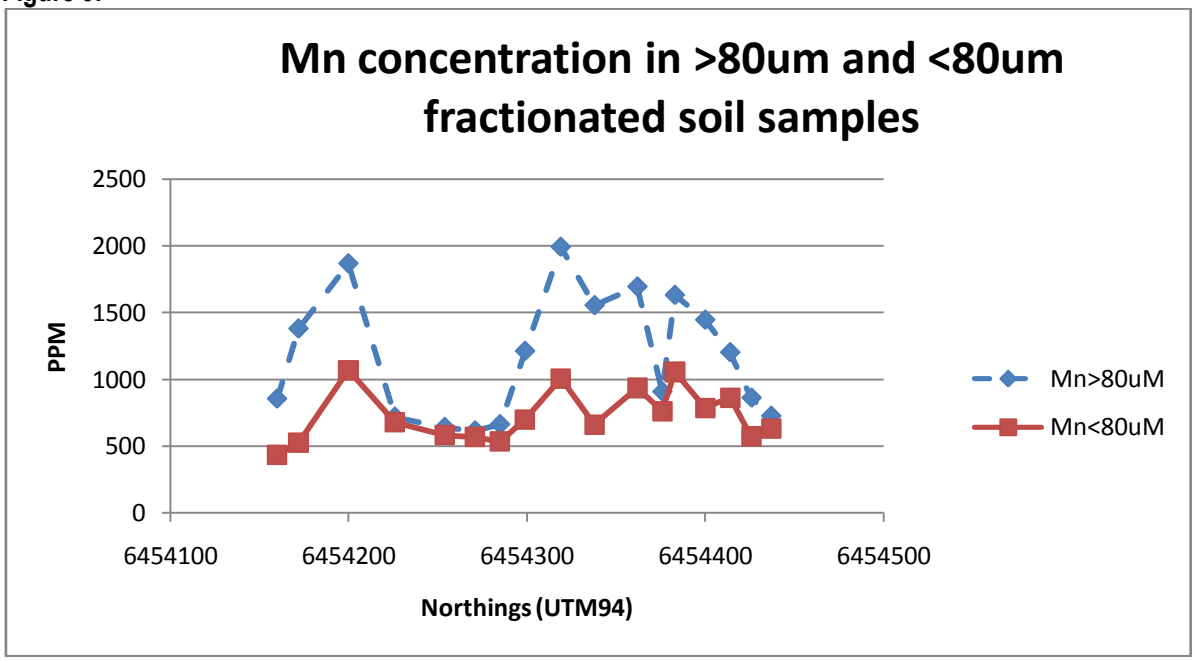
Mn concentration in >80um and <80um fractionated soil samples
2500
2000
1500
1000
500
0
PPM
6454100
6454200
6454300
6454400
6454500
Northings (UTM94)
Mn>80uM
Mn<80uM

Figure 10.

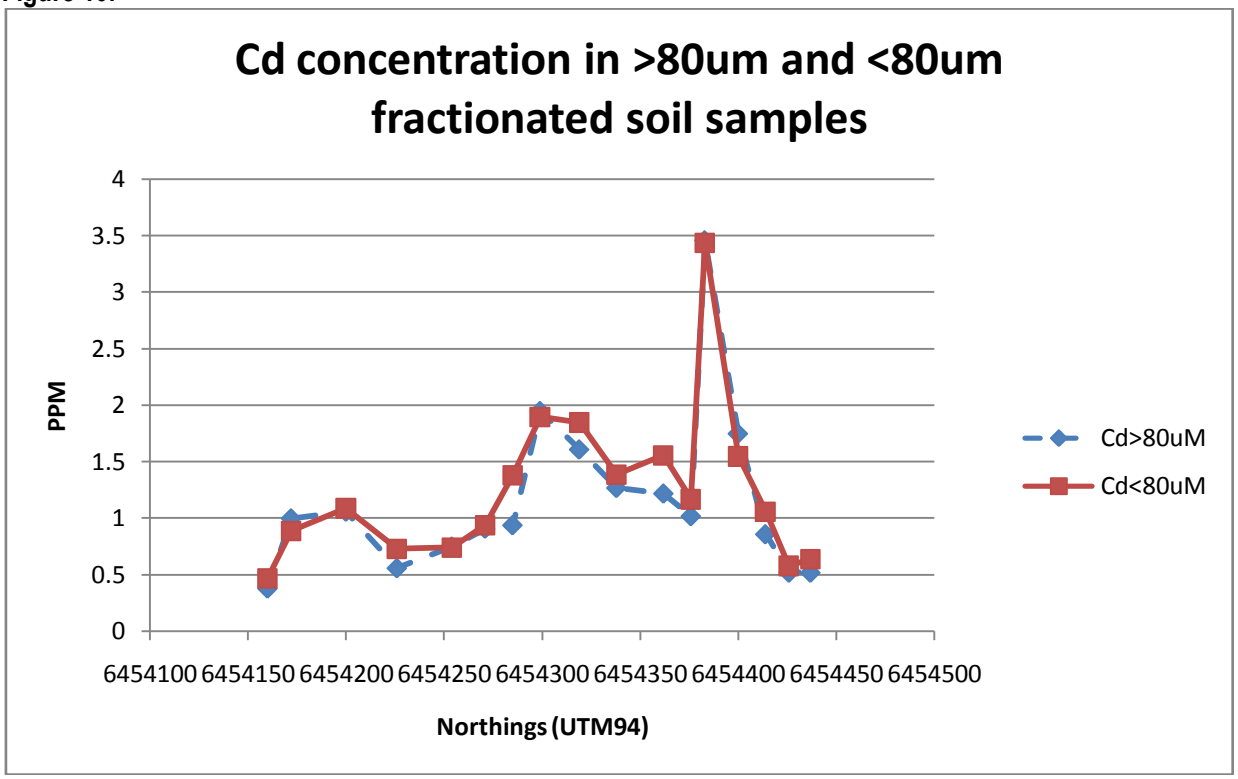
Cd concentration in >80um and <80um fractionated soil samples
PPM
4
3.5
3
2.5
2
1.5
1
0.5
0
6454100 6454150 6454200 6454250 6454300 6454350 6454400 6454450 6454500
Northings (UTM94)
Cd>80uM
Cd<80uM

Figure 11.

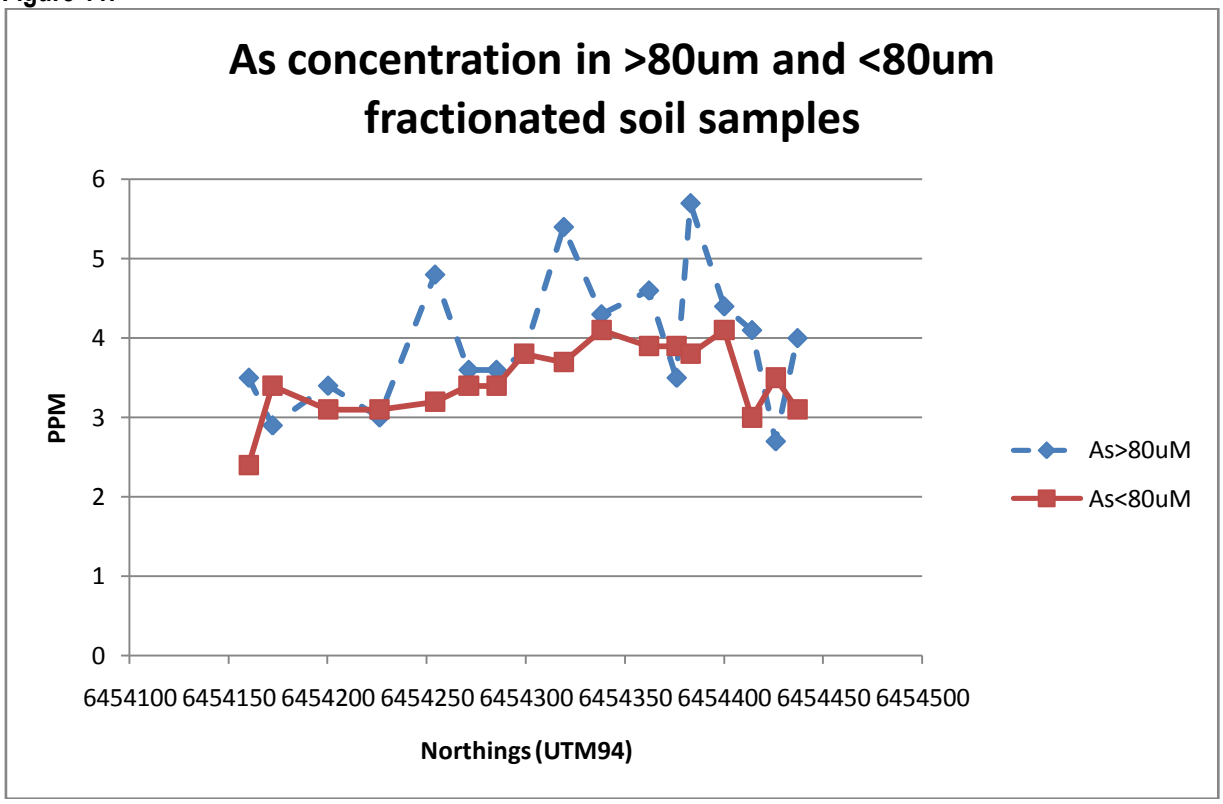
As concentration in >80um and <80um fractionated soil samples
PPM
0
1
2
3
4
5
6
6454100 6454150 6454200 6454250 6454300 6454350 6454400 6454450 6454500
Northings (UTM94)
As>80uM
As<80uM

Figure 12.

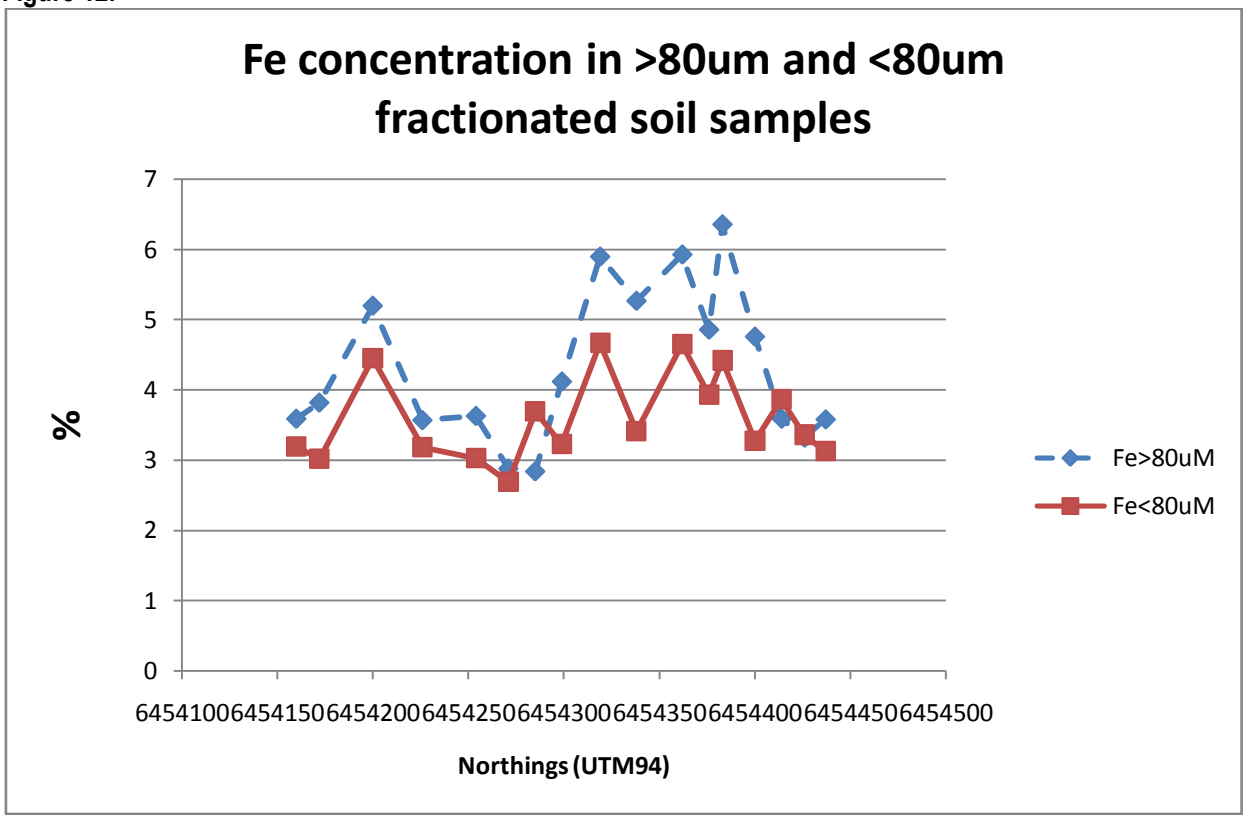
Fe concentration in >80um and <80um fractionated soil samples
%
7
6
5
4
3
2
1
0
6454100
6454150
6454200
6454250
6454300
6454350
6454400
6454450
6454500
Northings (UTM94)
Fe>80uM
Fe<80uM

Figure 13.

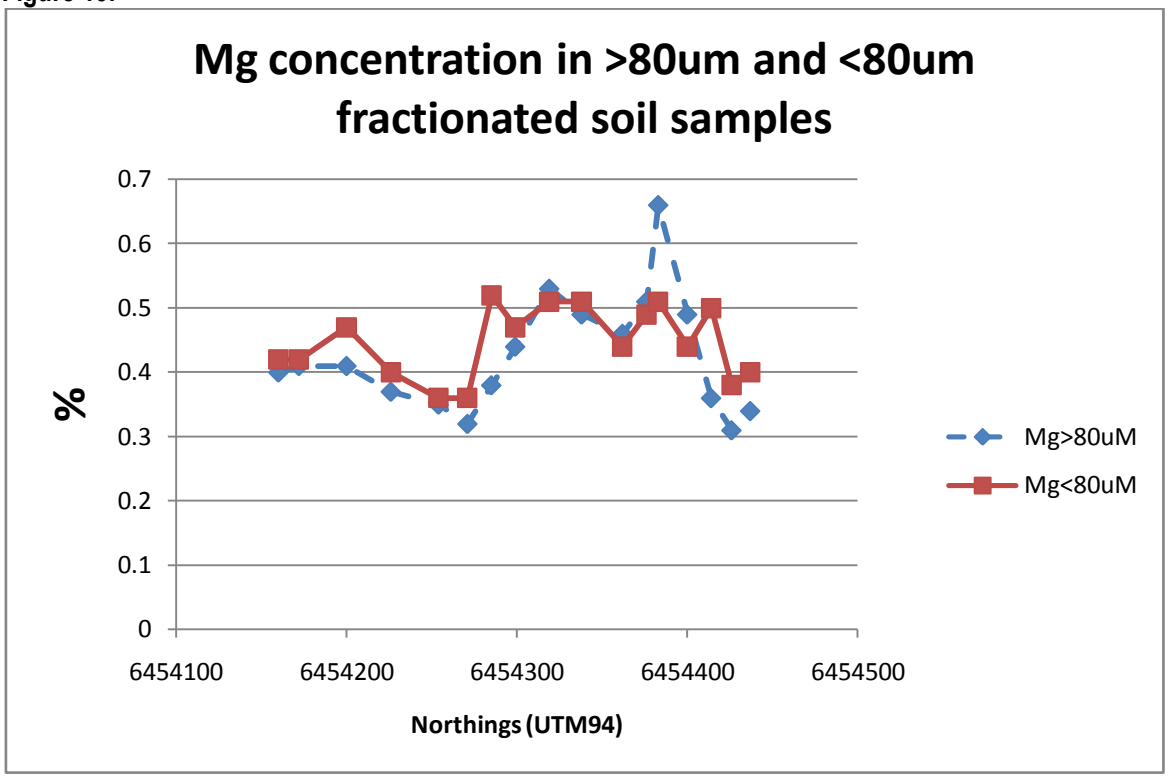
Mg concentration in >80um and <80um fractionated soil samples
0.7
0.6
0.5
0.4
0.3
0.2
0.1
0
%
6454100
6454200
6454300
6454400
6454500
Northings (UTM94)
Mg>80uM
Mg<80uM

Figure 14.

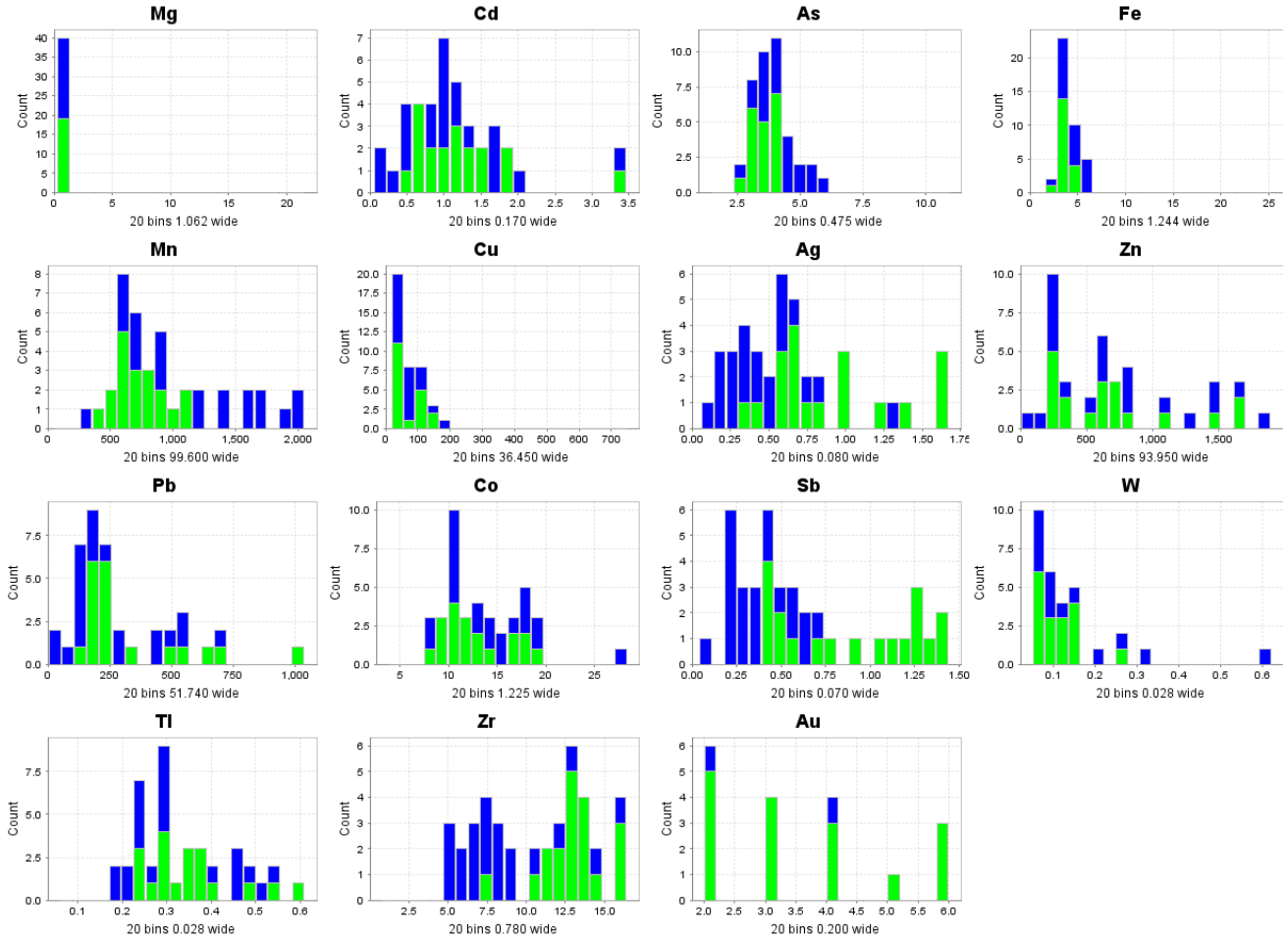
Mg
Count
20 bins 1.062 wide
Cd
Count
20 bins 0.170 wide
As
Count
20 bins 0.475 wide
Fe
Count
20 bins 1.244 wide
Mn
Count
20 bins 99.600 wide
Cu
Count
20 bins 36.450 wide
Ag
Count
20 bins 0.080 wide
Zn
Count
20 bins 93.950 wide
Pb
Count
20 bins 51.740 wide
Co
Count
20 bins 1.225 wide
Sb
Count
20 bins 0.070 wide
W
Count
20 bins 0.028 wide
Tl
Count
20 bins 0.028 wide
Zr
Count
20 bins 0.780 wide
Au
Count
20 bins 0.200 wide

Figure 15.

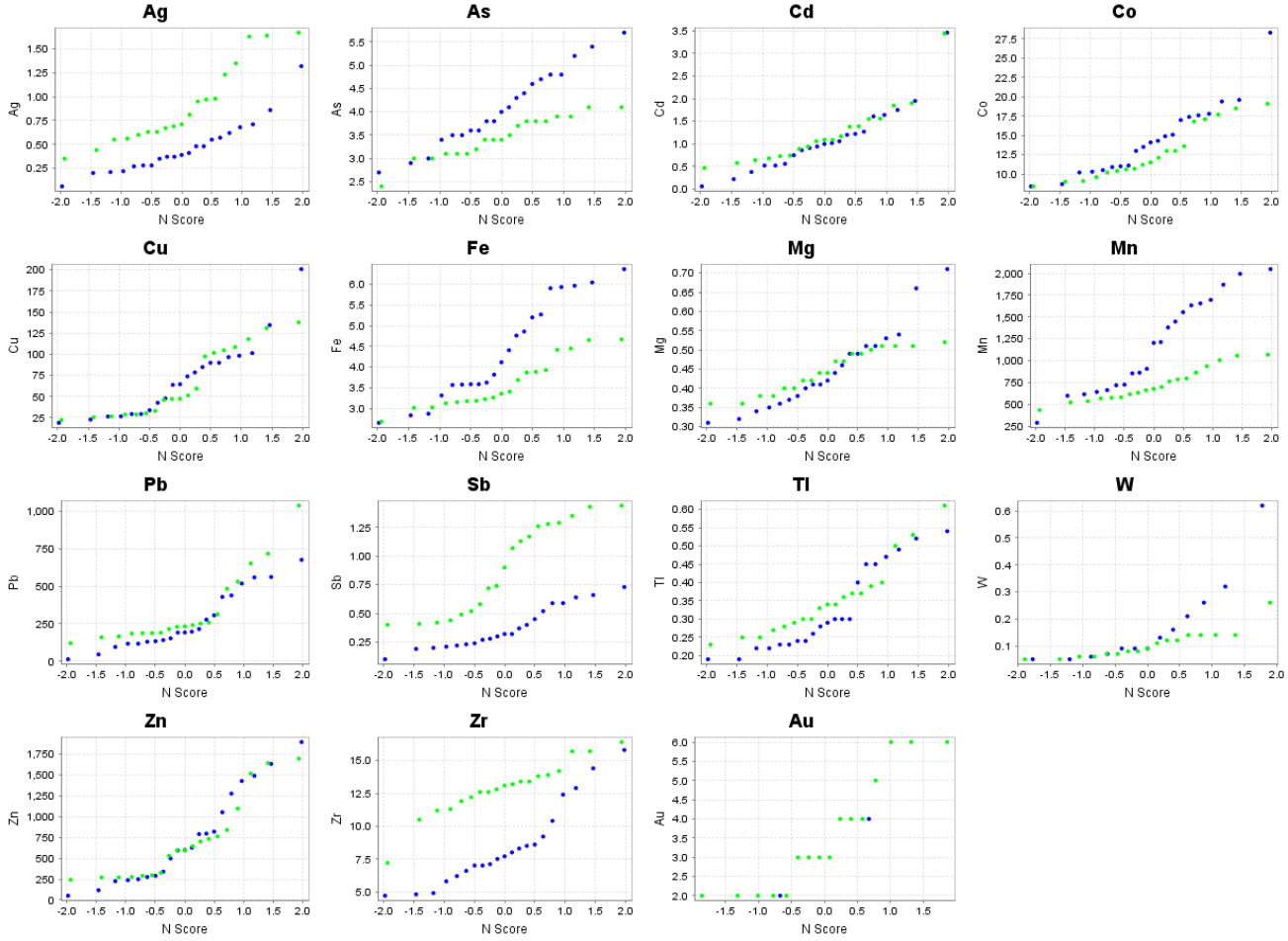

Figure 16a.

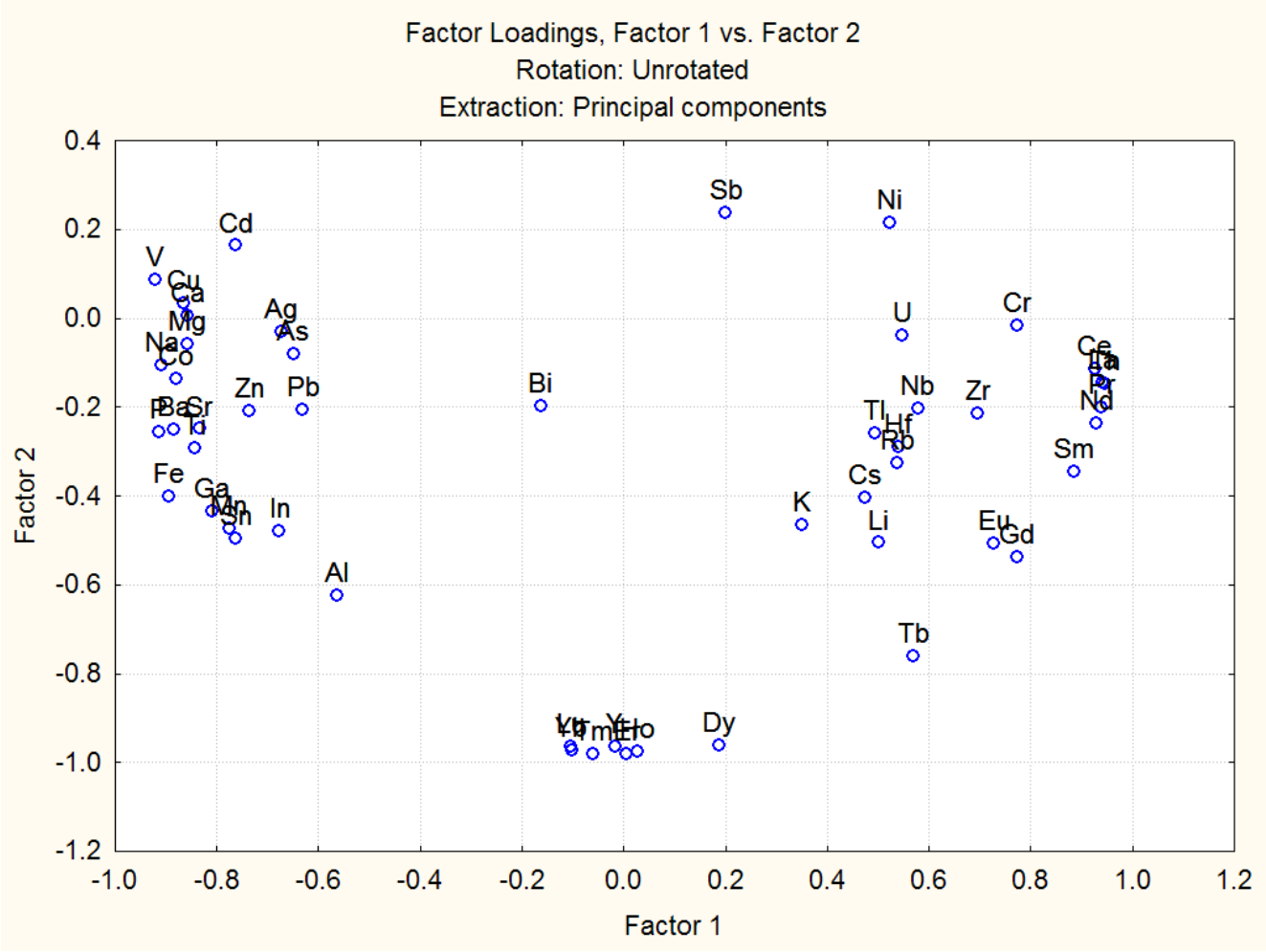
Factor Loadings, Factor 1 vs. Factor 2
Rotation: Unrotated
Extraction: Principal components
Factor 2
Factor 1
0.4
0.2
0.0
-0.2
-0.4
-0.6
-0.8
-1.0
-1.2
-1.0
-0.8
-0.6
-0.4
-0.2
0.0
0.2
0.4
0.6
0.8
1.0
1.2
Sb
Ni
Cd
V
Cu
Ag
As
U
Cr
Co
Bi
Zn
Pb
Nb
Zr
Sr
Tl
Hf
Rb
Sm
Fe
Cs
Ga
K
In
Li
Eu
Gd
Al
Tb
Dy
Ho

Figure 16b.

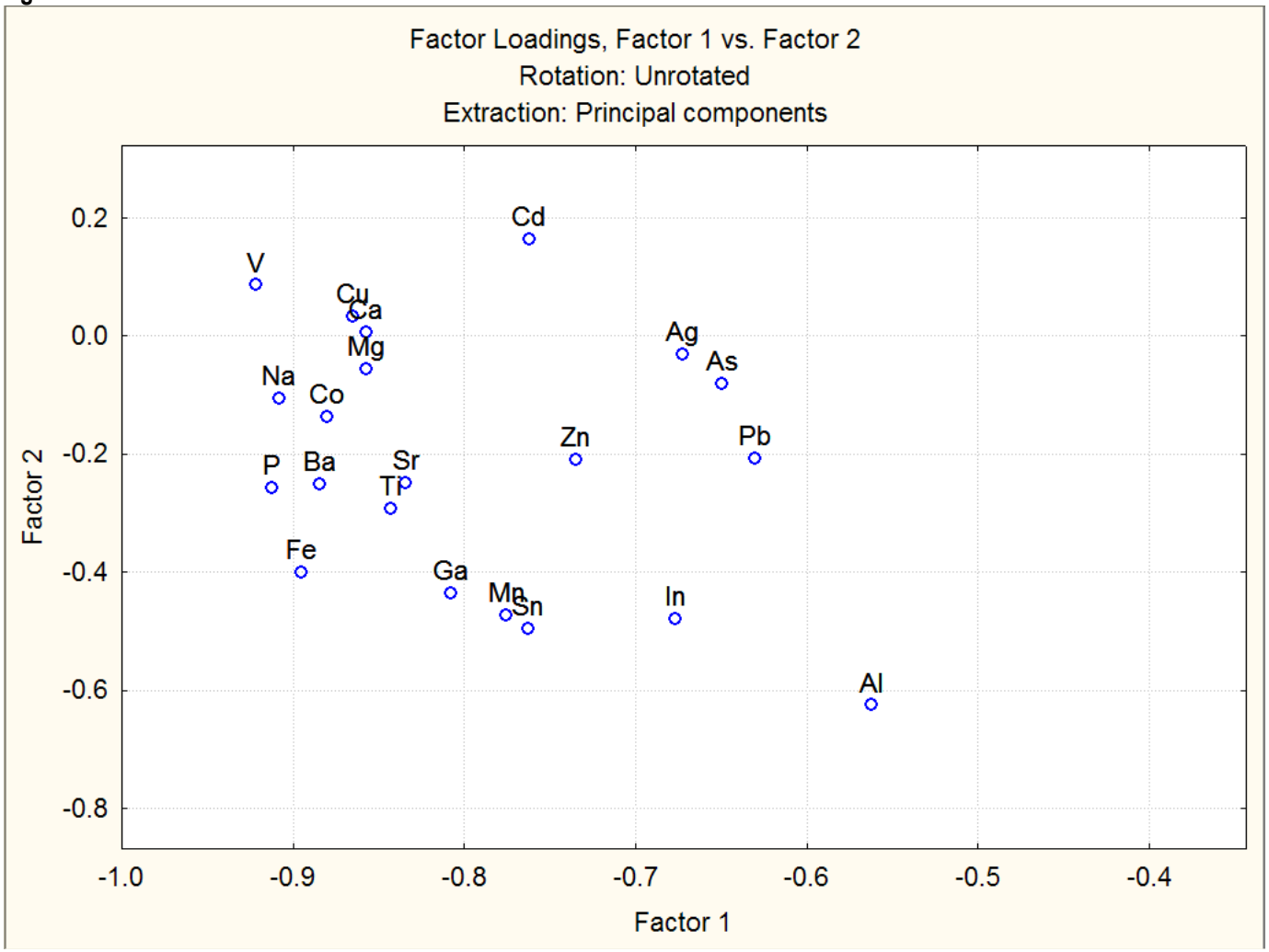
Factor Loadings, Factor 1 vs. Factor 2
Rotation: Unrotated
Extraction: Principal components
Cd
V
Cu
Ca
Mg
Ag
As
Na
Co
Zn
Pb
P
Ba
Sr
Ti
Fe
Ga
Mn
Sn
In
Al
0.2
0.0
-0.2
-0.4
-0.6
-0.8
Factor 2
-1.0
-0.9
-0.8
-0.7
-0.6
-0.5
-0.4
Factor 1

Figure 17a.

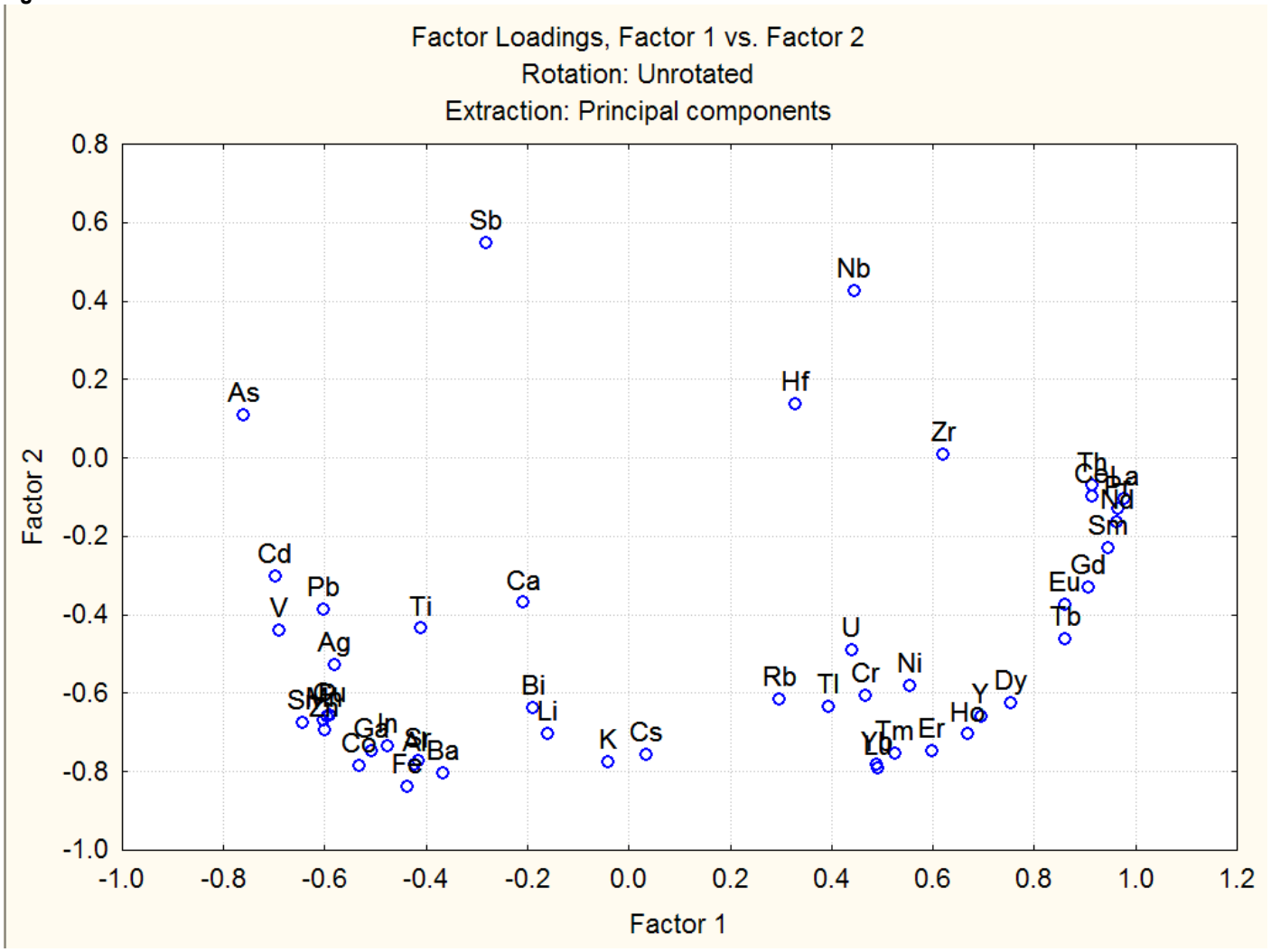
Factor Loadings, Factor 1 vs. Factor 2
Rotation: Unrotated
Extraction: Principal components
Factor 2
Factor 1
0.8
0.6
0.4
0.2
0.0
-0.2
-0.4
-0.6
-0.8
-1.0
-1.0
-0.8
-0.6
-0.4
-0.2
0.0
0.2
0.4
0.6
0.8
1.0
1.2
Sb
Nb
As
Hf
Zr
Th
La
Nd
Sm
Gd
Eu
Tb
Cd
Pb
V
Ti
Ca
Ag
U
Rb
Tl
Cr
Ni
Dy
Y
Ho
Bi
Li
K
Cs
Tm
Er
Ba
Fe

Figure 17b.

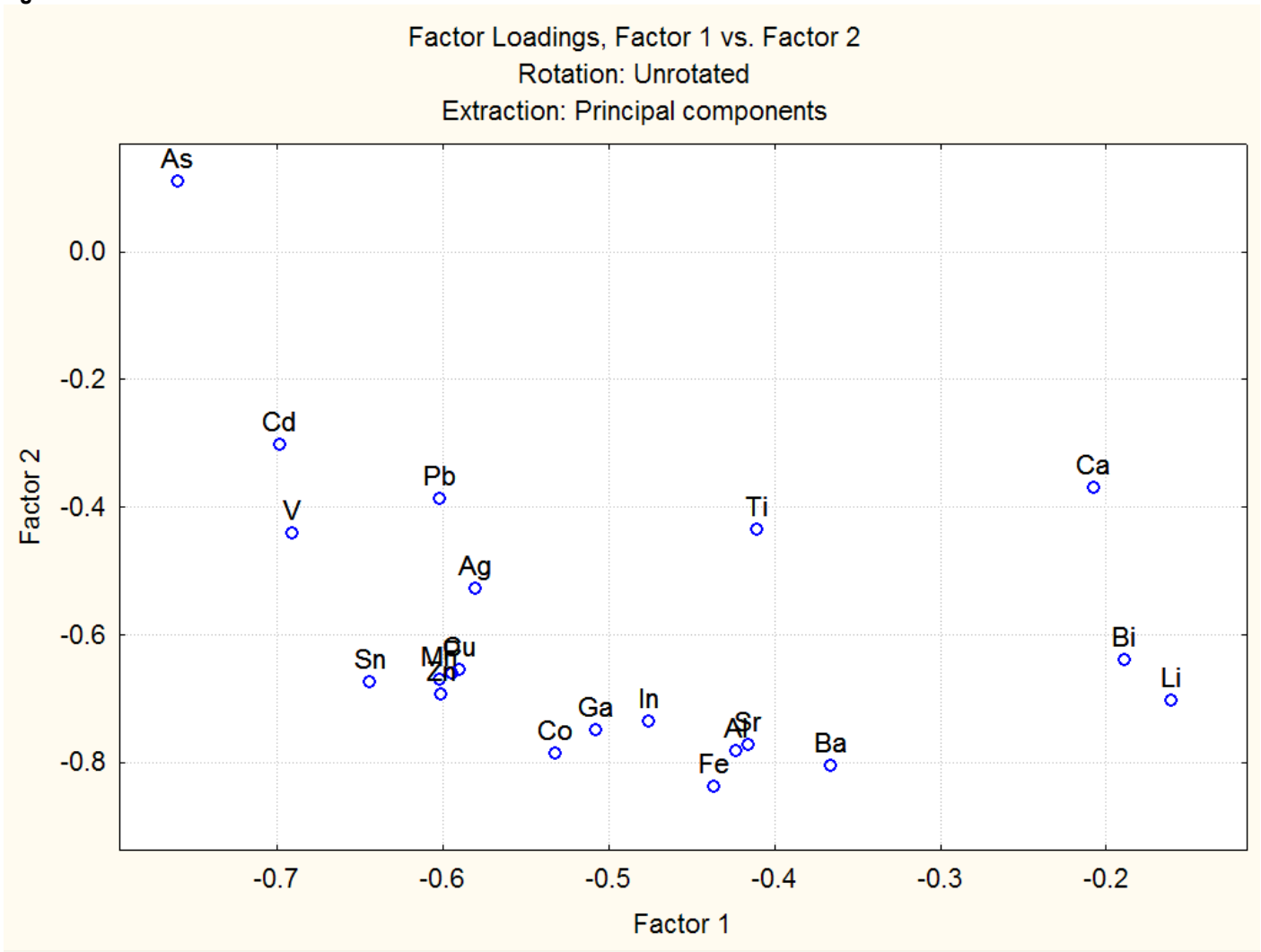
Factor Loadings, Factor 1 vs. Factor 2
Rotation: Unrotated
Extraction: Principal components
As
Cd
Pb
V
Ag
Ti
Ca
Bi
Li
Sn
Mn
Cu
Zn
Ga
In
Co
Al
Sr
Ba
Fe
0.0
-0.2
-0.4
-0.6
-0.8
Factor 2
-0.7
-0.6
-0.5
-0.4
-0.3
-0.2
Factor 1

Figure 18.

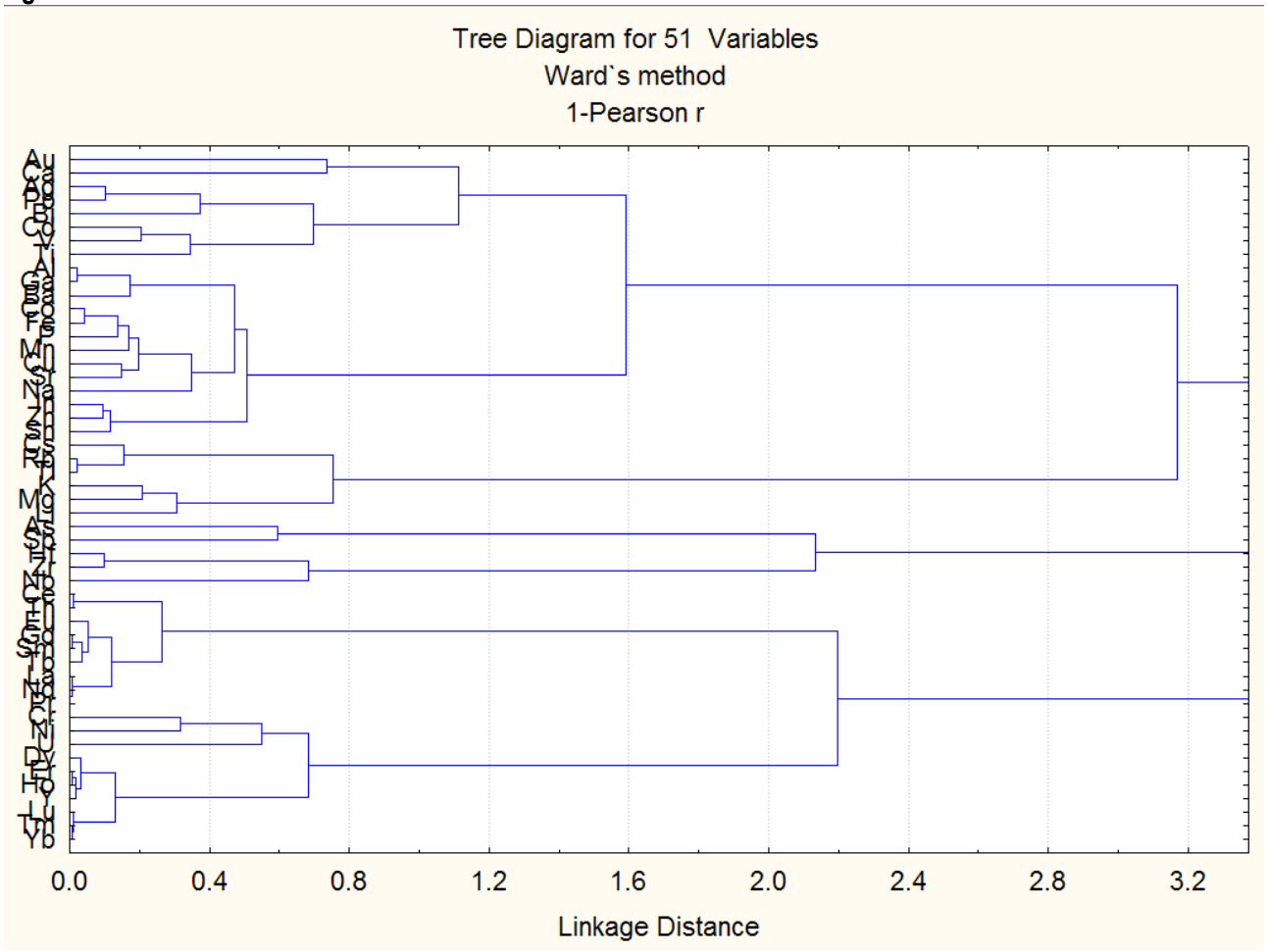
Tree Diagram for 51 Variables
Ward`s method
1-Pearson r
0.0
0.4
0.8
1.2
1.6
2.0
2.4
2.8
3.2
Linkage Distance

Figure 19.

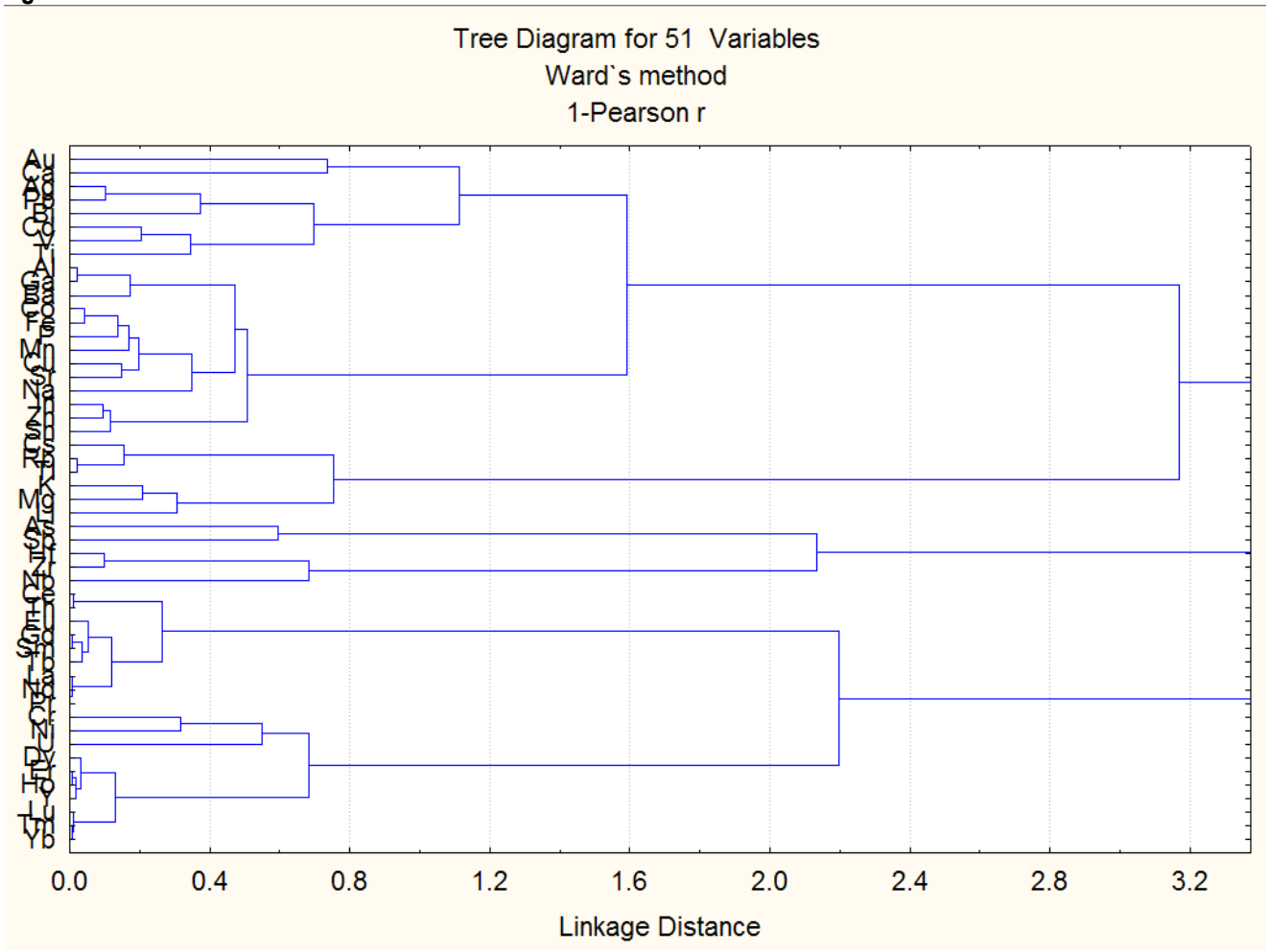
Tree Diagram for 51 Variables
Ward`s method
1-Pearson r
0.0
0.4
0.8
1.2
1.6
2.0
2.4
2.8
3.2
Linkage Distance

Figure 20.

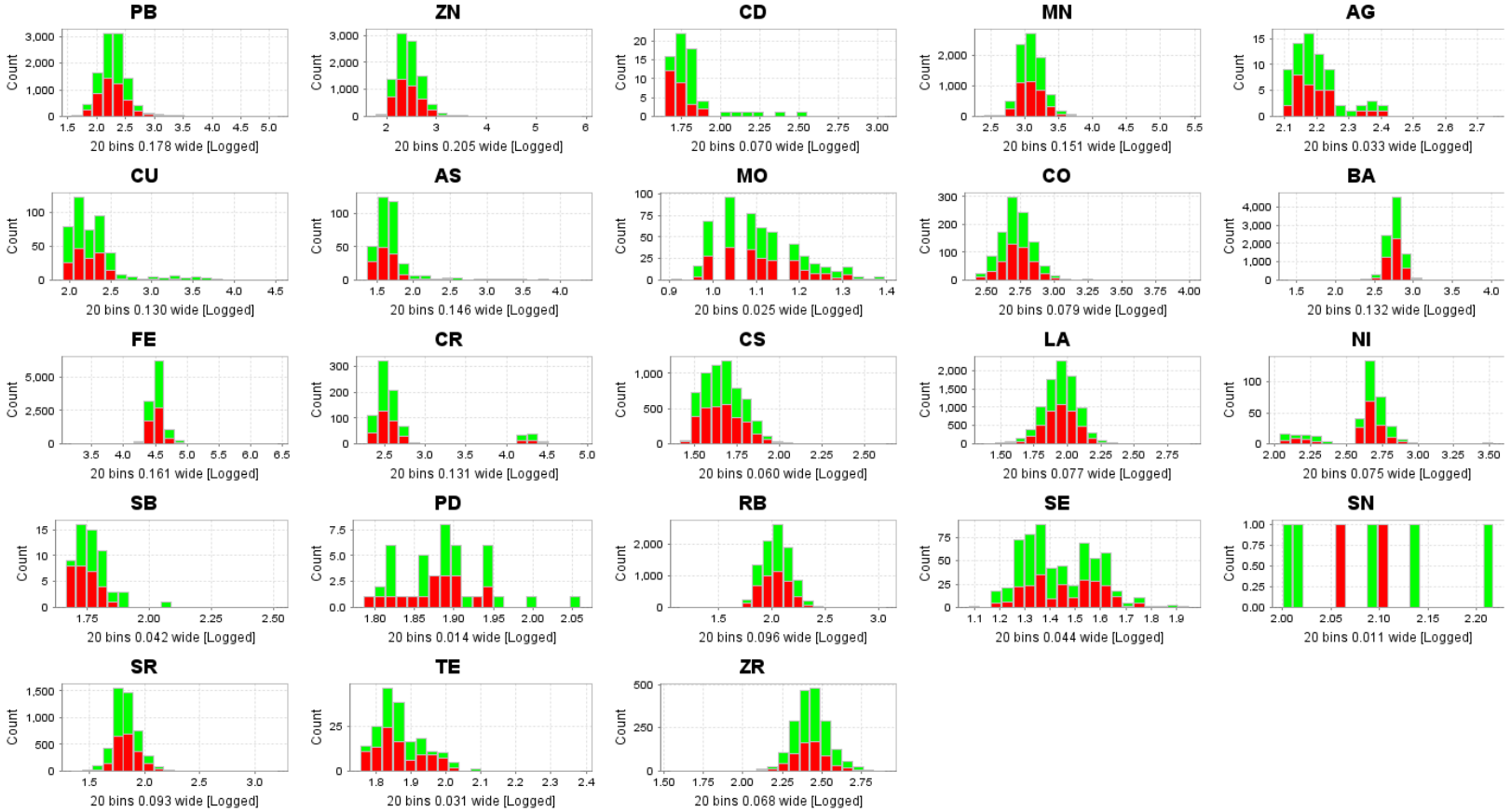
PB
Count
20 bins 0.178 wide [Logged]
ZN
Count
20 bins 0.205 wide [Logged]
CD
Count
20 bins 0.070 wide [Logged]
MN
Count
20 bins 0.151 wide [Logged]
AG
Count
20 bins 0.033 wide [Logged]
CU
Count
20 bins 0.130 wide [Logged]
AS
Count
20 bins 0.146 wide [Logged]
MO
Count
20 bins 0.025 wide [Logged]
CO
Count
20 bins 0.079 wide [Logged]
BA
Count
20 bins 0.132 wide [Logged]
FE
Count
20 bins 0.161 wide [Logged]
CR
Count
20 bins 0.131 wide [Logged]
CS
Count
20 bins 0.060 wide [Logged]
LA
Count
20 bins 0.077 wide [Logged]
NI
Count
20 bins 0.075 wide [Logged]
SB
Count
20 bins 0.042 wide [Logged]
PD
Count
20 bins 0.014 wide [Logged]
RB
Count
20 bins 0.096 wide [Logged]
SE
Count
20 bins 0.044 wide [Logged]
SN
Count
20 bins 0.011 wide [Logged]
SR
Count
20 bins 0.093 wide [Logged]
TE
Count
20 bins 0.031 wide [Logged]
ZR
Count
20 bins 0.068 wide [Logged]

Figure 21.

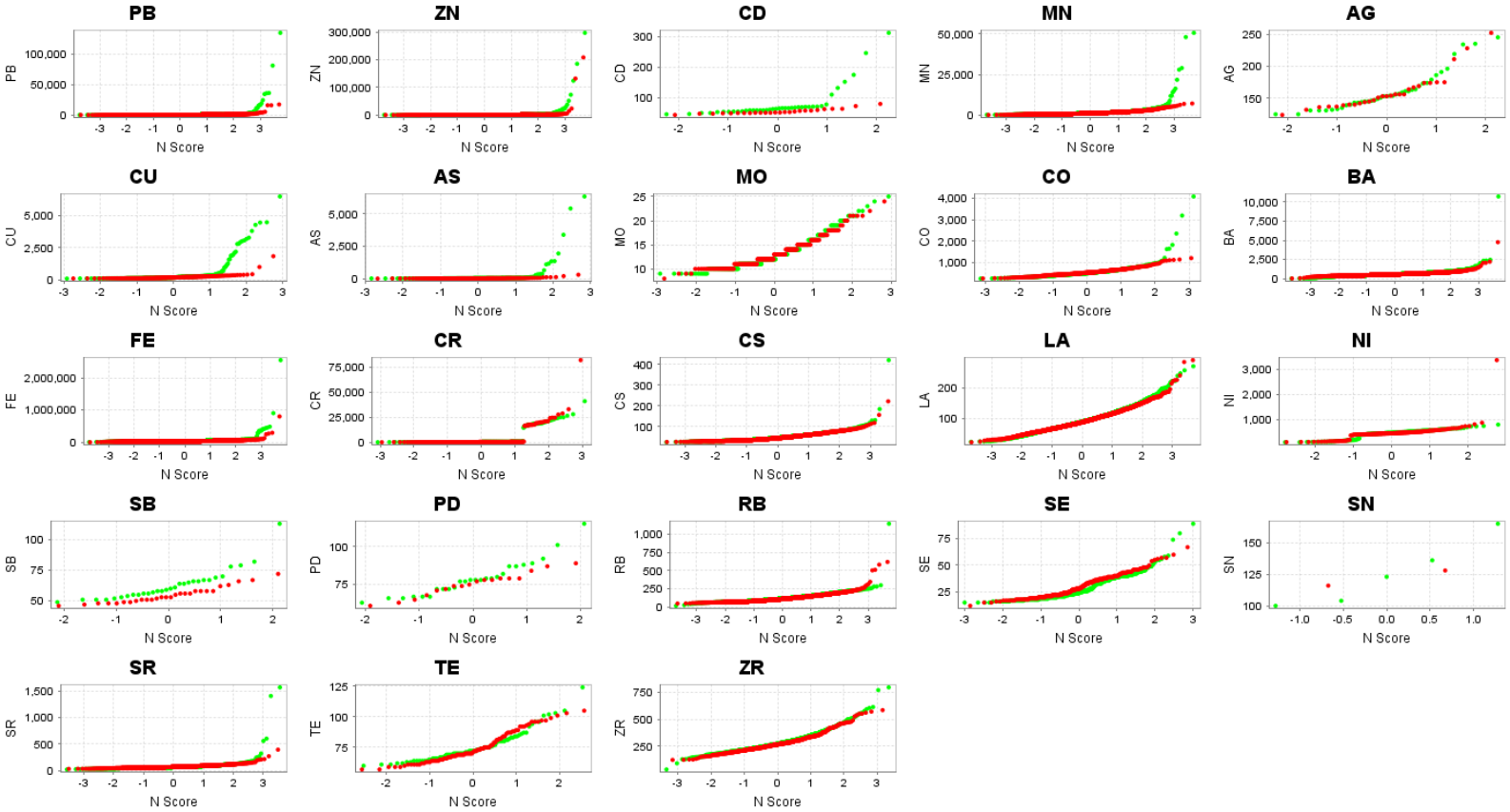
PB
ZN
CD
MN
AG
CU
AS
MO
CO
BA
FE
CR
CS
LA
NI
SB
PD
RB
SE
SN
SR
TE
ZR
N Score

Figure 22.

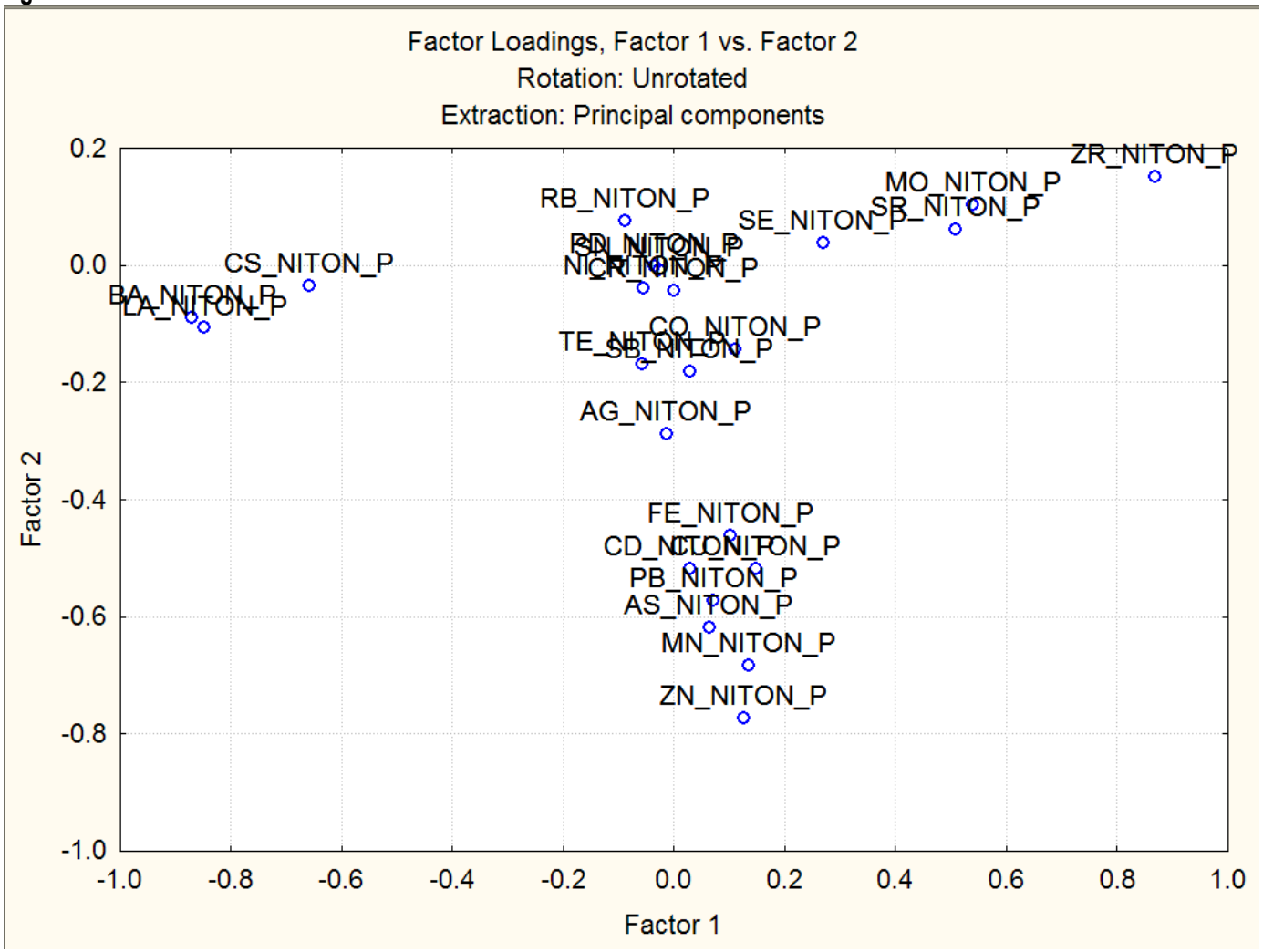
Factor Loadings, Factor 1 vs. Factor 2
Rotation: Unrotated
Extraction: Principal components
ZR_NITON_P
MO_NITON_P
SB_NITON_P
RB_NITON_P
SE_NITON_P
CS_NITON_P
BA_NITON_P
LA_NITON_P
CO_NITON_P
AG_NITON_P
FE_NITON_P
PB_NITON_P
AS_NITON_P
MN_NITON_P
ZN_NITON_P
Factor 2
Factor 1
0.2
0.0
-0.2
-0.4
-0.6
-0.8
-1.0
-1.0
-0.8
-0.6
-0.4
-0.2
0.0
0.2
0.4
0.6
0.8
1.0

Figure 23.

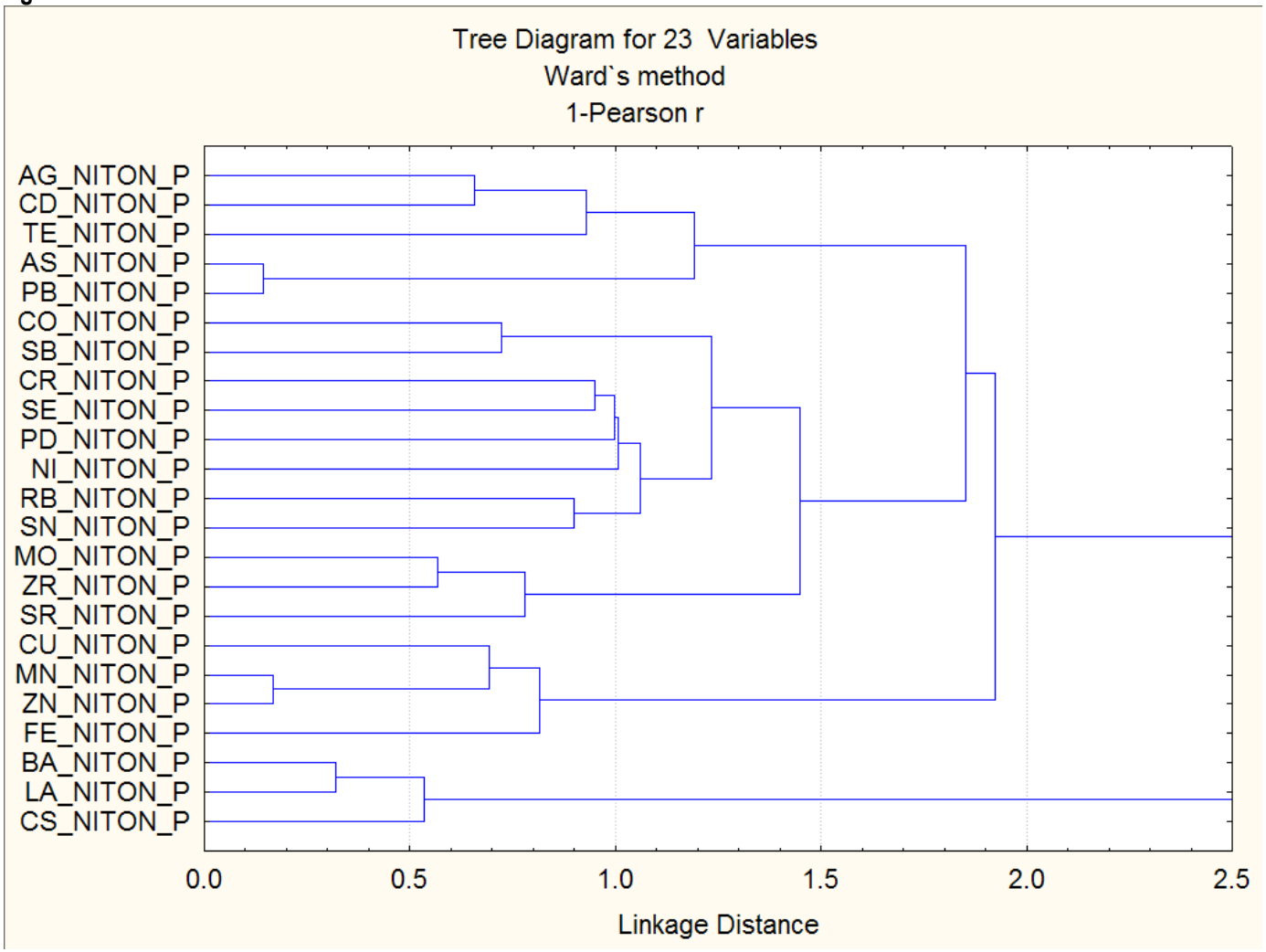
Tree Diagram for 23 Variables
Ward`s method
1-Pearson r
AG_NITON_P
CD_NITON_P
TE_NITON_P
AS_NITON_P
PB_NITON_P
CO_NITON_P
SB_NITON_P
CR_NITON_P
SE_NITON_P
PD_NITON_P
NI_NITON_P
RB_NITON_P
SN_NITON_P
MO_NITON_P
ZR_NITON_P
SR_NITON_P
CU_NITON_P
MN_NITON_P
ZN_NITON_P
FE_NITON_P
BA_NITON_P
LA_NITON_P
CS_NITON_P
0.0
0.5
1.0
1.5
2.0
2.5
Linkage Distance

Figure 24.

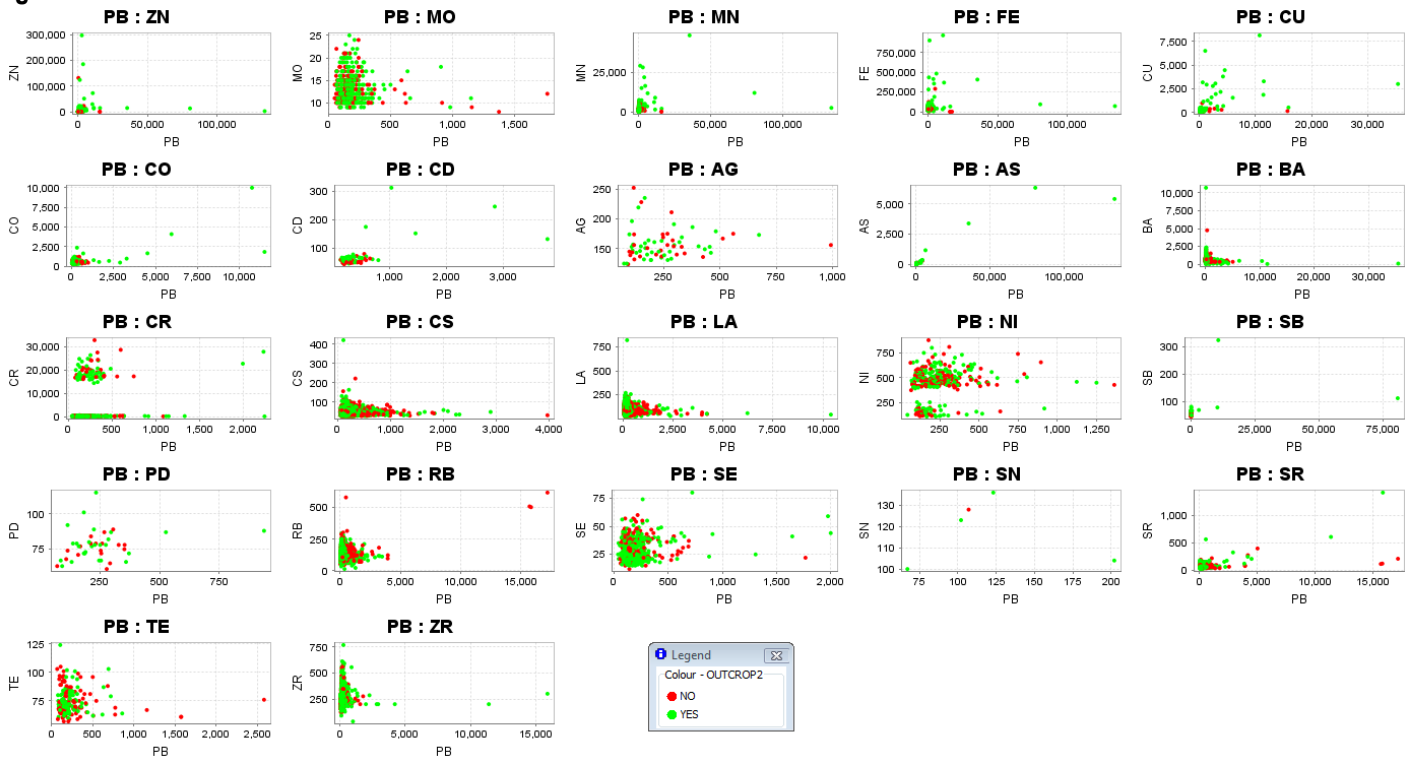
PB : ZN
PB : MO
PB : MN
PB : FE
PB : CU
PB : CO
PB : CD
PB : AG
PB : AS
PB : BA
PB : CR
PB : CS
PB : LA
PB : NI
PB : SB
PB : PD
PB : RB
PB : SE
PB : SN
PB : SR
PB : TE
PB : ZR
PB
Legend
Colour - OUTCROP2
NO
YES

Figure 25.

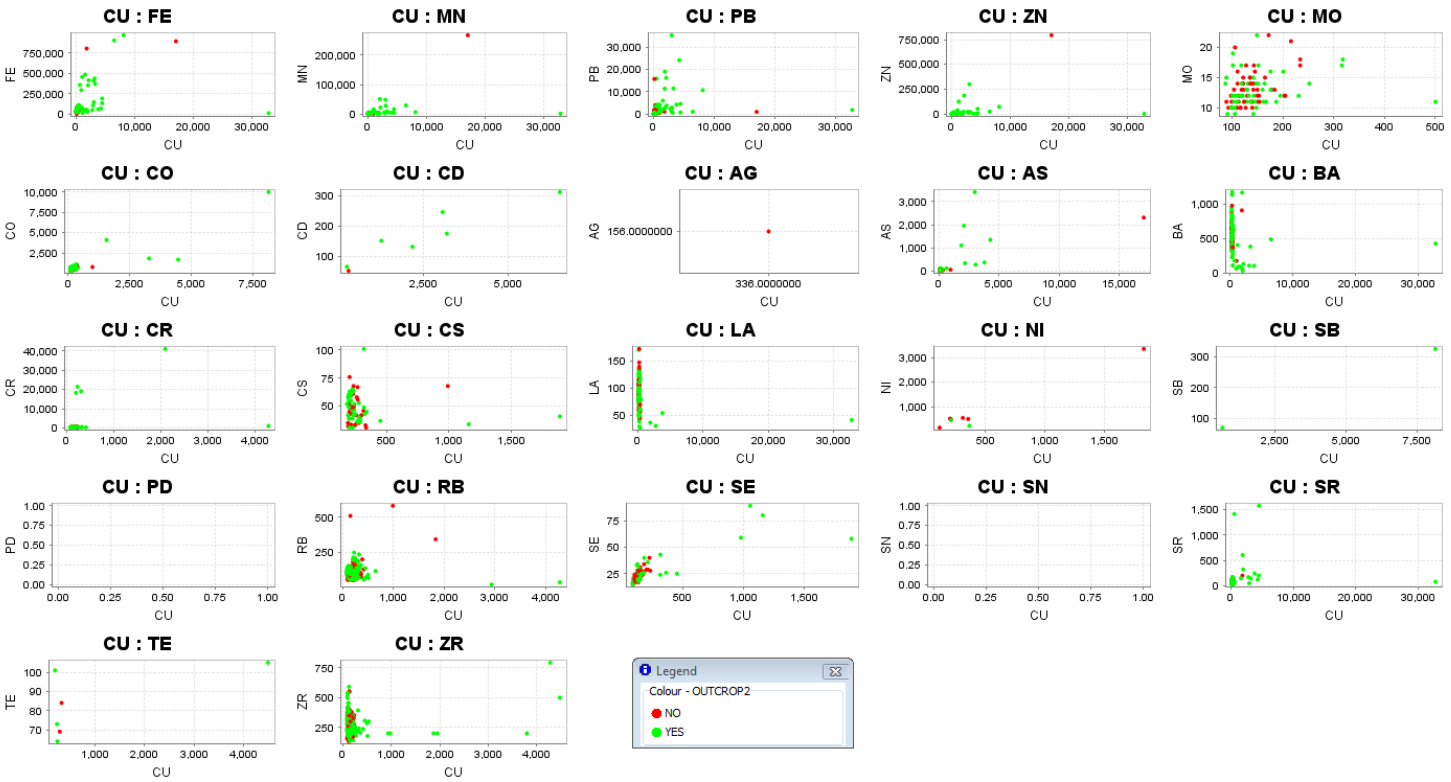
CU : FE
CU : MN
CU : PB
CU : ZN
CU : MO
CU : CO
CU : CD
CU : AG
CU : AS
CU : BA
CU : CR
CU : CS
CU : LA
CU : NI
CU : SB
CU : PD
CU : RB
CU : SE
CU : SN
CU : SR
CU : TE
CU : ZR
CU
Legend
Colour - OUTCROP2
NO
YES

Figure 26.

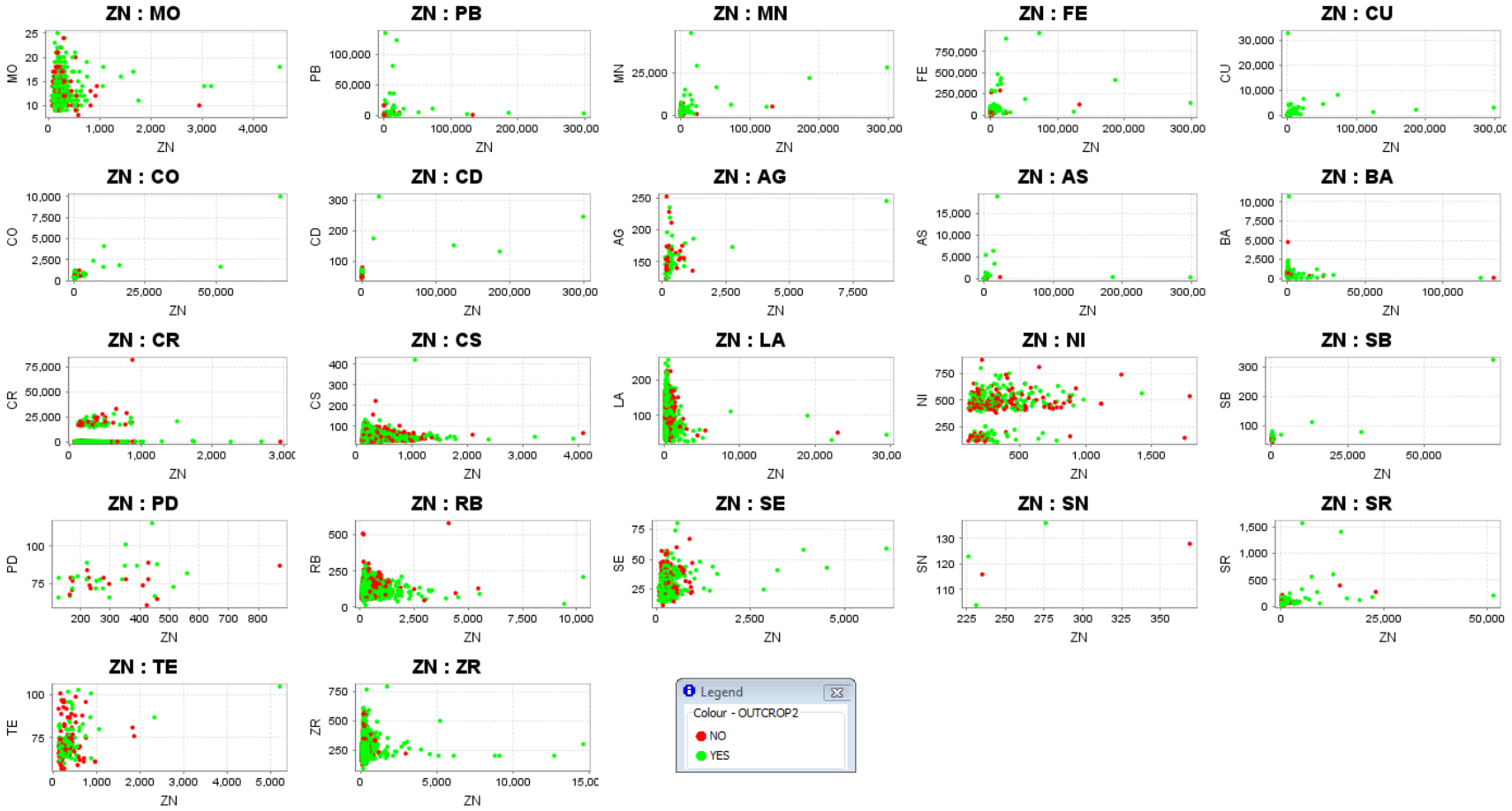
ZN : MO
ZN : PB
ZN : MN
ZN : FE
ZN : CU
ZN : CO
ZN : CD
ZN : AG
ZN : AS
ZN : BA
ZN : CR
ZN : CS
ZN : LA
ZN : NI
ZN : SB
ZN : PD
ZN : RB
ZN : SE
ZN : SN
ZN : SR
ZN : TE
ZN : ZR
ZN
Legend
Colour - OUTCROP2
NO
YES

Figure 27.

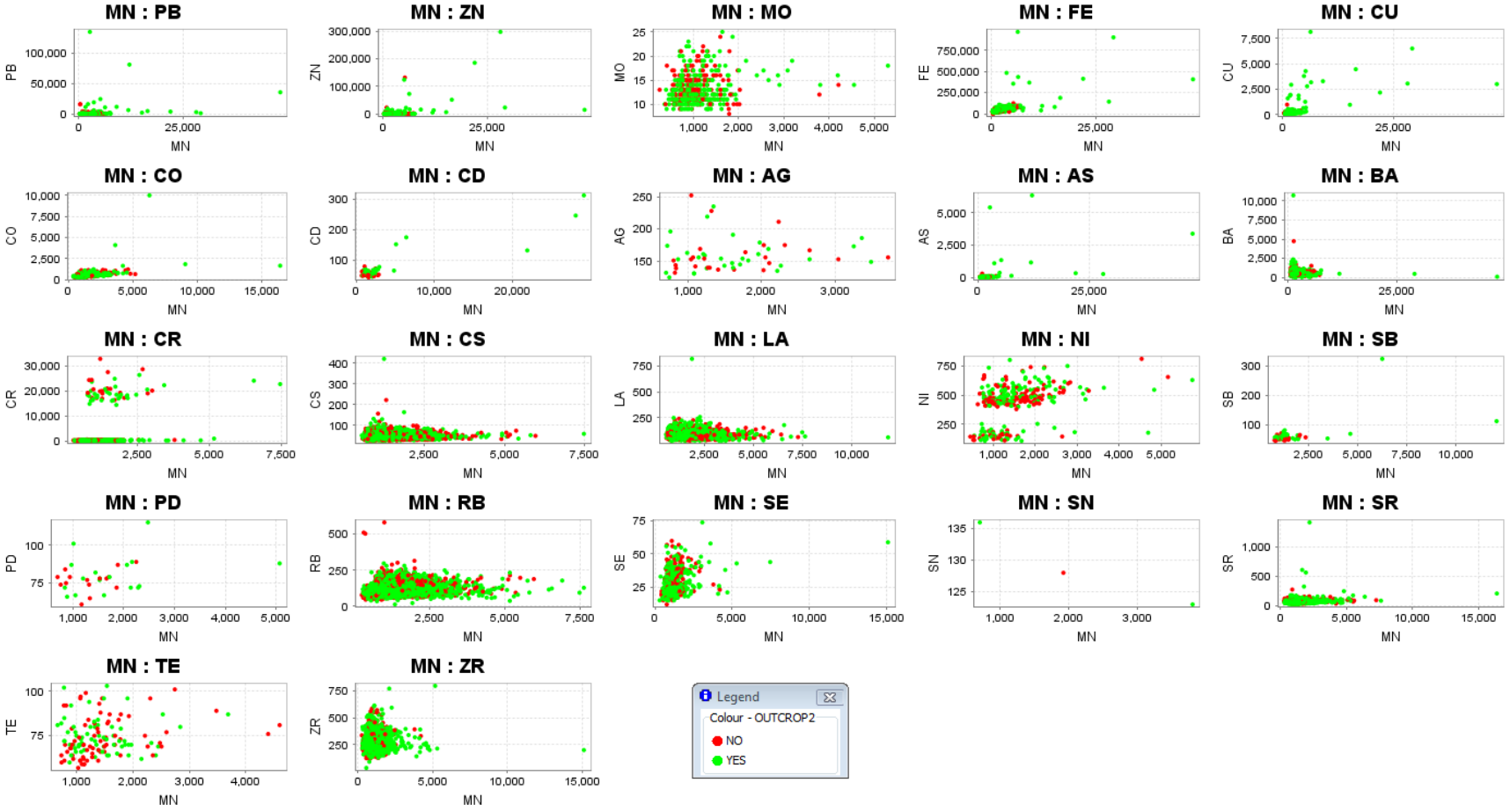
MN : PB
MN : ZN
MN : MO
MN : FE
MN : CU
MN : CO
MN : CD
MN : AG
MN : AS
MN : BA
MN : CR
MN : CS
MN : LA
MN : NI
MN : SB
MN : PD
MN : RB
MN : SE
MN : SN
MN : SR
MN : TE
MN : ZR
MN
Legend
Colour - OUTCROP2
NO
YES

Figure 28.

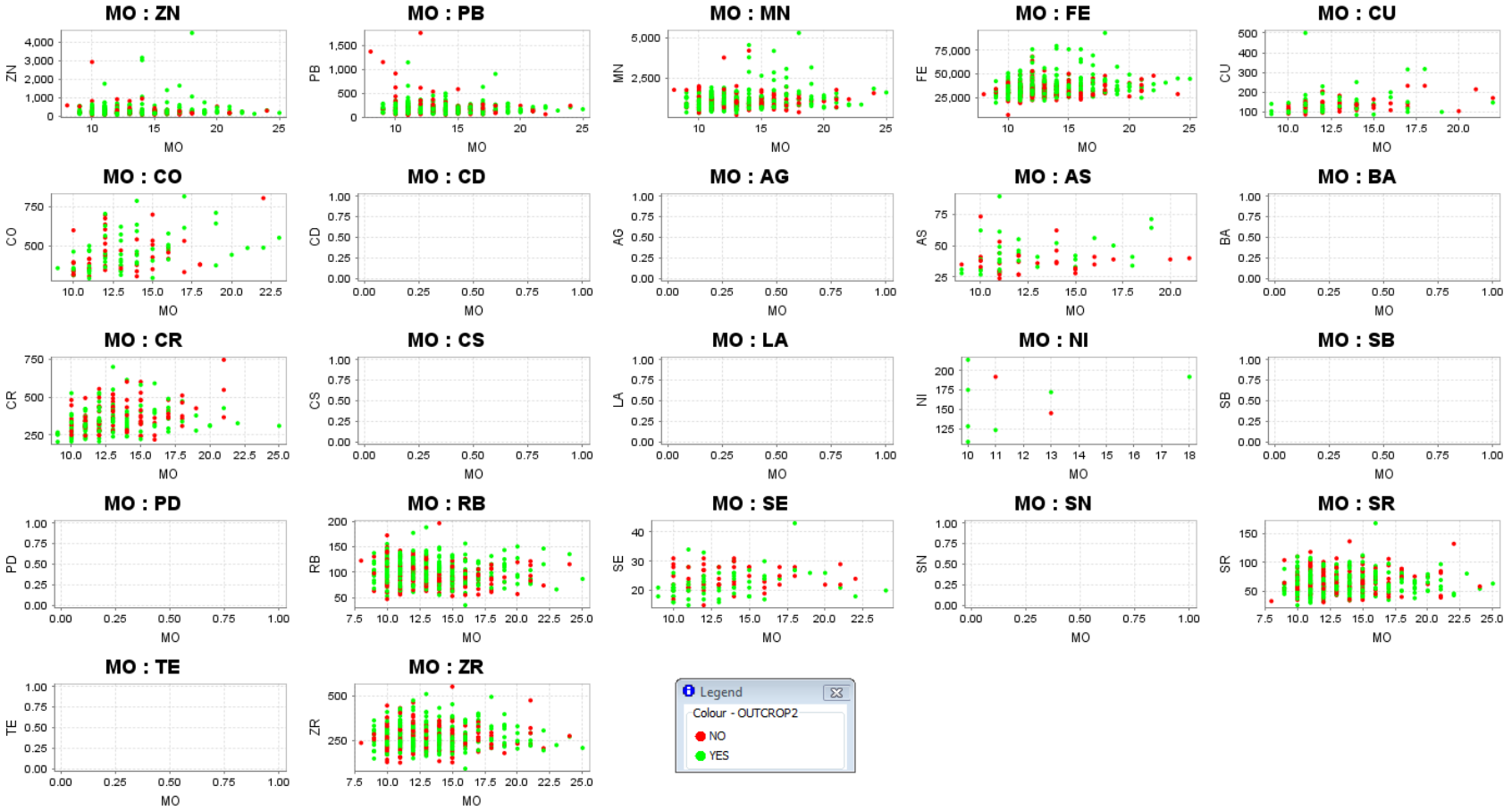
MO : ZN
MO : PB
MO : MN
MO : FE
MO : CU
MO : CO
MO : CD
MO : AG
MO : AS
MO : BA
MO : CR
MO : CS
MO : LA
MO : NI
MO : SB
MO : PD
MO : RB
MO : SE
MO : SN
MO : SR
MO : TE
MO : ZR
MO
Legend
Colour - OUTCROP2
NO
YES

Figure 29.

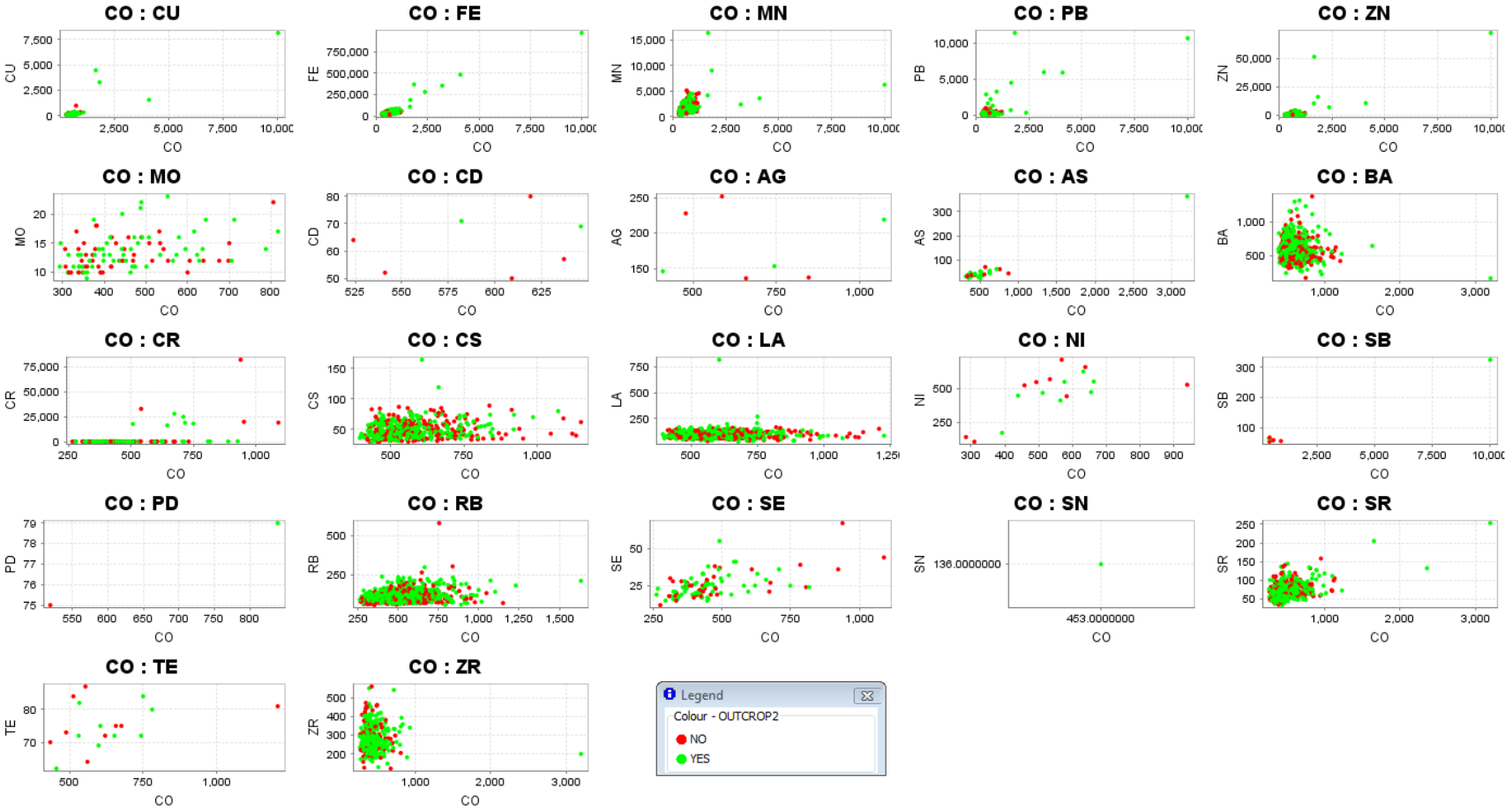
CO : CU
CO : FE
CO : MN
CO : PB
CO : ZN
CO : MO
CO : CD
CO : AG
CO : AS
CO : BA
CO : CR
CO : CS
CO : LA
CO : NI
CO : SB
CO : PD
CO : RB
CO : SE
CO : SN
CO : SR
CO : TE
CO : ZR
CO
Legend
Colour - OUTCROP2
NO
YES

Figure 30

.

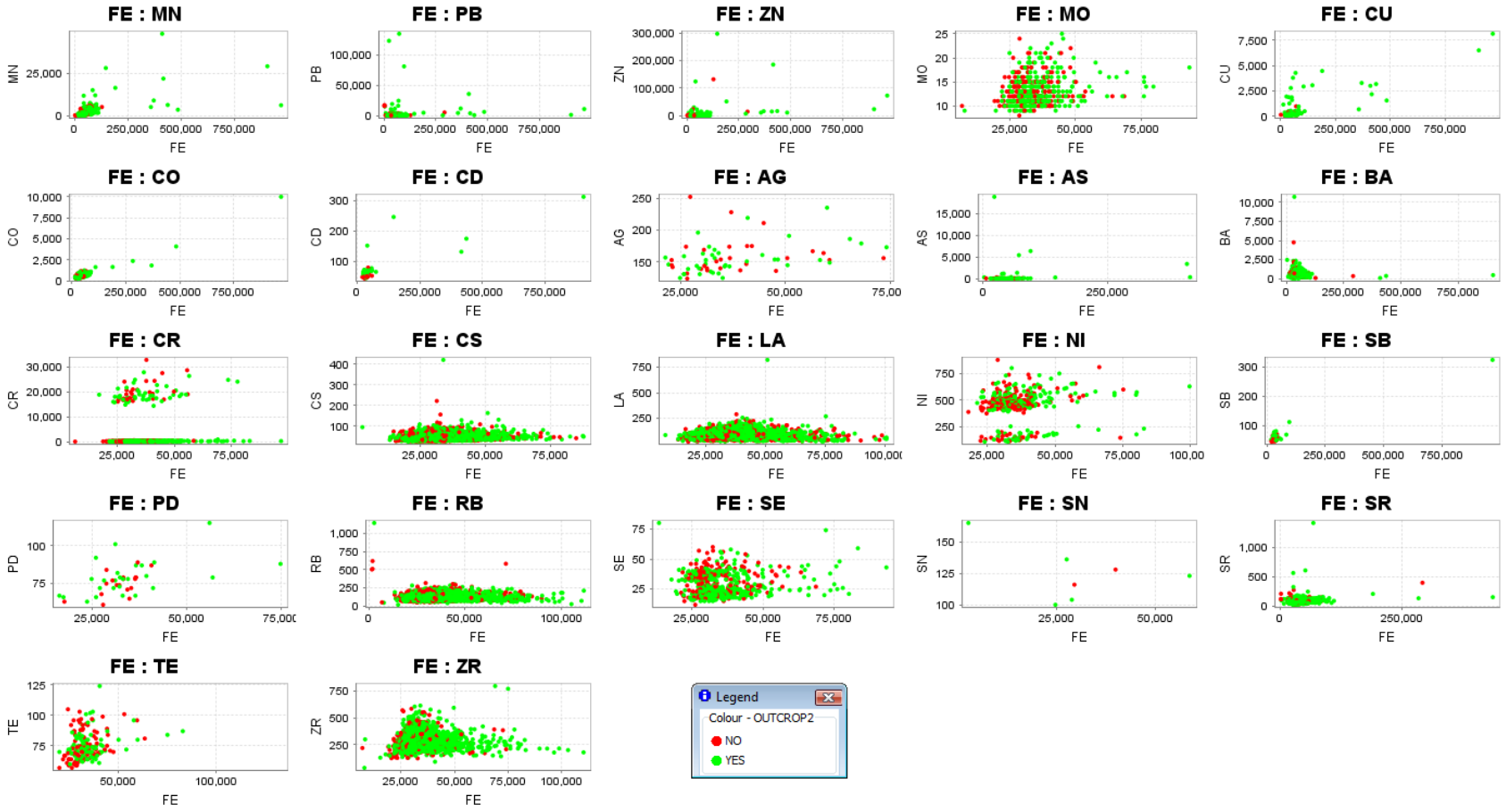
FE : MN
FE : PB
FE : ZN
FE : MO
FE : CU
FE : CO
FE : CD
FE : AG
FE : AS
FE : BA
FE : CR
FE : CS
FE : LA
FE : NI
FE : SB
FE : PD
FE : RB
FE : SE
FE : SN
FE : SR
FE : TE
FE : ZR
FE
Legend
Colour - OUTCROP2
NO
YES

Figure 31.

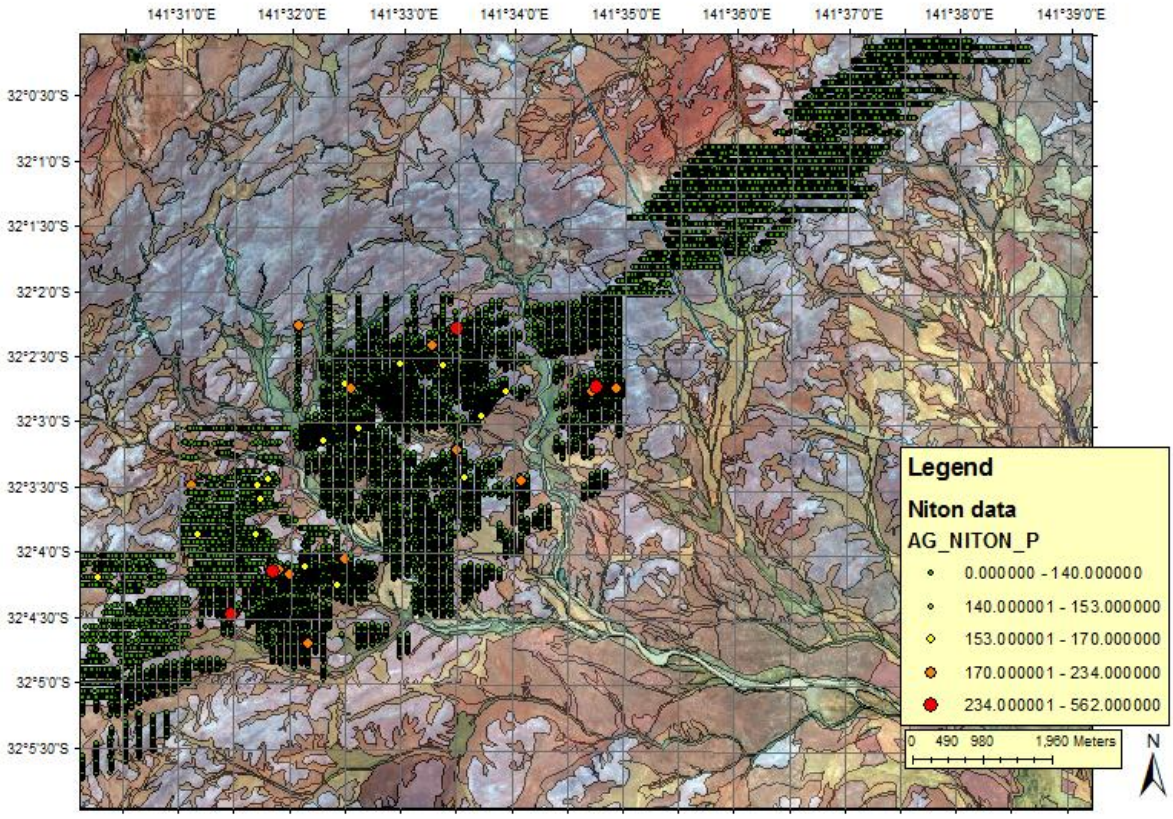
141°31'0"E
141°32'0"E
141°33'0"E
141°34'0"E
141°35'0"E
141°36'0"E
141°37'0"E
141°38'0"E
141°39'0"E
32°0'30"S
32°1'0"S
32°1'30"S
32°2'0"S
32°2'30"S
32°3'0"S
32°3'30"S
32°4'0"S
32°4'30"S
32°5'0"S
32°5'30"S
Legend
Niton data
AG_NITON_P
0.000000 - 140.000000
140.000001 - 153.000000
153.000001 - 170.000000
170.000001 - 234.000000
234.000001 - 562.000000
0 490 980 1,960 Meters
N

Figure 32.

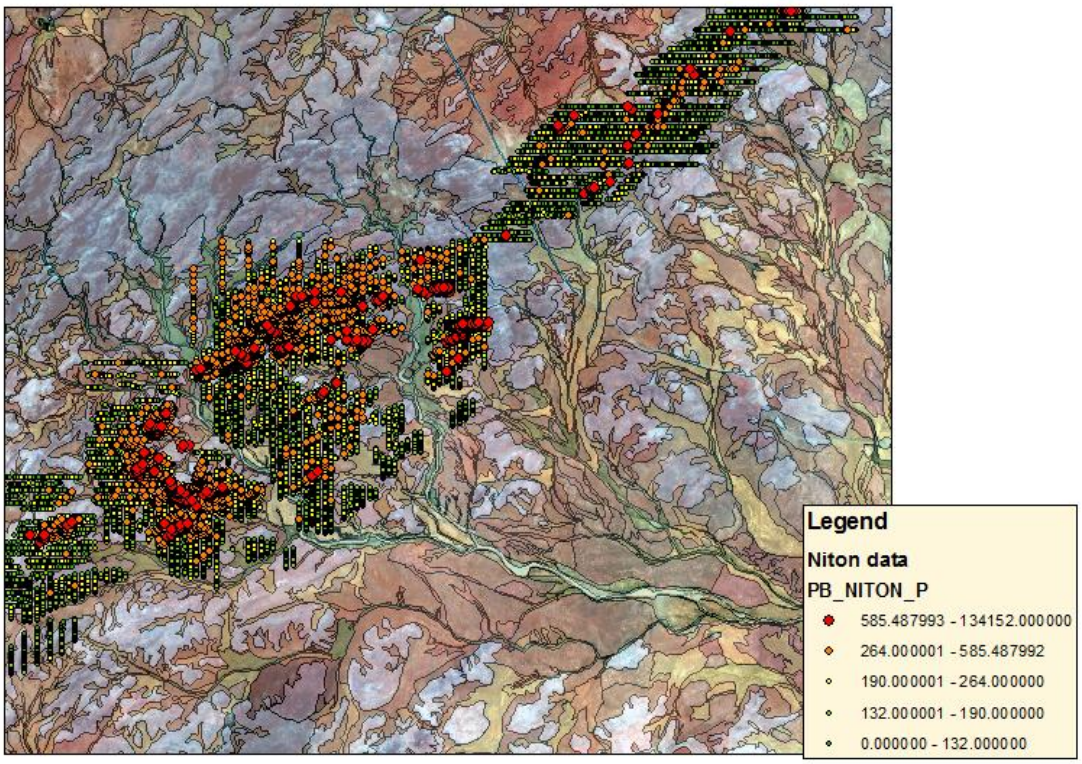
Legend
Niton data
PB_NITON_P
585.487993 - 134152.000000
264.000001 - 585.487992
190.000001 - 264.000000
132.000001 - 190.000000
0.000000 - 132.000000

Figure 33.

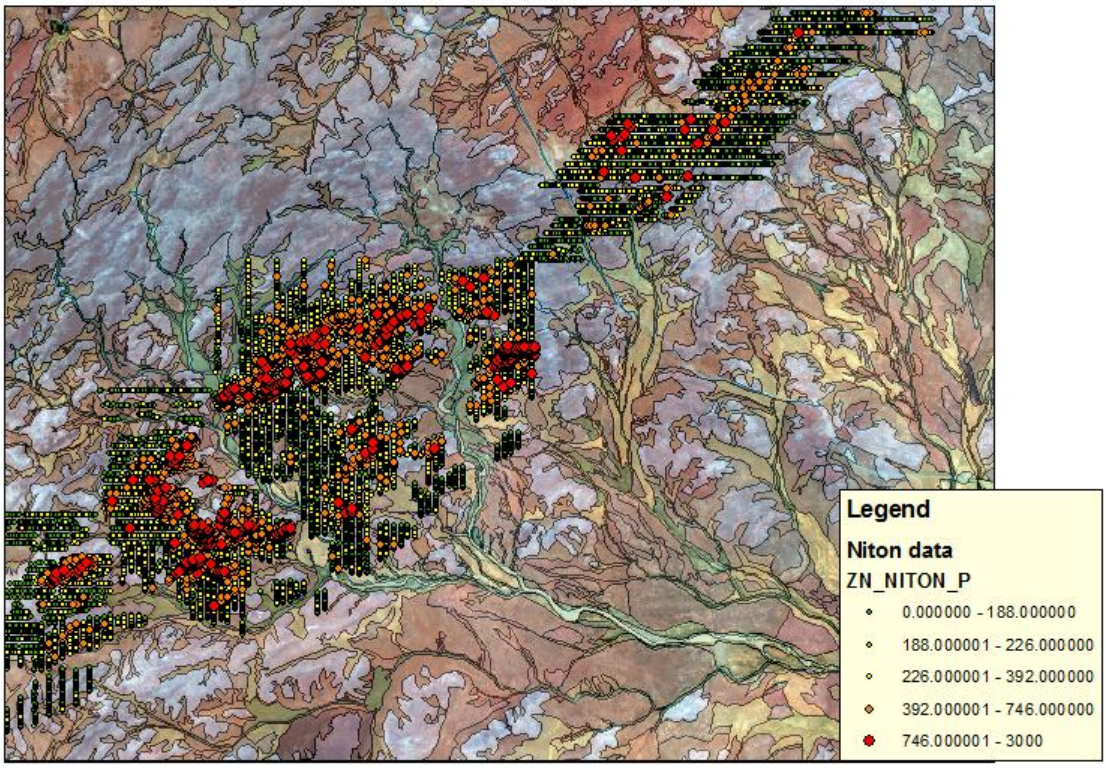
Legend
Niton data
ZN_NITON_P
0.000000 - 188.000000
188.000001 - 226.000000
226.000001 - 392.000000
392.000001 - 746.000000
746.000001 - 3000

Figure 34.

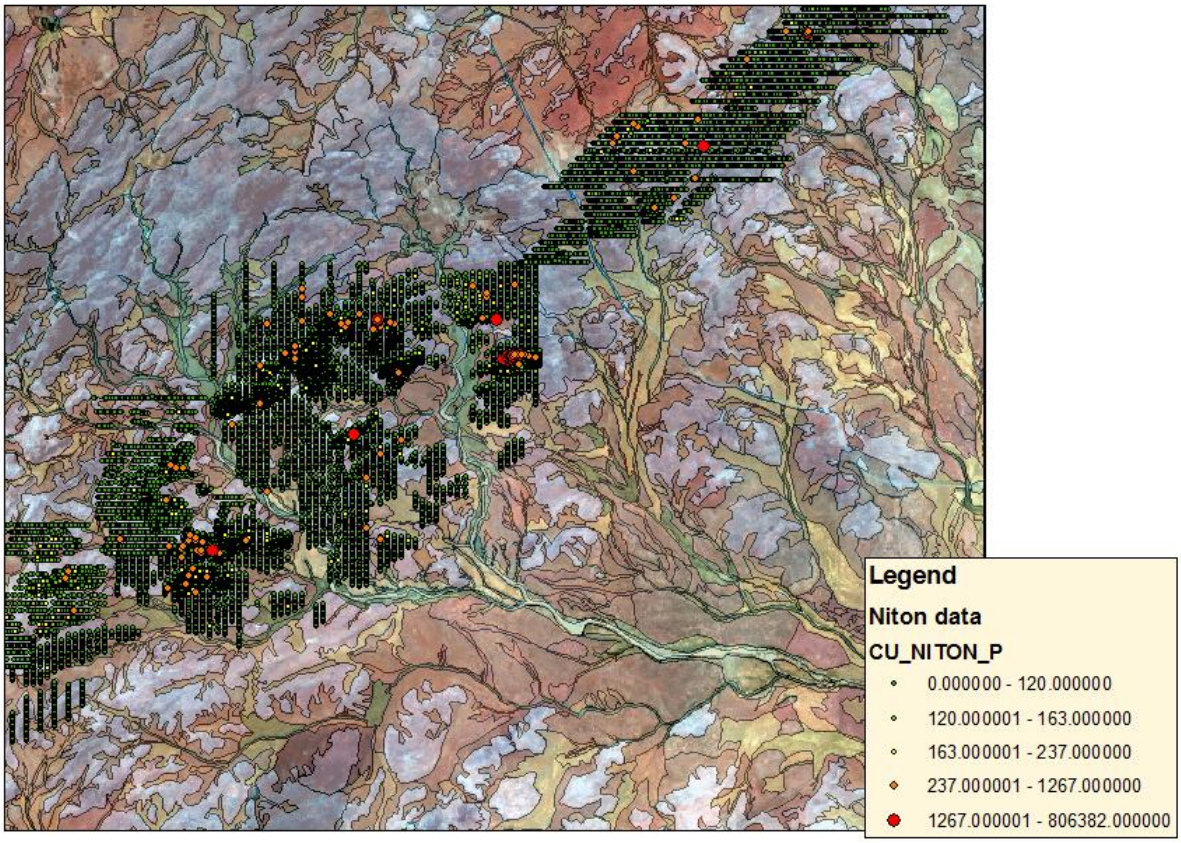
Legend
Niton data
CU_NITON_P
0.000000 - 120.000000
120.000001 - 163.000000
163.000001 - 237.000000
237.000001 - 1267.000000
1267.000001 - 806382.000000

Figure 35.

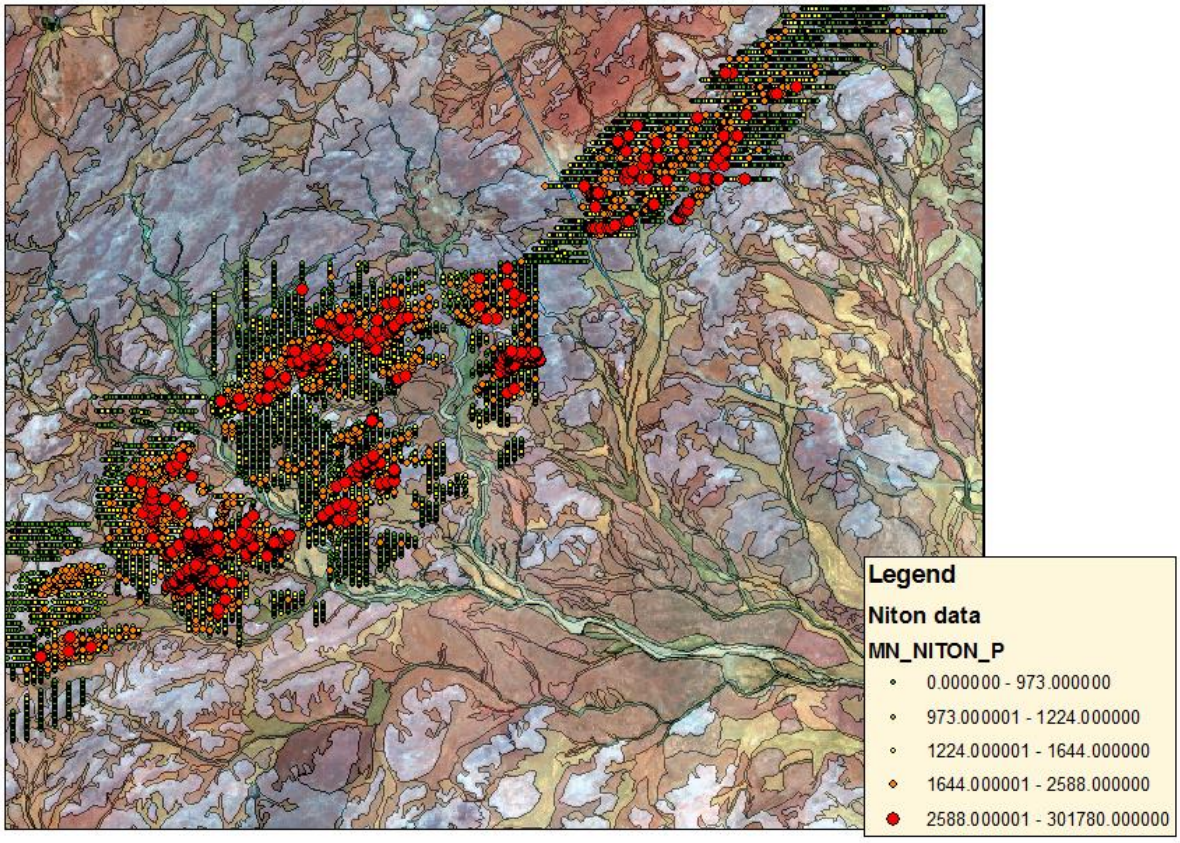
Legend
Niton data
MN_NITON_P
0.000000 - 973.000000
973.000001 - 1224.000000
1224.000001 - 1644.000000
1644.000001 - 2588.000000
2588.000001 - 301780.000000

Figure 36.

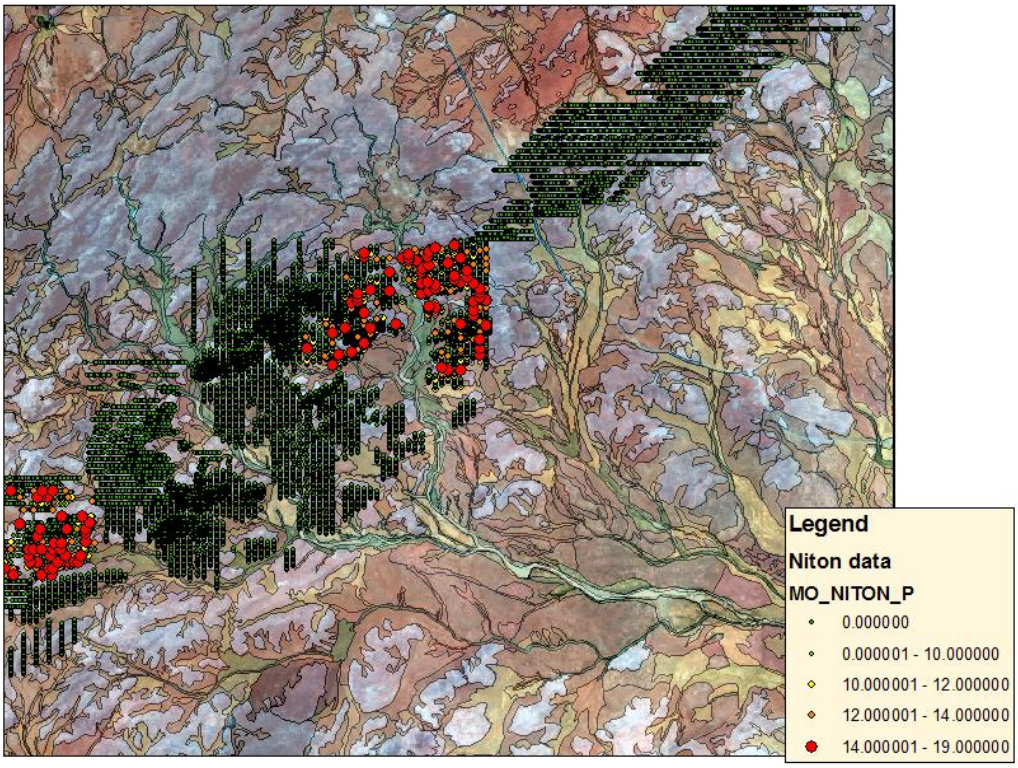
Legend
Niton data
MO_NITON_P
0.000000
0.000001 - 10.000000
10.000001 - 12.000000
12.000001 - 14.000000
14.000001 - 19.000000

Figure 37.

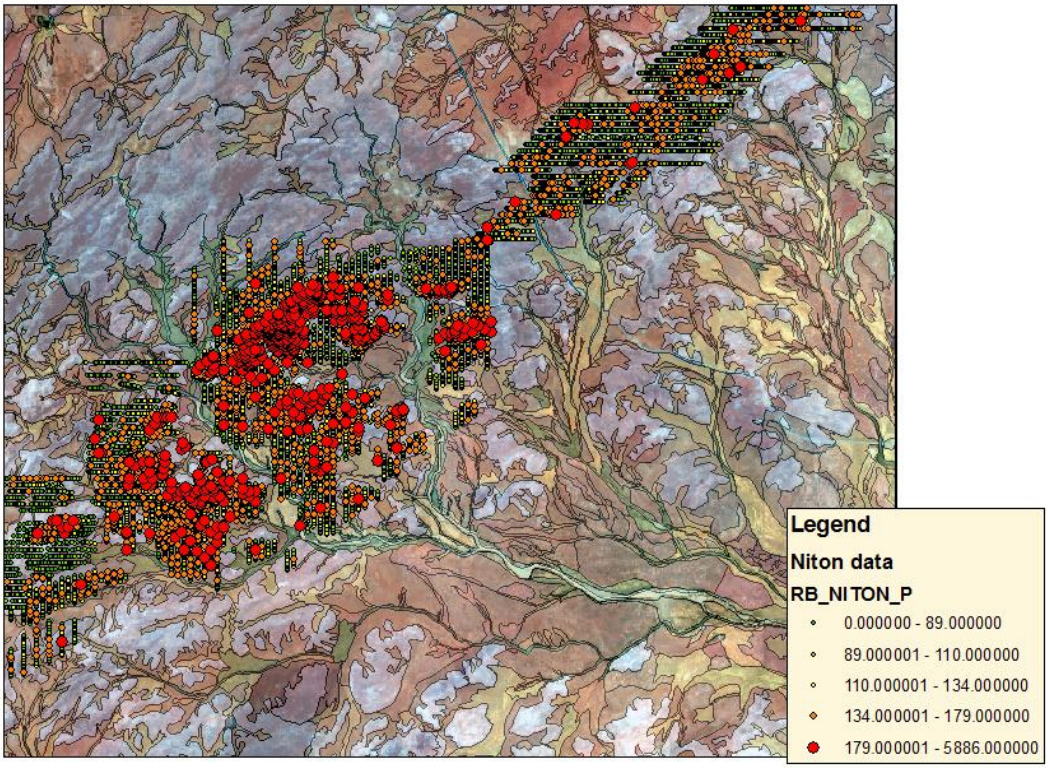
Legend
Niton data
RB_NITON_P
0.000000 - 89.000000
89.000001 - 110.000000
110.000001 - 134.000000
134.000001 - 179.000000
179.000001 - 5886.000000

Figure 38.

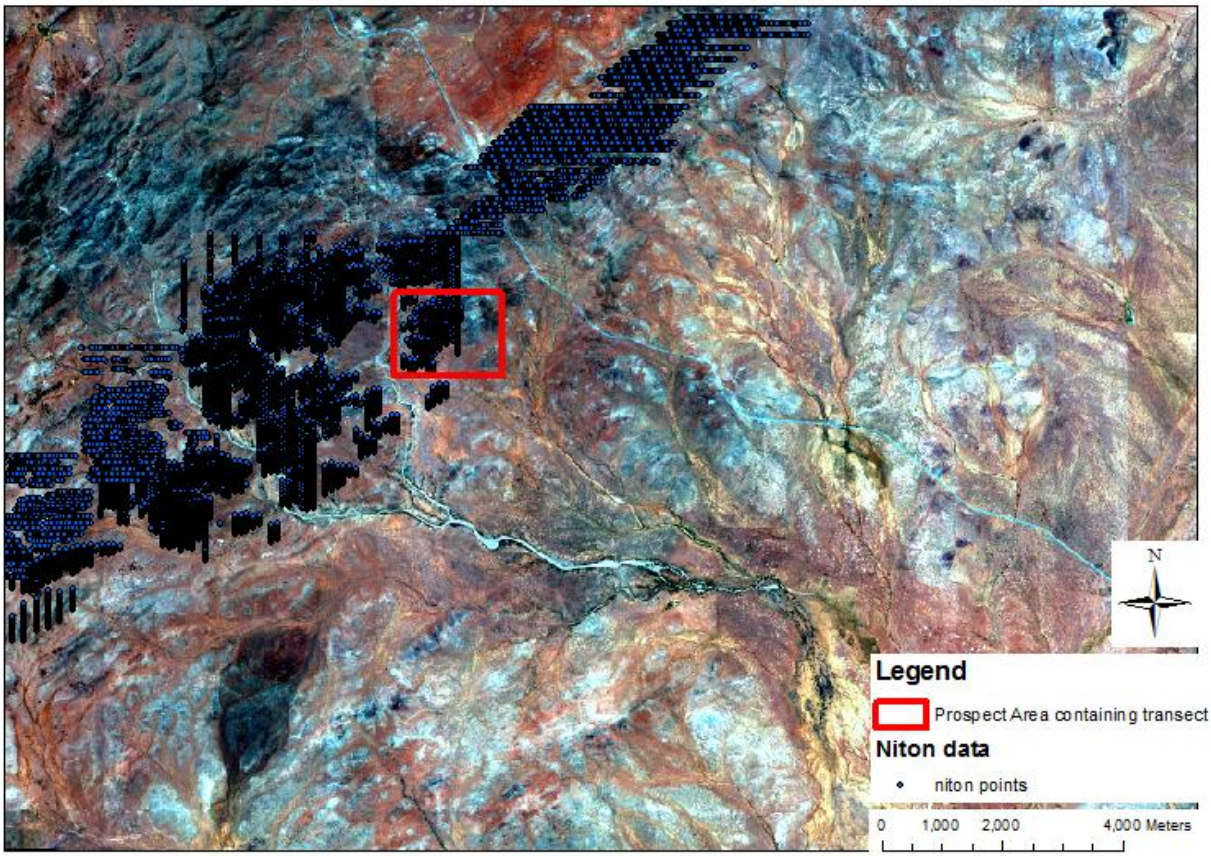
N
Legend
Prospect Area containing transect
Niton data
niton points
0
1,000
2,000
4,000 Meters

Figure 39.

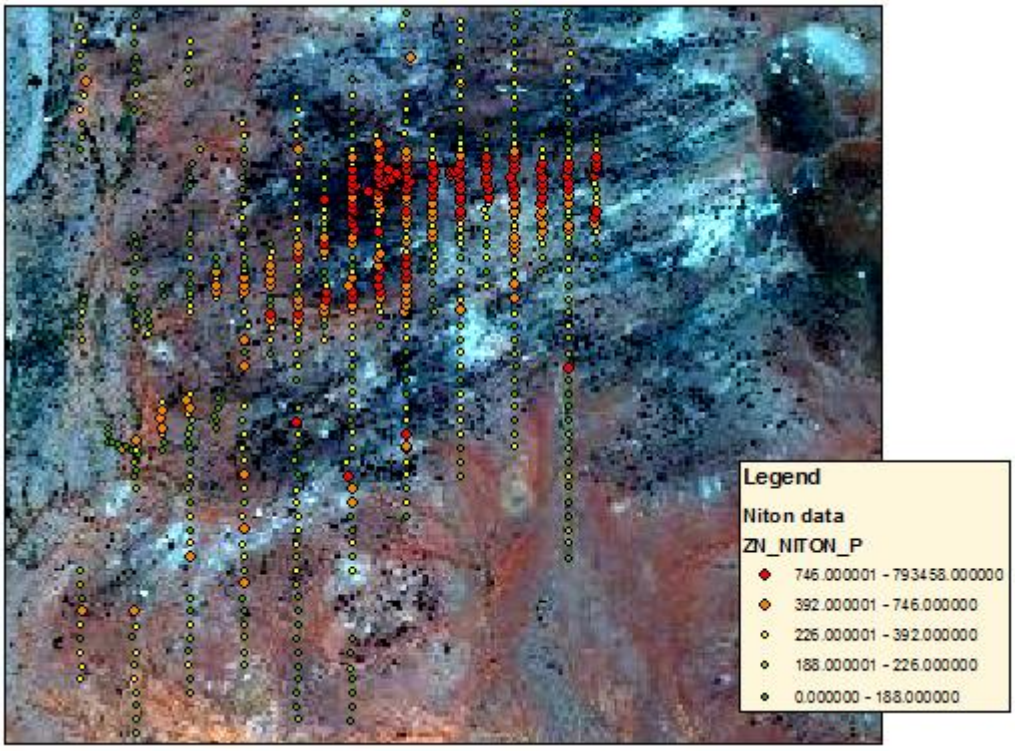
Legend
Niton data
ZN_NITON_P
746.000001 - 793458.000000
392.000001 - 746.000000
226.000001 - 392.000000
188.000001 - 226.000000
0.000000 - 188.000000

Figure 40.

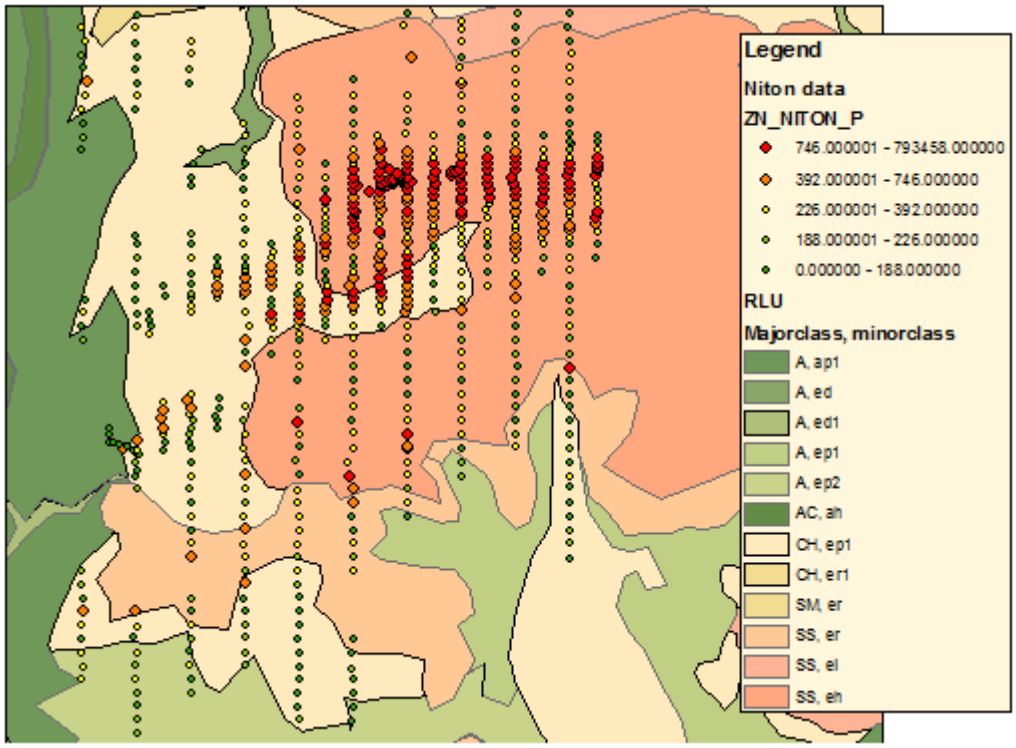
Legend
Niton data
ZN_NITON_P
746.000001 - 793458.000000
392.000001 - 746.000000
226.000001 - 392.000000
188.000001 - 226.000000
0.000000 - 188.000000
RLU
Majorclass, minorclass
A, ap1
A, ed
A, ed1
A, ep1
A, ep2
AC, ah
CH, ep1
CH, er1
SM, er
SS, er
SS, el
SS, eh

Figure 41.

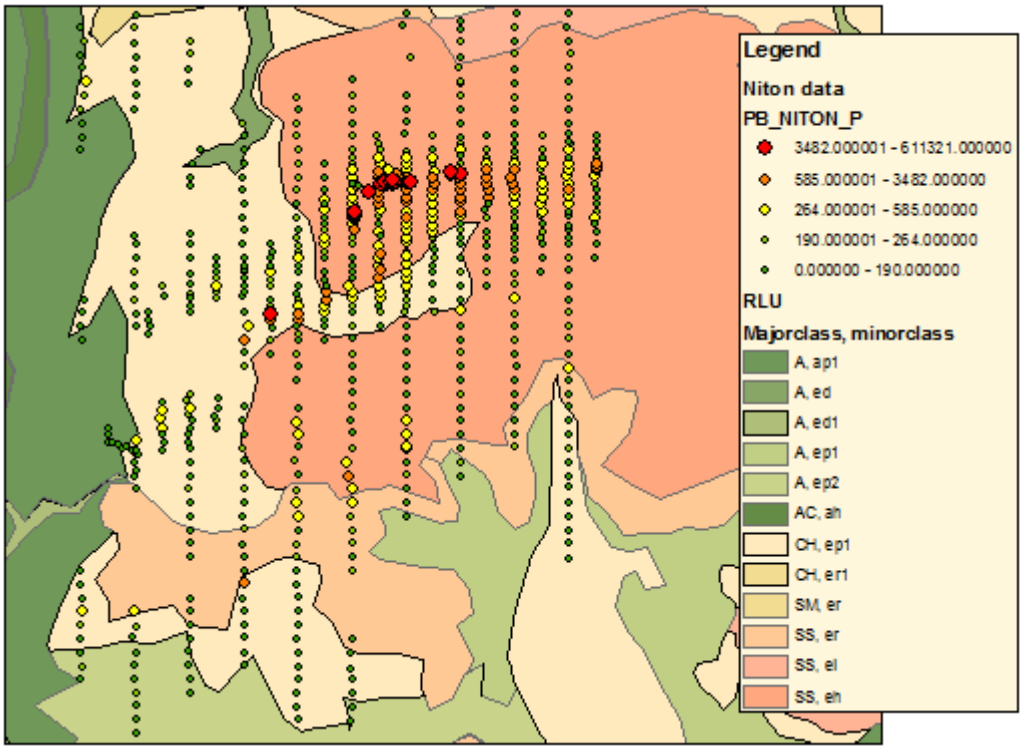
Legend
Niton data
PB_NITON_P
3482.000001 - 611321.000000
585.000001 - 3482.000000
264.000001 - 585.000000
190.000001 - 264.000000
0.000000 - 190.000000
RLU
Majorclass, minorclass
A, ap1
A, ed
A, ed1
A, ep1
A, ep2
AC, ah
CH, ep1
CH, er1
SM, er
SS, er
SS, el
SS, eh

Figure 42.

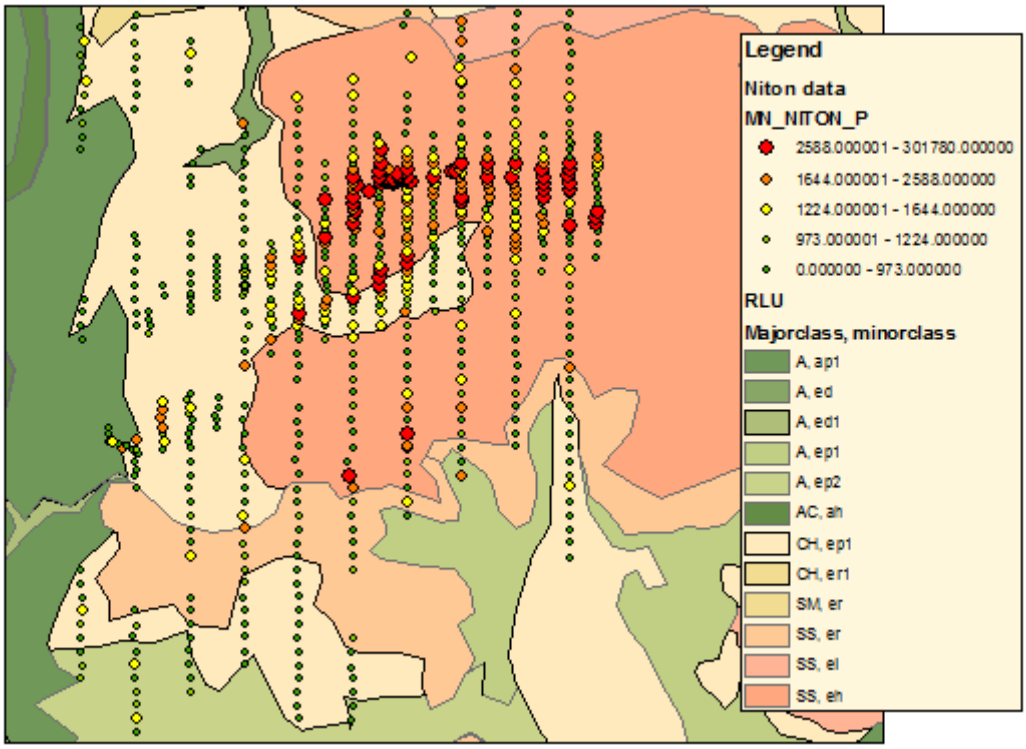
Legend
Niton data
MN_NITON_P
2588.000001 - 301780.000000
1644.000001 - 2588.000000
1224.000001 - 1644.000000
973.000001 - 1224.000000
0.000000 - 973.000000
RLU
Majorclass, minorclass
A, ap1
A, ed
A, ed1
A, ep1
A, ep2
AC, ah
CH, ep1
CH, er1
SM, er
SS, er
SS, el
SS, eh

Figure 43.

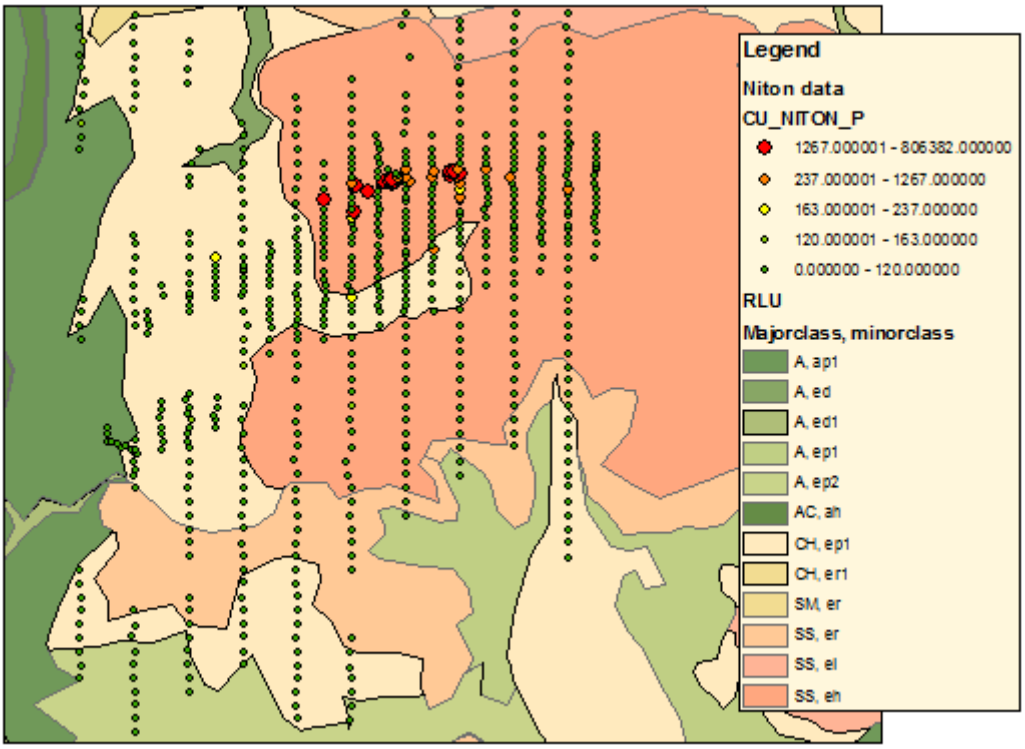
Legend
Niton data
CU_NITON_P
1267.000001 - 806382.000000
237.000001 - 1267.000000
163.000001 - 237.000000
120.000001 - 163.000000
0.000000 - 120.000000
RLU
Majorclass, minorclass
A, ap1
A, ed
A, ed1
A, ep1
A, ep2
AC, ah
CH, ep1
CH, er1
SM, er
SS, er
SS, el
SS, eh

Figure 44.

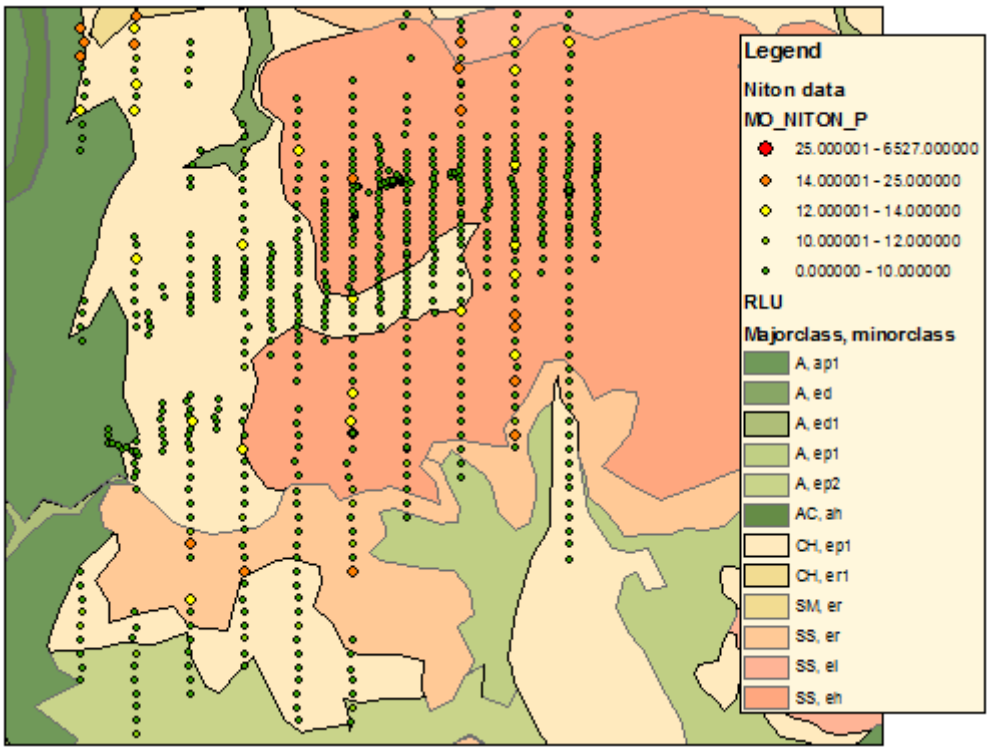
Legend
Niton data
MO_NITON_P
25.000001 - 6527.000000
14.000001 - 25.000000
12.000001 - 14.000000
10.000001 - 12.000000
0.000000 - 10.000000
RLU
Majorclass, minorclass
A, ap1
A, ed
A, ed1
A, ep1
A, ep2
AC, ah
CH, ep1
CH, er1
SM, er
SS, er
SS, el
SS, eh

Figure 45.

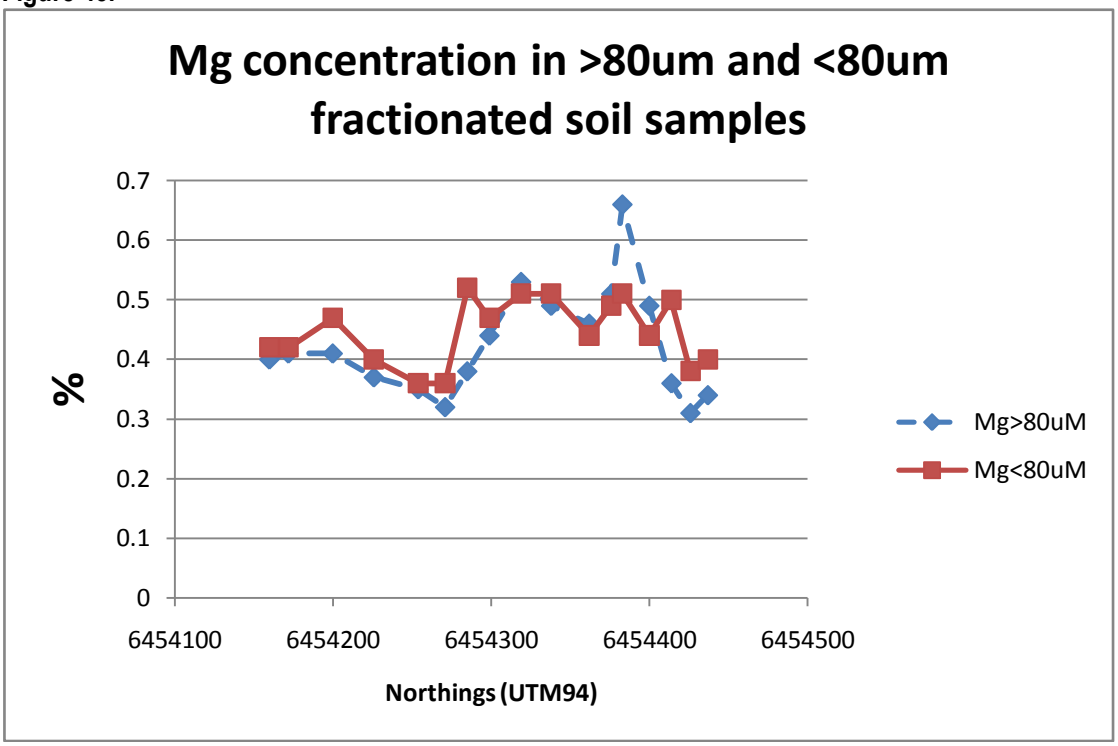
Mg concentration in >80um and <80um fractionated soil samples
0.7
0.6
0.5
0.4
0.3
0.2
0.1
0
%
6454100
6454200
6454300
6454400
6454500
Northings (UTM94)
Mg>80uM
Mg<80uM

Figure 46.

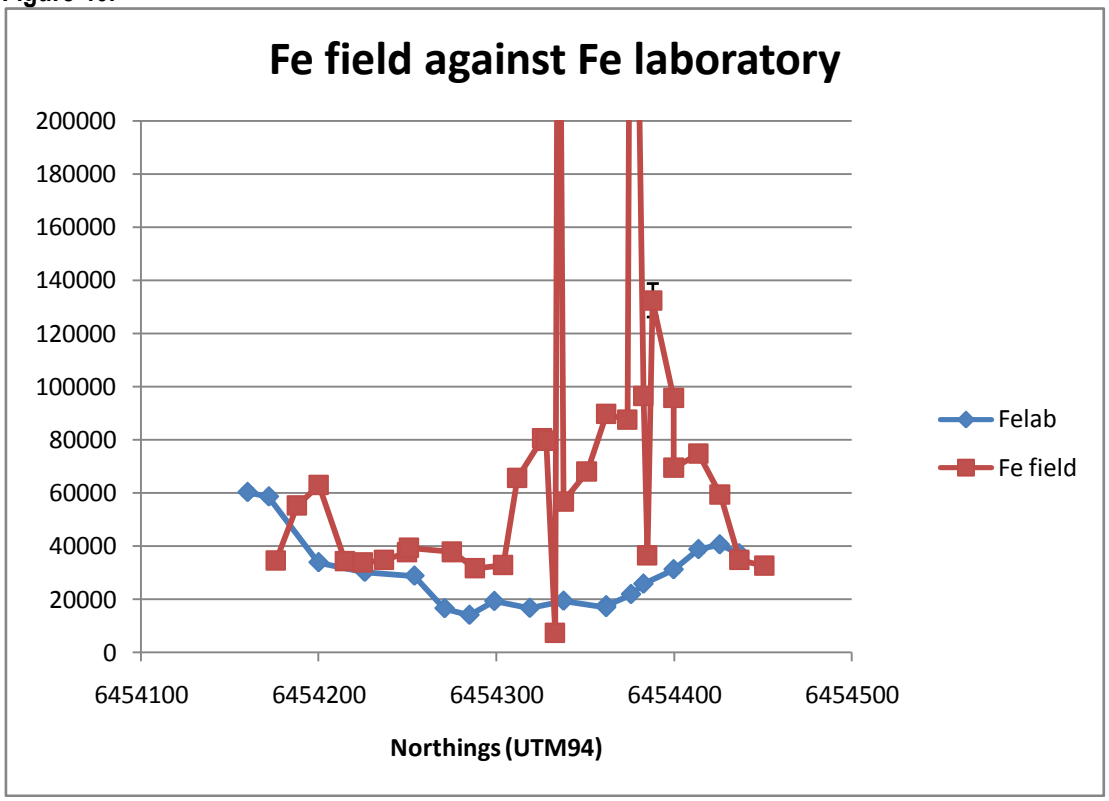
Fe field against Fe laboratory
200000
180000
160000
140000
120000
100000
80000
60000
40000
20000
0
6454100
6454200
6454300
6454400
6454500
Northings (UTM94)
Felab
Fe field

Figure 47.

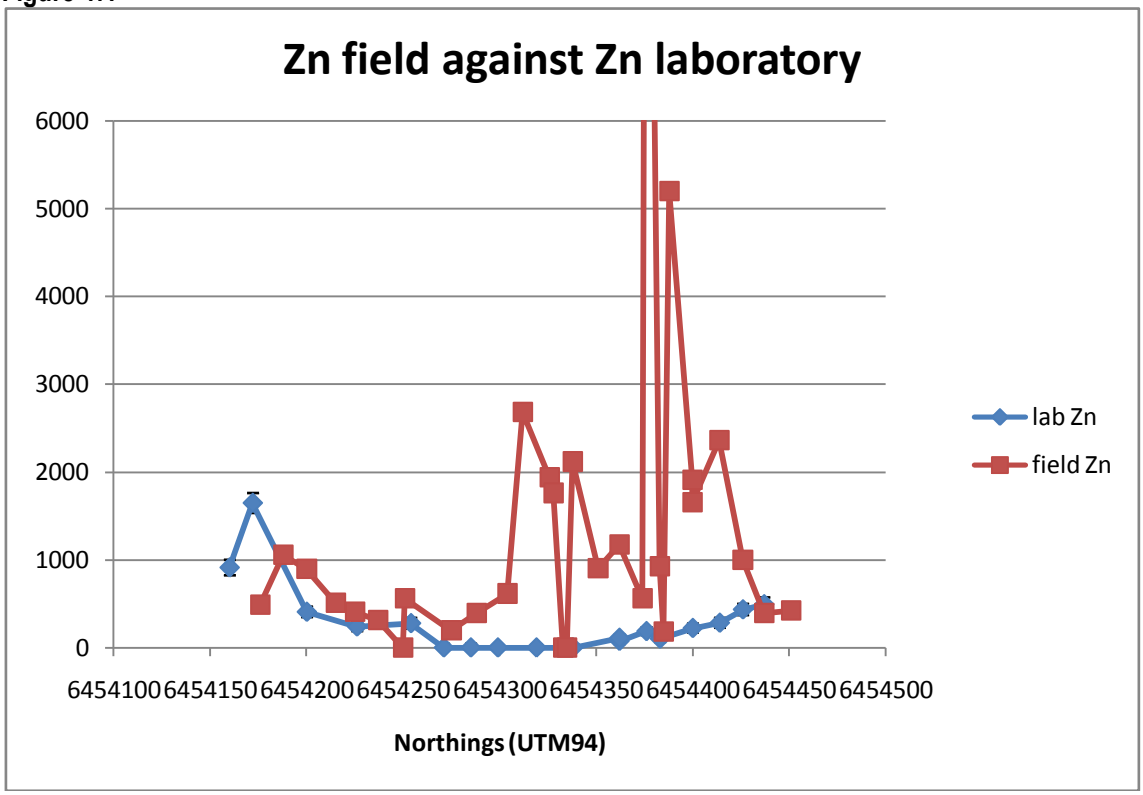
Zn field against Zn laboratory
6000
5000
4000
3000
2000
1000
0
6454100
6454150
6454200
6454250
6454300
6454350
6454400
6454450
6454500
Northings (UTM94)
lab Zn
field Zn

Figure 48.

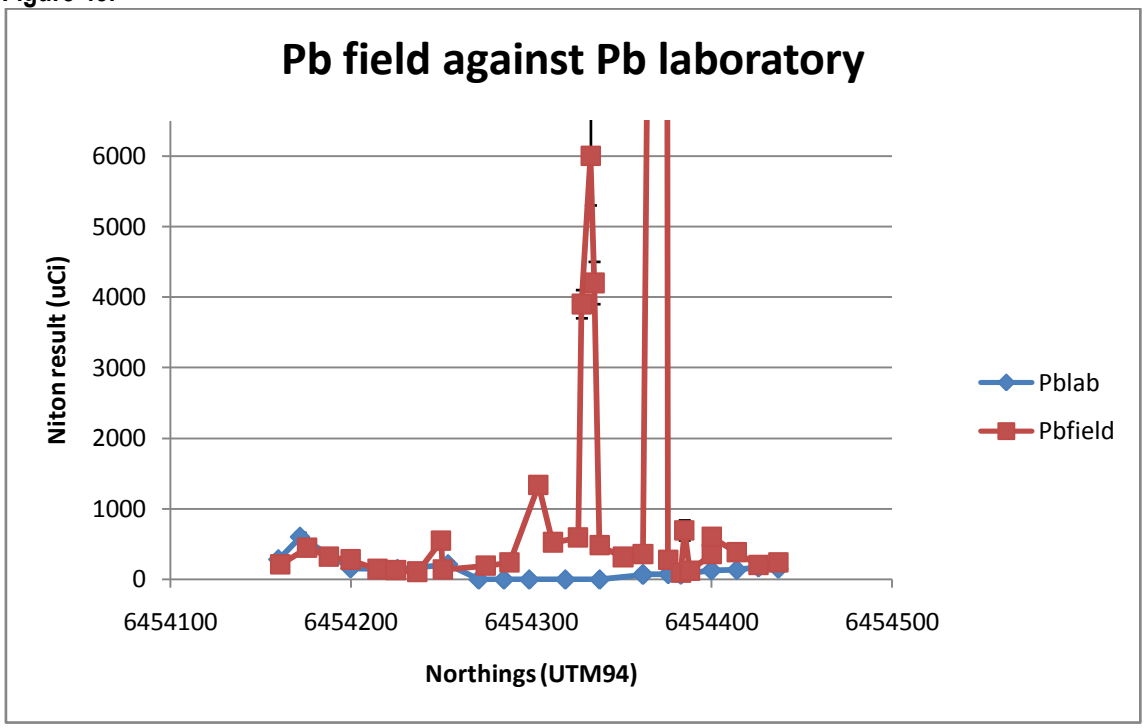
Pb field against Pb laboratory
Niton result (uCi)
6000
5000
4000
3000
2000
1000
0
6454100
6454200
6454300
6454400
6454500
Northings (UTM94)
Pblab
Pbfield

Figure 49.

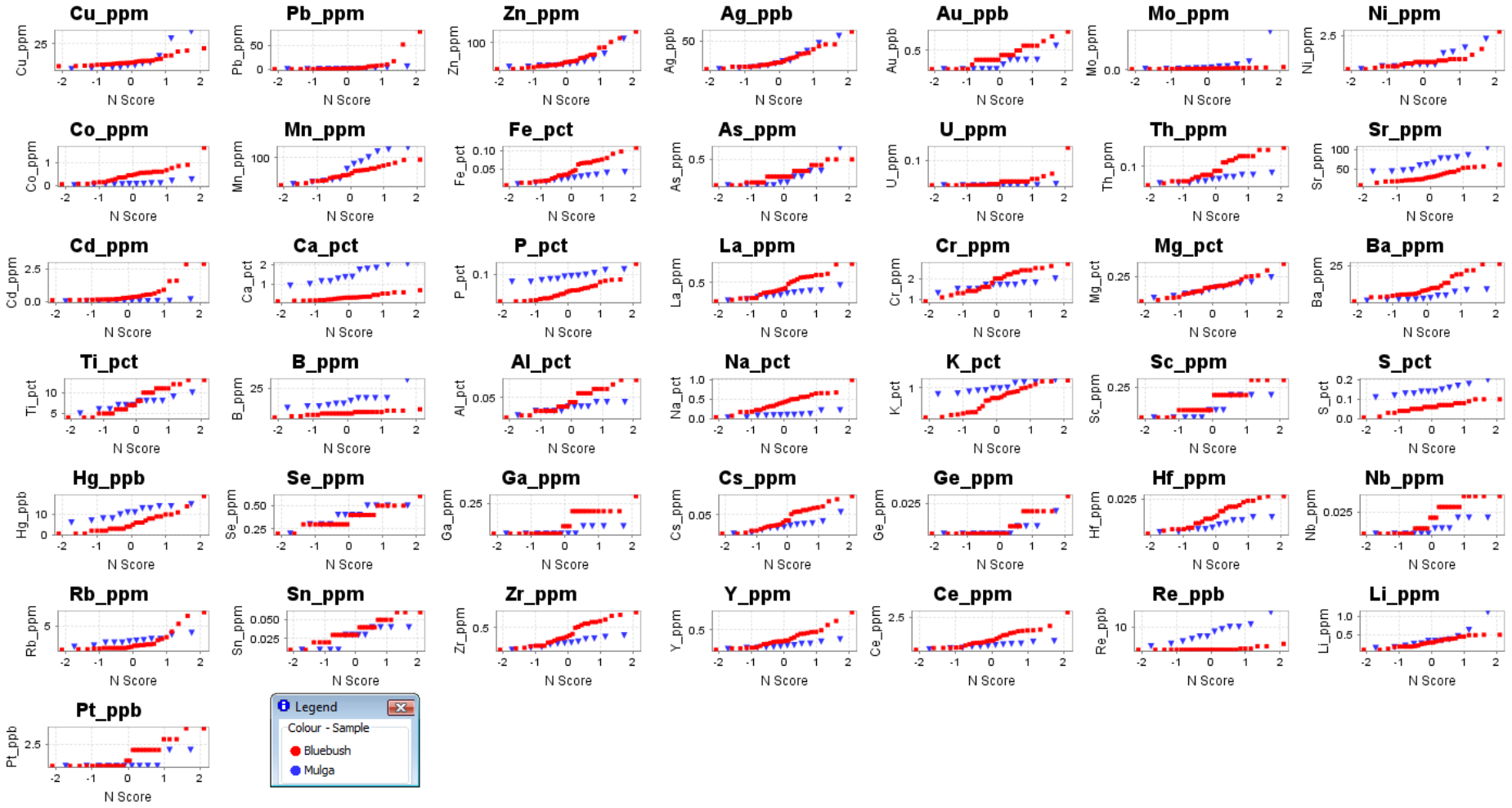
Cu_ppm
Pb_ppm
Zn_ppm
Ag_ppb
Au_ppb
Mo_ppm
Ni_ppm
Co_ppm
Mn_ppm
Fe_pct
As_ppm
U_ppm
Th_ppm
Sr_ppm
Cd_ppm
Ca_pct
P_pct
La_ppm
Cr_ppm
Mg_pct
Ba_ppm
Ti_pct
B_ppm
Al_pct
Na_pct
K_pct
Sc_ppm
S_pct
Hg_ppb
Se_ppm
Ga_ppm
Cs_ppm
Ge_ppm
Hf_ppm
Nb_ppm
Rb_ppm
Sn_ppm
Zr_ppm
Y_ppm
Ce_ppm
Re_ppb
Li_ppm
Pt_ppb
N Score
Legend
Colour - Sample
Bluebush
Mulga

Figure 50.

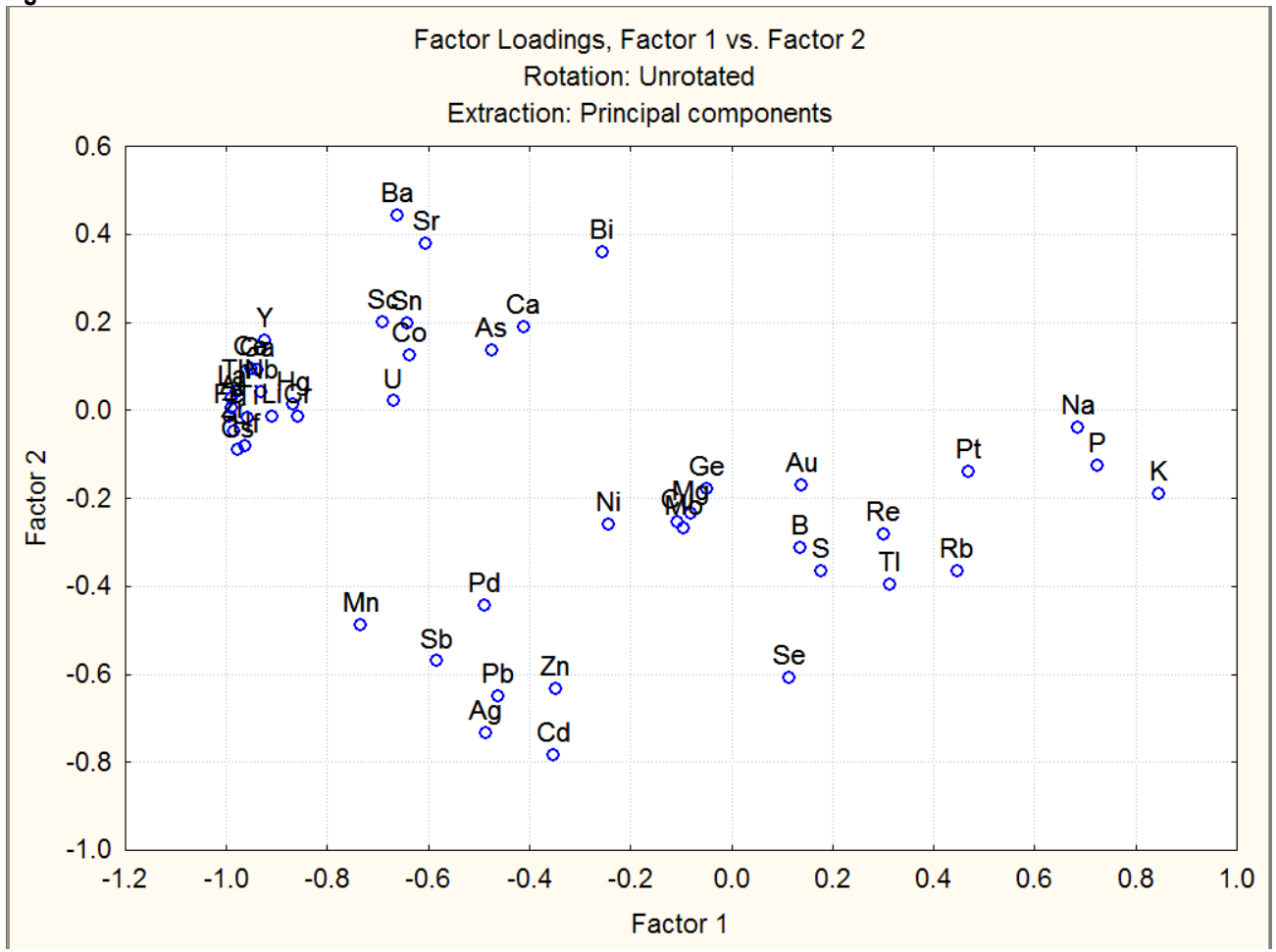
Factor Loadings, Factor 1 vs. Factor 2
Rotation: Unrotated
Extraction: Principal components
Factor 2
Factor 1
0.6
0.4
0.2
0.0
-0.2
-0.4
-0.6
-0.8
-1.0
-1.2
-1.0
-0.8
-0.6
-0.4
-0.2
0.0
0.2
0.4
0.6
0.8
1.0
Ba
Sr
Bi
Sc
Sn
Ca
Y
As
Co
U
Hg
Na
P
Pt
K
Ge
Au
Ni
Re
B
S
Rb
Tl
Mn
Pd
Sb
Se
Pb
Zn
Ag
Cd

Figure 51.

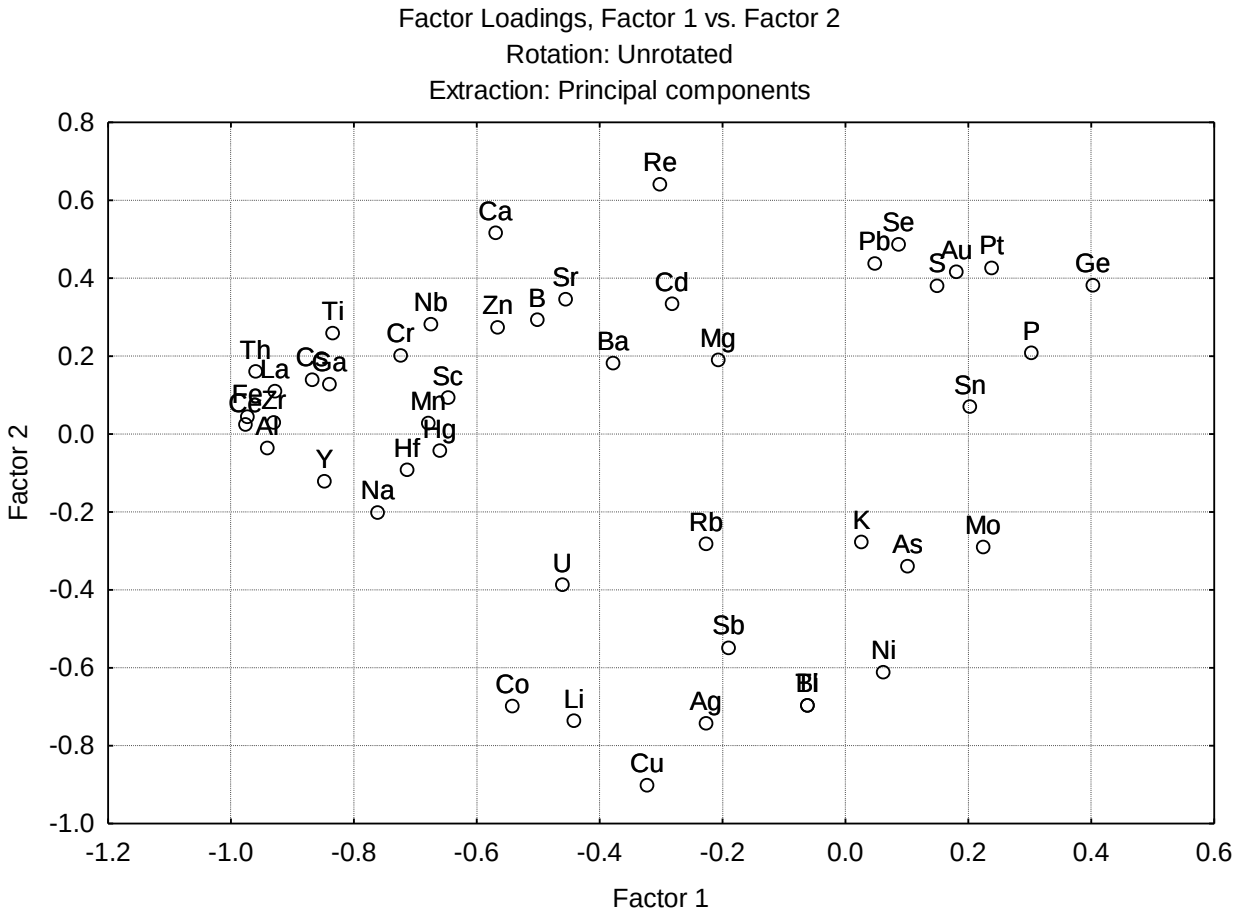
Factor Loadings, Factor 1 vs. Factor 2
Rotation: Unrotated
Extraction: Principal components
Factor 2
Factor 1
0.8
0.6
0.4
0.2
0.0
-0.2
-0.4
-0.6
-0.8
-1.0
-1.2
-1.0
-0.8
-0.6
-0.4
-0.2
0.0
0.2
0.4
0.6
Re
Ca
Se
Pb
Au
Pt
S
Ge
Sr
Cd
Nb
Zn
B
Ti
Cr
Ba
Mg
P
Th
La
Sc
Sn
Mn
Hg
Hf
Y
Na
Rb
K
Mo
As
U
Sb
Ni
Co
Li
Ag
Cu

Figure 52.

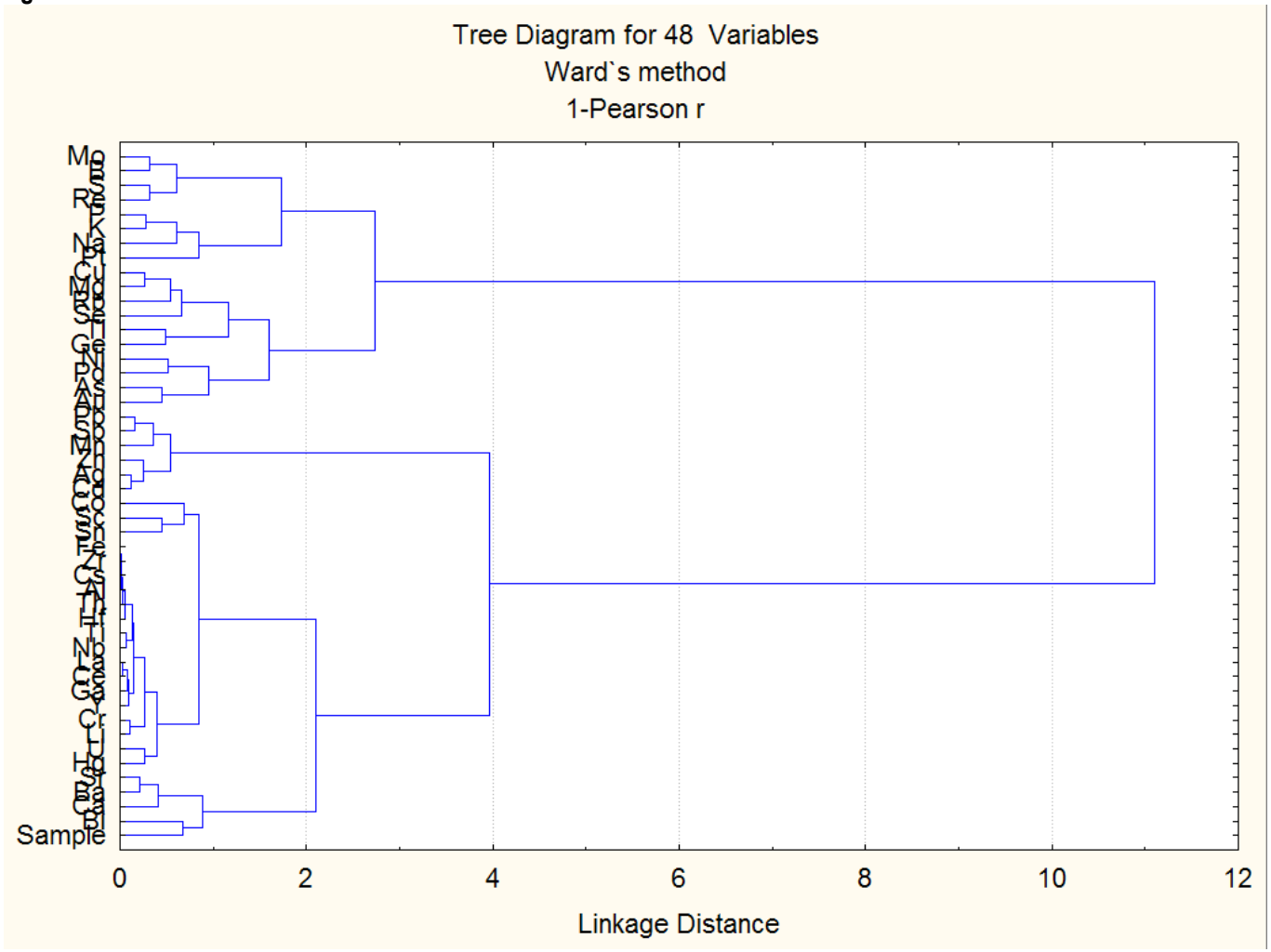
Tree Diagram for 48 Variables
Ward`s method
1-Pearson r
Sample
0
2
4
6
8
10
12
Linkage Distance

Figure 53.

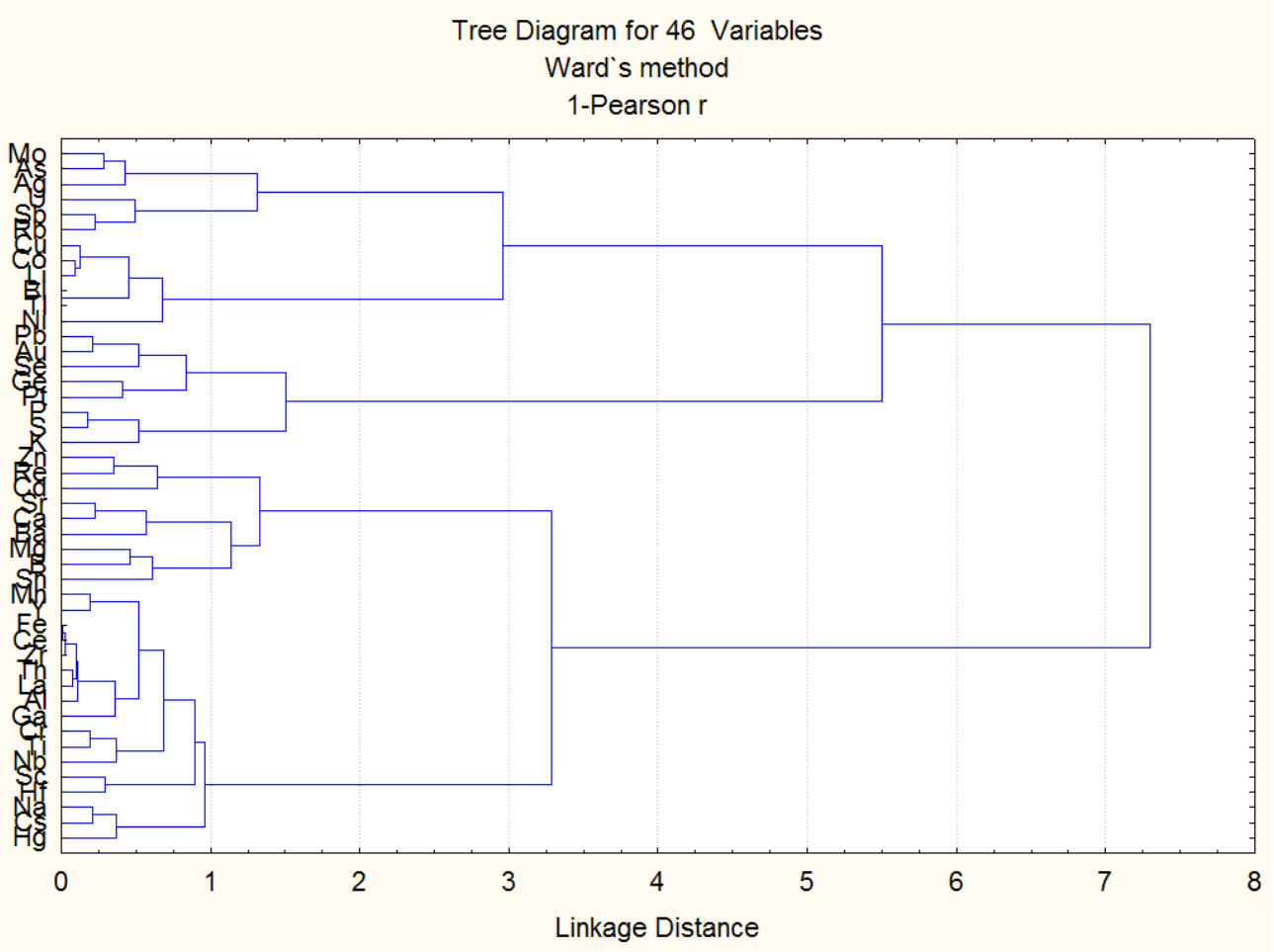
Tree Diagram for 46 Variables
Ward`s method
1-Pearson r
0
1
2
3
4
5
6
7
8
Linkage Distance

Figure 54.

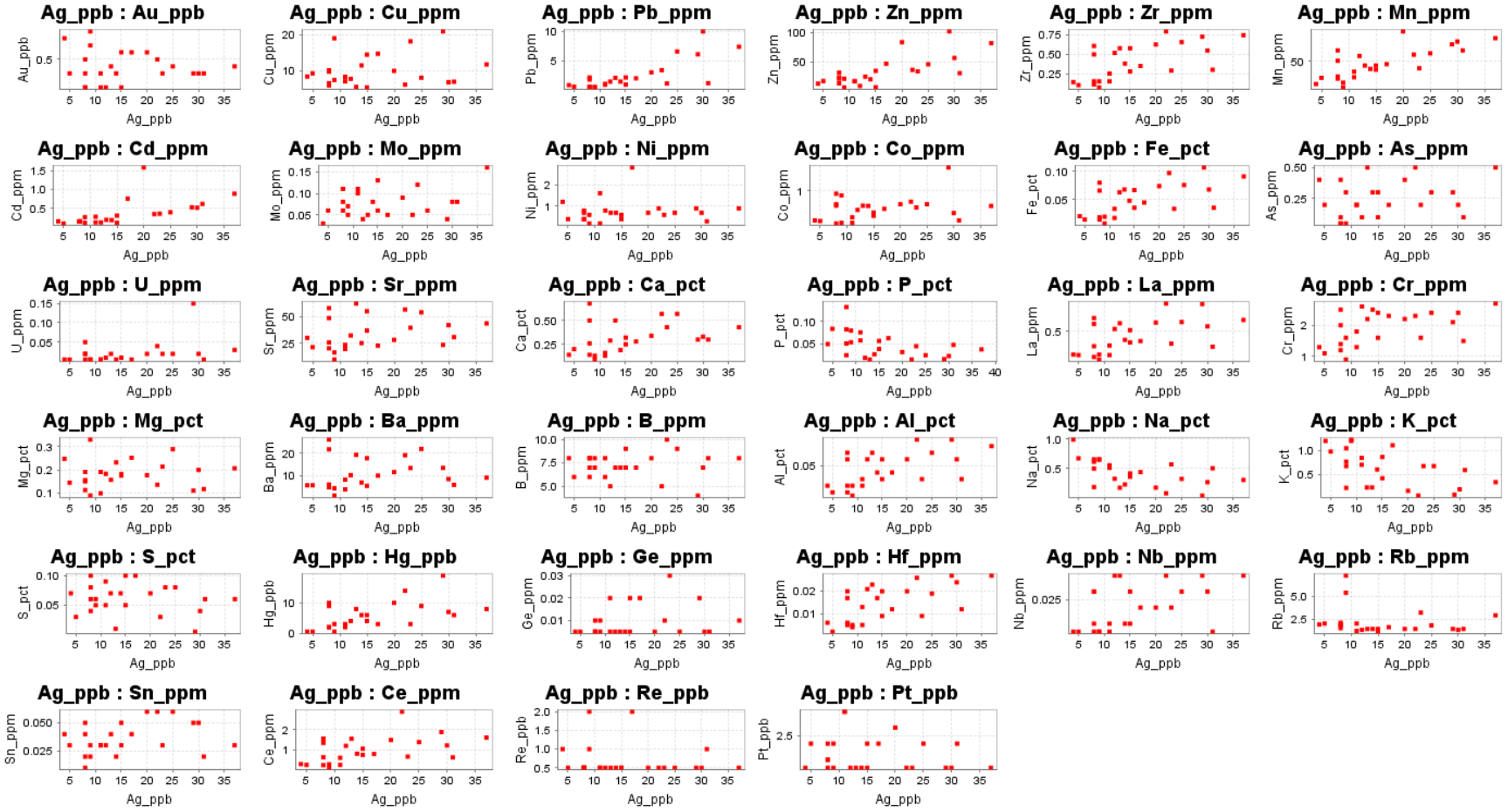
Ag_ppb : Au_ppb
Ag_ppb : Cu_ppm
Ag_ppb : Pb_ppm
Ag_ppb : Zn_ppm
Ag_ppb : Zr_ppm
Ag_ppb : Mn_ppm
Ag_ppb : Cd_ppm
Ag_ppb : Mo_ppm
Ag_ppb : Ni_ppm
Ag_ppb : Co_ppm
Ag_ppb : Fe_pct
Ag_ppb : As_ppm
Ag_ppb : U_ppm
Ag_ppb : Sr_ppm
Ag_ppb : Ca_pct
Ag_ppb : P_pct
Ag_ppb : La_ppm
Ag_ppb : Cr_ppm
Ag_ppb : Mg_pct
Ag_ppb : Ba_ppm
Ag_ppb : B_ppm
Ag_ppb : Al_pct
Ag_ppb : Na_pct
Ag_ppb : K_pct
Ag_ppb : S_pct
Ag_ppb : Hg_ppb
Ag_ppb : Ge_ppm
Ag_ppb : Hf_ppm
Ag_ppb : Nb_ppm
Ag_ppb : Rb_ppm
Ag_ppb : Sn_ppm
Ag_ppb : Ce_ppm
Ag_ppb : Re_ppb
Ag_ppb : Pt_ppb
Au_ppb
Cu_ppm
Pb_ppm
Zn_ppm
Zr_ppm
Mn_ppm
Cd_ppm
Mo_ppm
Ni_ppm
Co_ppm
Fe_pct
As_ppm
U_ppm
Sr_ppm
Ca_pct
P_pct
La_ppm
Cr_ppm
Mg_pct
Ba_ppm
B_ppm
Al_pct
Na_pct
K_pct
S_pct
Hg_ppb
Ge_ppm
Hf_ppm
Nb_ppm
Rb_ppm
Sn_ppm
Ce_ppm
Re_ppb
Pt_ppb
Ag_ppb

Figure 55.

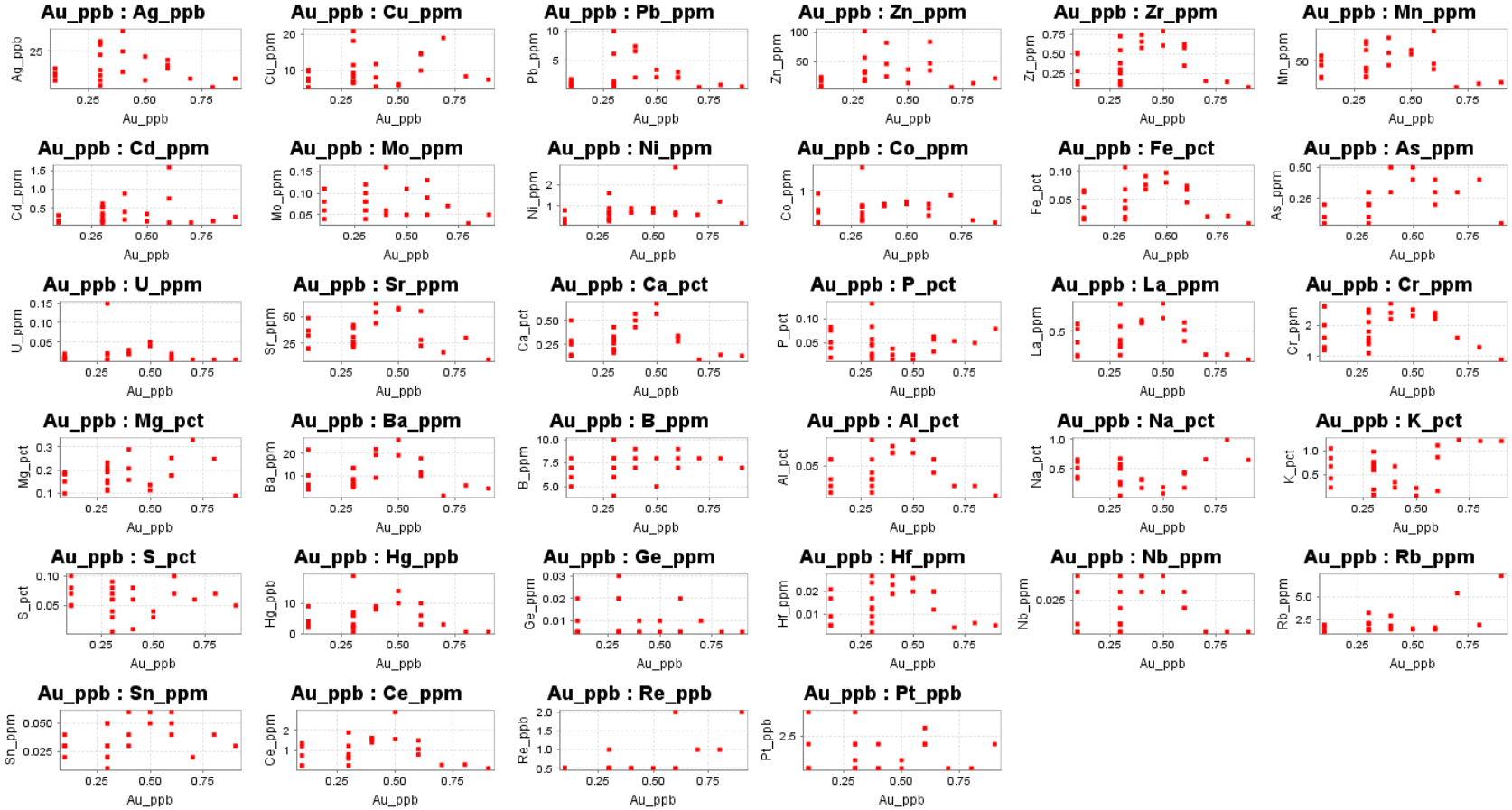
Au_ppb : Ag_ppb
Au_ppb : Cu_ppm
Au_ppb : Pb_ppm
Au_ppb : Zn_ppm
Au_ppb : Zr_ppm
Au_ppb : Mn_ppm
Au_ppb : Cd_ppm
Au_ppb : Mo_ppm
Au_ppb : Ni_ppm
Au_ppb : Co_ppm
Au_ppb : Fe_pct
Au_ppb : As_ppm
Au_ppb : U_ppm
Au_ppb : Sr_ppm
Au_ppb : Ca_pct
Au_ppb : P_pct
Au_ppb : La_ppm
Au_ppb : Cr_ppm
Au_ppb : Mg_pct
Au_ppb : Ba_ppm
Au_ppb : B_ppm
Au_ppb : Al_pct
Au_ppb : Na_pct
Au_ppb : K_pct
Au_ppb : S_pct
Au_ppb : Hg_ppb
Au_ppb : Ge_ppm
Au_ppb : Hf_ppm
Au_ppb : Nb_ppm
Au_ppb : Rb_ppm
Au_ppb : Sn_ppm
Au_ppb : Ce_ppm
Au_ppb : Re_ppb
Au_ppb : Pt_ppb
Au_ppb

Figure 56.

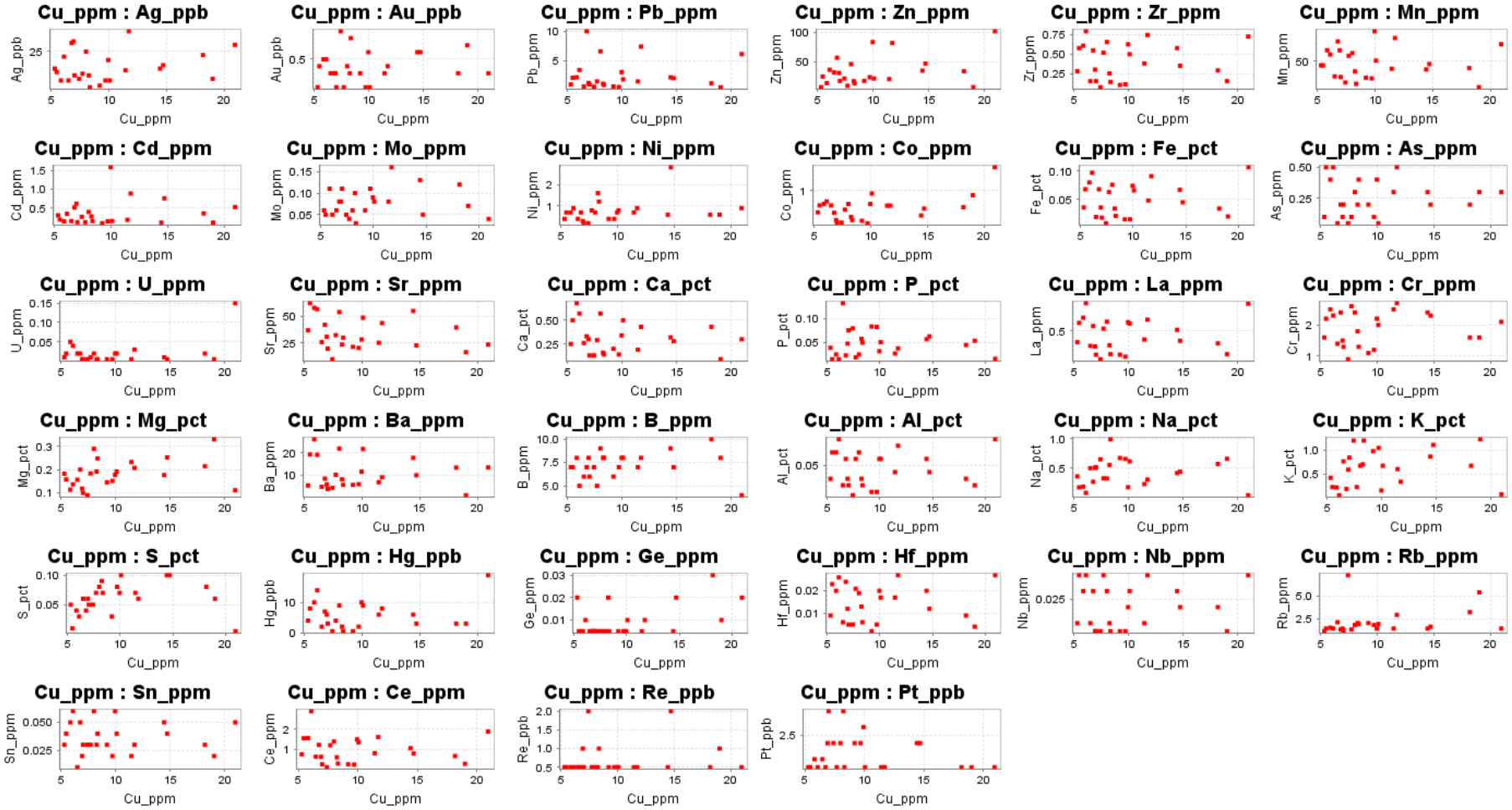
Cu_ppm : Ag_ppb
Cu_ppm : Au_ppb
Cu_ppm : Pb_ppm
Cu_ppm : Zn_ppm
Cu_ppm : Zr_ppm
Cu_ppm : Mn_ppm
Cu_ppm : Cd_ppm
Cu_ppm : Mo_ppm
Cu_ppm : Ni_ppm
Cu_ppm : Co_ppm
Cu_ppm : Fe_pct
Cu_ppm : As_ppm
Cu_ppm : U_ppm
Cu_ppm : Sr_ppm
Cu_ppm : Ca_pct
Cu_ppm : P_pct
Cu_ppm : La_ppm
Cu_ppm : Cr_ppm
Cu_ppm : Mg_pct
Cu_ppm : Ba_ppm
Cu_ppm : B_ppm
Cu_ppm : Al_pct
Cu_ppm : Na_pct
Cu_ppm : K_pct
Cu_ppm : S_pct
Cu_ppm : Hg_ppb
Cu_ppm : Ge_ppm
Cu_ppm : Hf_ppm
Cu_ppm : Nb_ppm
Cu_ppm : Rb_ppm
Cu_ppm : Sn_ppm
Cu_ppm : Ce_ppm
Cu_ppm : Re_ppb
Cu_ppm : Pt_ppb
Cu_ppm

Figure 57.

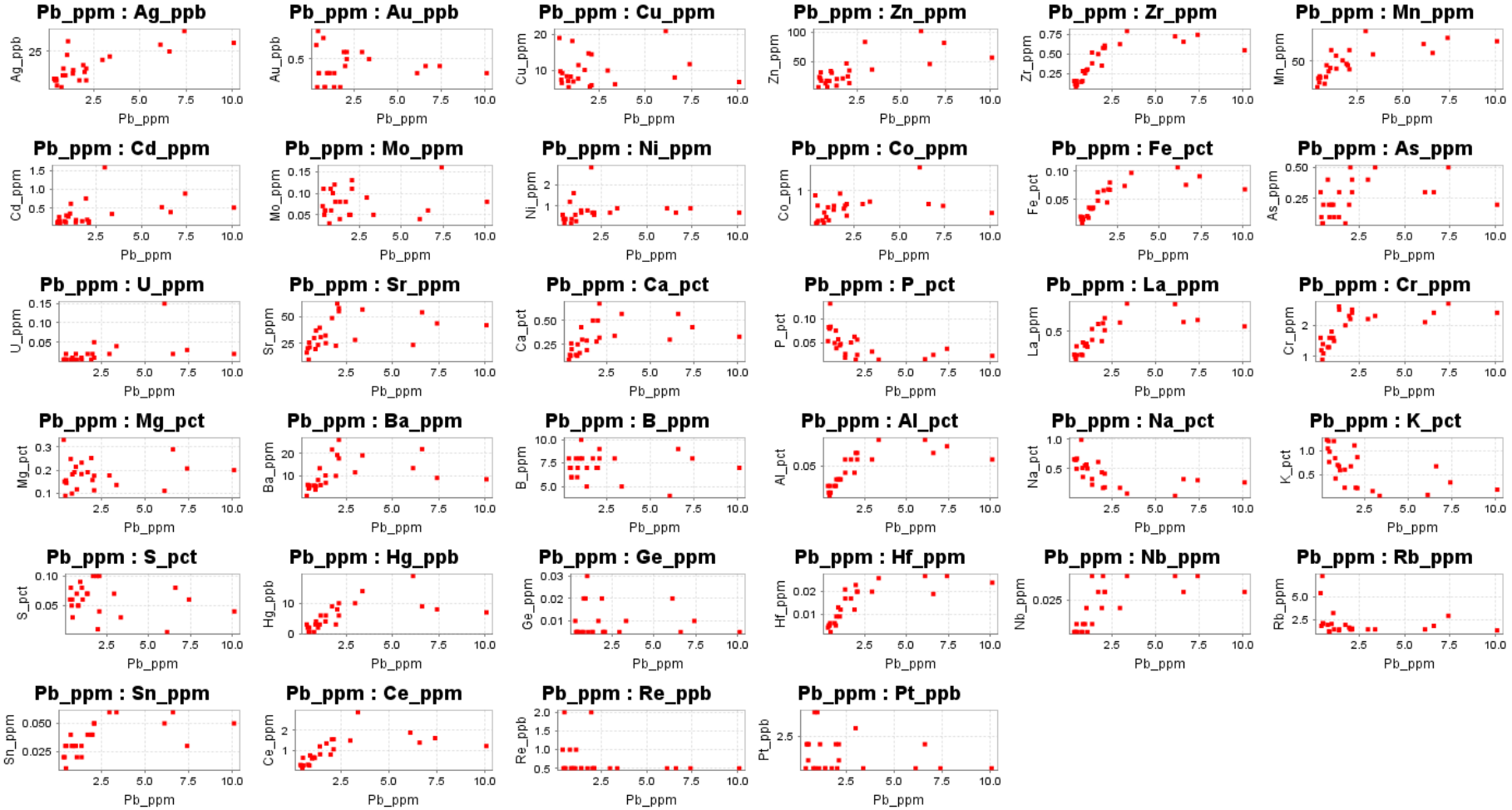
Pb_ppm : Ag_ppb
Pb_ppm : Au_ppb
Pb_ppm : Cu_ppm
Pb_ppm : Zn_ppm
Pb_ppm : Zr_ppm
Pb_ppm : Mn_ppm
Pb_ppm : Cd_ppm
Pb_ppm : Mo_ppm
Pb_ppm : Ni_ppm
Pb_ppm : Co_ppm
Pb_ppm : Fe_pct
Pb_ppm : As_ppm
Pb_ppm : U_ppm
Pb_ppm : Sr_ppm
Pb_ppm : Ca_pct
Pb_ppm : P_pct
Pb_ppm : La_ppm
Pb_ppm : Cr_ppm
Pb_ppm : Mg_pct
Pb_ppm : Ba_ppm
Pb_ppm : B_ppm
Pb_ppm : Al_pct
Pb_ppm : Na_pct
Pb_ppm : K_pct
Pb_ppm : S_pct
Pb_ppm : Hg_ppb
Pb_ppm : Ge_ppm
Pb_ppm : Hf_ppm
Pb_ppm : Nb_ppm
Pb_ppm : Rb_ppm
Pb_ppm : Sn_ppm
Pb_ppm : Ce_ppm
Pb_ppm : Re_ppb
Pb_ppm : Pt_ppb
Pb_ppm

Figure 58.

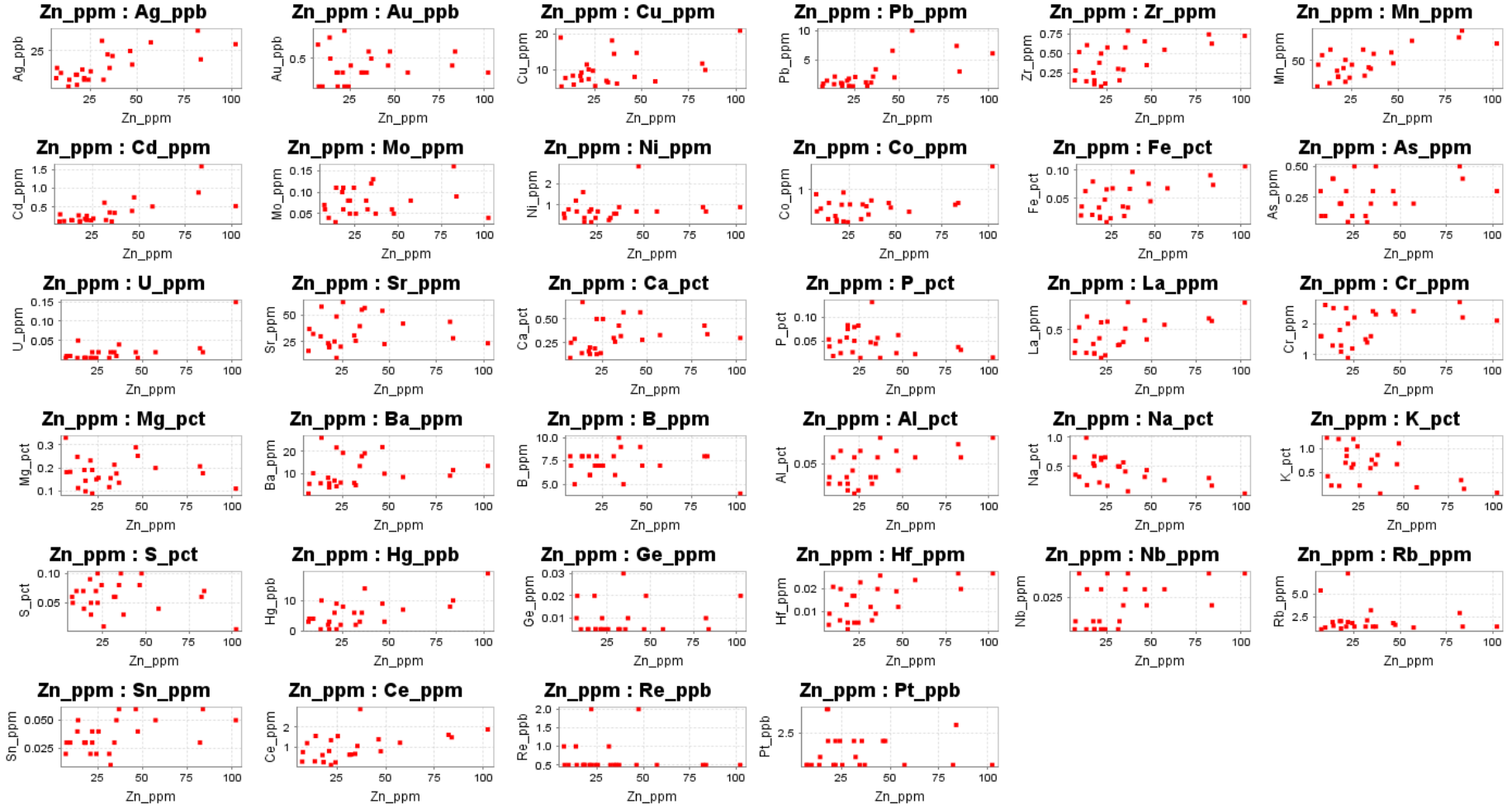
Zn_ppm : Ag_ppb
Zn_ppm : Au_ppb
Zn_ppm : Cu_ppm
Zn_ppm : Pb_ppm
Zn_ppm : Zr_ppm
Zn_ppm : Mn_ppm
Zn_ppm : Cd_ppm
Zn_ppm : Mo_ppm
Zn_ppm : Ni_ppm
Zn_ppm : Co_ppm
Zn_ppm : Fe_pct
Zn_ppm : As_ppm
Zn_ppm : U_ppm
Zn_ppm : Sr_ppm
Zn_ppm : Ca_pct
Zn_ppm : P_pct
Zn_ppm : La_ppm
Zn_ppm : Cr_ppm
Zn_ppm : Mg_pct
Zn_ppm : Ba_ppm
Zn_ppm : B_ppm
Zn_ppm : Al_pct
Zn_ppm : Na_pct
Zn_ppm : K_pct
Zn_ppm : S_pct
Zn_ppm : Hg_ppb
Zn_ppm : Ge_ppm
Zn_ppm : Hf_ppm
Zn_ppm : Nb_ppm
Zn_ppm : Rb_ppm
Zn_ppm : Sn_ppm
Zn_ppm : Ce_ppm
Zn_ppm : Re_ppb
Zn_ppm : Pt_ppb
Zn_ppm

Figure 59

.

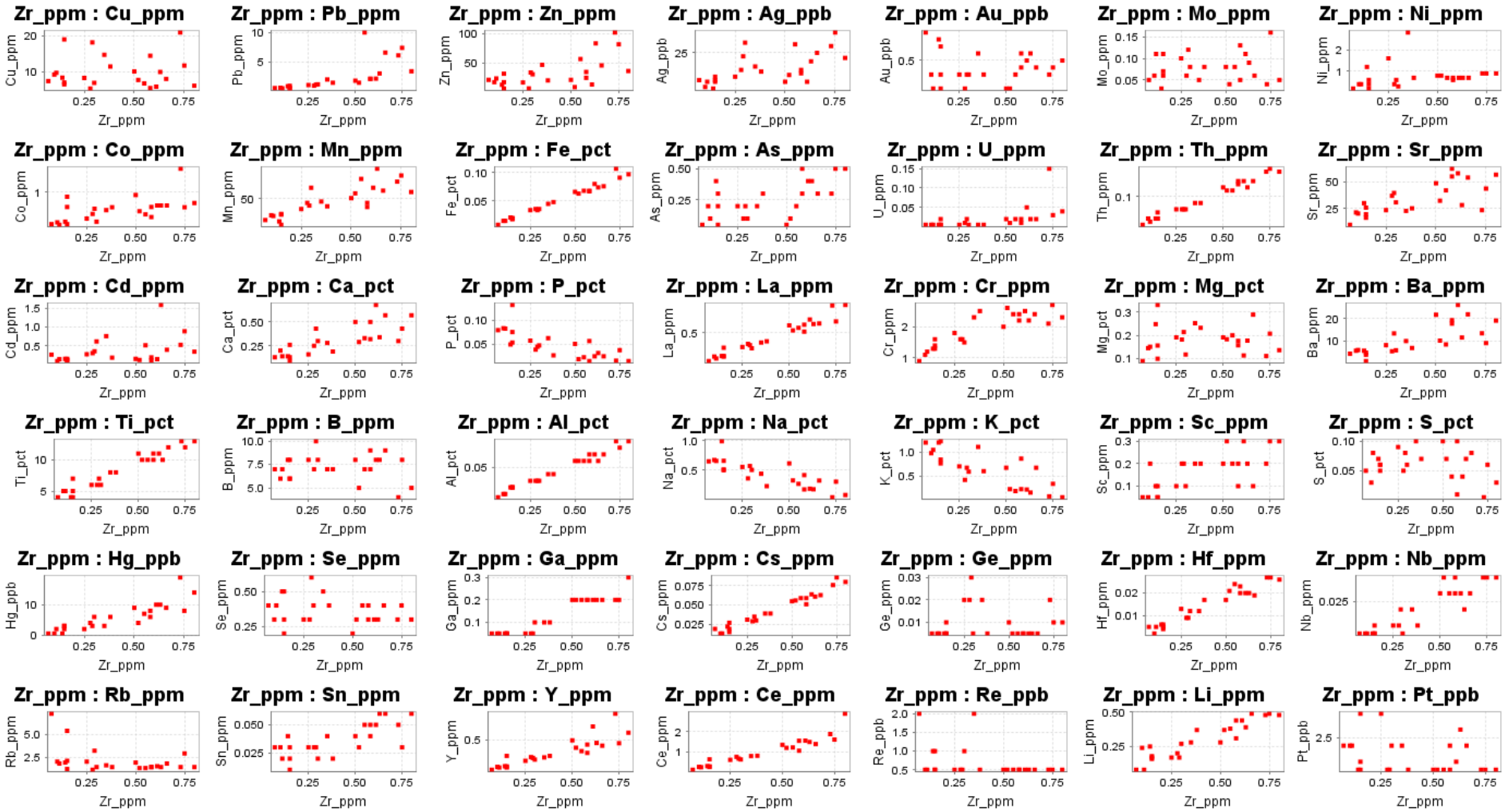
Zr_ppm : Cu_ppm
Zr_ppm : Pb_ppm
Zr_ppm : Zn_ppm
Zr_ppm : Ag_ppb
Zr_ppm : Au_ppb
Zr_ppm : Mo_ppm
Zr_ppm : Ni_ppm
Zr_ppm : Co_ppm
Zr_ppm : Mn_ppm
Zr_ppm : Fe_pct
Zr_ppm : As_ppm
Zr_ppm : U_ppm
Zr_ppm : Th_ppm
Zr_ppm : Sr_ppm
Zr_ppm : Cd_ppm
Zr_ppm : Ca_pct
Zr_ppm : P_pct
Zr_ppm : La_ppm
Zr_ppm : Cr_ppm
Zr_ppm : Mg_pct
Zr_ppm : Ba_ppm
Zr_ppm : Ti_pct
Zr_ppm : B_ppm
Zr_ppm : Al_pct
Zr_ppm : Na_pct
Zr_ppm : K_pct
Zr_ppm : Sc_ppm
Zr_ppm : S_pct
Zr_ppm : Hg_ppb
Zr_ppm : Se_ppm
Zr_ppm : Ga_ppm
Zr_ppm : Cs_ppm
Zr_ppm : Ge_ppm
Zr_ppm : Hf_ppm
Zr_ppm : Nb_ppm
Zr_ppm : Rb_ppm
Zr_ppm : Sn_ppm
Zr_ppm : Y_ppm
Zr_ppm : Ce_ppm
Zr_ppm : Re_ppb
Zr_ppm : Li_ppm
Zr_ppm : Pt_ppb
Zr_ppm

Figure 60.

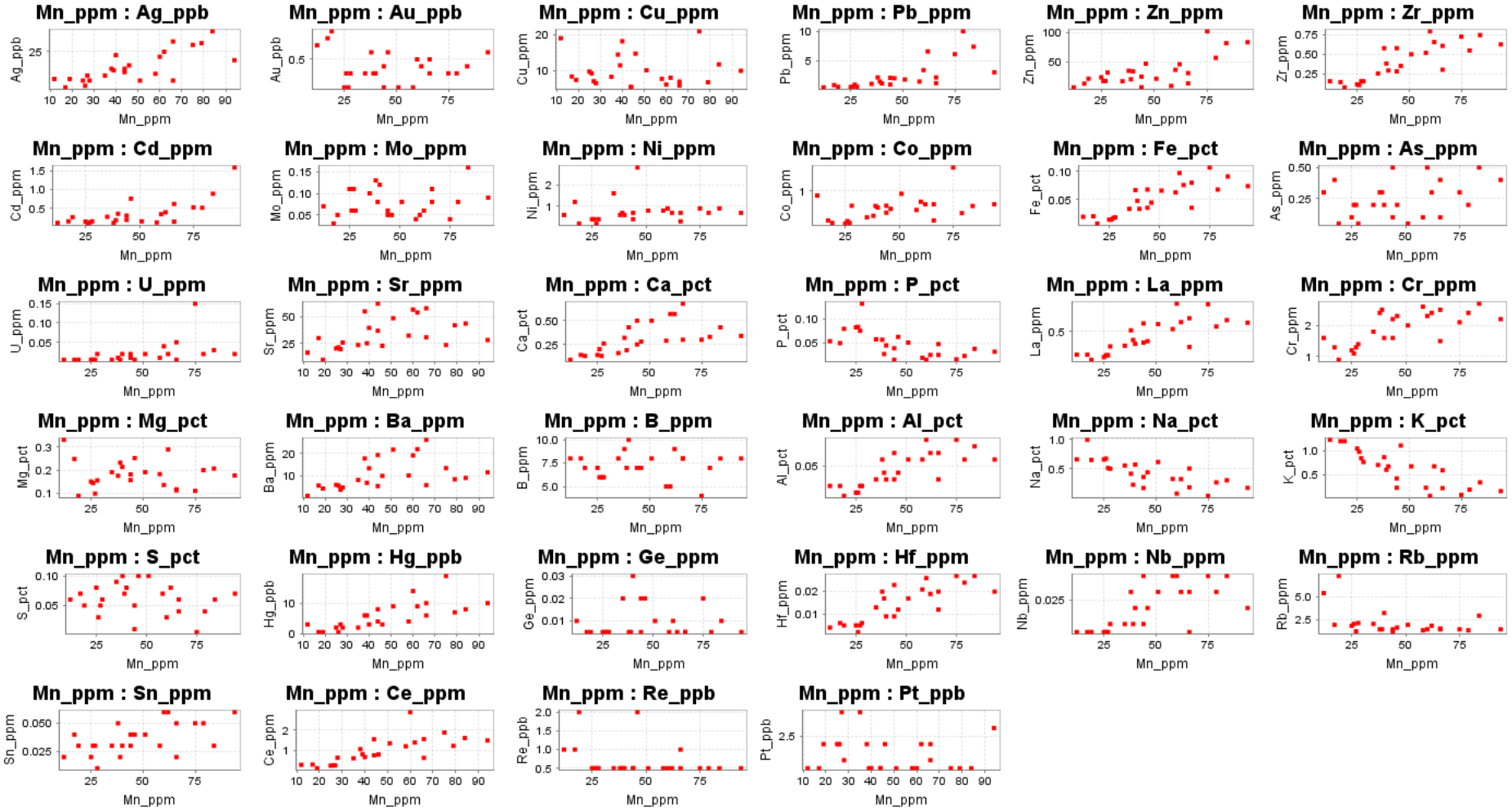
Mn_ppm : Ag_ppb
Mn_ppm : Au_ppb
Mn_ppm : Cu_ppm
Mn_ppm : Pb_ppm
Mn_ppm : Zn_ppm
Mn_ppm : Zr_ppm
Mn_ppm : Cd_ppm
Mn_ppm : Mo_ppm
Mn_ppm : Ni_ppm
Mn_ppm : Co_ppm
Mn_ppm : Fe_pct
Mn_ppm : As_ppm
Mn_ppm : U_ppm
Mn_ppm : Sr_ppm
Mn_ppm : Ca_pct
Mn_ppm : P_pct
Mn_ppm : La_ppm
Mn_ppm : Cr_ppm
Mn_ppm : Mg_pct
Mn_ppm : Ba_ppm
Mn_ppm : B_ppm
Mn_ppm : Al_pct
Mn_ppm : Na_pct
Mn_ppm : K_pct
Mn_ppm : S_pct
Mn_ppm : Hg_ppb
Mn_ppm : Ge_ppm
Mn_ppm : Hf_ppm
Mn_ppm : Nb_ppm
Mn_ppm : Rb_ppm
Mn_ppm : Sn_ppm
Mn_ppm : Ce_ppm
Mn_ppm : Re_ppb
Mn_ppm : Pt_ppb
Mn_ppm

Figure 61.

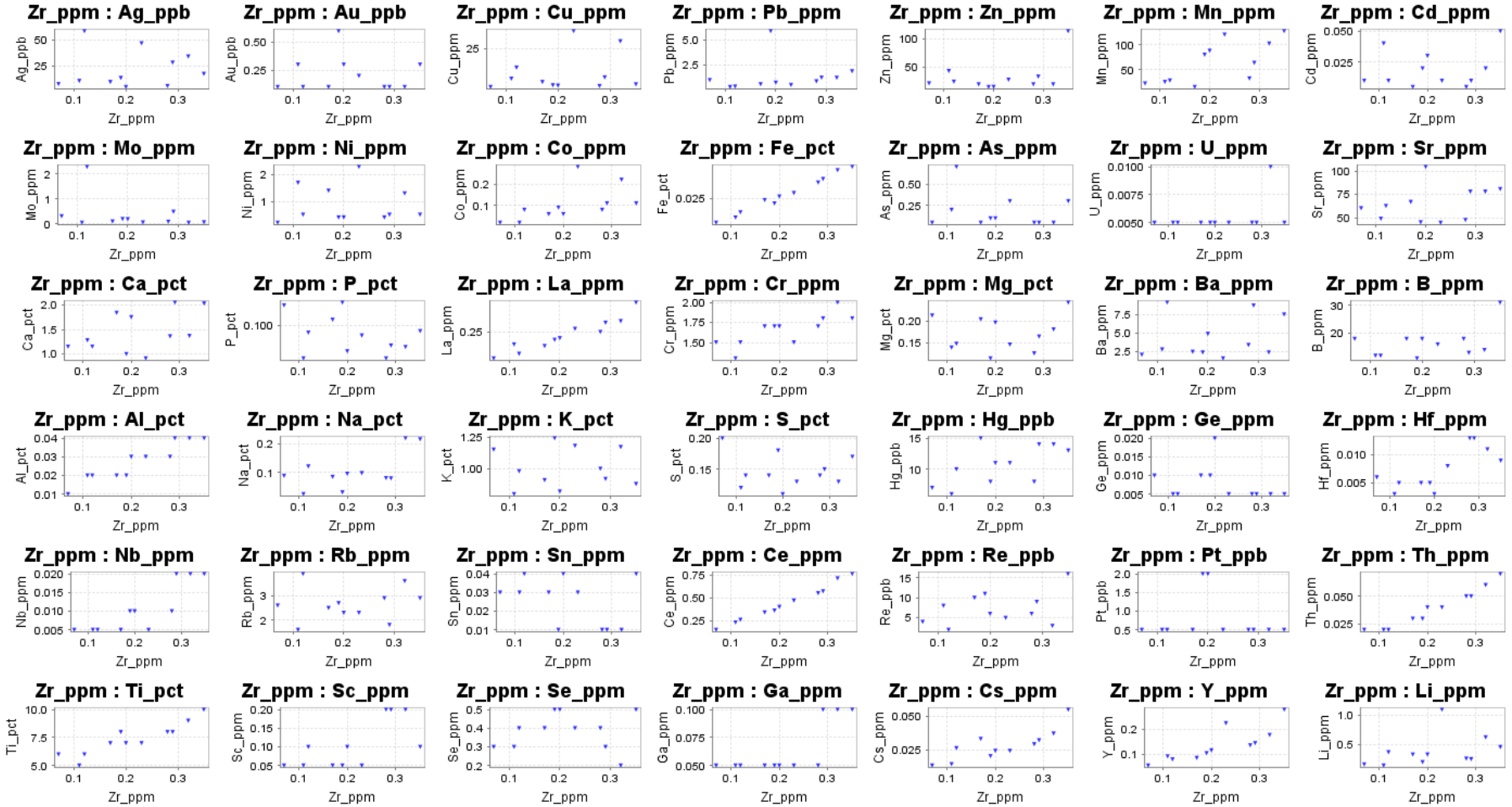
Zr_ppm : Ag_ppb
Zr_ppm : Au_ppb
Zr_ppm : Cu_ppm
Zr_ppm : Pb_ppm
Zr_ppm : Zn_ppm
Zr_ppm : Mn_ppm
Zr_ppm : Cd_ppm
Zr_ppm : Mo_ppm
Zr_ppm : Ni_ppm
Zr_ppm : Co_ppm
Zr_ppm : Fe_pct
Zr_ppm : As_ppm
Zr_ppm : U_ppm
Zr_ppm : Sr_ppm
Zr_ppm : Ca_pct
Zr_ppm : P_pct
Zr_ppm : La_ppm
Zr_ppm : Cr_ppm
Zr_ppm : Mg_pct
Zr_ppm : Ba_ppm
Zr_ppm : B_ppm
Zr_ppm : Al_pct
Zr_ppm : Na_pct
Zr_ppm : K_pct
Zr_ppm : S_pct
Zr_ppm : Hg_ppb
Zr_ppm : Ge_ppm
Zr_ppm : Hf_ppm
Zr_ppm : Nb_ppm
Zr_ppm : Rb_ppm
Zr_ppm : Sn_ppm
Zr_ppm : Ce_ppm
Zr_ppm : Re_ppb
Zr_ppm : Pt_ppb
Zr_ppm : Th_ppm
Zr_ppm : Ti_pct
Zr_ppm : Sc_ppm
Zr_ppm : Se_ppm
Zr_ppm : Ga_ppm
Zr_ppm : Cs_ppm
Zr_ppm : Y_ppm
Zr_ppm : Li_ppm
Zr_ppm

Figure 62.

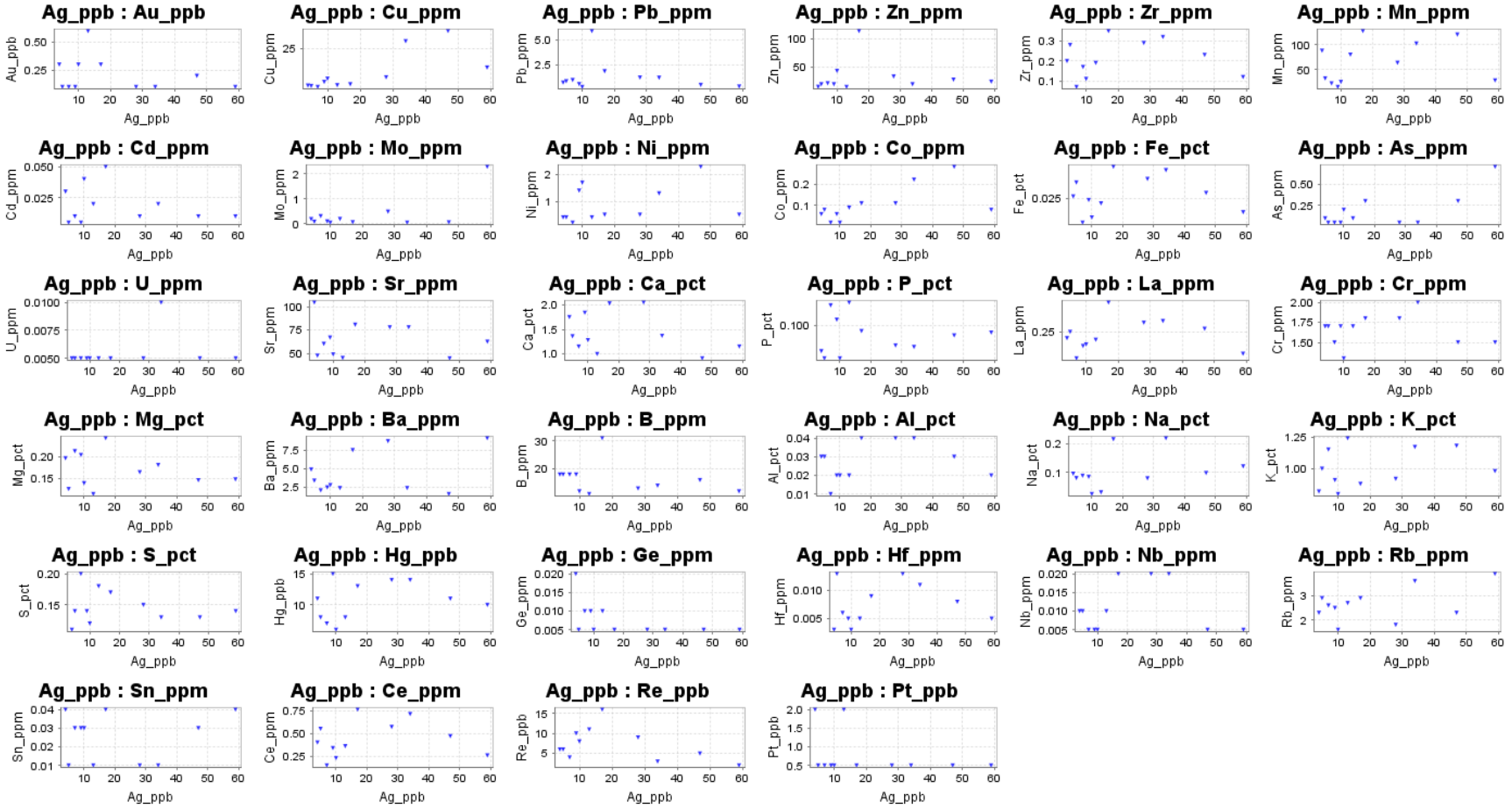
Ag_ppb : Au_ppb
Au_ppb
Ag_ppb : Cu_ppm
Cu_ppm
Ag_ppb : Pb_ppm
Pb_ppm
Ag_ppb : Zn_ppm
Zn_ppm
Ag_ppb : Zr_ppm
Zr_ppm
Ag_ppb : Mn_ppm
Mn_ppm
Ag_ppb : Cd_ppm
Cd_ppm
Ag_ppb : Mo_ppm
Mo_ppm
Ag_ppb : Ni_ppm
Ni_ppm
Ag_ppb : Co_ppm
Co_ppm
Ag_ppb : Fe_pct
Fe_pct
Ag_ppb : As_ppm
As_ppm
Ag_ppb : U_ppm
U_ppm
Ag_ppb : Sr_ppm
Sr_ppm
Ag_ppb : Ca_pct
Ca_pct
Ag_ppb : P_pct
P_pct
Ag_ppb : La_ppm
La_ppm
Ag_ppb : Cr_ppm
Cr_ppm
Ag_ppb : Mg_pct
Mg_pct
Ag_ppb : Ba_ppm
Ba_ppm
Ag_ppb : B_ppm
B_ppm
Ag_ppb : Al_pct
Al_pct
Ag_ppb : Na_pct
Na_pct
Ag_ppb : K_pct
K_pct
Ag_ppb : S_pct
S_pct
Ag_ppb : Hg_ppb
Hg_ppb
Ag_ppb : Ge_ppm
Ge_ppm
Ag_ppb : Hf_ppm
Hf_ppm
Ag_ppb : Nb_ppm
Nb_ppm
Ag_ppb : Rb_ppm
Rb_ppm
Ag_ppb : Sn_ppm
Sn_ppm
Ag_ppb : Ce_ppm
Ce_ppm
Ag_ppb : Re_ppb
Re_ppb
Ag_ppb : Pt_ppb
Pt_ppb
Ag_ppb

Figure 63.

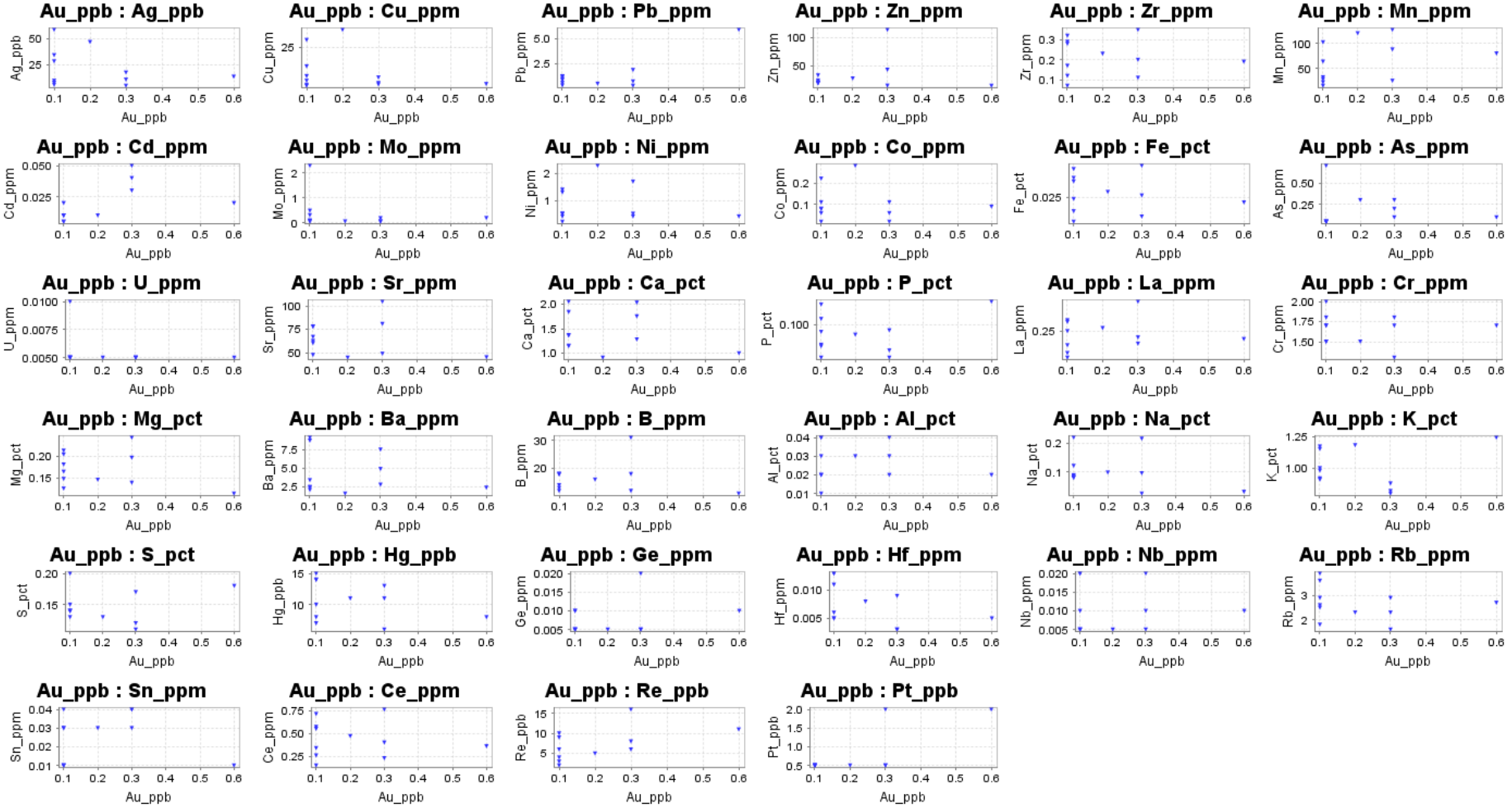
Au_ppb : Ag_ppb
Au_ppb : Cu_ppm
Au_ppb : Pb_ppm
Au_ppb : Zn_ppm
Au_ppb : Zr_ppm
Au_ppb : Mn_ppm
Au_ppb : Cd_ppm
Au_ppb : Mo_ppm
Au_ppb : Ni_ppm
Au_ppb : Co_ppm
Au_ppb : Fe_pct
Au_ppb : As_ppm
Au_ppb : U_ppm
Au_ppb : Sr_ppm
Au_ppb : Ca_pct
Au_ppb : P_pct
Au_ppb : La_ppm
Au_ppb : Cr_ppm
Au_ppb : Mg_pct
Au_ppb : Ba_ppm
Au_ppb : B_ppm
Au_ppb : Al_pct
Au_ppb : Na_pct
Au_ppb : K_pct
Au_ppb : S_pct
Au_ppb : Hg_ppb
Au_ppb : Ge_ppm
Au_ppb : Hf_ppm
Au_ppb : Nb_ppm
Au_ppb : Rb_ppm
Au_ppb : Sn_ppm
Au_ppb : Ce_ppm
Au_ppb : Re_ppb
Au_ppb : Pt_ppb
Au_ppb

Figure 64.

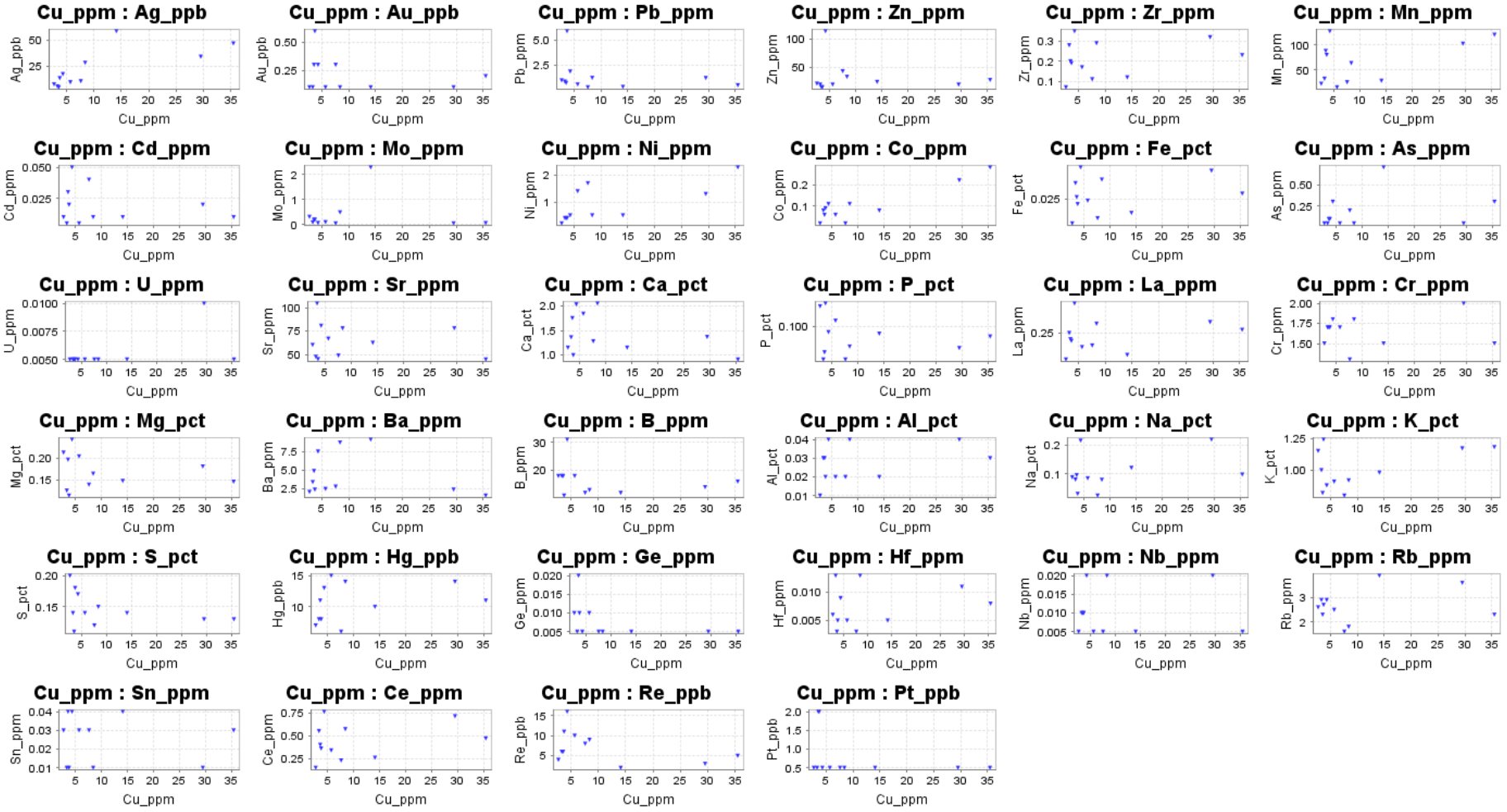
Cu_ppm : Ag_ppb
Cu_ppm : Au_ppb
Cu_ppm : Pb_ppm
Cu_ppm : Zn_ppm
Cu_ppm : Zr_ppm
Cu_ppm : Mn_ppm
Cu_ppm : Cd_ppm
Cu_ppm : Mo_ppm
Cu_ppm : Ni_ppm
Cu_ppm : Co_ppm
Cu_ppm : Fe_pct
Cu_ppm : As_ppm
Cu_ppm : U_ppm
Cu_ppm : Sr_ppm
Cu_ppm : Ca_pct
Cu_ppm : P_pct
Cu_ppm : La_ppm
Cu_ppm : Cr_ppm
Cu_ppm : Mg_pct
Cu_ppm : Ba_ppm
Cu_ppm : B_ppm
Cu_ppm : Al_pct
Cu_ppm : Na_pct
Cu_ppm : K_pct
Cu_ppm : S_pct
Cu_ppm : Hg_ppb
Cu_ppm : Ge_ppm
Cu_ppm : Hf_ppm
Cu_ppm : Nb_ppm
Cu_ppm : Rb_ppm
Cu_ppm : Sn_ppm
Cu_ppm : Ce_ppm
Cu_ppm : Re_ppb
Cu_ppm : Pt_ppb
Cu_ppm

Figure 65.

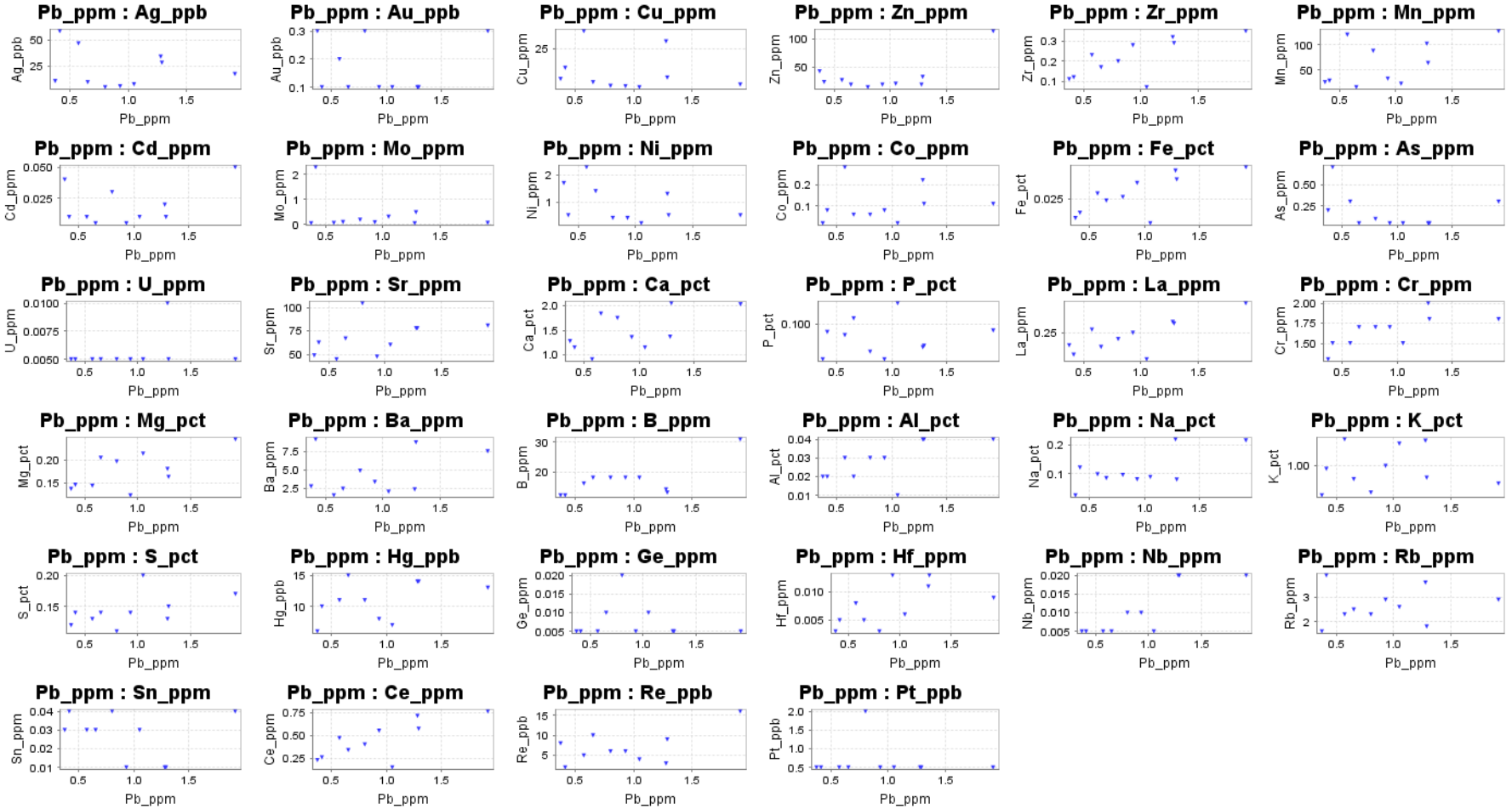
Pb_ppm : Ag_ppb
Pb_ppm : Au_ppb
Pb_ppm : Cu_ppm
Pb_ppm : Zn_ppm
Pb_ppm : Zr_ppm
Pb_ppm : Mn_ppm
Pb_ppm : Cd_ppm
Pb_ppm : Mo_ppm
Pb_ppm : Ni_ppm
Pb_ppm : Co_ppm
Pb_ppm : Fe_pct
Pb_ppm : As_ppm
Pb_ppm : U_ppm
Pb_ppm : Sr_ppm
Pb_ppm : Ca_pct
Pb_ppm : P_pct
Pb_ppm : La_ppm
Pb_ppm : Cr_ppm
Pb_ppm : Mg_pct
Pb_ppm : Ba_ppm
Pb_ppm : B_ppm
Pb_ppm : Al_pct
Pb_ppm : Na_pct
Pb_ppm : K_pct
Pb_ppm : S_pct
Pb_ppm : Hg_ppb
Pb_ppm : Ge_ppm
Pb_ppm : Hf_ppm
Pb_ppm : Nb_ppm
Pb_ppm : Rb_ppm
Pb_ppm : Sn_ppm
Pb_ppm : Ce_ppm
Pb_ppm : Re_ppb
Pb_ppm : Pt_ppb
Pb_ppm

Figure 66.

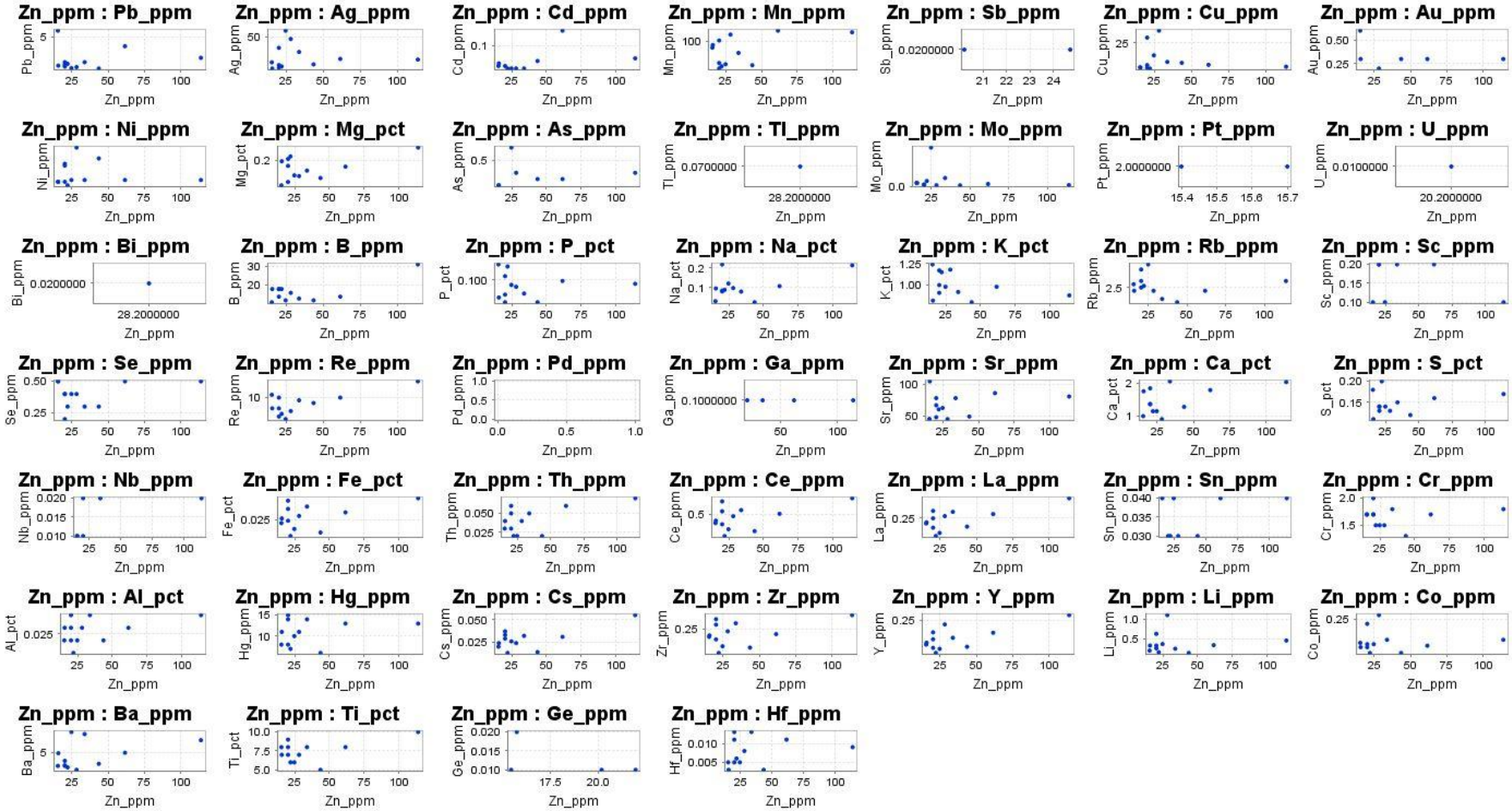
Zn_ppm : Pb_ppm
Zn_ppm : Ag_ppm
Zn_ppm : Cd_ppm
Zn_ppm : Mn_ppm
Zn_ppm : Sb_ppm
Zn_ppm : Cu_ppm
Zn_ppm : Au_ppm
Zn_ppm : Ni_ppm
Zn_ppm : Mg_pct
Zn_ppm : As_ppm
Zn_ppm : Tl_ppm
Zn_ppm : Mo_ppm
Zn_ppm : Pt_ppm
Zn_ppm : U_ppm
Zn_ppm : Bi_ppm
Zn_ppm : B_ppm
Zn_ppm : P_pct
Zn_ppm : Na_pct
Zn_ppm : K_pct
Zn_ppm : Rb_ppm
Zn_ppm : Sc_ppm
Zn_ppm : Se_ppm
Zn_ppm : Re_ppm
Zn_ppm : Pd_ppm
Zn_ppm : Ga_ppm
Zn_ppm : Sr_ppm
Zn_ppm : Ca_pct
Zn_ppm : S_pct
Zn_ppm : Nb_ppm
Zn_ppm : Fe_pct
Zn_ppm : Th_ppm
Zn_ppm : Ce_ppm
Zn_ppm : La_ppm
Zn_ppm : Sn_ppm
Zn_ppm : Cr_ppm
Zn_ppm : Al_pct
Zn_ppm : Hg_ppm
Zn_ppm : Cs_ppm
Zn_ppm : Zr_ppm
Zn_ppm : Y_ppm
Zn_ppm : Li_ppm
Zn_ppm : Co_ppm
Zn_ppm : Ba_ppm
Zn_ppm : Ti_pct
Zn_ppm : Ge_ppm
Zn_ppm : Hf_ppm
Zn_ppm

Figure 67.

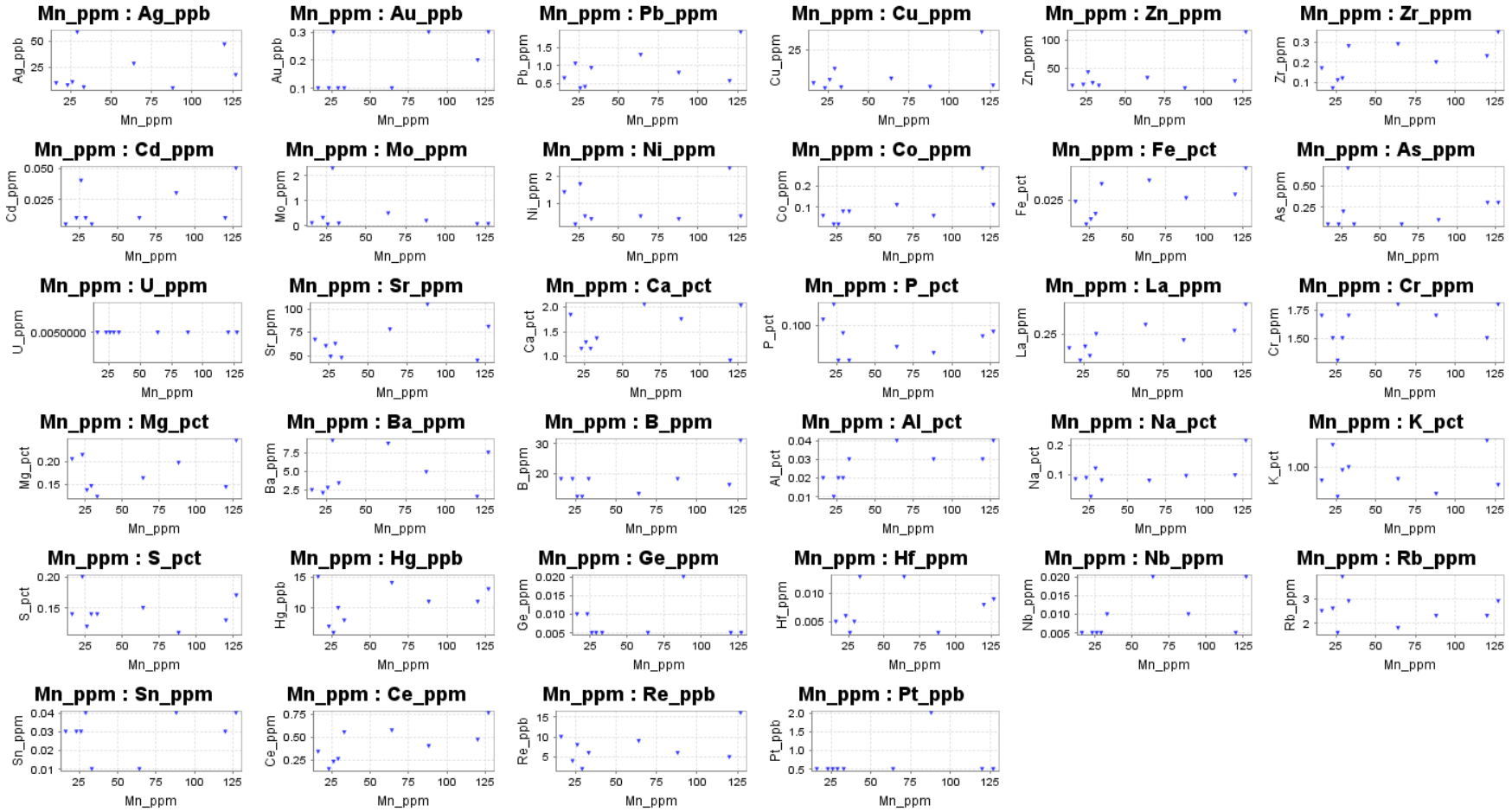

Figure 68.

Figure 68.

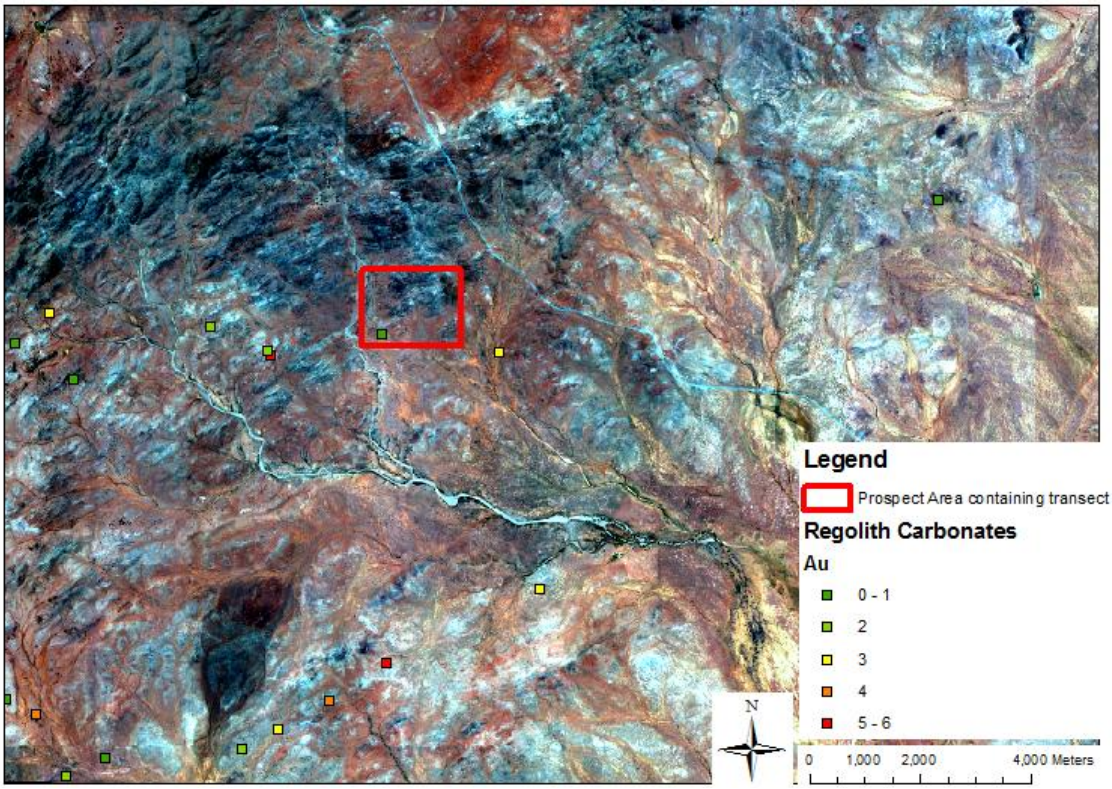
Legend
Prospect Area containing transect
Regolith Carbonates
Au
0 - 1
2
3
4
5 - 6
N
0
1,000
2,000
4,000 Meters

Figure 69.

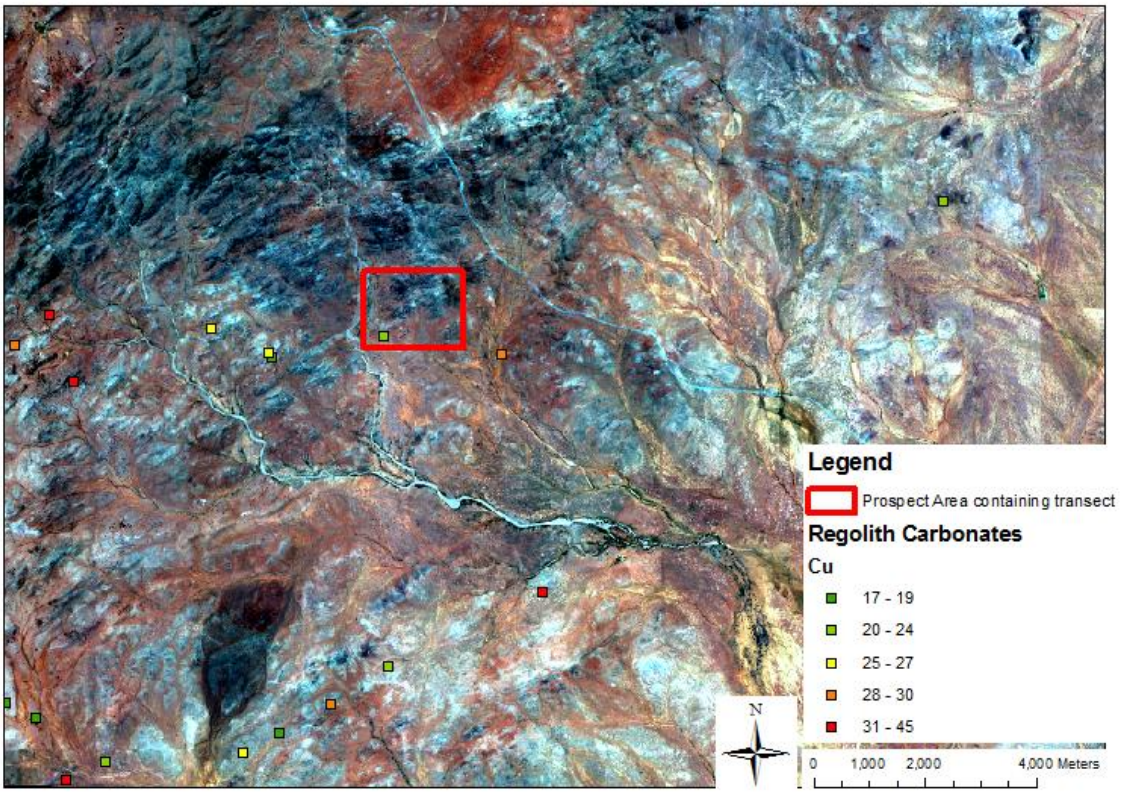
Legend
Prospect Area containing transect
Regolith Carbonates
Cu
17 - 19
20 - 24
25 - 27
28 - 30
31 - 45
N
0
1,000
2,000
4,000 Meters

Figure 70.

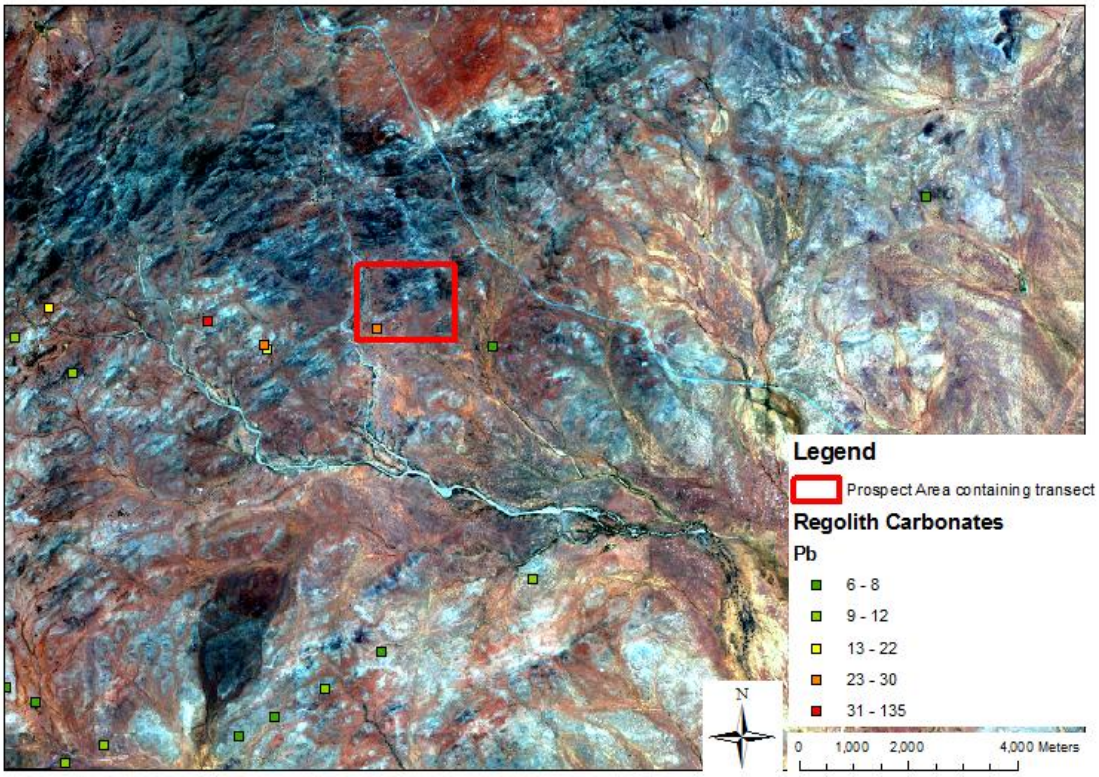
Legend
Prospect Area containing transect
Regolith Carbonates
Pb
6 - 8
9 - 12
13 - 22
23 - 30
31 - 135
N
0
1,000
2,000
4,000 Meters

Figure 71.

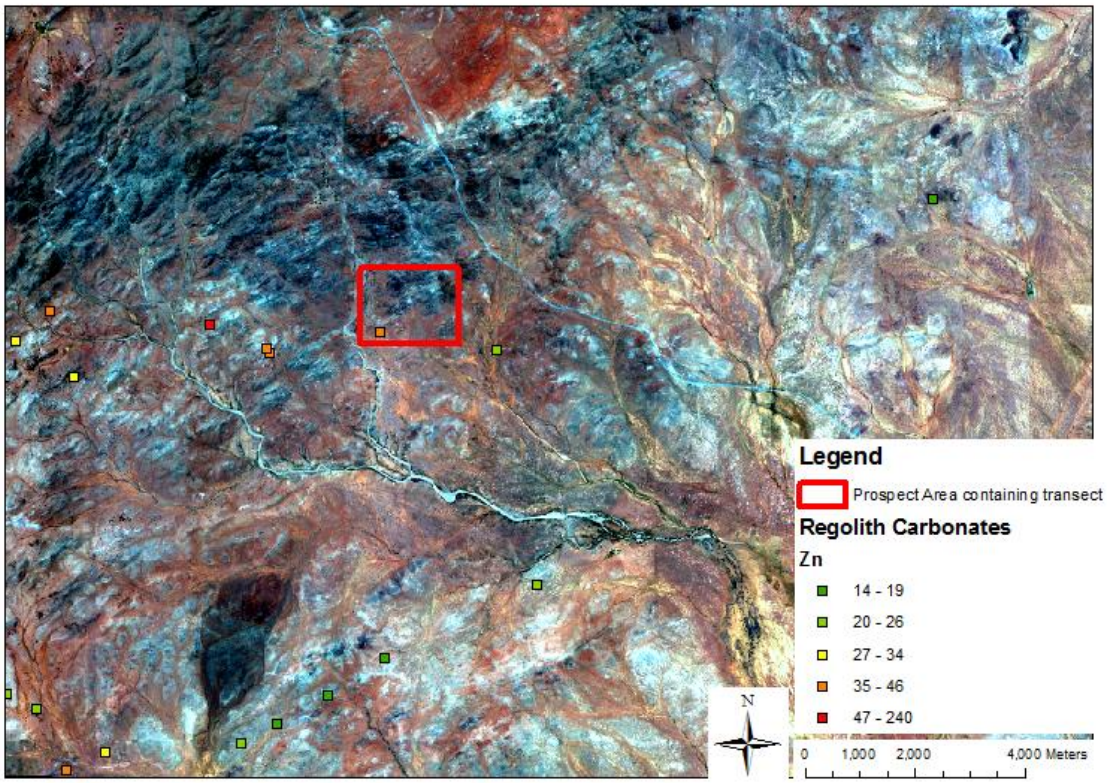
Legend
Prospect Area containing transect
Regolith Carbonates
Zn
14 - 19
20 - 26
27 - 34
35 - 46
47 - 240
N
0
1,000
2,000
4,000 Meters

Figure 72.

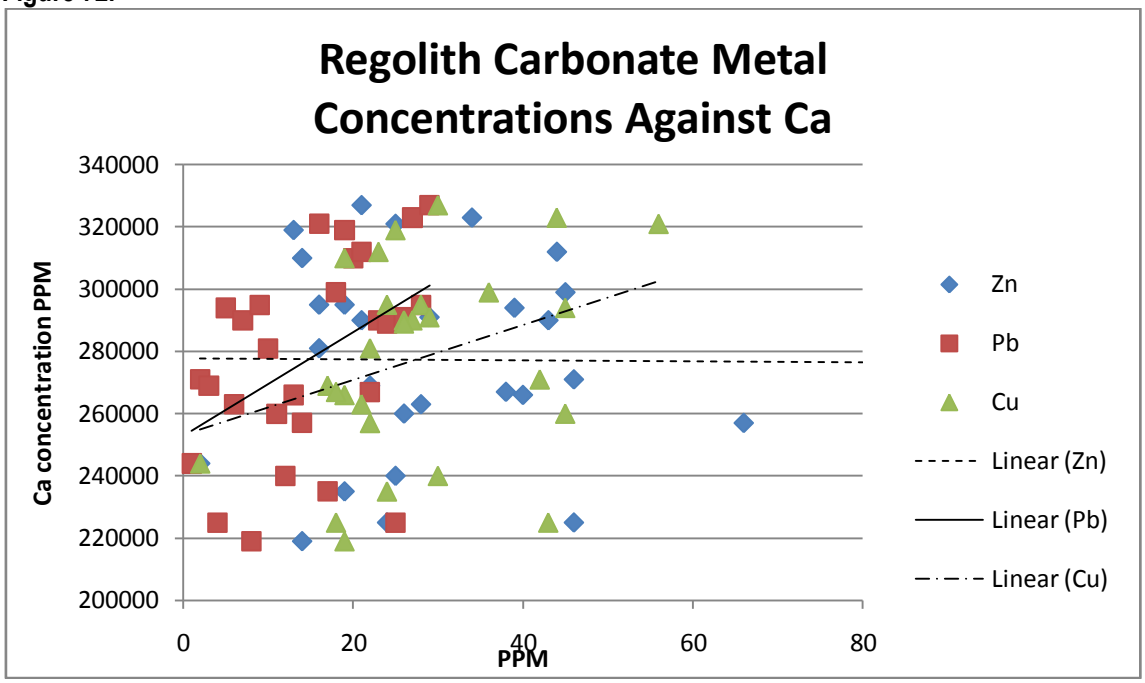
Regolith Carbonate Metal Concentrations Against Ca
Ca concentration PPM
340000
320000
300000
280000
260000
240000
220000
200000
0
20
40
60
80
PPM
Zn
Pb
Cu
Linear (Zn)
Linear (Pb)
Linear (Cu)

Appendix II – Additional plots used to establish conclusions

Appendix 2.1

Geochemical Correlations of R^2 >0.8		
Element	**<80**	**>80**
Ag	Pb, Cd	Mn, Pb, Zn
Cd	Co, Cu, Mg, Zn, Ag	Pb
Co	Zn, Cd, Mg, Cu	Zn, Mn, Fe, Ag
Cu	Cd, Co, Mg	Mn, Fe
Fe	Co, Mn, Mg	Zn, Mn, Cu
Mg	Cd, Co, Cu, Fe	-
Mn	Zn, Fe	Zn, Fe, Ag, Cu
Pb	Zn, Ag	Cd
Zn	Cd, Pb, Co, Mn	Mn, Fe, Ag

Geochemical XY scatter plots for selected elements
Appendix 2.2.1

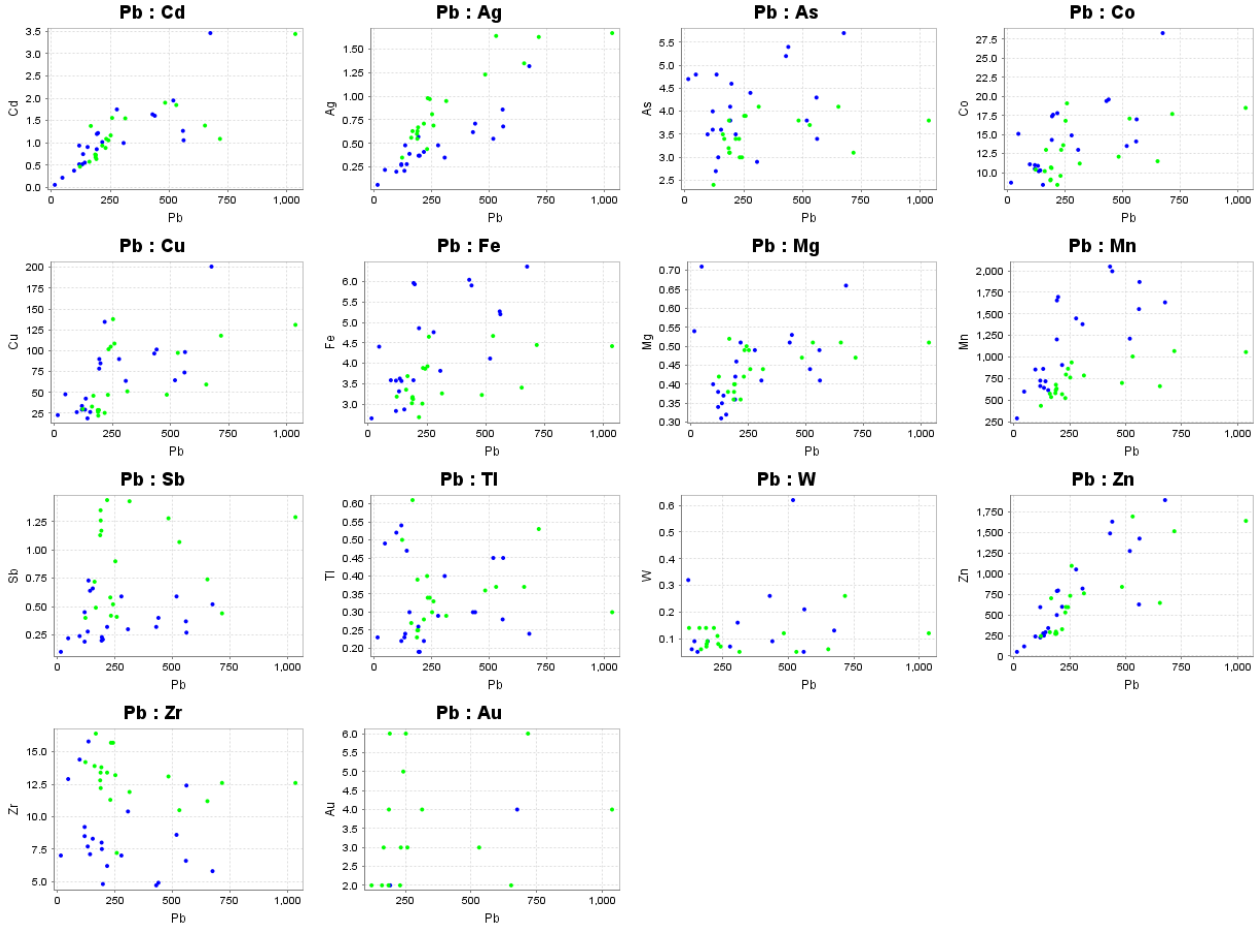

Appendix 2.2.2

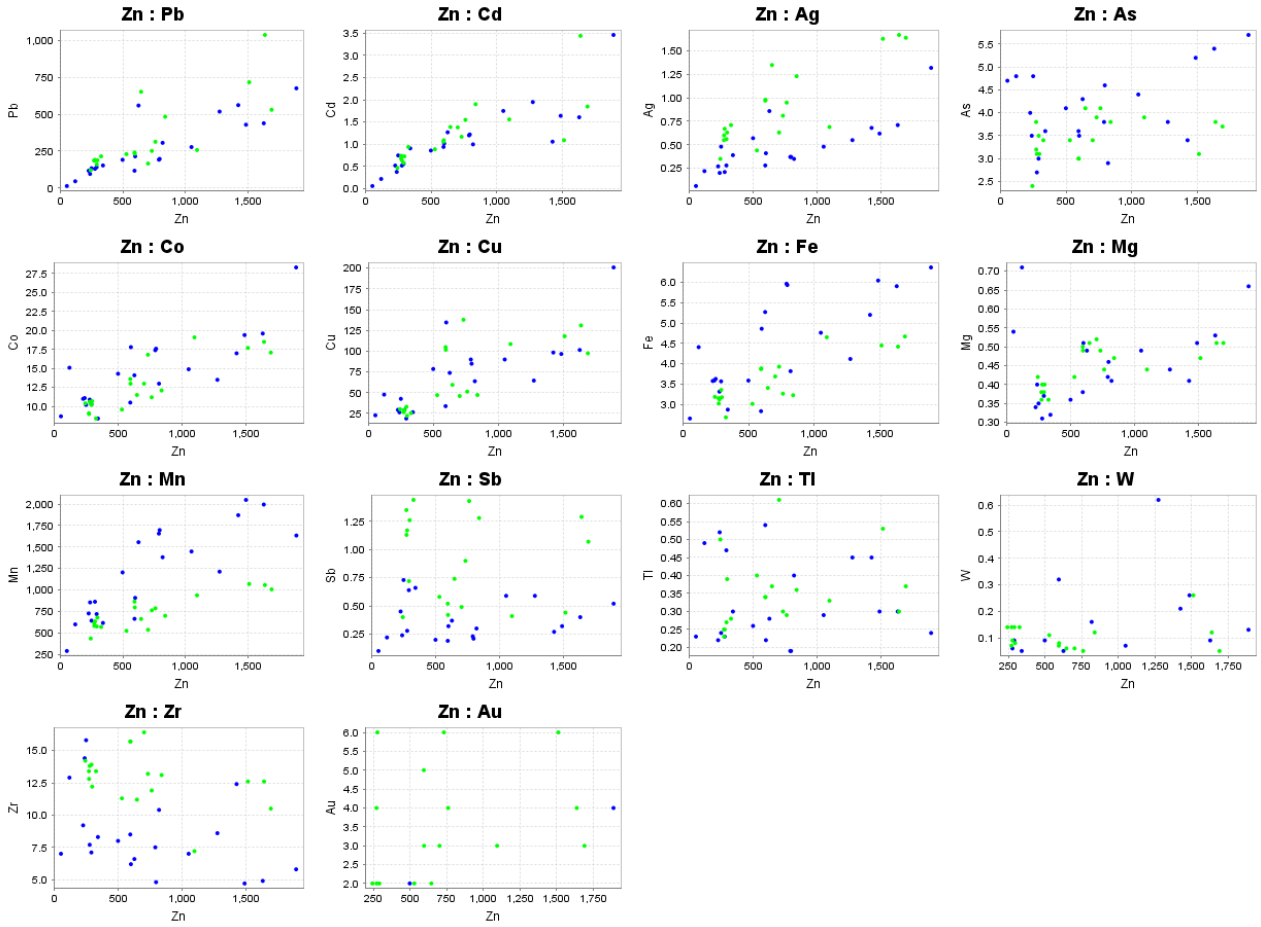

Appendix 2.2.3

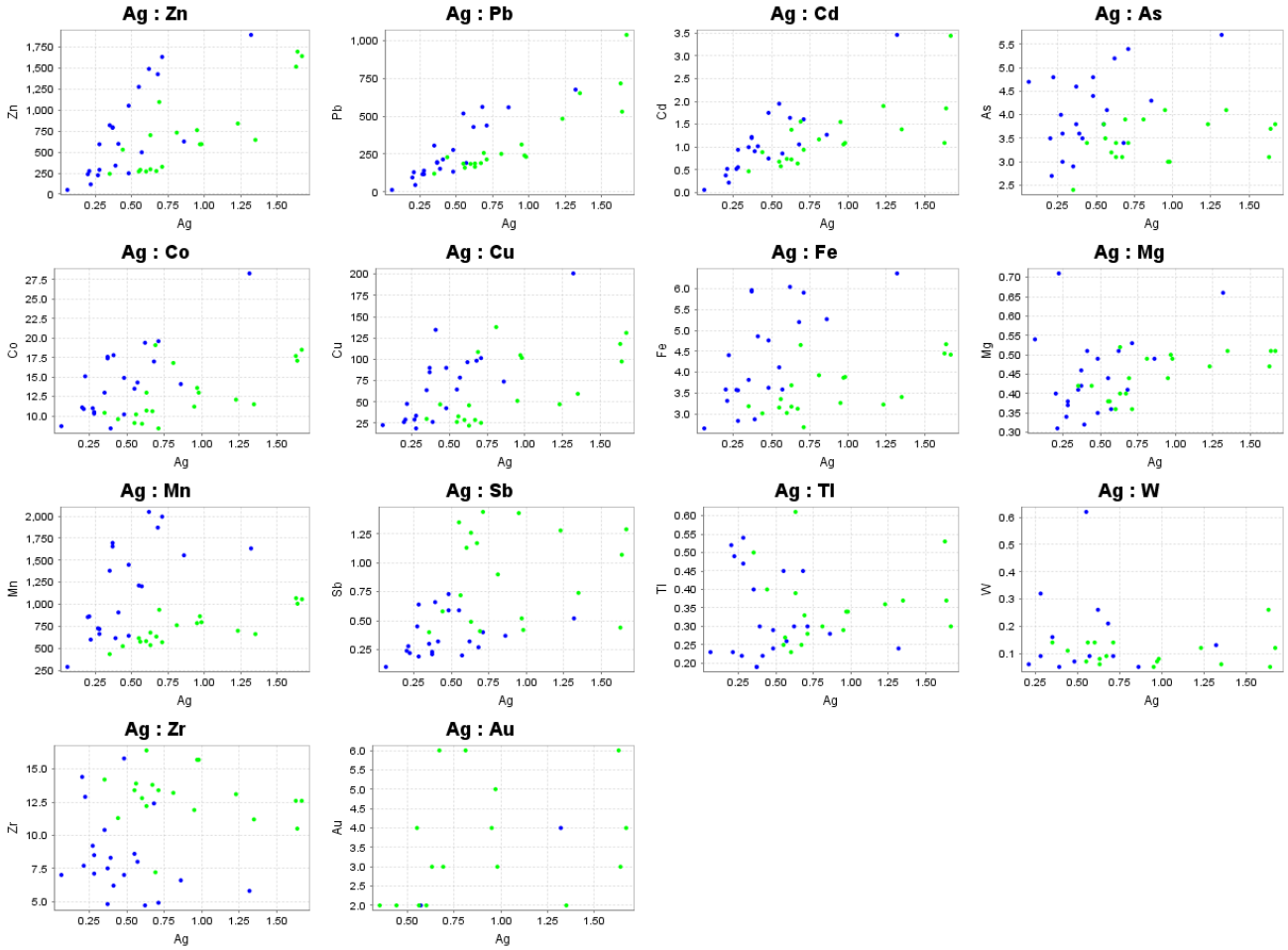

Appendix 2.2.4

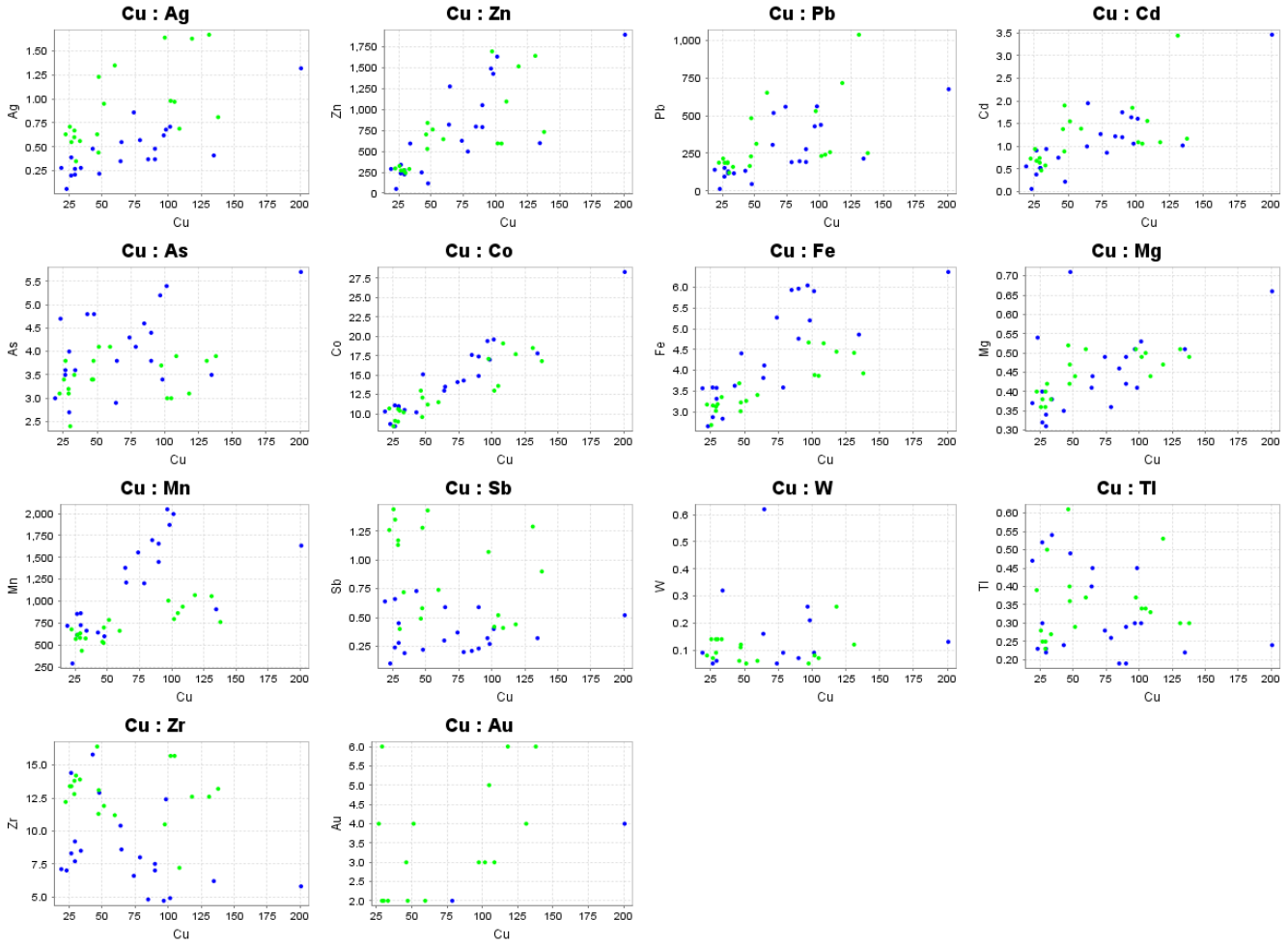

Appendix 2.2.5

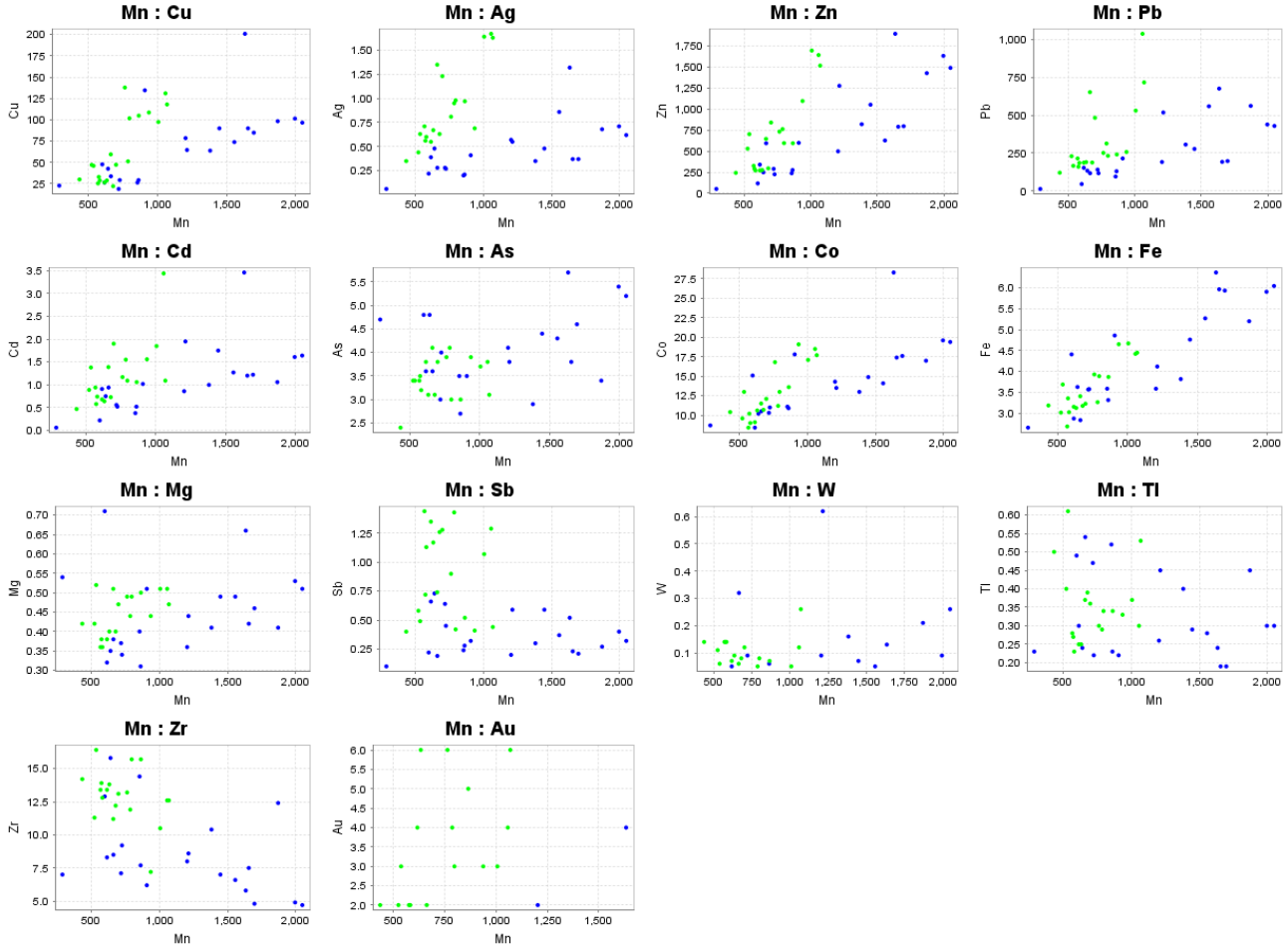

Appendix 2.2.6

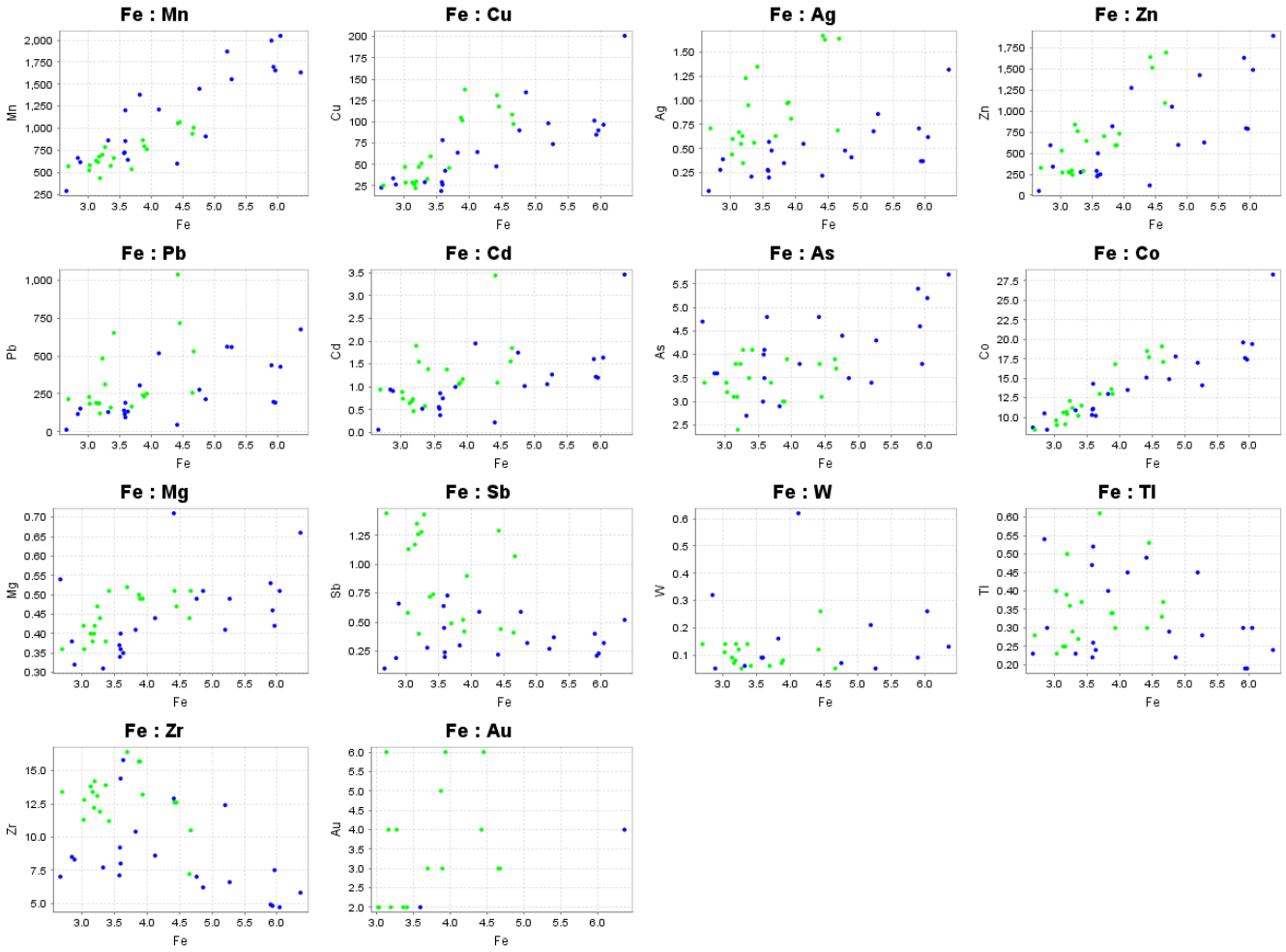

Appendix 2.2.8

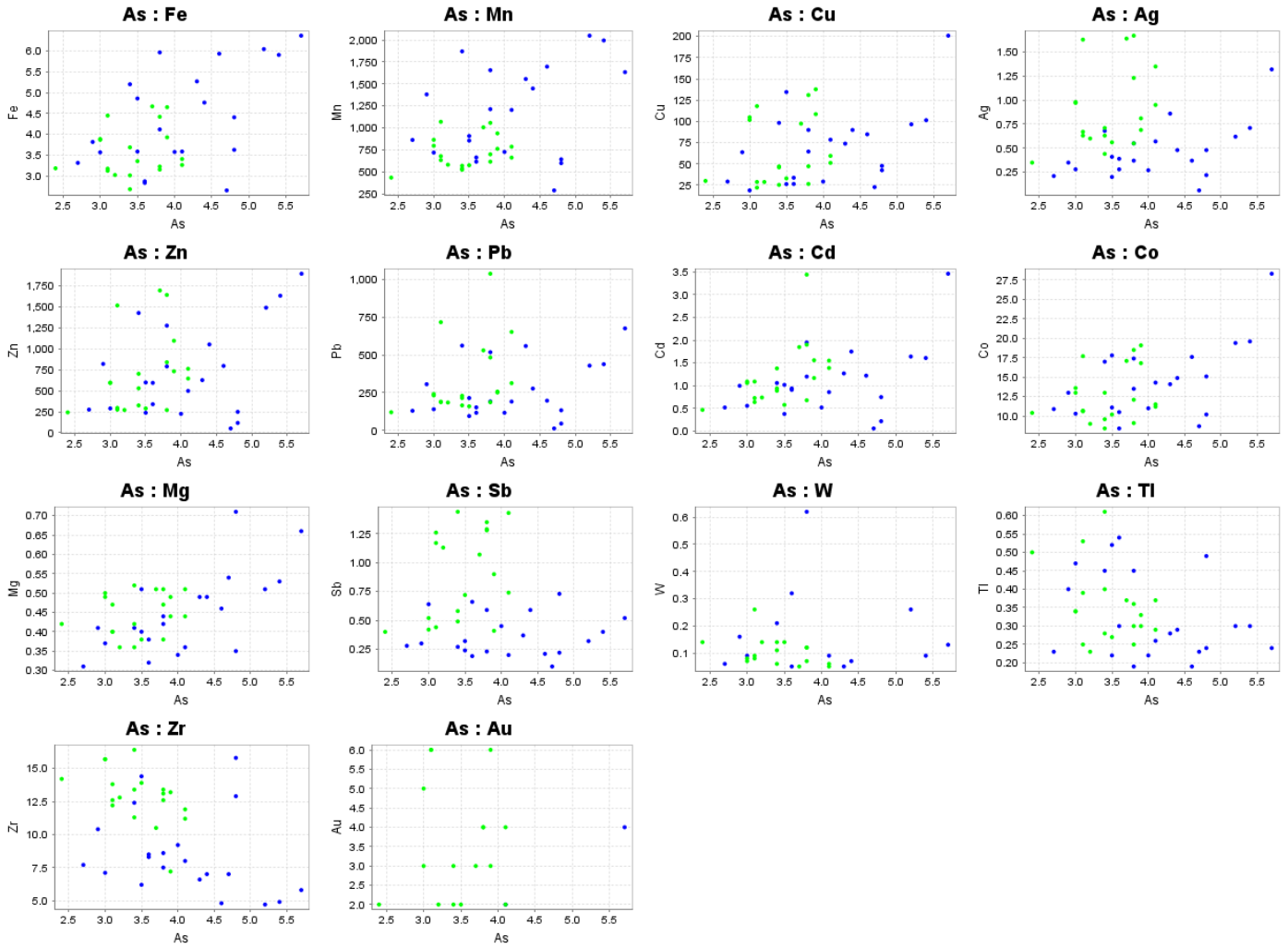

Appendix 2.2.9

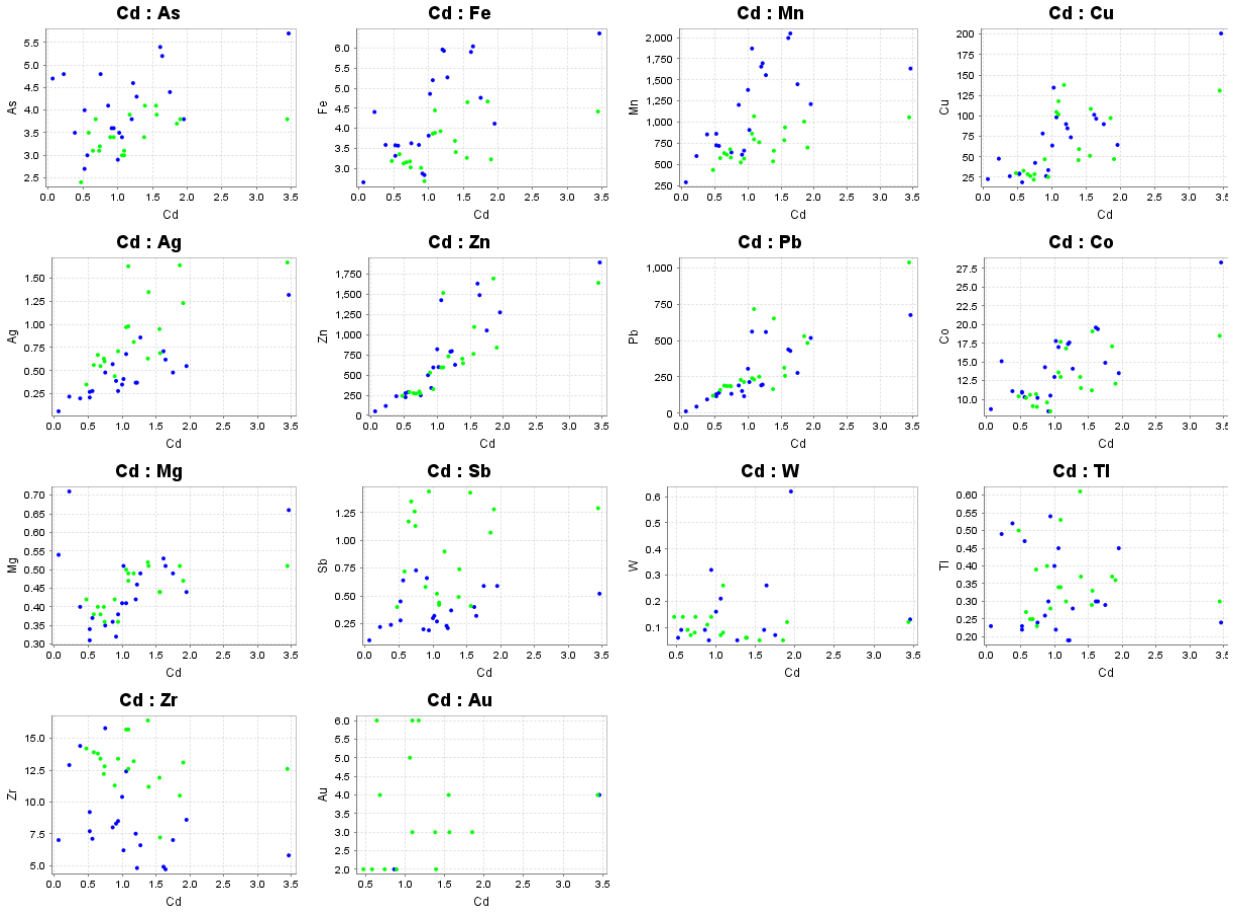

Appendix 2.2.11

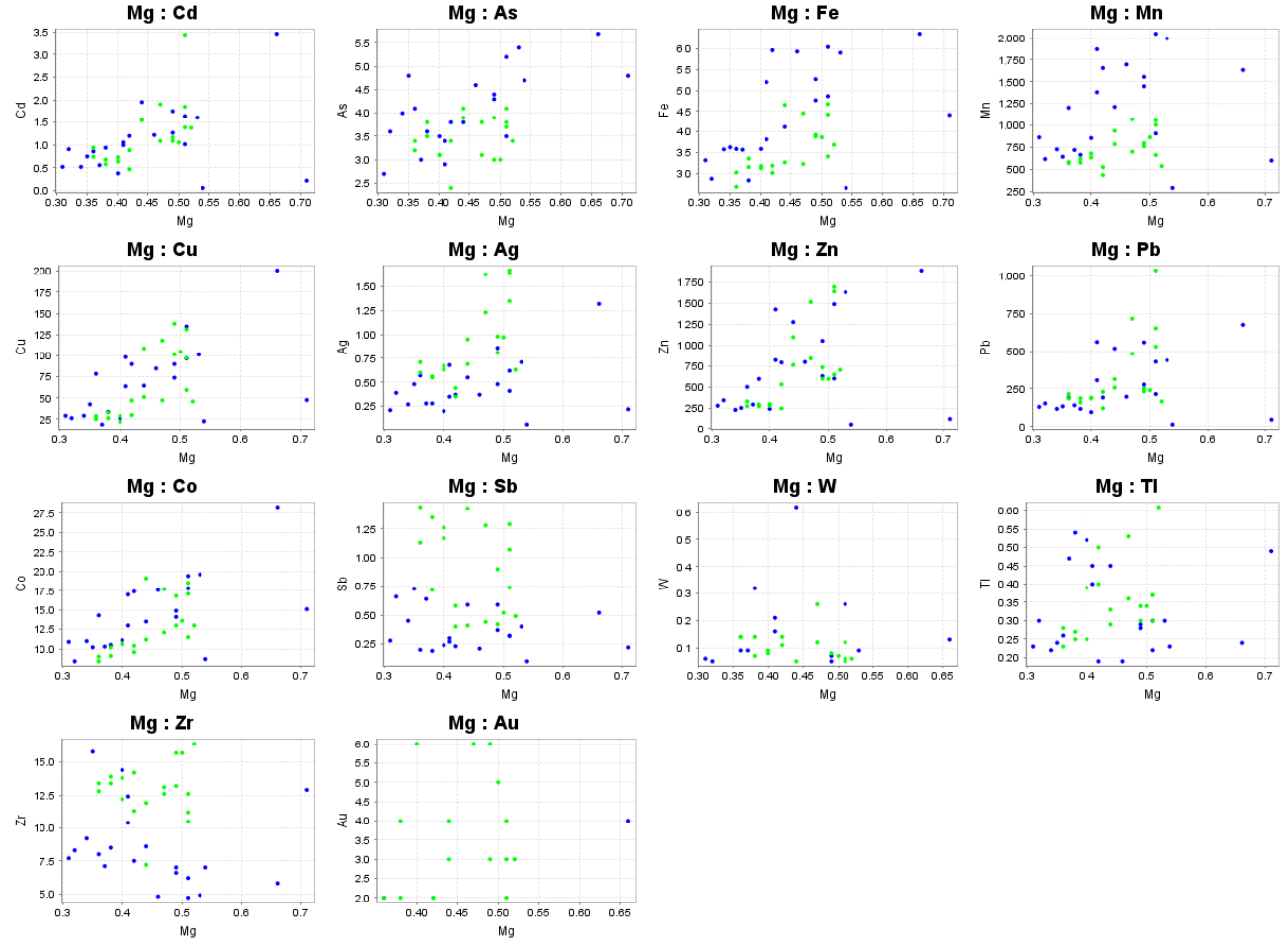

Comparison of niton data sets and geochemistry

Appendix 2.3.1

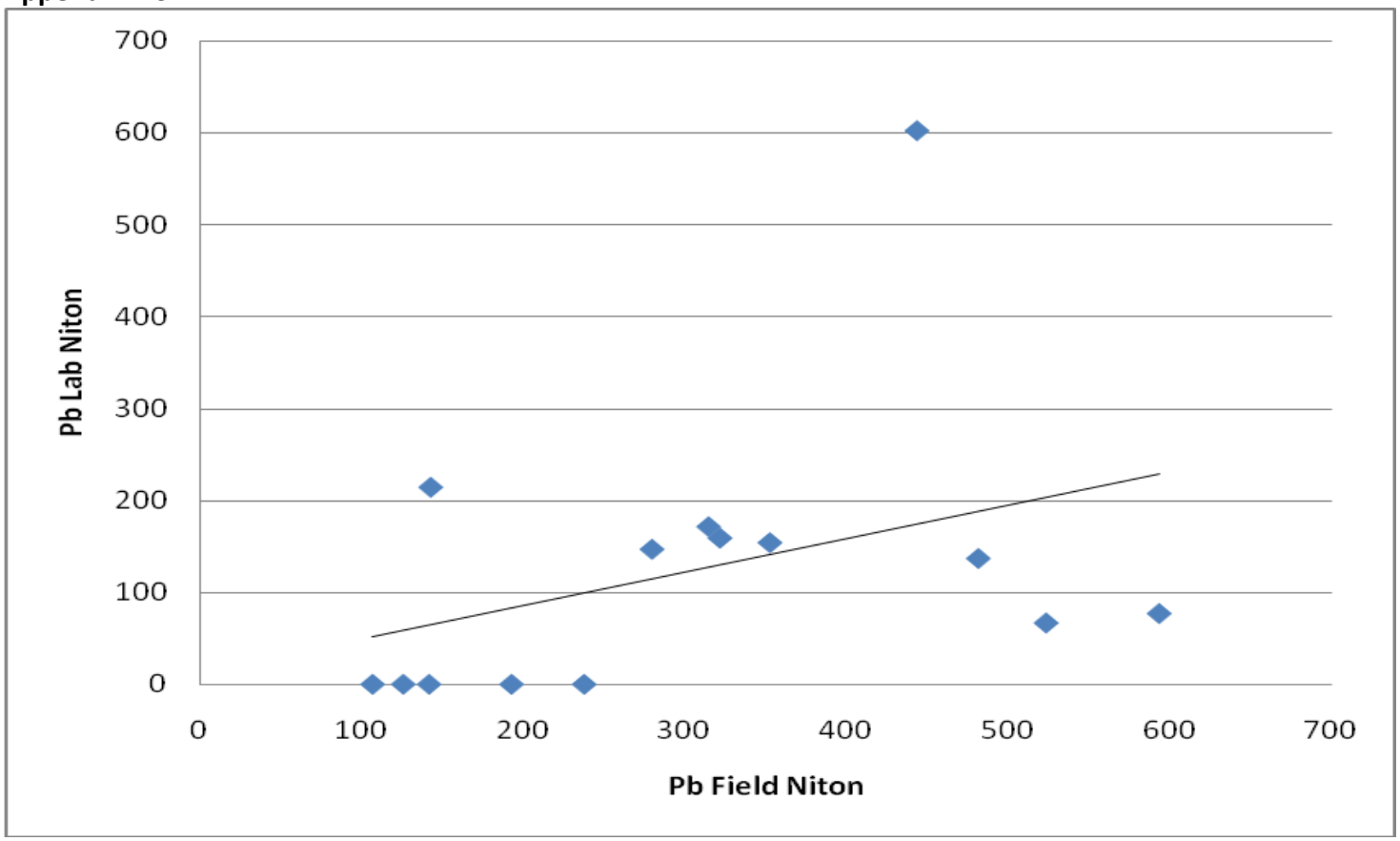

Appendix 2.3.2

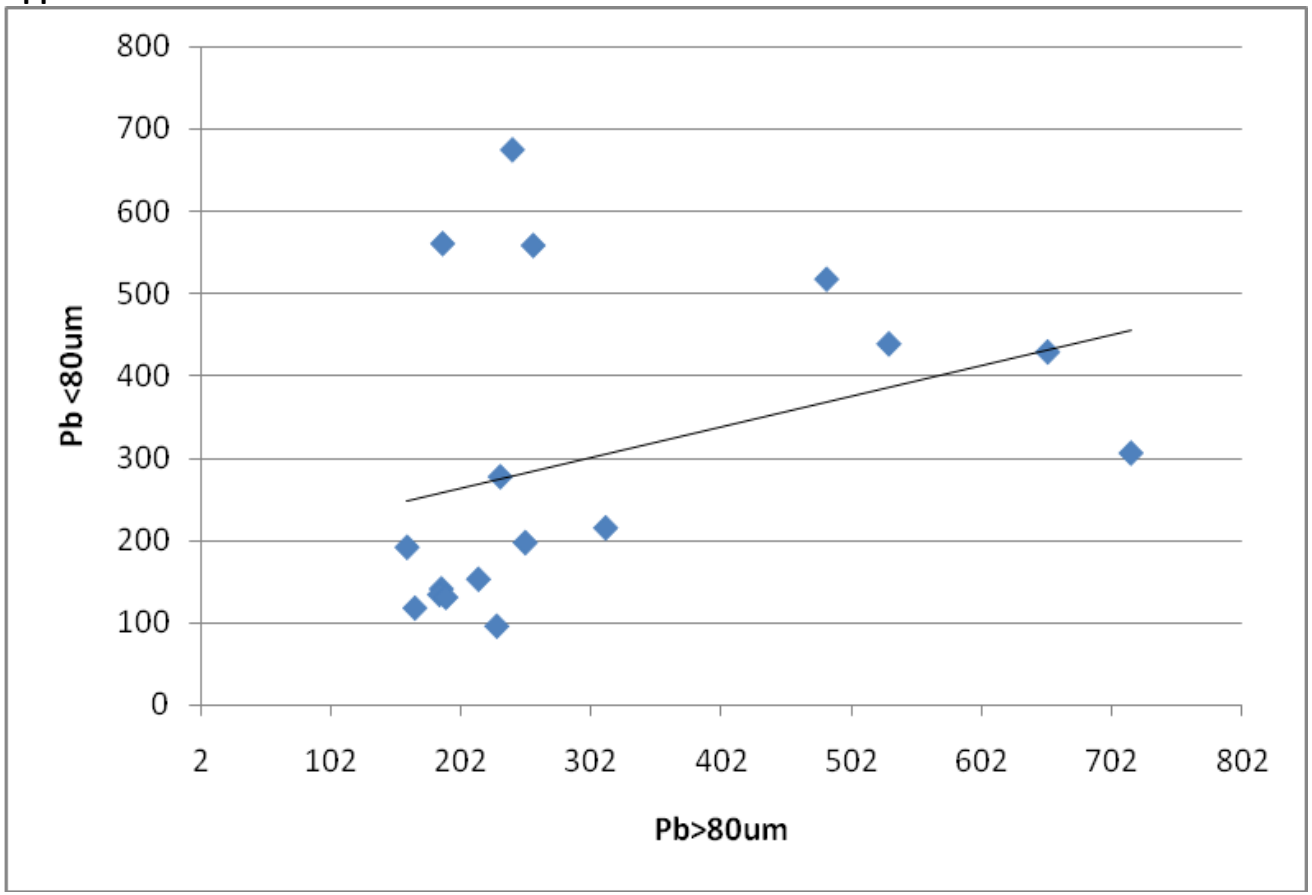

Appendix 2.3.3

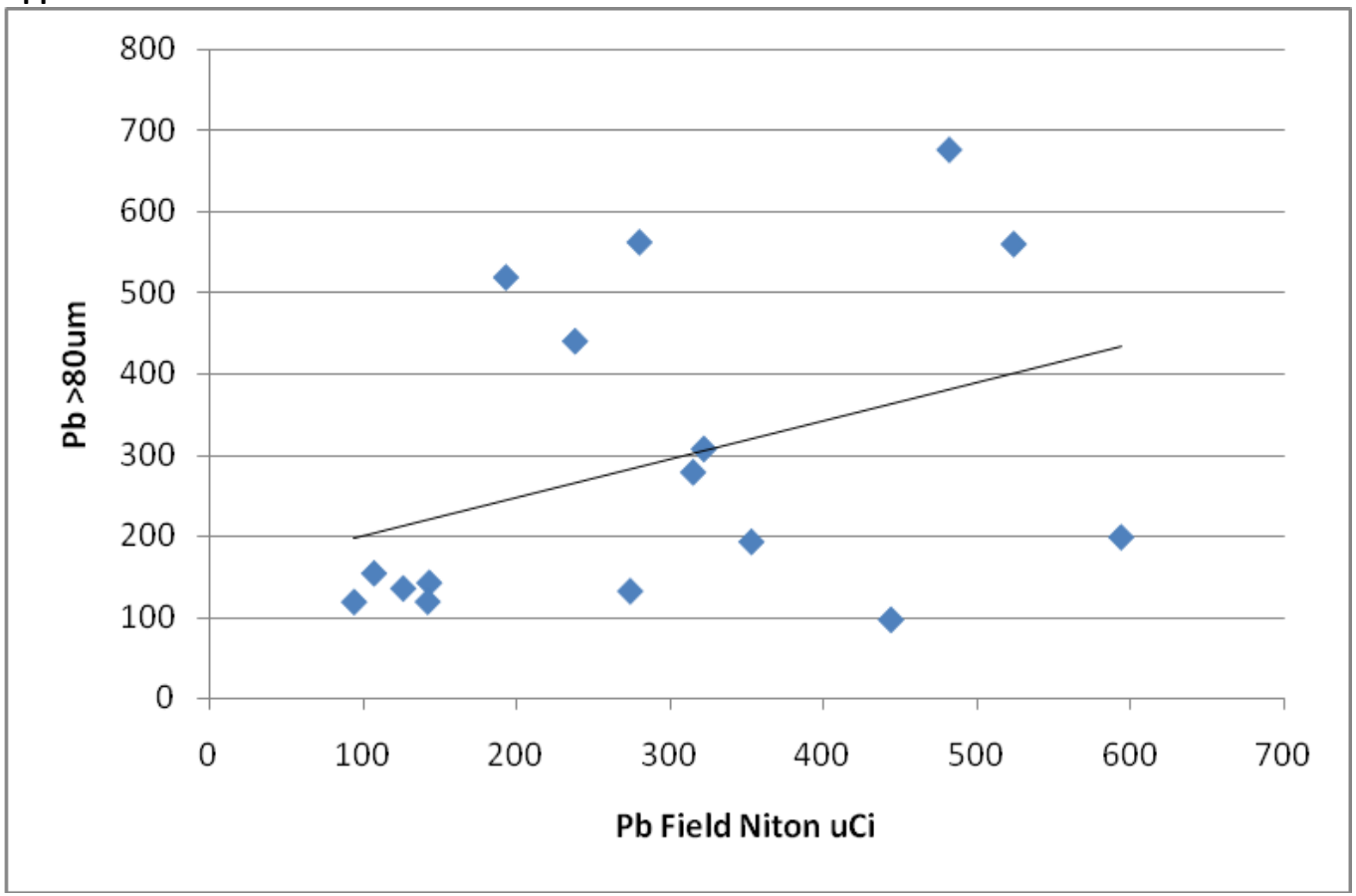

Appendix 2.3.4

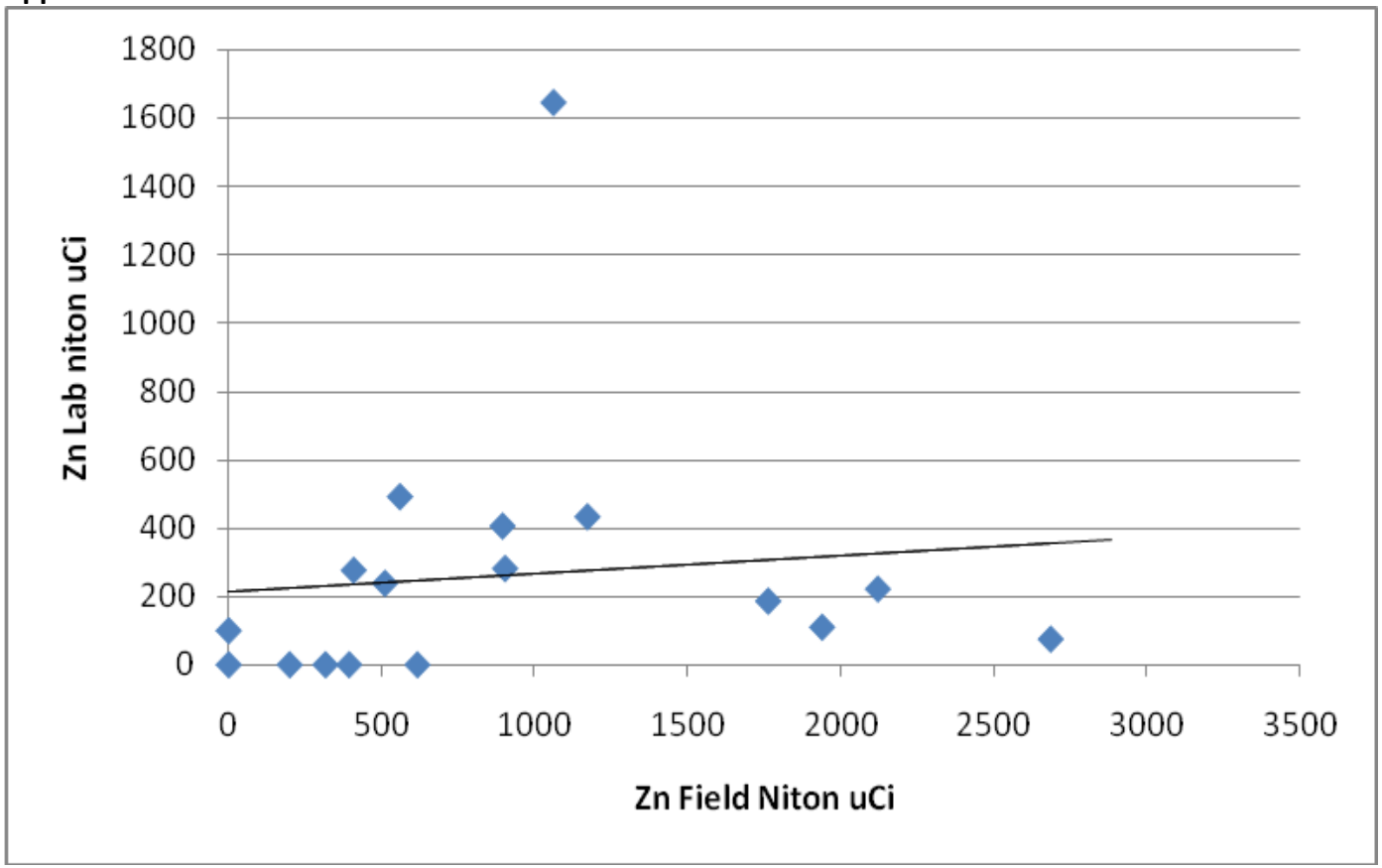

Appendix 2.3.5

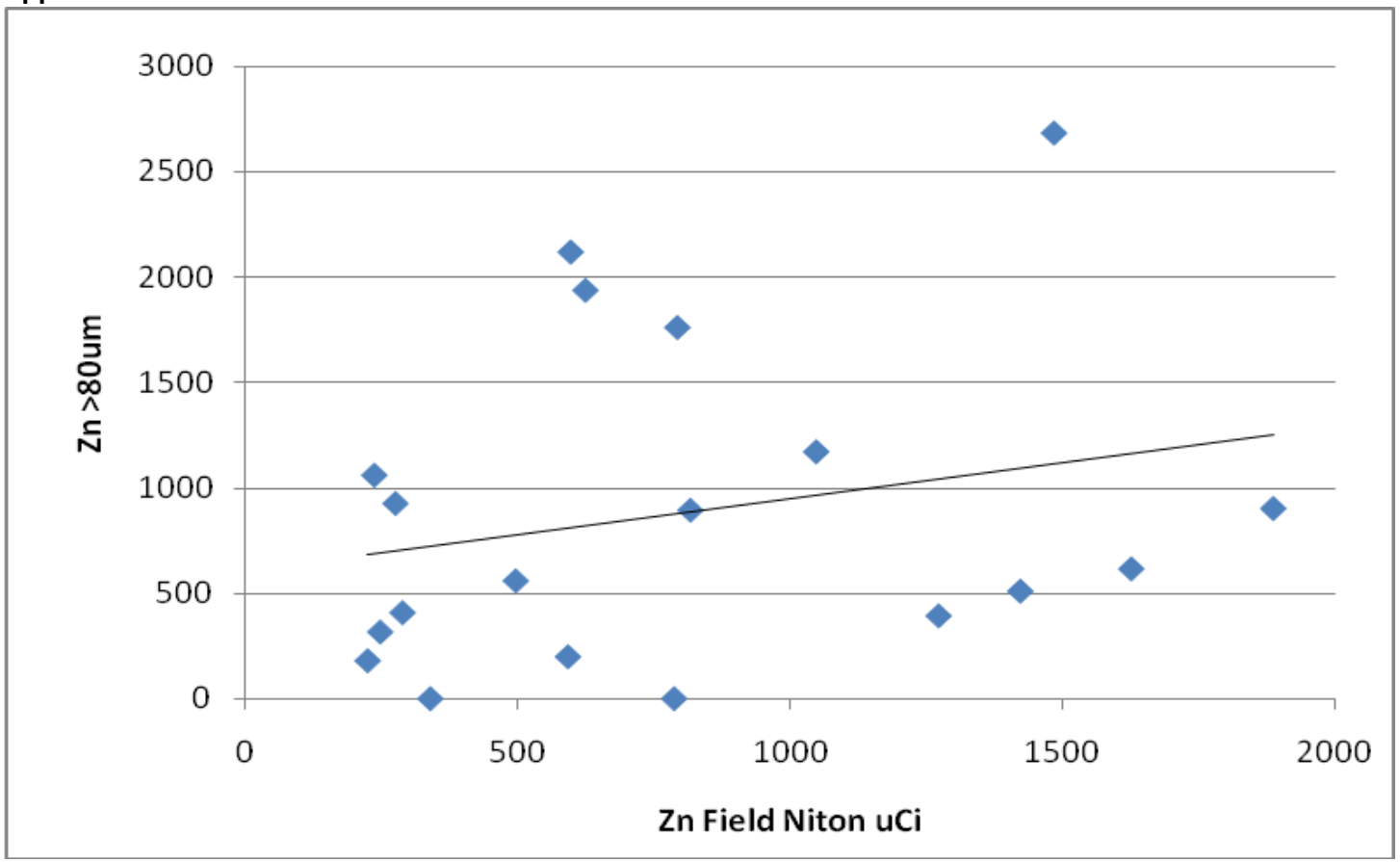

Appendix 2.3.6

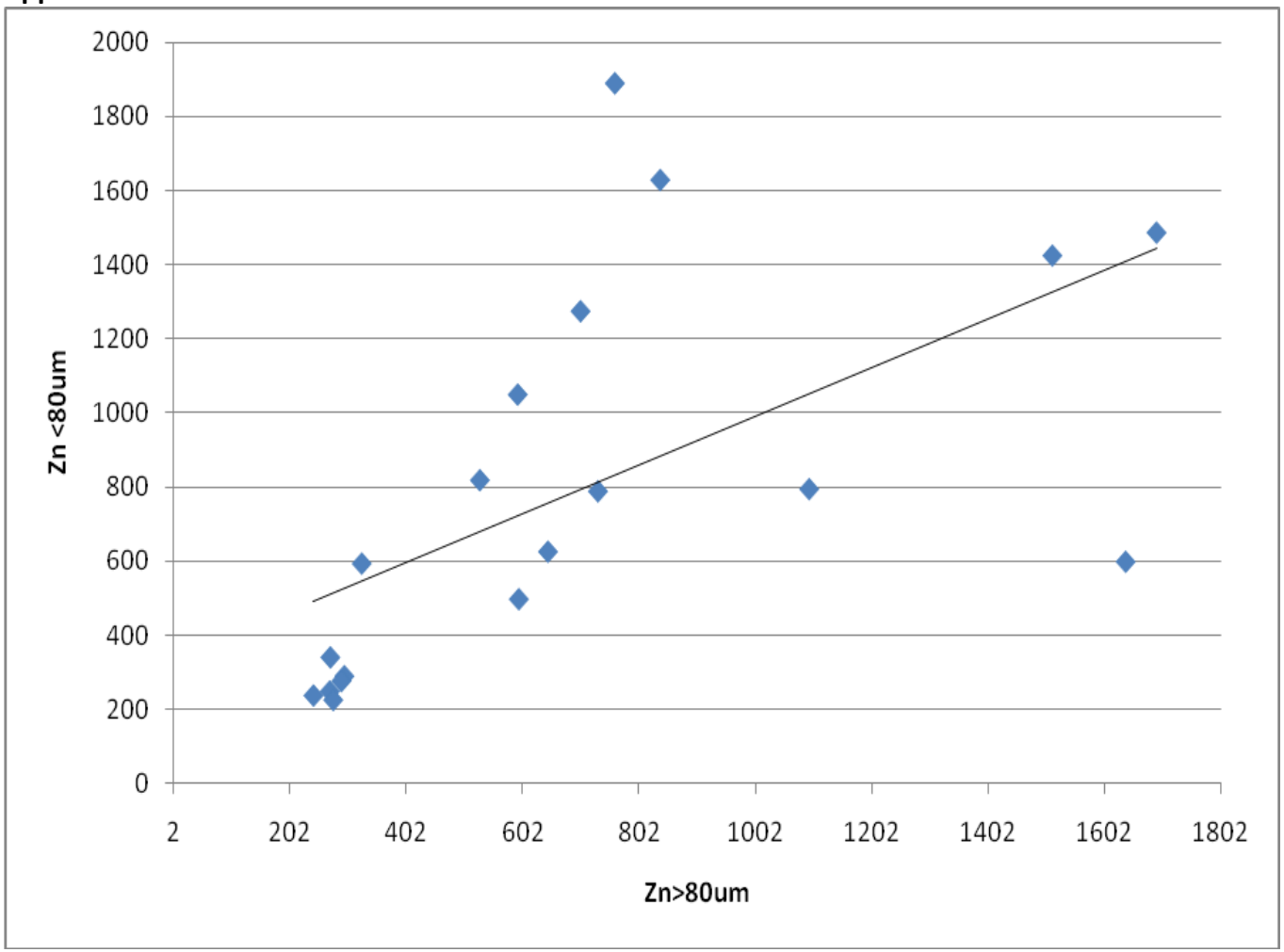

Appendix 2.3.7

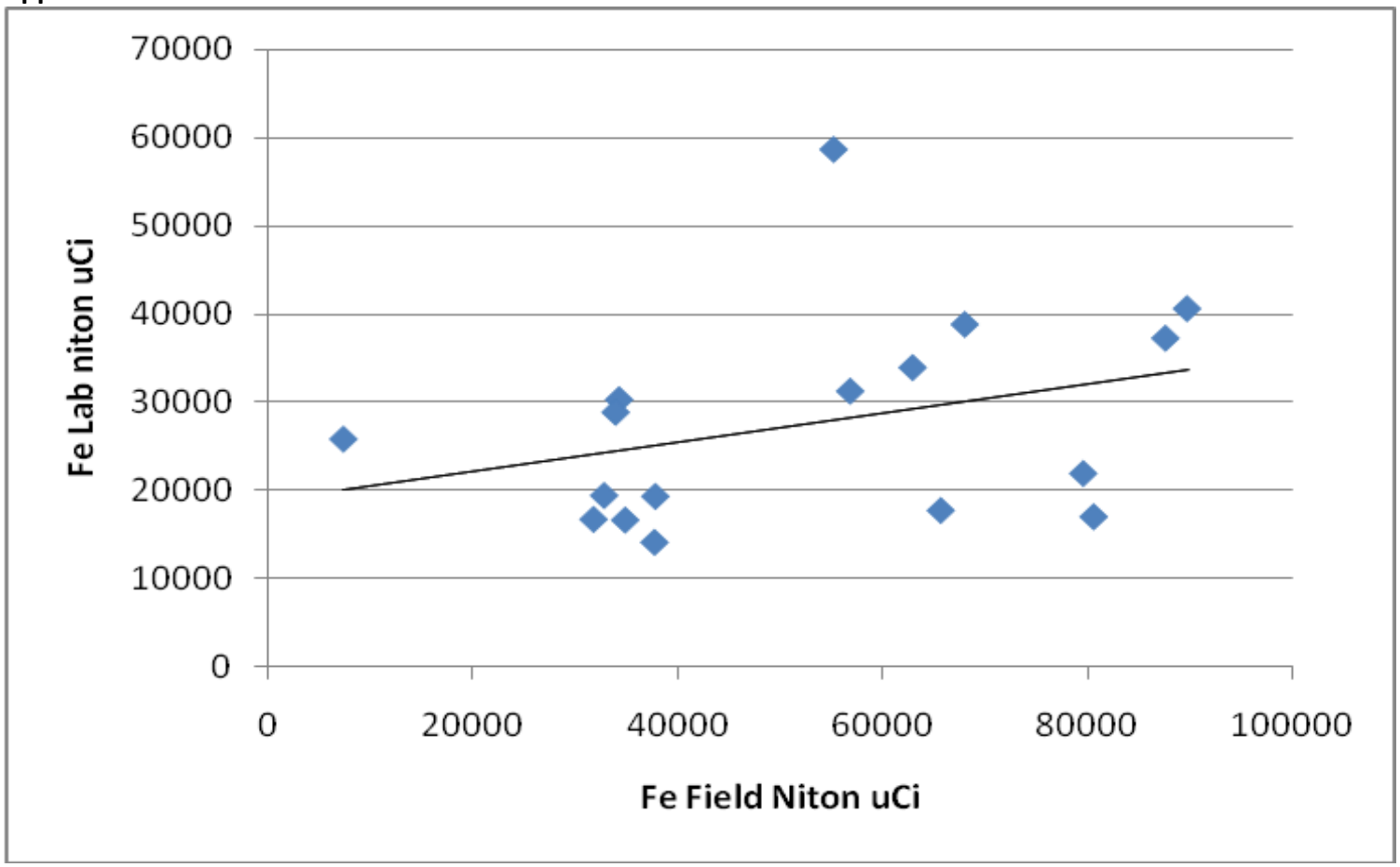

Appendix 2.3.8

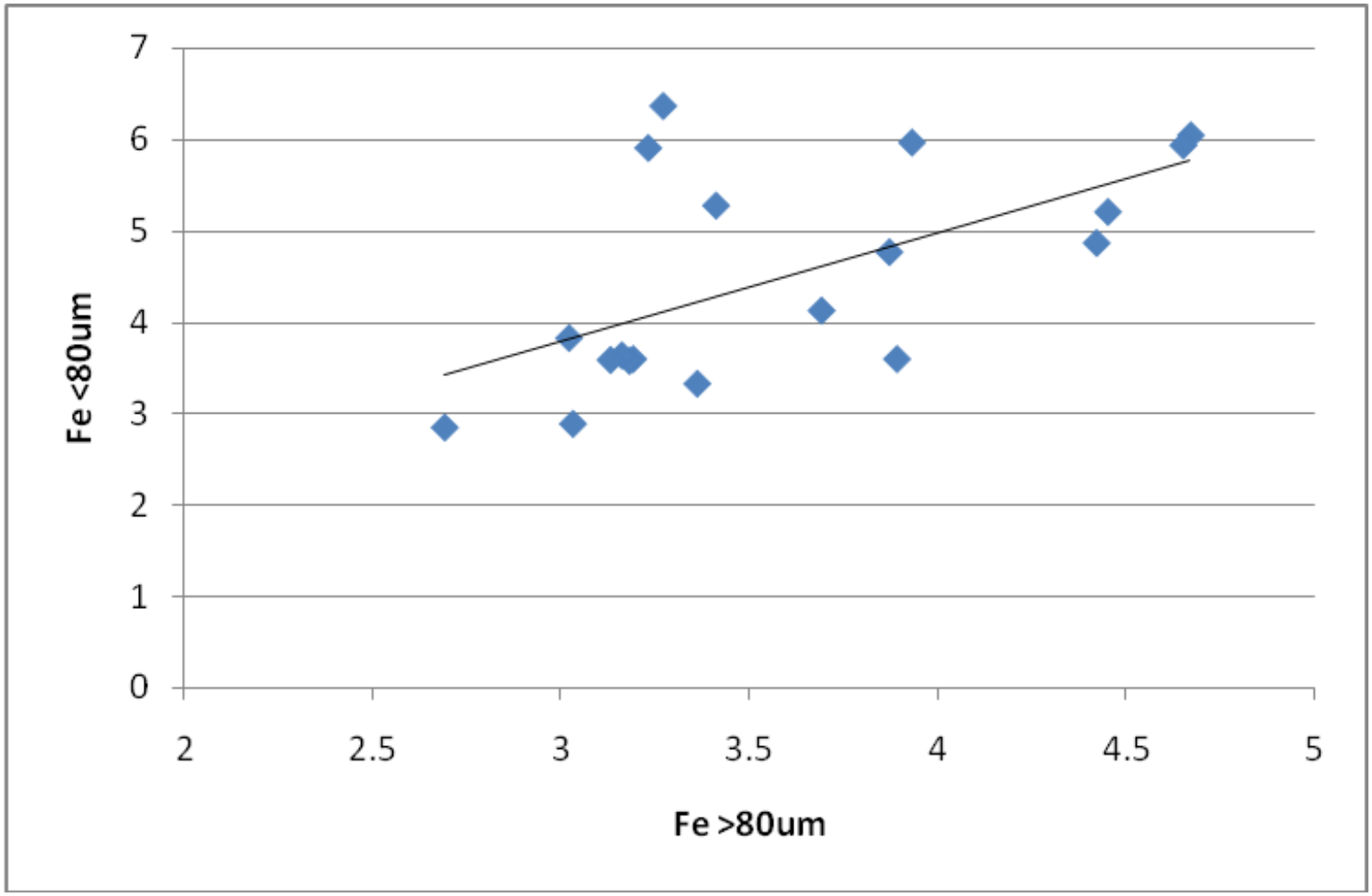
Fe <80um
Fe >80um
0
1
2
3
4
5
6
7
2
2.5
3
3.5
4
4.5
5

Appendix 2.3.9

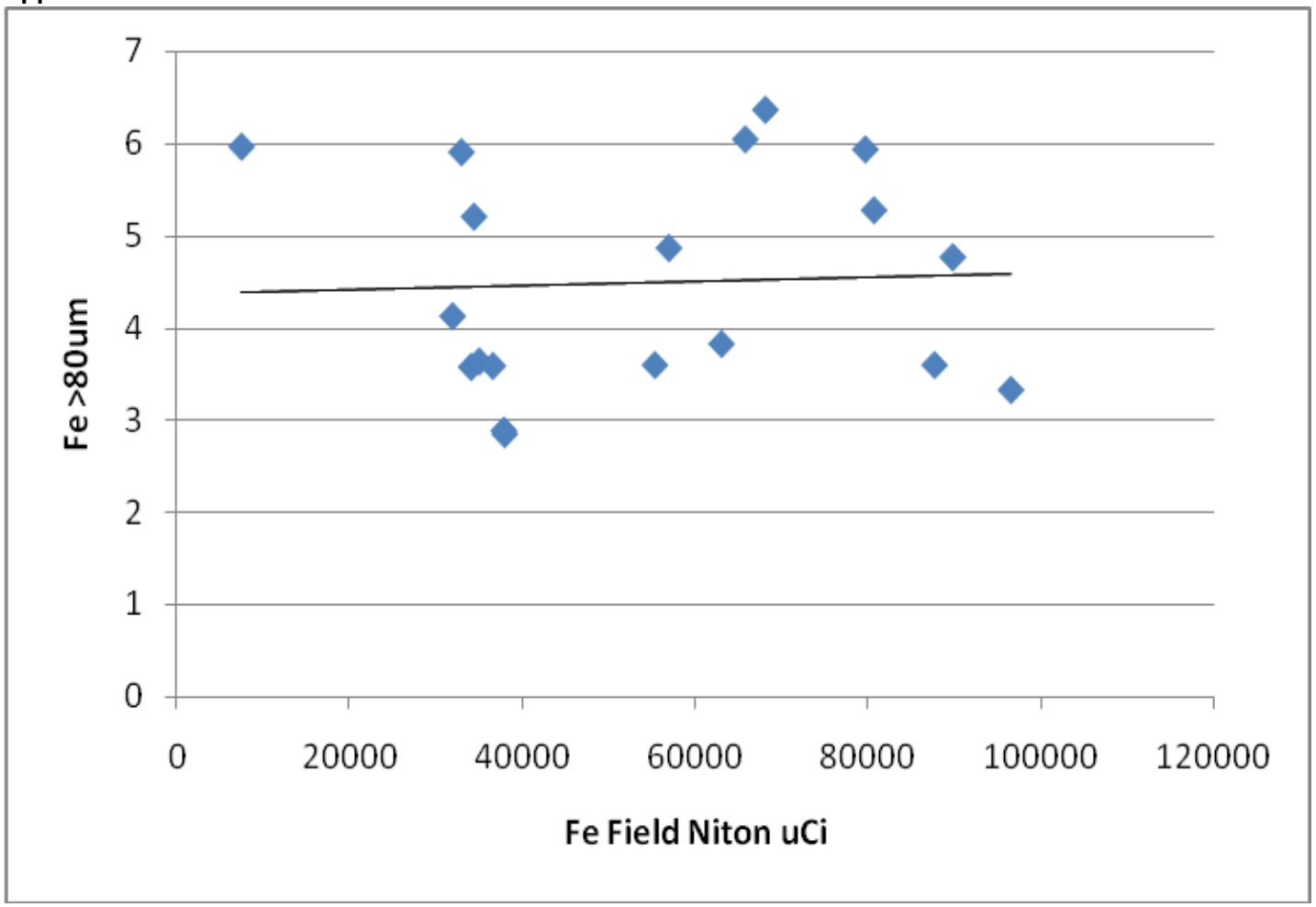

Appendix 2.3.10

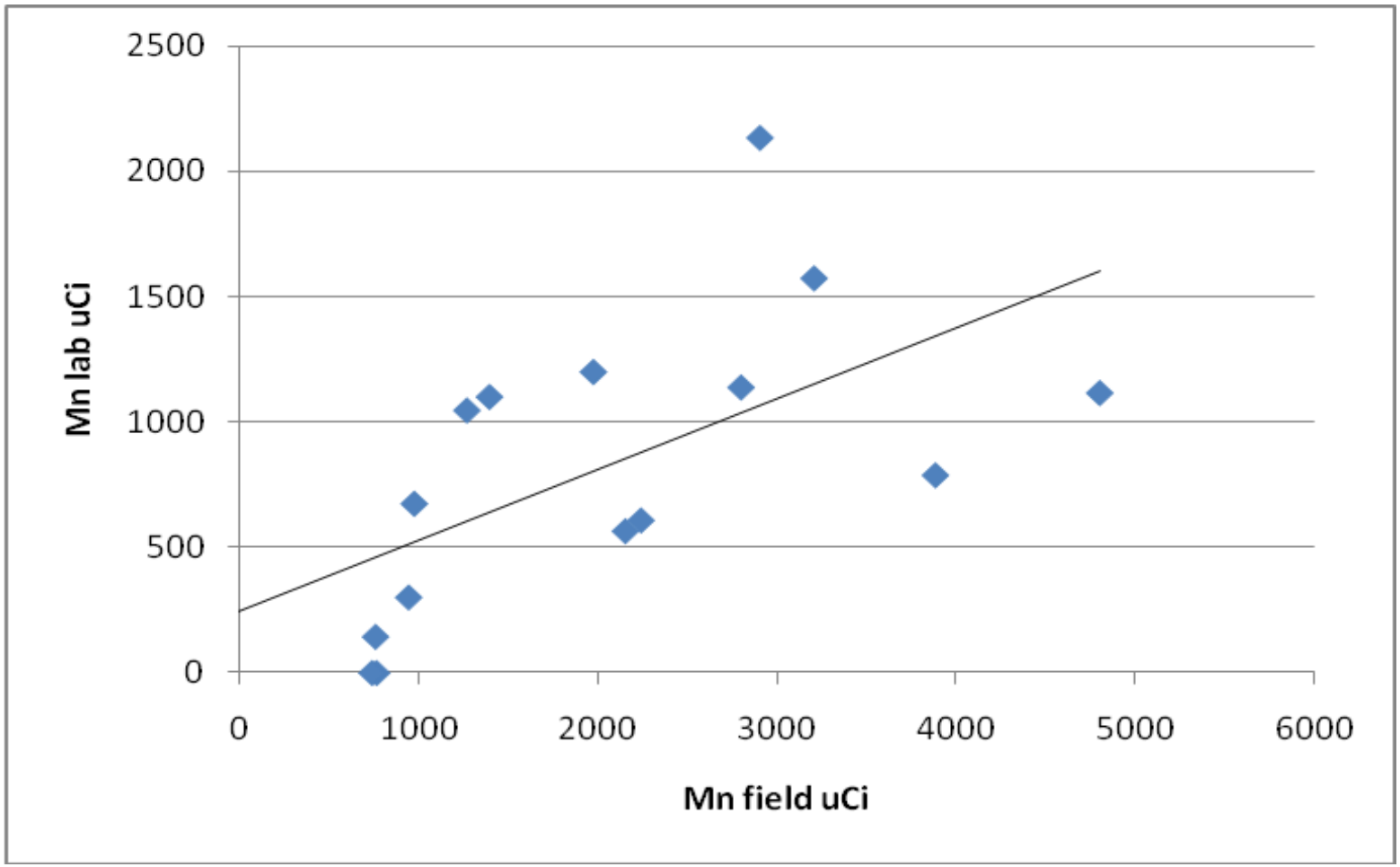

Appendix 2.3.11

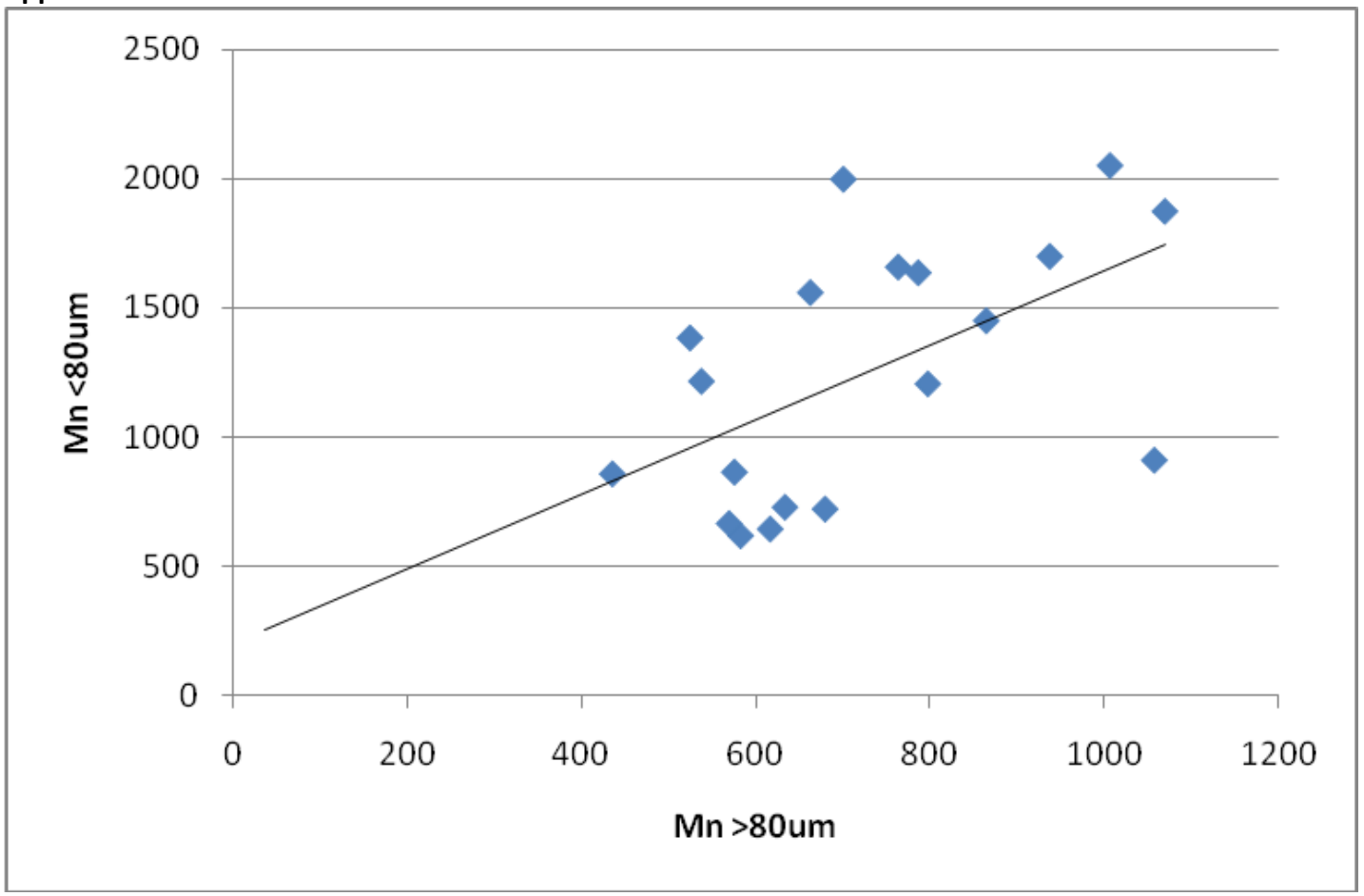

Appendix 2.3.12

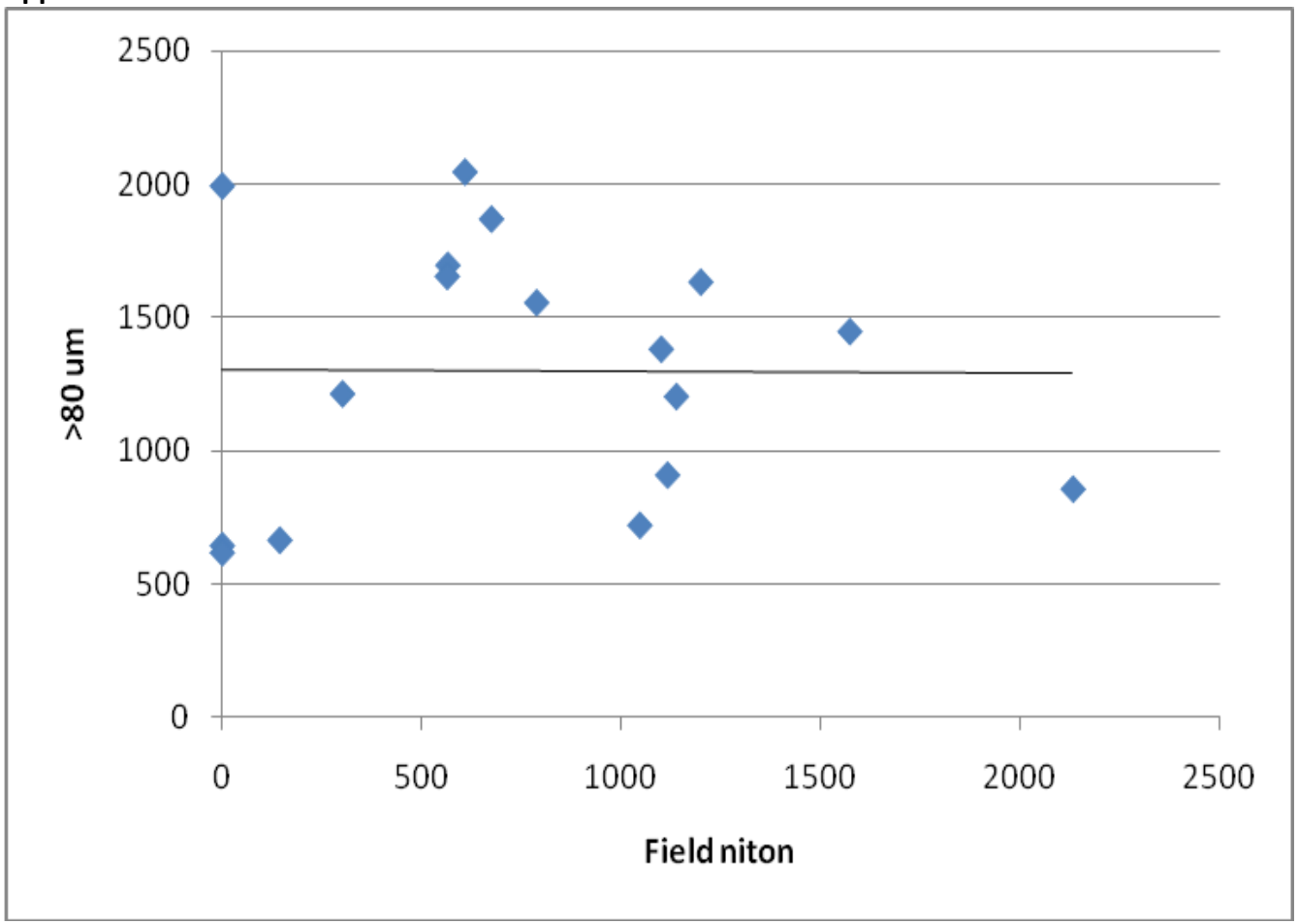

Biogeochemistry
Appendix 2.4.1

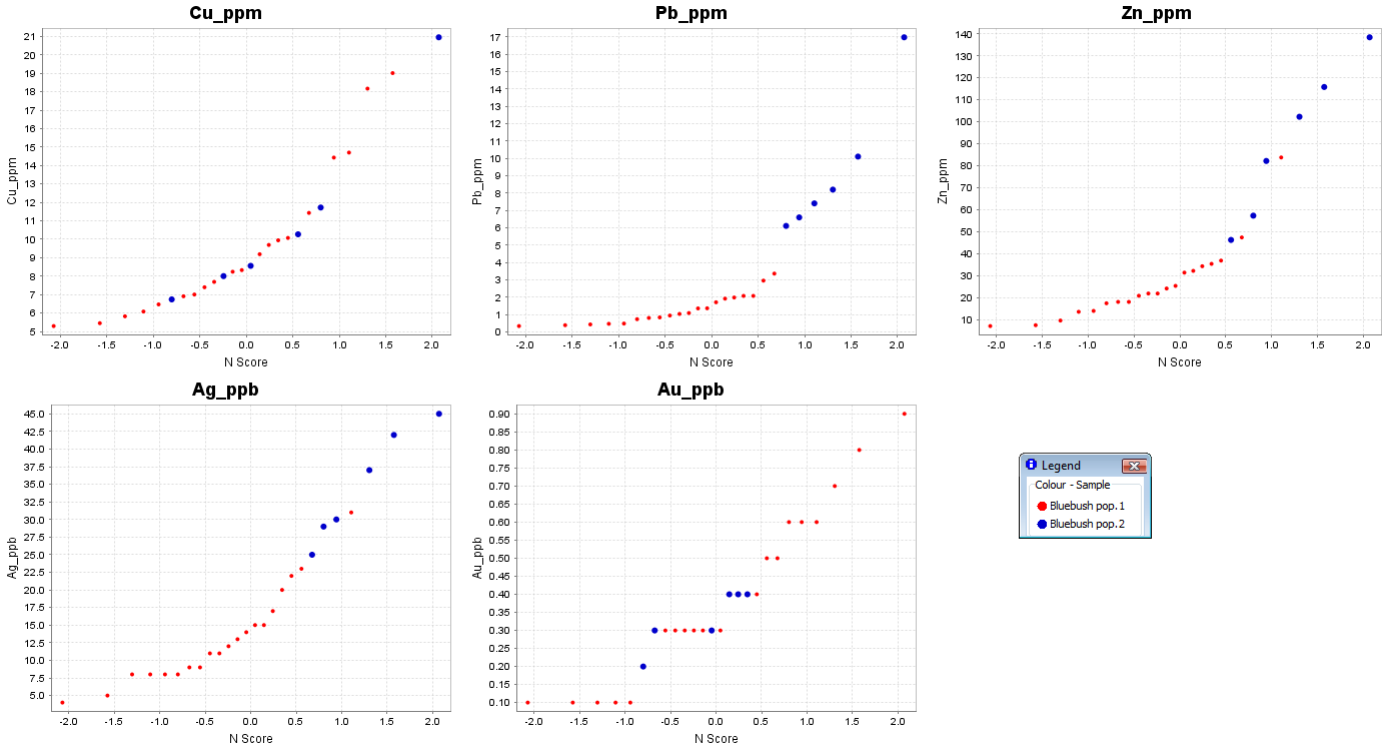

Appendix 2.4.2

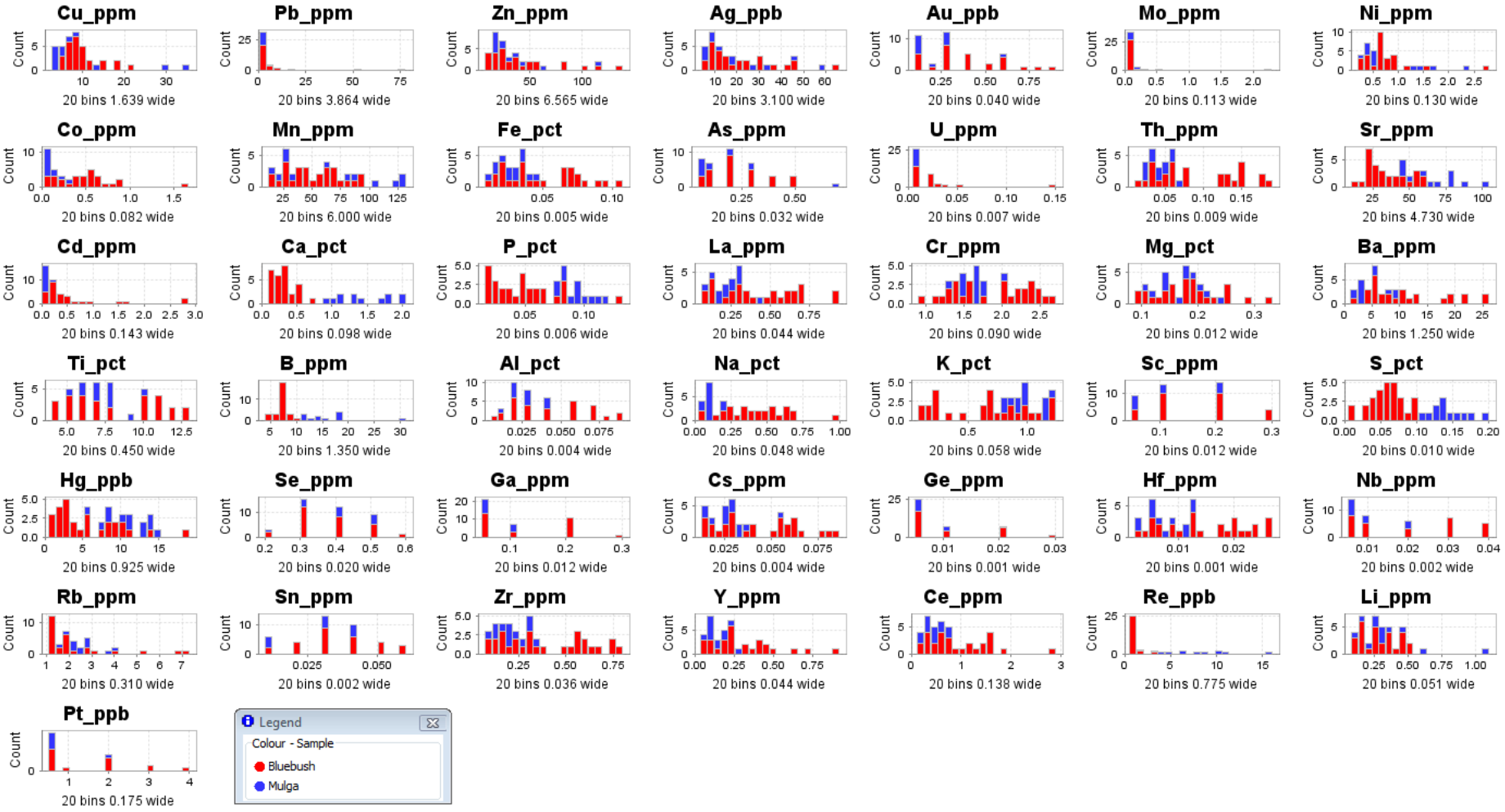

Appendix 2.4.3

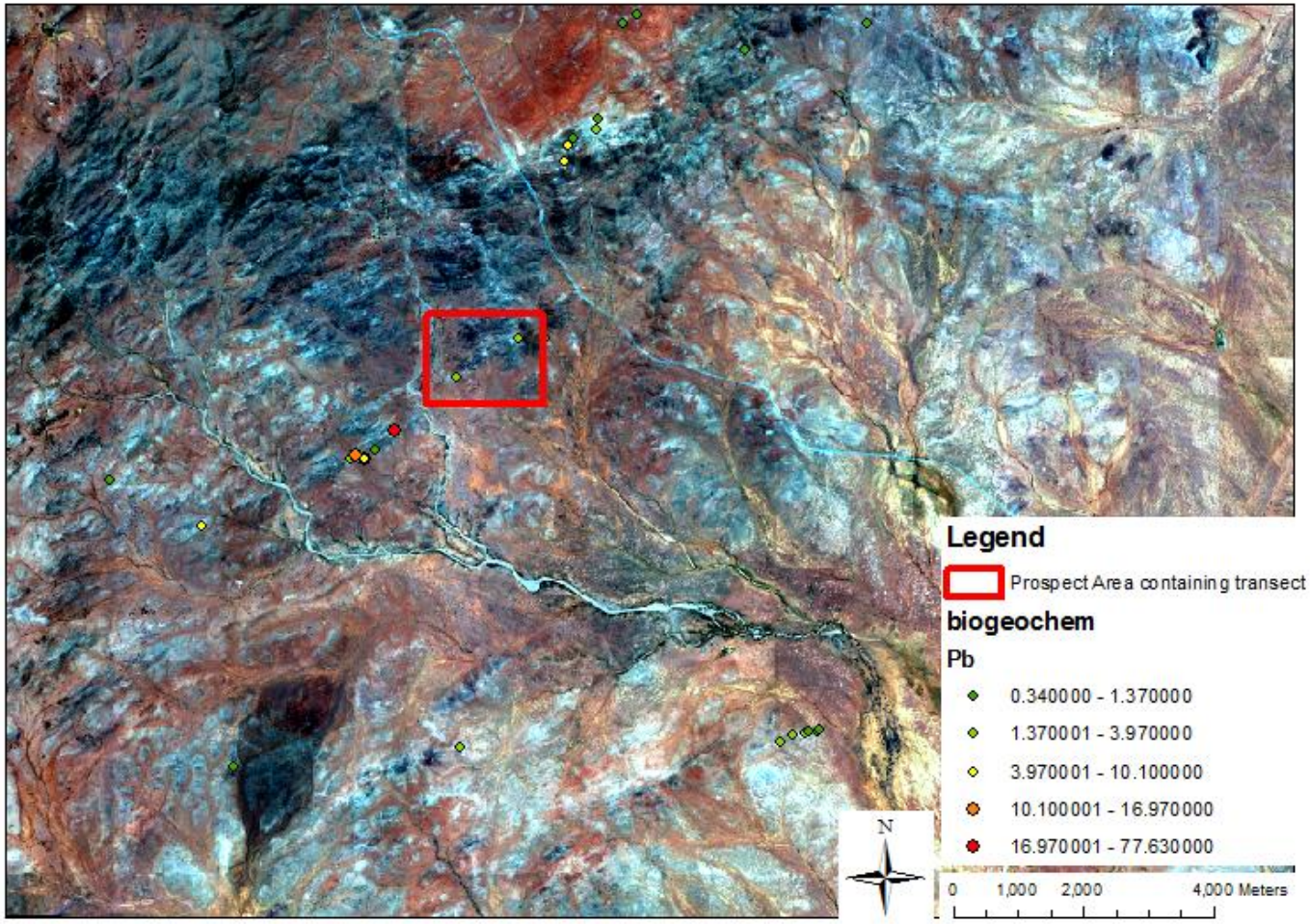

Appendix 2.4.4

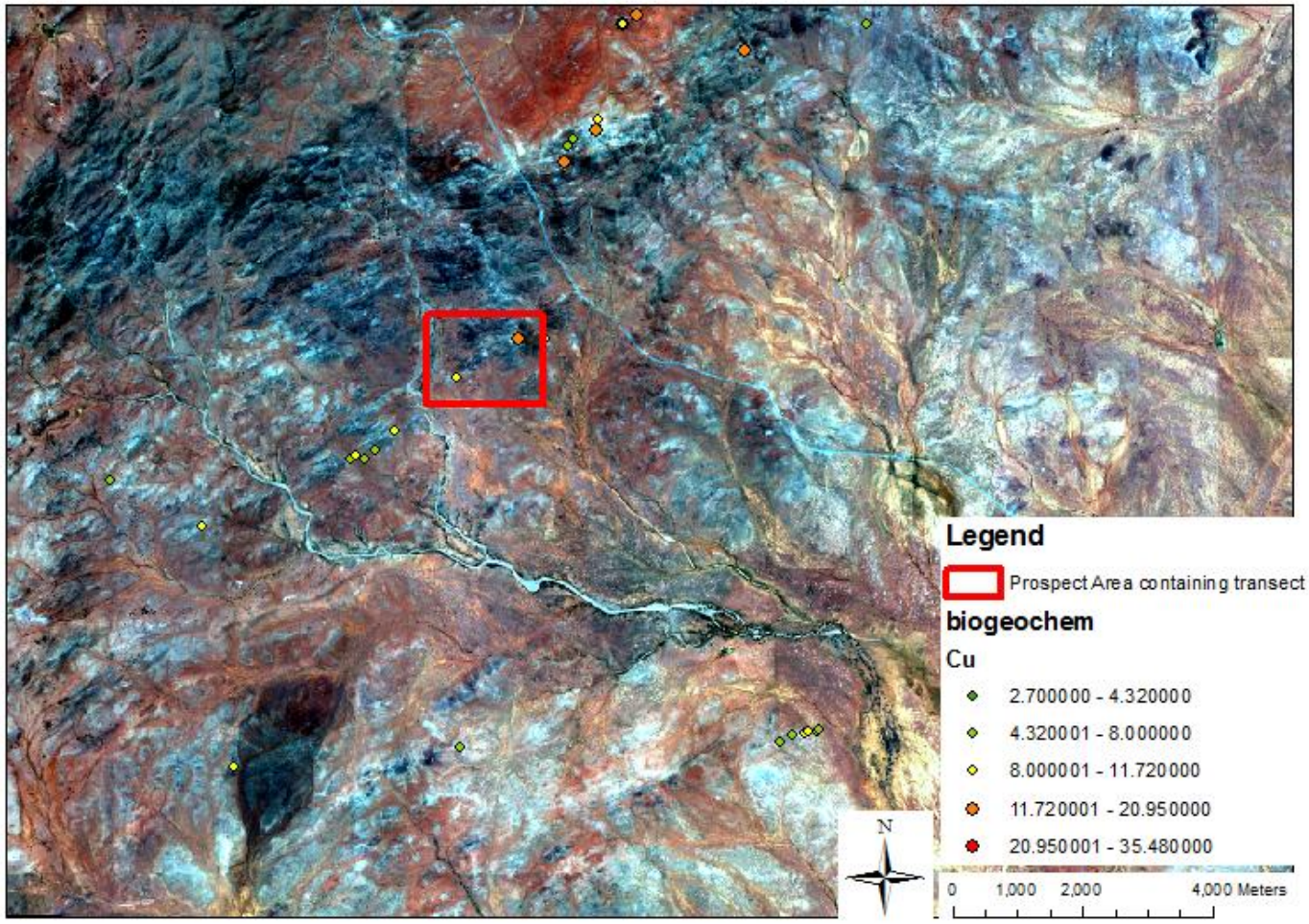

Appendix 2.4.5

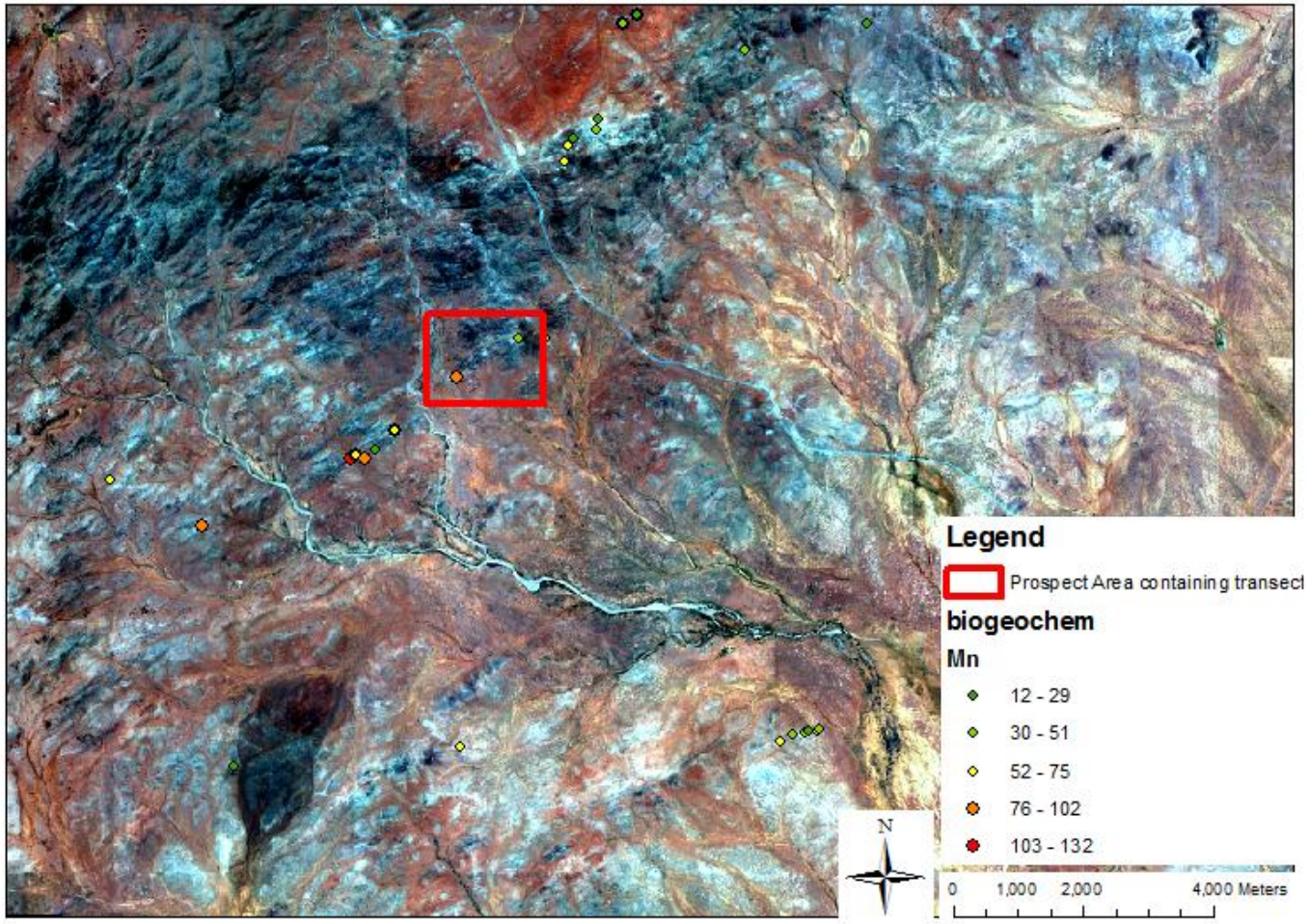

Appendix 2.4.6

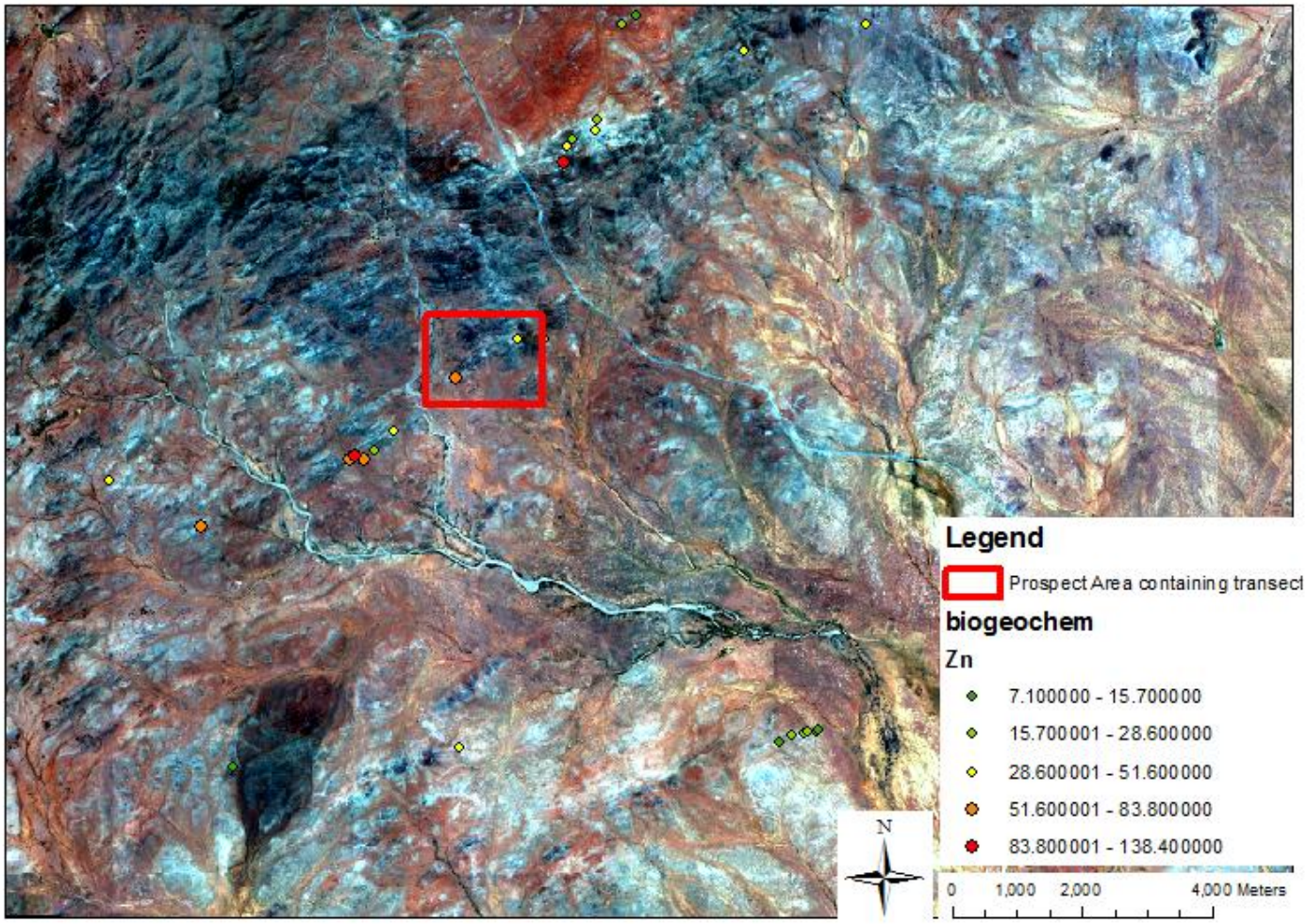

Appendix 2.4.7

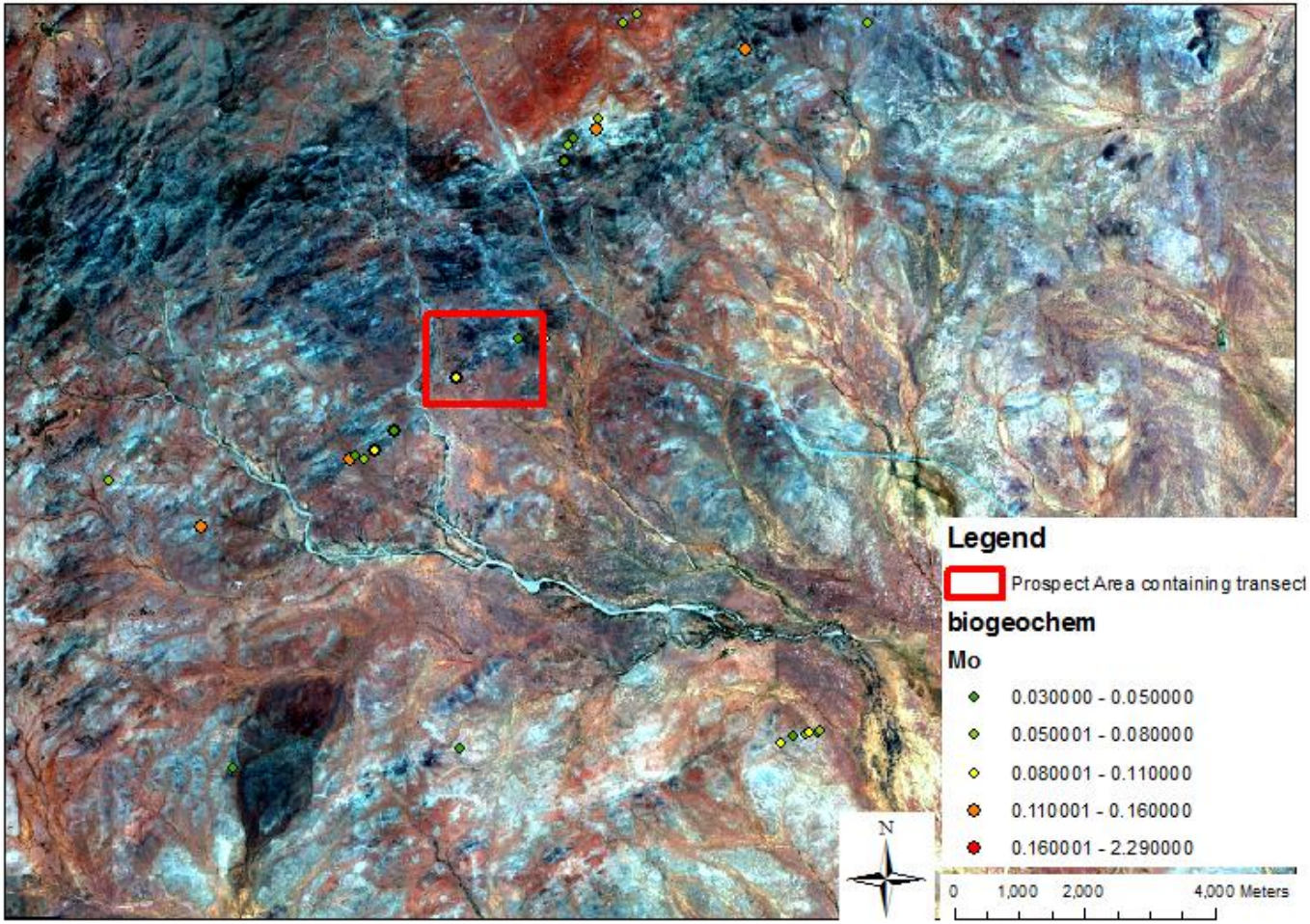

Appendix 2.4.8

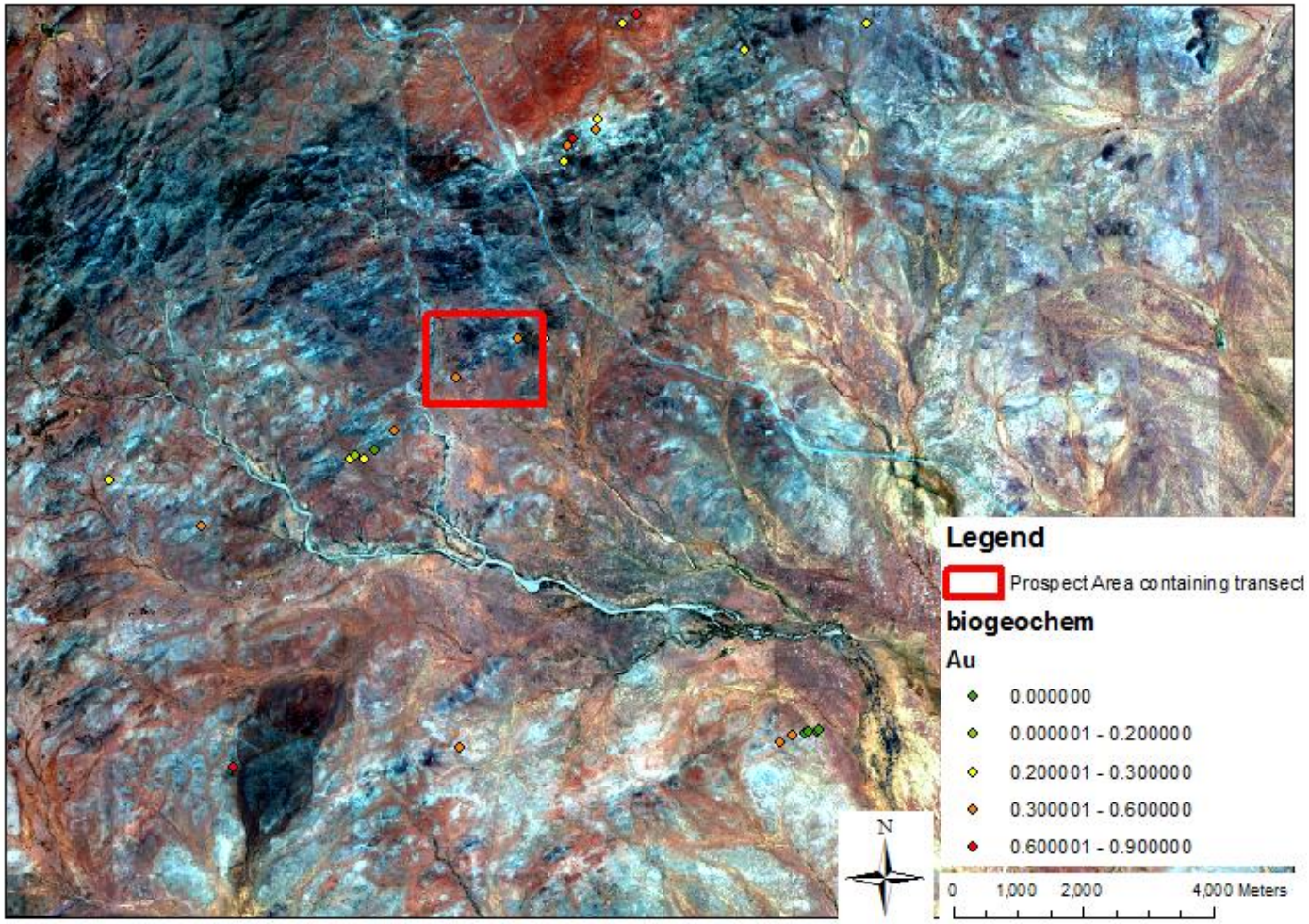

Appendix 2.4.9

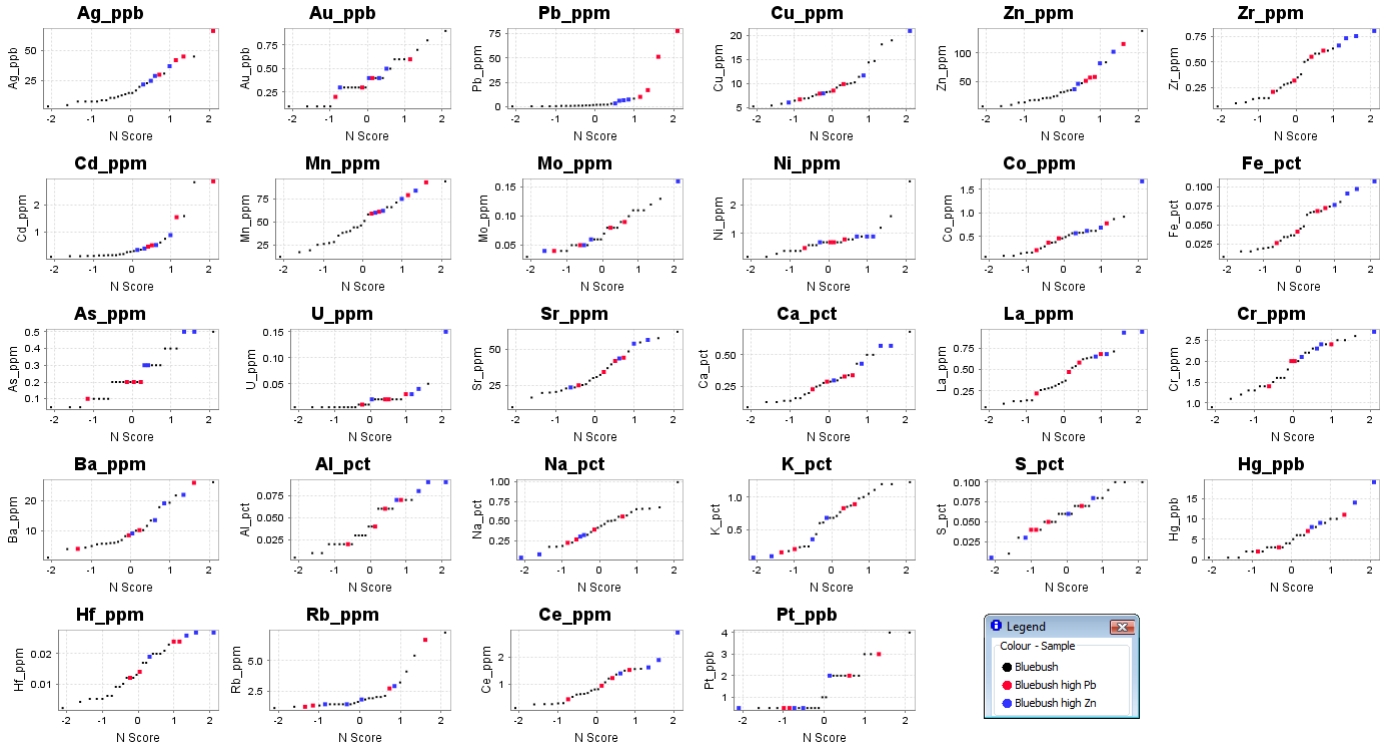

Appendix 2.4.10

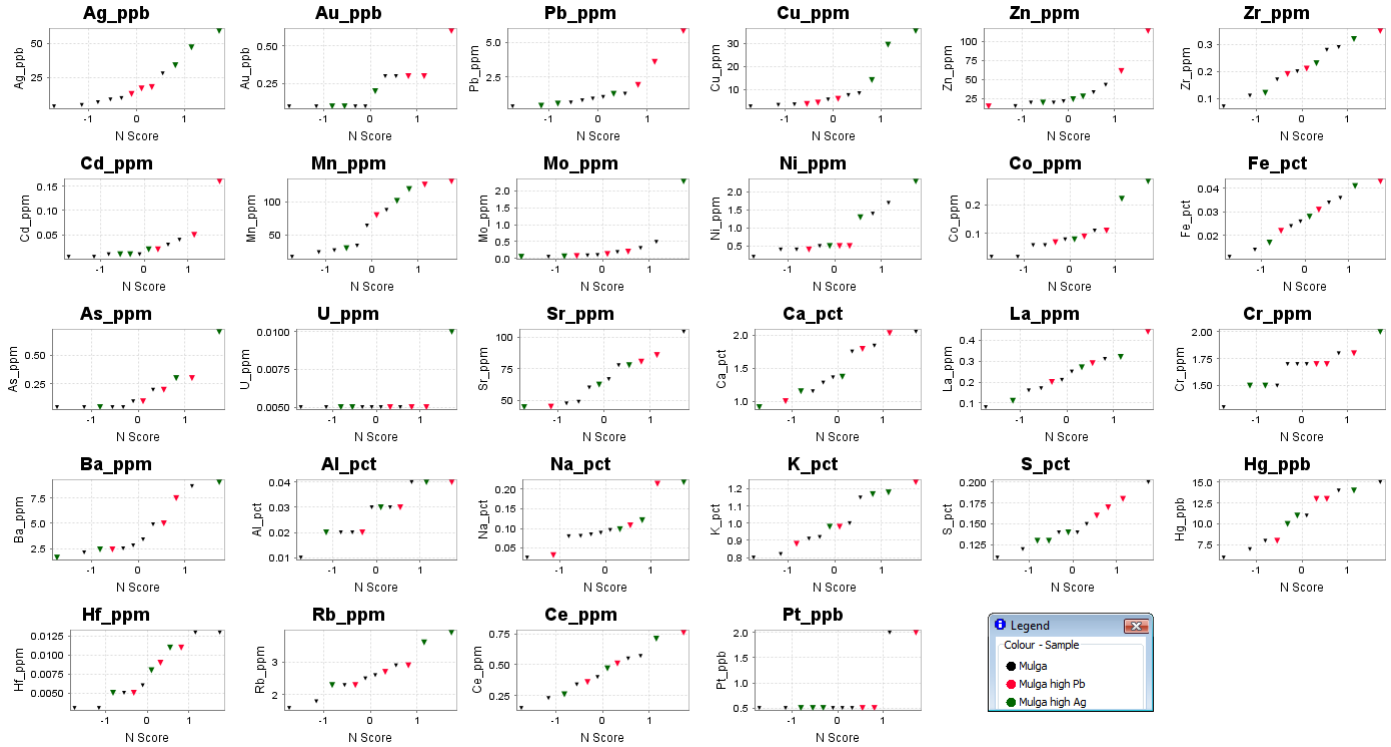

Biogeochemisty of mineralization styles Bluebush
Appendix 2.4.11

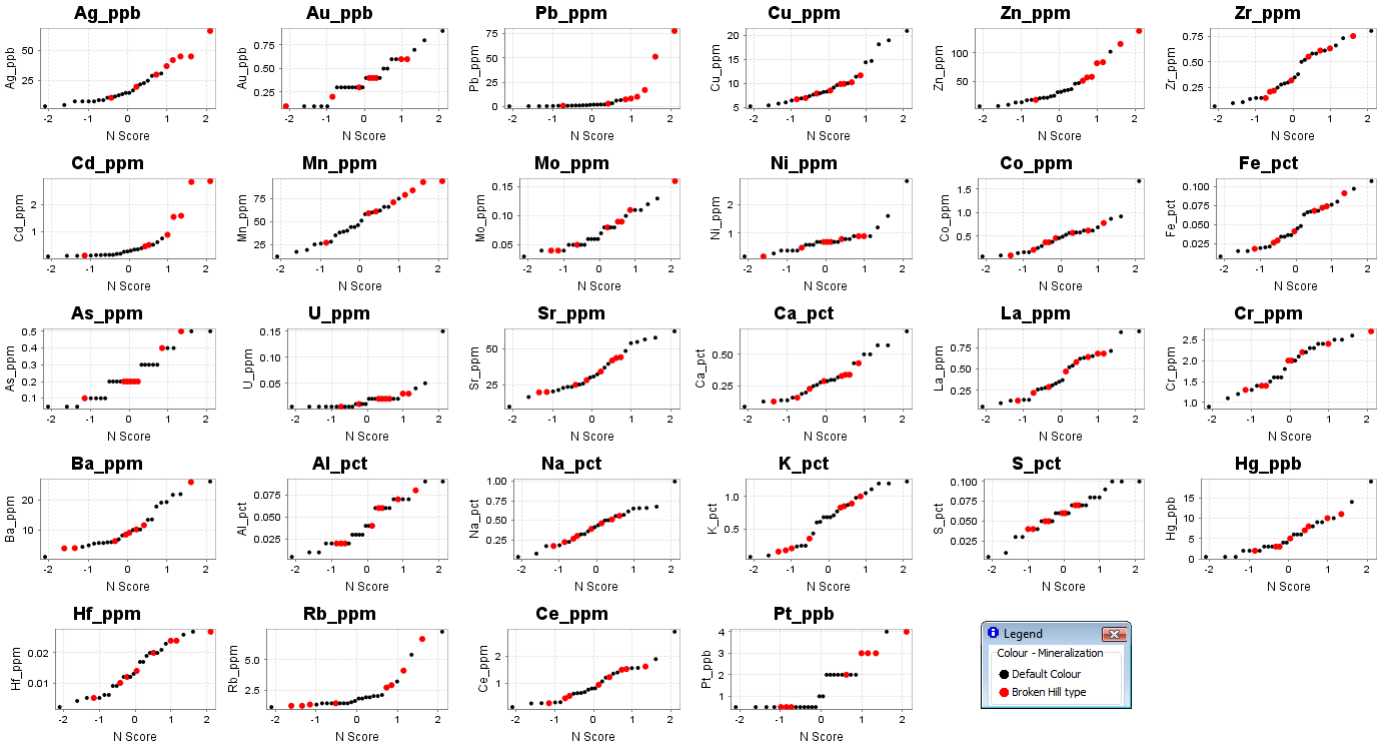

Appendix 2.4.12

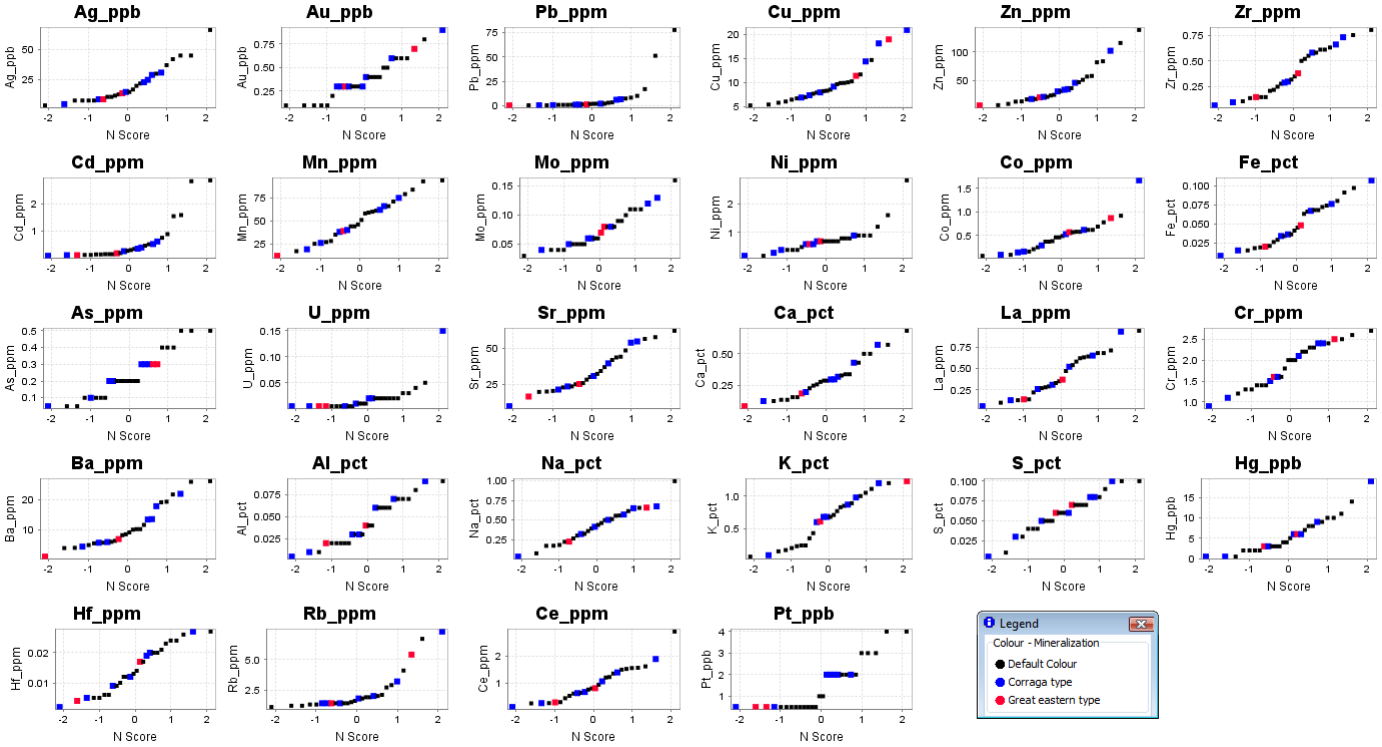

Biogeochemisty of mineralization styles Mulga
Appendix 2.4.13

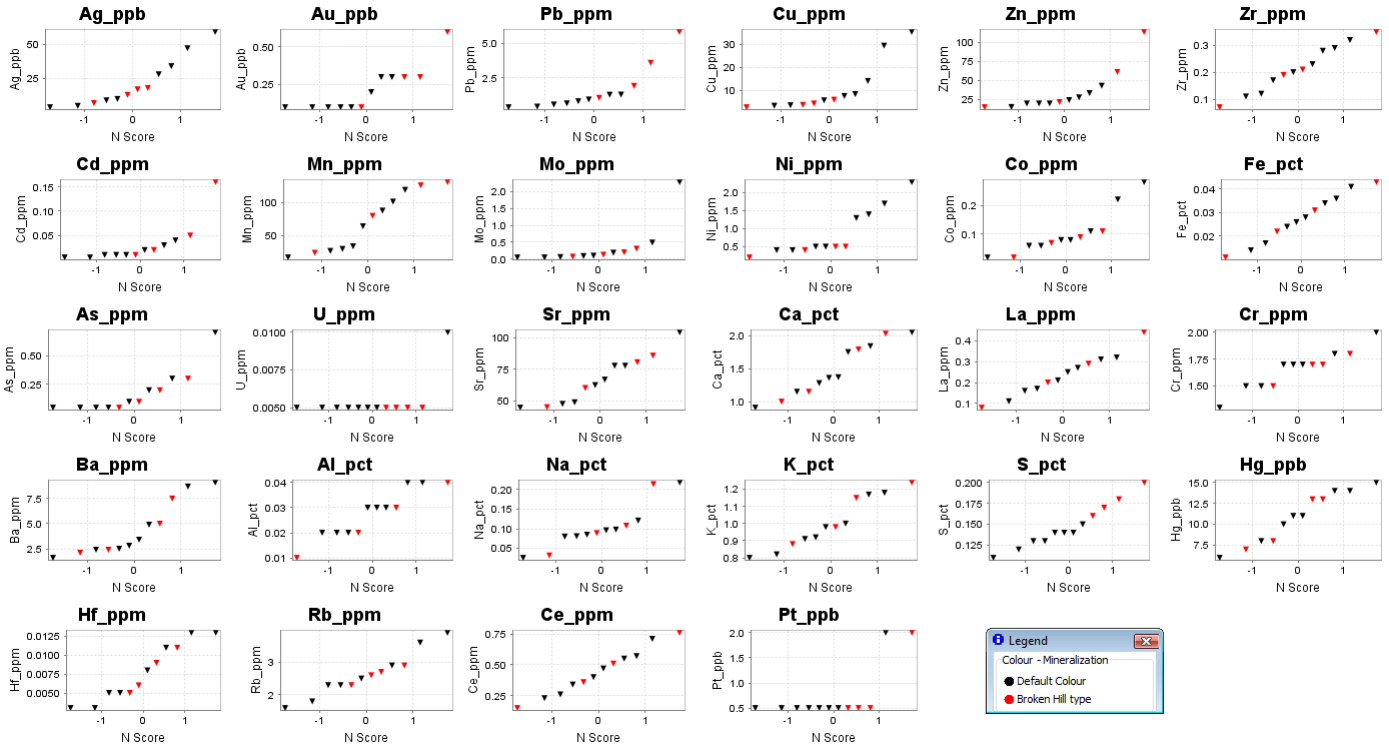

Appendix 2.4.14

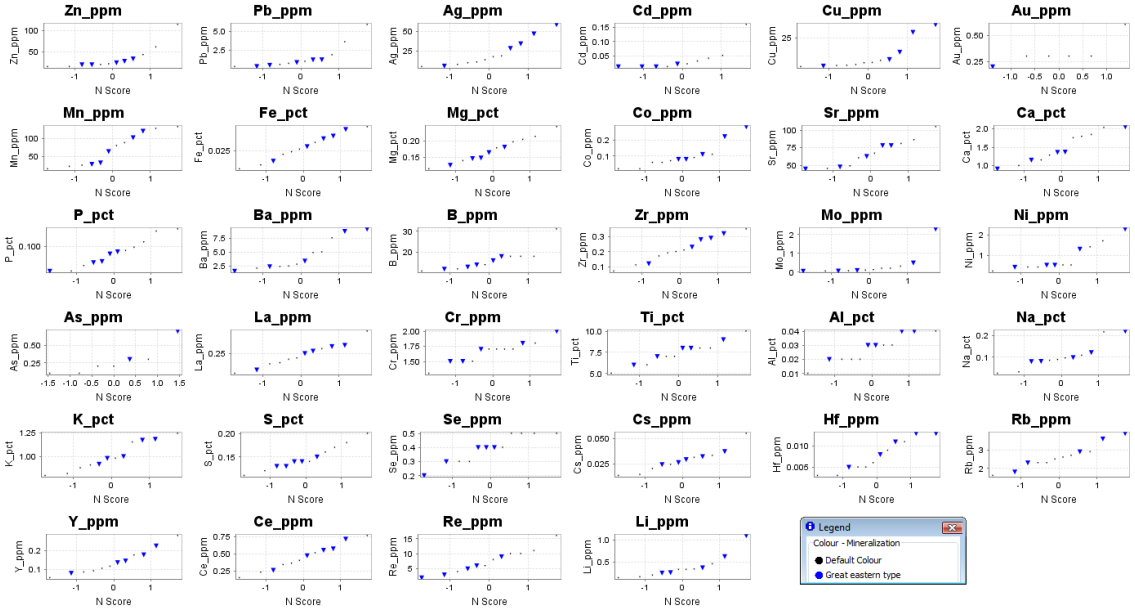

Niton additional plots
Appendix 2.5.1

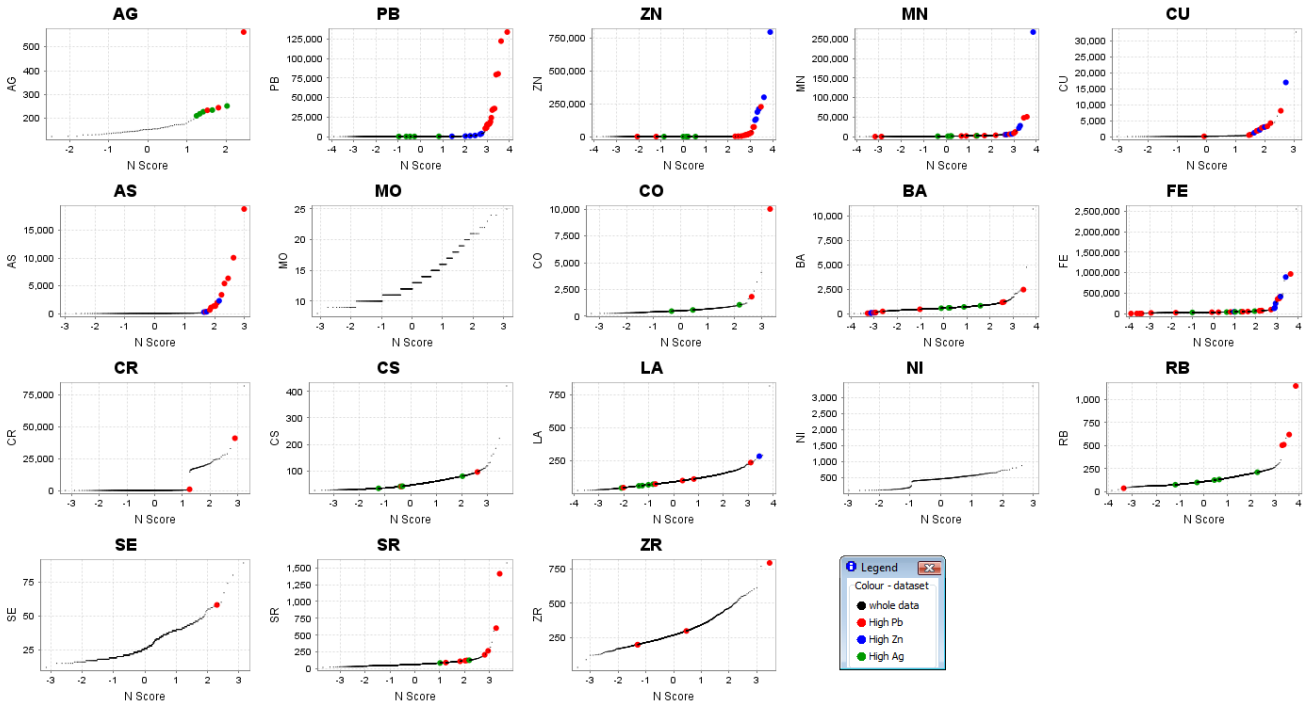

Appendix 2.5.2

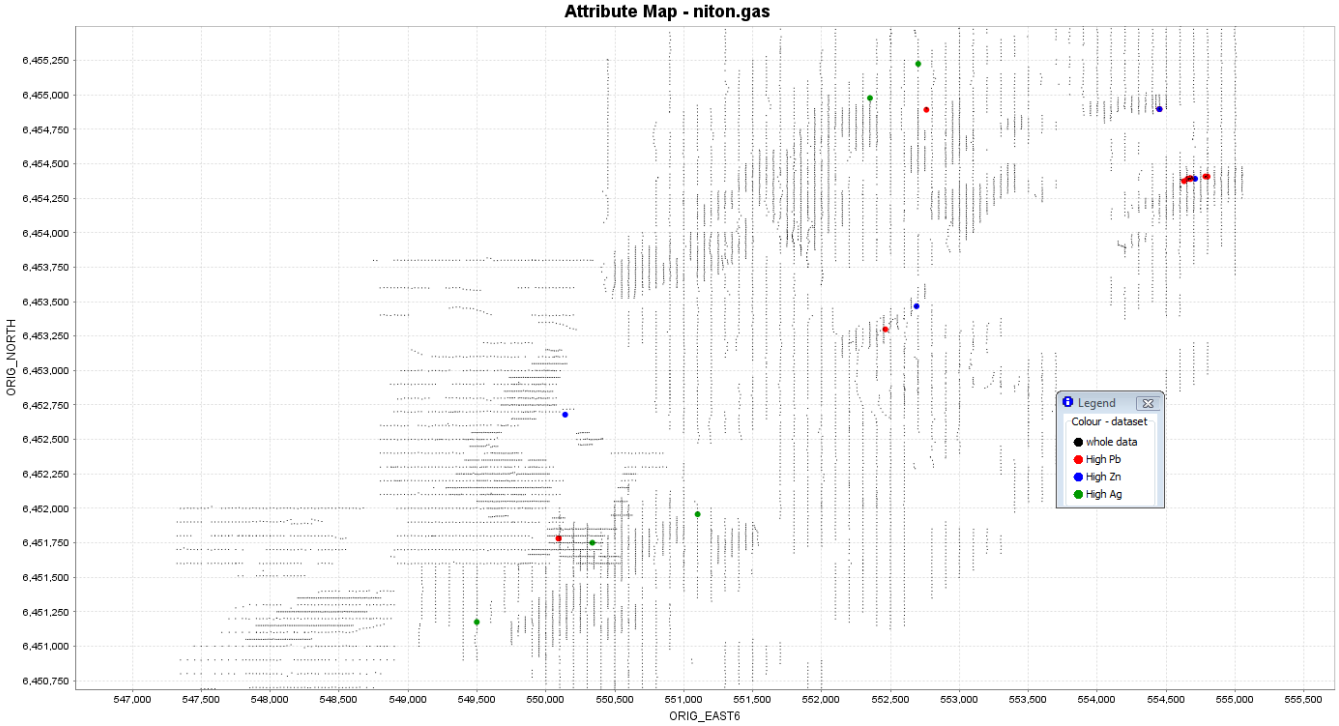

Appendix III – Raw data used in analysis

Appendix 3.1 Soil geochemical data

ELEMENTS	Au	Ag	Al	As	Ba	Be	Bi	Ca	Cd	Ce	Co	Cr	Cs
UNITS	ppb	ppm	ppm	ppm	ppm	ppm	ppm	%	ppm	ppm	ppm	ppm	ppm
DETECTION	1	0.02	20	0.5	1	0.05	0.01	0.01	0.01	0.01	0.1	1	0.01
METHOD	AR01/MS	AR01/MS	AR01/OE	AR01/MS	AR01/MS	AR01/MS	AR01/MS	AR01/OE	AR01/MS	AR01/MS	AR01/MS	AR01/MS	AR01/MS
COMMENTS: 1027.1/1010673 (03/09/2010) CLIENT O/N: STEVE HILL 1/1													
MINUS 01	6	0.67	28989	3.1	75	0.96	0.26	0.22	0.64	98.51	10.6	31	1.95
MINUS 02	2	0.56	29632	3.5	72	0.95	0.36	0.25	0.58	104.05	10.2	30	1.85
MINUS 03	5	0.97	35328	3	100	1.2	0.56	1.25	1.06	84.05	13.6	31	2.21
MINUS 04	4	0.95	30867	4.1	84	1.03	0.49	0.28	1.55	62.91	11.2	30	2.23
MINUS 05	4	1.67	33457	3.8	103	1.07	0.89	0.73	3.44	57.13	18.5	28	2.03
MINUS 06	4	0.55	31194	3.8	62	1.04	0.27	0.18	0.68	81.52	9.1	30	2.09
MINUS 07	3	0.69	44972	3.9	141	1.25	0.4	0.42	1.56	53.4	19.1	31	2.45
MINUS 08	2	1.35	33562	4.1	119	1.09	0.57	0.55	1.39	57.1	11.5	28	2.45
MINUS 09	3	1.64	40600	3.7	121	1.28	0.87	0.42	1.85	72.14	17.1	31	2.47
MINUS 10	X	1.23	29648	3.8	93	1.06	1.16	0.32	1.9	65.17	12.1	31	2.36
MINUS 11	3	0.63	34859	3.4	131	1.59	0.65	0.33	1.38	102.35	13	36	2.99
MINUS 12	X	0.71	24873	3.4	63	0.92	0.3	0.19	0.94	66.46	8.4	28	1.98
MINUS 13	2	0.6	25614	3.2	60	0.91	0.26	0.17	0.74	72.3	9	28	1.77
MINUS 14	X	0.63	28561	3.1	84	1.46	0.26	0.21	0.73	91.26	10.7	32	2.35
MINUS 15	6	1.63	38560	3.1	129	1.62	1.86	0.34	1.09	81.51	17.7	32	2.86
MINUS 16	2	0.44	24182	3.4	88	0.99	0.75	0.26	0.89	76.62	9.6	27	2.25
MINUS 17	2	0.35	27132	2.4	82	1.35	0.36	0.2	0.47	87.53	10.4	29	2.21
MINUS 18	3	0.98	31979	3	100	1.06	0.53	1.22	1.09	76.68	13	30	2.14
MINUS 19	6	0.81	37198	3.9	125	1.64	0.34	0.38	1.17	51.59	16.8	27	2.27
CHECKS													
MINUS 02	1	0.45	27601	3.7	70	1.23	0.28	0.29	0.6	95.02	10.1	31	1.83
PLUS 01	X	0.27	22222	3.7	69	1.33	0.2	0.67	0.51	90.98	11.9	27	1.27
PLUS 21	1	0.2	37791	4.1	126	2.03	0.31	0.55	0.23	60.24	14.6	41	3.12
STANDARDS													
AE19	77	1.07	19371	80.8	14	0.2	9.93	0.73	1.02	13.58	43.5	93	0.18
NGL-24	19	0.21	9812	17.7	85	0.08	1.87	0.88	0.24	7.42	8.5	49	0.09
AE19	78	1.31	20248	85.4	14	0.19	11.25	0.82	1.08	14.91	44.4	101	0.17
NGL-24	17	0.23	9303	18.3	84	X	1.95	0.95	0.23	7.22	8	49	0.08
AE19	66	1.23	18740	78.9	14	0.19	10.12	0.75	0.98	13.81	42.3	96	0.18
NGL-24	15	0.21	8936	18.6	85	X	1.82	0.9	0.22	7.01	7.8	48	0.08
AE19	66	1.08	17626	83.4	12	0.21	9.54	0.9	1.05	12.67	43.5	102	0.15
NGL-24	15	0.18	9036	18.3	85	0.09	1.86	0.93	0.25	6.63	8.5	52	0.08
BLANKS													
Control Blank	X	0.03	X	X	X	X	0.04	0.01	0.01	0.02	X	1	X

Cu	Dy	Er	Eu	Fe	Ga	Gd	Hf	Ho	In	K	La	Li	Lu
ppm	ppm	ppm	ppm	%	ppm	ppm	ppm	ppm	ppm	ppm	ppm	ppm	ppm
0.2	0.01	0.01	0.01	0.01	0.05	0.05	0.01	0.01	0.005	20	0.01	0.1	0.01
AR01/MS	AR01/MS	AR01/MS	AR01/MS	AR01/OE	AR01/MS	AR01/MS	AR01/MS	AR01/MS	AR01/MS	AR01/OE	AR01/MS	AR01/MS	AR01/MS
28.9	3.93	1.73	1.31	3.13	7.47	6.71	0.38	0.69	0.04	5117	51.05	15	0.21
33.1	4.11	1.78	1.4	3.36	7.23	7.2	0.44	0.71	0.041	5093	54.15	5.9	0.22
104.8	4.04	1.97	1.27	3.87	8.89	6.1	0.47	0.76	0.057	6533	43.59	16.2	0.26
51.3	2.92	1.37	0.94	3.27	8.04	4.55	0.38	0.52	0.048	5998	30.97	13.9	0.16
131	3.16	1.53	0.95	4.42	9.22	4.48	0.43	0.58	0.081	5429	26.94	13.6	0.2
26.6	3.68	1.75	1.16	3.16	7.8	5.84	0.41	0.67	0.035	5572	43.53	14.8	0.21
108.5	3.56	1.72	1.18	4.65	13.01	5.15	0.21	0.67	0.108	6158	26.45	17.1	0.22
59.5	2.97	1.41	0.99	3.41	8.94	4.5	0.39	0.54	0.057	6409	28.5	15.2	0.17
97.4	3.7	1.74	1.18	4.67	11.02	5.61	0.31	0.67	0.155	6738	35.7	16.7	0.21
47.3	3.12	1.46	1.06	3.23	7.88	4.83	0.39	0.58	0.073	6555	34.6	14.8	0.18
46.1	4.79	2.22	1.74	3.69	9.26	8.06	0.46	0.87	0.053	7570	61.68	18.8	0.27
25.4	3.04	1.46	1.01	2.69	6.59	4.72	0.41	0.56	0.034	4815	35.5	11.3	0.18
28.8	3.59	1.67	1.13	3.03	6.75	5.6	0.42	0.65	0.033	5124	41.12	5.2	0.2
22.2	4.38	2	1.42	3.18	7.65	6.96	0.33	0.79	0.037	5347	53.59	14.1	0.25
118	4.95	2.5	1.34	4.45	10.55	7.1	0.36	0.94	0.129	7005	46.18	18.1	0.33
47.1	3.18	1.39	1.07	3.02	6.67	5.35	0.33	0.56	0.058	4994	40.89	11.6	0.17
30.1	4.22	1.86	1.7	3.19	6.78	8.3	0.43	0.75	0.038	5843	62.13	13.4	0.22
101.8	3.81	1.88	1.2	3.89	8.59	5.65	0.5	0.72	0.058	6304	42.31	15.1	0.23
137.8	3.23	1.57	0.98	3.93	10.61	4.37	0.46	0.61	0.065	6153	25.37	15.8	0.2
32.8	3.89	1.66	1.28	3.19	7.86	6.43	0.4	0.66	0.04	4579	50.29	16.9	0.21
29.2	4.14	2.03	1.14	4.06	6.53	6.09	0.32	0.75	0.041	3406	44.99	12.2	0.26
37.3	4.1	2.07	1.17	3.82	11.15	5.08	0.54	0.77	0.042	8205	27.99	23.1	0.25
101.2	0.26	0.37	0.09	4.42	17.34	0.58	2.1	0.29	0.067	416	12.72	2.6	0.02
103.7	0.17	0.08	0.05	3.39	8.32	0.2	1.26	0.03	0.04	253	1.99	1.4	0.01
109.4	0.29	0.4	0.1	5.15	18.97	0.65	2.26	0.34	0.075	364	13.96	2.6	0.02
104.3	0.15	0.07	0.04	3.34	8.61	0.19	1.41	0.03	0.038	180	1.8	1.2	0.01
106.4	0.26	0.38	0.09	4.76	18.7	0.59	1.82	0.3	0.074	361	13.37	2.7	0.02
105.8	0.14	0.06	0.04	3.46	8.78	0.18	1.1	0.03	0.036	180	1.75	1.2	0.01
106.8	0.26	0.37	0.09	4.87	19.64	0.55	1.95	0.3	0.072	307	11.49	3.1	0.02
108.9	0.14	0.07	0.04	3.44	9.2	0.18	1.25	0.03	0.039	172	1.73	1.6	0.01
1.1	X	X	X	X	X	X	X	X	X	22	0.01	X	X

Mg	Mn	Mo	Na	Nb	Nd	Ni	P	Pb	Pd	Pr	Pt	Rb	Re
%	ppm	ppm	%	ppm	ppm	ppm	ppm	ppm	ppb	ppm	ppb	ppm	ppm
0.01	1	0.1	0.01	0.02	0.01	0.2	10	0.5	10	0.005	5	0.02	0.001
AR01/OE	AR01/OE	AR01/MS	AR01/OE	AR01/MS	AR01/MS	AR01/MS	AR01/OE	AR01/MS	AR01/MS	AR01/MS	AR01/MS	AR01/MS	AR01/MS
0.4	634	0.4	0.07	0.22	44.52	18.8	426	190.4	X	11.739	X	36.05	X
0.38	576	0.4	0.08	0.21	48.9	18.7	446	160.6	X	13.111	7	34.77	X
0.5	865	0.4	0.08	0.22	39.14	21	487	241.5	20	10.235	X	41.22	X
0.44	787	0.4	0.07	0.16	28.46	16.8	459	313.1	X	7.433	X	41.07	X
0.51	1058	0.5	0.09	0.24	25.32	19.7	579	1036.5	X	6.577	X	38.31	X
0.38	617	0.5	0.07	0.29	38.61	18.4	416	187	X	10.182	X	37.6	X
0.44	938	0.4	0.09	0.09	27.55	16.3	688	257.5	X	6.848	X	43.93	X
0.51	663	0.4	0.08	0.19	26.56	16.9	488	652.5	X	6.82	X	49.03	X
0.51	1007	0.4	0.08	0.12	32.88	18.9	568	530.6	X	8.512	6	47.93	X
0.47	701	0.4	0.07	0.18	30.69	17.9	402	482.8	11	7.95	X	47.78	X
0.52	538	0.4	0.07	0.2	53.55	23.3	435	166.6	20	13.822	X	67.5	X
0.36	570	0.4	0.07	0.24	30.7	15.7	417	215.4	X	8.055	X	38.31	X
0.36	583	0.5	0.07	0.37	35.64	17.1	424	185.5	X	9.258	X	33.99	0.002
0.4	680	0.6	0.05	0.23	45.79	18.7	402	187.9	X	11.979	X	48.09	X
0.47	1070	0.6	0.09	0.19	41.97	19.6	600	716.5	X	10.844	X	60.04	X
0.42	525	0.3	0.07	0.14	35.57	17	410	229.5	13	9.381	6	47.44	X
0.42	436	0.4	0.07	0.28	54.58	19.7	356	120.7	X	14.389	X	55.6	X
0.49	798	0.4	0.08	0.16	36.98	20.8	493	232.2	X	9.687	X	40.76	X
0.49	764	0.4	0.08	0.19	24.13	16.2	486	251.3	X	6.113	X	42.41	X
0.37	541	0.4	0.07	0.13	44.49	18	411	149.3	13	11.855	X	33.9	X
0.34	784	0.5	0.05	0.17	39.33	19.4	346	115.5	12	10.44	X	26	X
0.69	570	0.4	0.07	0.17	27.89	24.1	373	43.9	X	7.122	X	59.57	X
0.07	291	26.5	0.8	0.31	2.04	101.8	124	51.5	267	0.576	231	2.01	X
0.31	89	6.3	0.42	0.22	1.17	20.9	69	12.7	217	0.328	198	1.4	0.002
0.07	297	29.1	0.83	0.32	2.13	111.1	127	58.4	296	0.598	260	1.71	X
0.32	86	6.1	0.38	0.32	1.07	21.1	71	11.4	226	0.31	200	0.97	X
0.07	291	24.9	0.77	0.25	2.01	103.4	126	53.2	215	0.564	235	1.79	X
0.29	81	5.9	0.39	0.21	1.04	19.5	57	11	213	0.289	195	0.96	X
0.09	285	26.7	0.73	0.3	1.83	100.7	123	50.8	182	0.517	201	1.52	X
0.31	84	5.9	0.38	0.2	1	20.5	67	10.9	199	0.283	186	0.98	X
X	X	X	0.04	X	0.01	0.4	X	X	X	X	X	0.06	X

Sb	Sc	Se	Sm	Sn	Sr	Ta	Tb	Te	Th	Ti	Tl	Tm	U
ppm	ppm	ppm	ppm	ppm	ppm	ppm	ppm	ppm	ppm	ppm	ppm	ppm	ppm
0.02	0.1	0.5	0.01	0.05	0.02	0.01	0.005	0.01	0.01	5	0.01	0.01	0.01
AR01/MS	AR01/MS	AR01/MS	AR01/MS	AR01/MS	AR01/MS	AR01/MS	AR01/MS	AR01/MS	AR01/MS	AR01/OE	AR01/MS	AR01/MS	AR01/MS
1.17	8.2	X	7.97	1	27.24	X	0.852	0.06	17.58	553	0.25	0.23	1.37
0.72	7.8	X	8.64	0.89	27.29	X	0.907	0.06	19.78	612	0.27	0.23	1.64
0.52	9.7	X	7.07	1.03	40.77	X	0.81	0.07	14.77	833	0.34	0.27	1.72
1.43	9.1	X	5.3	1.1	28.55	X	0.602	0.06	11.15	619	0.29	0.18	1.07
1.29	11.5	X	5.02	1.2	35.46	X	0.63	0.08	10.04	1004	0.3	0.2	1.47
1.35	8.8	X	7.01	0.95	28.04	X	0.762	0.03	14.5	505	0.25	0.23	1.28
0.41	14.6	X	5.62	1.36	44.74	X	0.699	0.06	8.73	462	0.33	0.23	0.91
0.74	9.8	X	5.04	1.07	32.71	X	0.603	0.07	9.49	580	0.37	0.18	0.92
1.07	12.9	X	6.35	1.41	37.86	X	0.751	0.06	12.8	764	0.37	0.23	1.41
1.28	9	X	5.65	1.12	27.53	X	0.647	0.09	11.72	507	0.36	0.19	1
0.49	10.5	X	9.53	1.02	30.86	X	1.003	0.09	18.09	479	0.61	0.29	1.38
1.44	7.8	X	5.72	0.95	23.54	X	0.616	0.08	11.24	432	0.28	0.2	0.97
1.13	8.5	X	6.58	0.93	25.08	X	0.733	0.06	13.18	381	0.23	0.22	1.2
1.26	8.5	X	8.22	0.98	30.02	X	0.897	0.08	15.95	491	0.39	0.27	1.46
0.44	12.8	X	7.87	1.4	39.63	X	0.973	0.09	14.76	696	0.53	0.34	1.66
0.58	7.7	X	6.42	0.95	28.08	X	0.692	0.05	14.14	601	0.4	0.18	1.23
0.4	7.8	X	9.77	0.83	24.51	X	0.982	0.06	16.83	469	0.5	0.23	1.22
0.42	9.7	X	6.79	0.99	39.64	X	0.77	0.06	14.08	647	0.34	0.26	1.45
0.9	13.9	X	4.81	1.28	35.18	X	0.622	0.06	9.39	636	0.3	0.22	1.22
0.71	7.8	X	8.12	0.95	29.96	X	0.858	0.02	18.95	559	0.25	0.21	1.52
0.41	8.9	X	7.28	0.86	24.55	X	0.852	0.05	18.98	470	0.21	0.28	1.74
0.14	10.9	X	5.56	1.26	57.86	X	0.762	0.02	9.87	237	0.43	0.27	1.11
7.82	5.3	1.8	0.39	2.37	54.8	0.02	0.053	8.63	51.08	1293	7.52	0.02	12.71
1.41	2.9	9.1	0.23	1.15	34.65	X	0.032	5.39	26.85	691	1.48	0.01	9.62
8.77	4.6	1.9	0.43	2.69	60.61	0.01	0.059	9.43	56.9	1353	8.62	0.02	14.69
1.44	2	8.7	0.21	1.18	34.43	X	0.03	5.79	28.12	645	1.49	0.01	9.66
7.8	4	1.8	0.39	2.53	56.74	X	0.052	8.38	52.34	1196	8.32	0.02	13.83
1.34	1.8	8.1	0.19	1.12	33.76	X	0.028	5.24	27.09	630	1.48	X	9.6
7.97	5.2	1.6	0.37	2.48	55.96	X	0.049	8.35	48.91	1203	7.56	0.02	13.21
1.34	2	8.7	0.2	1.21	37.37	X	0.029	5.81	27.89	621	1.48	0.01	9.76
X	0.2	X	X	X	X	X	X	X	X	10	X	X	X

V	W	Y	Yb	Zn	Zr	Eastings	Northings	Duplicate					
ppm	ppm	ppm	ppm	ppm	ppm	GDA94	GDA94						
2	0.05	0.02	0.01	1	0.1								
AR01/OE	AR01/MS	AR01/MS	AR01/MS	AR01/OE	AR01/MS								
51	0.09	18.64	1.44	276	13.8	554600	6454437						
53	0.14	17.63	1.47	290	13.9	554601	6454426						
63	0.07	18.82	1.74	593	15.7	554601	6454414						
72	0.05	13.56	1.09	760	11.9	554602	6454400						
122	0.12	14.43	1.31	1638	12.6	554600	6454383						
50	0.07	17.41	1.45	270	13.4	554605	6454254						
77	X	17.02	1.46	1094	7.2	554600	6454362						
60	0.06	13.94	1.17	645	11.2	554600	6454338						
88	0.05	16.82	1.44	1691	10.5	554600	6454319						
57	0.12	14.74	1.2	838	13.1	554603	6454299						
59	0.06	23.25	1.81	701	16.4	554599	6454285						
43	0.14	14.57	1.2	325	13.4	554601	6454271						
47	0.14	17.17	1.38	271	12.8	554605	6454254						
49	0.08	21.12	1.69	295	12.2	554599	6454226						
72	0.26	25.22	2.19	1512	12.6	554602	6454200						
57	0.11	14.5	1.14	528	11.3	554600	6454172						
49	0.14	19.61	1.43	242	14.2	554602	6454160						
61	0.08	18.26	1.62	595	15.7	554601	6454414	3					
102	X	15.44	1.38	731	13.2	554601	6454376	6					
48	0.06	16.62	1.39	266	13.3								
39	X	19.08	1.82	223	12								
52	X	20.09	1.72	109	16.6								
320	0.13	1.09	0.12	115	77.8								
100	0.14	0.69	0.07	23	43.8								
355	0.16	1.11	0.13	126	81.7								
98	0.17	0.64	0.07	20	45.4								
316	0.08	1.08	0.12	118	68.9								
90	0.19	0.59	0.07	18	38								
323	0.14	1.03	0.12	114	73.5								
99	0.1	0.62	0.07	19	42.6								
X	X	X	X	X	X								

Appendix 3.2 Biogeochemical data

Eastings	Northings	co-ord system	repeats	Sample	Sample
556183	6451440	GDA94		RKBBB	RKBBB 001
556183	6457440	GDA94		RKBBB	RKBBB 002
556066	6457067	GDA94		RKBBB	RKBBB 003
556570	6457715	GDA94		RKBBB	RKBBB 004
556534	6457577	GDA94		RKBBB	RKBBB 005
556939	6459196	GDA94		RKBBB	RKBBB 006
557165	6459330	GDA94		RKBBB	RKBBB 007
558838	6458790	GDA94		RKBBB	RKBBB 008
560703	6459199	GDA94		RKBBB	RKBBB 009
555756	6454368	GDA94		RKBBB	RKBBB 010
555362	6454346	GDA94		RKBBB	RKBBB 011
554387	6453770	GDA94		RKBBB	RKBBB 012
553437	6452956	GDA94		RKBBB	RKBBB 013
553149	6452639	GDA94		RKBBB	RKBBB 014
552980	6452513	GDA94		RKBBB	RKBBB 015
552982	6452517	GDA94		RKBBB	RKBBB 016
552861	6452565	GDA94		RKBBB	RKBBB 017
552861	6452565	GDA94		RKBBB	RKBBB 018
550481	6451486	GDA94		RKBBB	RKBBB 019
549072	6452194	GDA94		RKBBB	RKBBB 020
550973	6447768	GDA94		RKBBB	RKBBB 021
554444	6448088	GDA94		RKBBB	RKBBB 022
559362	6448158	GDA94		RKBBB	RKBBB 023
559564	6448264	GDA94		RKBBB	RKBBB 024
559748	6448303	GDA94		RKBBB	RKBBB 025
559811	6448324	GDA94		RKBBB	RKBBB 026
559935	6448319	GDA94		RKBBB	RKBBB 027
559972	6448356	GDA94		RKBBB	RKBBB 028
		GDA94	RKBBB001	RKBBB	RKBBB 029
		GDA94	RKBBB025	RKBBB	RKBBB 030
		GDA94	RKBBB015	RKBBB	RKBBB 031
556066	6457067	GDA94		RKMU	RKMU 001
556534	6457577	GDA94		RKMU	RKMU 002
556939	6459196	GDA94		RKMU	RKMU 003
557165	6459330	GDA94		RKMU	RKMU 004
558838	6458790	GDA94		RKMU	RKMU 005
555756	6454368	GDA94		RKMU	RKMU 006
555362	6454346	GDA94		RKMU	RKMU 007
554387	6453770	GDA94		RKMU	RKMU 008
553437	6452956	GDA94		RKMU	RKMU 009
553149	6452639	GDA94		RKMU	RKMU 010
552754	6452506	GDA94		RKMU	RKMU 011
552861	6452565	GDA94		RKMU	RKMU 012
		GDA94	RKMU007	RKMU	RKMU 013
		GDA94	RKMU008	RKMU	RKMU 014

Mineralization	Mo	Cu	Pb	Zn	Ag	Ni
Corraga type	0.06	8	6.6	46.3	25	0.7
Corraga type	0.05	7.4	0.44	21.9	9	0.2
Corraga type	0.04	20.95	6.11	102.3	29	0.9
Corraga type +Pb Zn	0.06	9.19	0.49	18.1	5	0.4
Corraga type +Pb Zn	0.13	14.43	2.08	35.4	15	0.6
Thackeringa type and Great e	0.08	11.43	1.37	20.9	14	0.7
Great eastern type	0.07	19.01	0.34	7.1	9	0.6
Corraga type +Pb Zn	0.12	18.17	1.04	34.3	23	0.6
Haematite breccia and ferrug	0.06	6.47	0.47	32.2	8	0.4
Mulga springs type	0.1	8.24	0.95	17.5	11	1.6
Mulga springs type	0.05	14.7	1.92	47.4	17	2.8
related to Broken hill type	0.09	9.94	2.96	83.8	20	0.7
Broken Hill type	0.04	9.91	77.63	51.6	66	0.7
Broken Hill type	0.11	7	0.81	18.1	11	0.2
Broken Hill type	0.09	7.94	51.19	58.4	45	0.8
Broken Hill type	0.08	6.74	10.1	57.3	30	0.7
Broken Hill type	0.04	10.27	8.2	138.4	45	0.9
Broken Hill type	0.05	8.56	16.97	115.8	42	0.5
related to Broken hill type	0.16	11.72	7.41	82.2	37	0.9
Corraga type	0.08	6.91	1.09	31.4	31	0.3
Copper bearing quartz veins i	0.03	8.33	0.74	13.6	4	1.2
Laminated pyritic quartz vein	0.05	6.08	3.36	36.9	22	0.9
pyritic	0.11	5.82	2.08	14	8	0.7
Gold bearing quartz	0.05	5.45	1.99	25.4	13	0.7
Pyrite quartz veins	0.08	10.07	1.71	21.9	8	0.8
Gold bearing quartz	0.11	9.69	0.39	24.2	8	0.4
Gold bearing quartz	0.04	7.69	1.36	9.6	12	0.8
Gold bearing quartz	0.06	5.29	0.84	7.5	15	0.4
Corraga type	0.03	6.67	3.97	28.6	28	0.4
Pyrite quartz veins	0.08	9.28	1.34	20.4	8	0.6
Broken Hill type	0.13	10.05	64.48	76.4	62	1.1
Corraga type	0.49	8.39	1.29	33.8	28	0.5
Corraga type +Pb Zn	0.09	3.31	0.93	20.2	5	0.4
Thackeringa type and Great e	0.05	29.52	1.28	20.2	34	1.3
Great eastern type	0.06	35.48	0.57	28.2	47	2.3
Corraga type +Pb Zn	2.29	14.1	0.41	24.7	59	0.5
Mulga springs type	0.1	5.68	0.65	20.2	9	1.4
Mulga springs type	0.05	7.58	0.37	43.5	10	1.7
related to Broken hill type	0.19	3.55	0.8	15.7	4	0.4
Broken Hill type	0.2	3.73	5.85	15.4	13	0.4
Broken Hill type	0.31	2.7	1.05	22	7	0.2
Broken Hill type	0.13	5.94	3.6	61.5	18	0.5
Broken Hill type	0.07	4.31	1.92	113.7	17	0.5
Mulga springs type	0.16	4.32	0.81	18.2	3	2.2
related to Broken hill type	0.19	3.34	0.81	15.3	4	0.3

Co	Mn	Fe	As	U	Au	Th	Sr	Cd
0.62	62	0.076	0.3	0.02	0.4	0.15	53.8	0.4
0.09	19	0.008	<0.1	<0.01	0.9	0.01	10	0.27
1.67	75	0.107	0.3	0.15	0.3	0.18	23.6	0.53
0.14	26	0.015	0.2	<0.01	0.3	0.03	21.5	0.1
0.29	38	0.067	0.3	0.01	0.6	0.14	54.7	0.12
0.57	39	0.048	0.3	<0.01	0.3	0.08	25.3	0.19
0.87	12	0.02	0.3	<0.01	0.7	0.03	16.6	0.12
0.53	40	0.034	0.2	0.02	0.3	0.06	39.5	0.36
0.58	28	0.019	<0.1	0.02	0.3	0.05	25.9	0.16
0.25	35	0.034	0.2	<0.01	0.3	0.06	23.6	0.28
0.49	46	0.045	0.2	<0.01	0.6	0.08	22.9	0.76
0.62	94	0.074	0.4	0.02	0.6	0.13	28.3	1.59
0.78	61	0.041	0.2	0.02	0.6	0.08	44.1	0.47
0.09	27	0.018	0.2	<0.01	<0.2	0.03	19.8	0.13
0.46	93	0.072	0.1	0.03	0.4	0.15	34.3	2.86
0.37	79	0.068	0.2	0.02	0.3	0.12	41.9	0.52
0.37	71	0.029	0.2	0.02	0.4	0.05	20.1	2.83
0.21	59	0.026	0.2	0.01	0.2	0.04	25.1	1.55
0.57	84	0.091	0.5	0.03	0.4	0.19	43.6	0.89
0.16	66	0.036	0.1	<0.01	0.3	0.06	30.8	0.62
0.16	17	0.021	0.4	<0.01	0.8	0.03	30.1	0.16
0.69	60	0.097	0.5	0.04	0.5	0.18	56.4	0.35
0.62	66	0.08	0.4	0.05	0.5	0.15	57.6	0.15
0.58	44	0.068	0.5	0.02	0.4	0.15	62	0.2
0.92	51	0.066	<0.1	0.02	<0.2	0.13	48.4	0.16
0.07	25	0.015	0.1	<0.01	<0.2	0.02	20.5	0.15
0.46	58	0.063	0.1	0.01	<0.2	0.12	32.3	0.13
0.38	44	0.036	0.1	0.01	<0.2	0.06	36.9	0.31
0.36	40	0.04	0.2	0.01	<0.2	0.07	48.2	0.29
0.84	44	0.049	0.1	0.02	<0.2	0.09	48.2	0.12
0.67	122	0.113	0.2	0.04	<0.2	0.19	40	3.39
0.11	64	0.036	<0.1	<0.01	<0.2	0.05	77.9	0.01
0.08	33	0.034	<0.1	<0.01	<0.2	0.05	47.5	<0.01
0.22	102	0.041	<0.1	0.01	<0.2	0.06	77.9	0.02
0.28	120	0.028	0.3	<0.01	0.2	0.04	44.5	0.01
0.08	29	0.017	0.7	<0.01	<0.2	0.02	62.4	0.01
0.06	16	0.024	<0.1	<0.01	<0.2	0.03	66.8	<0.01
0.02	26	0.014	0.2	<0.01	0.3	0.02	48.8	0.04
0.06	88	0.026	0.1	<0.01	0.3	0.04	104.6	0.03
0.09	80	0.022	0.1	<0.01	0.6	0.03	44.9	0.02
0.02	23	0.011	<0.1	<0.01	<0.2	0.02	60.1	0.01
0.07	132	0.031	0.2	<0.01	0.3	0.06	86	0.16
0.11	127	0.043	0.3	<0.01	0.3	0.07	80.7	0.05
0.07	15	0.02	0.3	<0.01	0.2	0.03	54.2	0.01
0.08	82	0.026	0.2	<0.01	0.2	0.04	103.6	0.03

Sb	Bi	V	Ca	P	La	Cr	Mg	Ba
<0.02	<0.02	<2	0.57	0.025	0.65	2.4	0.289	21.9
<0.02	<0.02	<2	0.13	0.08	0.06	0.9	0.089	4.4
0.02	0.02	<2	0.3	0.016	0.93	2.1	0.111	13.5
<0.02	<0.02	<2	0.2	0.084	0.13	1.1	0.145	5.7
<0.02	<0.02	<2	0.32	0.057	0.52	2.4	0.176	17.8
<0.02	<0.02	<2	0.19	0.027	0.37	2.5	0.232	6.9
<0.02	<0.02	<2	0.09	0.054	0.14	1.6	0.331	1.1
<0.02	<0.02	<2	0.43	0.045	0.31	1.6	0.214	13.4
<0.02	<0.02	<2	0.26	0.133	0.27	1.4	0.156	4.9
<0.02	<0.02	<2	0.16	0.058	0.28	1.8	0.191	8.2
<0.02	<0.02	<2	0.28	0.063	0.35	2.3	0.252	10
<0.02	<0.02	2	0.34	0.032	0.64	2.2	0.177	11.6
<0.02	<0.02	<2	0.34	0.034	0.47	2	0.256	25.9
<0.02	<0.02	<2	0.13	0.076	0.13	1.3	0.099	3.9
0.03	<0.02	<2	0.29	0.018	0.68	2	0.187	10.2
0.03	<0.02	<2	0.33	0.023	0.58	2.4	0.2	8.5
<0.02	<0.02	<2	0.16	0.065	0.29	1.4	0.14	6.3
0.03	<0.02	<2	0.23	0.05	0.22	1.4	0.193	4
0.03	<0.02	2	0.43	0.038	0.68	2.7	0.207	9.1
<0.02	<0.02	<2	0.3	0.048	0.26	1.5	0.117	5.9
<0.02	<0.02	<2	0.14	0.05	0.14	1.3	0.248	5.7
0.02	<0.02	<2	0.57	0.015	0.94	2.3	0.136	19.1
<0.02	0.12	<2	0.68	0.025	0.71	2.5	0.113	26.1
<0.02	0.04	<2	0.5	0.015	0.63	2.2	0.157	19.3
<0.02	0.04	<2	0.5	0.051	0.62	2	0.191	21.7
<0.02	0.06	<2	0.14	0.083	0.1	1.2	0.151	6
<0.02	<0.02	<2	0.29	0.019	0.54	2.6	0.183	10.2
<0.02	<0.02	<2	0.25	0.039	0.33	1.6	0.182	5.5
<0.02	<0.02	<2	0.5	0.016	0.34	1.6	0.169	17.7
<0.02	<0.02	<2	0.47	0.044	0.42	1.9	0.17	20.9
0.06	0.02	3	0.33	0.026	0.95	2.9	0.233	13
<0.02	<0.02	<2	2.05	0.086	0.31	1.8	0.164	8.7
<0.02	<0.02	<2	1.36	0.077	0.25	1.7	0.124	3.4
0.02	<0.02	<2	1.37	0.085	0.32	2	0.181	2.4
<0.02	0.02	<2	0.91	0.093	0.27	1.5	0.145	1.6
0.02	<0.02	<2	1.15	0.095	0.11	1.5	0.147	9.1
<0.02	<0.02	<2	1.84	0.104	0.16	1.7	0.205	2.5
<0.02	<0.02	<2	1.28	0.077	0.17	1.3	0.138	2.8
<0.02	<0.02	<2	1.75	0.082	0.21	1.7	0.197	4.9
<0.02	<0.02	<2	1	0.116	0.2	1.7	0.112	2.4
<0.02	<0.02	<2	1.15	0.114	0.08	1.5	0.214	2.1
<0.02	<0.02	<2	1.79	0.099	0.29	1.7	0.178	5
<0.02	<0.02	<2	2.03	0.096	0.44	1.8	0.245	7.5
<0.02	<0.02	<2	1.31	0.086	0.13	1.7	0.285	2.6
<0.02	<0.02	<2	1.83	0.08	0.21	1.6	0.197	5

Ti	B	Al	Na	K	W	Sc	Tl	S
12	9	0.07	0.32	0.68	<0.1	0.1	<0.02	0.08
4	7	<0.01	0.65	1.2	<0.1	<0.1	0.03	0.05
13	4	0.09	0.033	0.09	<0.1	0.2	<0.02	<0.01
5	6	0.01	0.674	0.98	<0.1	<0.1	<0.02	0.03
11	9	0.06	0.414	0.87	<0.1	0.1	<0.02	0.1
8	7	0.04	0.224	0.61	<0.1	0.2	<0.02	0.07
4	8	0.02	0.658	1.23	<0.1	0.1	<0.02	0.06
7	10	0.03	0.57	0.68	<0.1	0.2	0.02	0.08
7	6	0.02	0.499	0.77	<0.1	<0.1	<0.02	0.06
6	8	0.03	0.555	0.71	<0.1	0.1	<0.02	0.09
8	7	0.04	0.438	1.11	<0.1	0.2	0.02	0.1
10	8	0.06	0.172	0.17	<0.1	0.2	<0.02	0.07
7	9	0.04	0.391	0.83	<0.1	0.1	0.03	0.05
5	6	0.02	0.511	0.85	<0.1	<0.1	<0.02	0.05
11	7	0.07	0.222	0.15	<0.1	0.1	<0.02	0.04
10	7	0.06	0.264	0.2	<0.1	0.2	<0.02	0.04
6	7	0.02	0.462	1	<0.1	0.1	0.03	0.06
5	7	0.02	0.558	0.89	<0.1	0.1	<0.02	0.07
12	8	0.08	0.302	0.35	<0.1	0.3	<0.02	0.06
6	8	0.03	0.502	0.6	<0.1	0.1	<0.02	0.06
4	8	0.02	0.996	1.2	<0.1	0.1	<0.02	0.07
13	5	0.09	0.074	0.07	<0.1	0.3	<0.02	0.03
11	8	0.07	0.181	0.23	<0.1	0.3	<0.02	0.04
10	7	0.07	0.17	0.24	<0.1	0.2	<0.02	0.01
11	8	0.06	0.614	0.68	<0.1	0.2	<0.02	0.1
5	7	0.01	0.656	1.05	<0.1	0.2	<0.02	0.08
10	5	0.06	0.324	0.24	<0.1	0.3	<0.02	0.07
6	7	0.03	0.359	0.43	<0.1	0.2	<0.02	0.05
7	4	0.04	0.183	0.42	<0.1	0.1	<0.02	0.04
8	7	0.05	0.56	0.63	<0.1	0.2	<0.02	0.1
15	8	0.11	0.283	0.19	<0.1	0.2	<0.02	0.12
8	13	0.04	0.08	0.92	<0.1	0.2	<0.02	0.15
8	18	0.03	0.081	1	<0.1	0.2	<0.02	0.14
9	14	0.04	0.218	1.17	<0.1	0.2	<0.02	0.13
7	16	0.03	0.098	1.18	<0.1	<0.1	0.07	0.13
6	12	0.02	0.121	0.98	<0.1	0.1	<0.02	0.14
7	18	0.02	0.085	0.91	<0.1	<0.1	<0.02	0.14
5	12	0.02	0.026	0.8	<0.1	<0.1	<0.02	0.12
7	18	0.03	0.096	0.82	<0.1	0.1	<0.02	0.11
8	11	0.02	0.032	1.24	<0.1	<0.1	<0.02	0.18
6	18	0.01	0.089	1.15	<0.1	<0.1	<0.02	0.2
8	14	0.03	0.108	0.98	<0.1	0.2	<0.02	0.16
10	31	0.04	0.214	0.88	<0.1	0.1	<0.02	0.17
6	14	0.02	0.113	0.69	<0.1	0.1	<0.02	0.15
7	20	0.03	0.093	0.83	<0.1	0.2	<0.02	0.13

Hg	Se	Te	Ga	Cs	Ge	Hf	Nb	Rb	Sn
9	0.4	<0.02	0.2	0.063	<0.01	0.019	0.03	1.8	0.06
<1	0.4	<0.02	<0.1	0.019	<0.01	0.005	<0.01	7.3	0.03
19	0.3	<0.02	0.2	0.076	0.02	0.027	0.04	1.4	0.05
<1	0.3	<0.02	<0.1	0.013	<0.01	0.002	<0.01	2	0.03
6	0.4	<0.02	0.2	0.051	<0.01	0.02	0.03	1.4	0.05
6	0.4	<0.02	0.1	0.039	<0.01	0.017	0.01	1.4	0.02
3	0.5	<0.02	<0.1	0.019	0.01	0.004	<0.01	5.4	0.02
3	0.6	<0.02	<0.1	0.035	0.03	0.009	0.02	3.2	0.03
2	0.2	<0.02	<0.1	0.027	<0.01	0.006	0.01	2.1	<0.02
2	0.3	<0.02	<0.1	0.031	0.02	0.013	0.01	2	0.03
3	0.5	<0.02	0.1	0.039	0.02	0.012	0.02	1.6	0.04
10	0.3	<0.02	0.2	0.061	<0.01	0.02	0.02	1.4	0.06
3	0.3	<0.02	<0.1	0.056	<0.01	0.014	0.03	6.7	0.04
3	0.3	<0.02	<0.1	0.015	<0.01	0.005	<0.01	1.2	0.03
11	0.5	<0.02	0.2	0.066	0.02	0.024	0.03	1.2	0.04
7	0.4	<0.02	0.2	0.059	<0.01	0.024	0.03	1.3	0.05
5	0.3	<0.02	<0.1	0.025	0.02	0.01	0.01	4.1	<0.02
2	0.5	<0.02	<0.1	0.028	<0.01	0.012	<0.01	2.7	0.03
8	0.4	<0.02	0.2	0.086	0.01	0.027	0.04	2.9	0.03
6	0.4	<0.02	0.1	0.03	<0.01	0.012	<0.01	1.4	0.02
<1	0.5	<0.02	<0.1	0.022	<0.01	0.006	<0.01	1.9	0.04
14	0.3	<0.02	0.3	0.08	0.01	0.026	0.04	1.4	0.06
10	0.3	0.02	0.2	0.064	<0.01	0.02	0.03	1.5	0.05
8	0.3	<0.02	0.2	0.059	<0.01	0.023	0.04	1.4	0.04
9	0.2	<0.02	0.2	0.055	0.01	0.017	0.03	1.9	0.04
2	0.4	<0.02	<0.1	0.013	<0.01	0.005	<0.01	1.8	0.02
4	0.3	<0.02	0.2	0.056	<0.01	0.021	0.04	1.3	0.03
4	0.3	<0.02	<0.1	0.029	0.02	0.009	0.01	1.1	0.03
4	0.4	<0.02	0.1	0.034	0.01	0.012	0.02	1	0.02
7	0.3	<0.02	0.1	0.042	0.03	0.018	0.02	1.7	0.03
11	0.5	<0.02	0.3	0.1	<0.01	0.034	0.05	1.9	0.04
14	0.3	<0.02	0.1	0.032	<0.01	0.013	0.02	1.8	<0.02
8	0.4	<0.02	<0.1	0.029	<0.01	0.013	0.01	2.9	<0.02
14	0.2	<0.02	0.1	0.037	<0.01	0.011	0.02	3.6	<0.02
11	0.4	<0.02	<0.1	0.024	<0.01	0.008	<0.01	2.3	0.03
10	0.4	<0.02	<0.1	0.026	<0.01	0.005	<0.01	3.9	0.04
15	0.4	<0.02	<0.1	0.033	0.01	0.005	<0.01	2.5	0.03
6	0.3	<0.02	<0.1	0.014	<0.01	0.003	<0.01	1.6	0.03
11	0.5	<0.02	<0.1	0.024	0.02	0.003	0.01	2.3	0.04
8	0.5	<0.02	<0.1	0.02	0.01	0.005	0.01	2.7	<0.02
7	0.3	0.02	<0.1	0.013	0.01	0.006	<0.01	2.6	0.03
13	0.5	<0.02	0.1	0.031	<0.01	0.011	<0.01	2.3	0.04
13	0.5	<0.02	0.1	0.055	<0.01	0.009	0.02	2.9	0.04
13	0.5	0.02	<0.1	0.029	<0.01	0.007	<0.01	1.8	0.04
11	0.4	<0.02	<0.1	0.027	<0.01	0.006	0.02	2.4	0.03

Ta	Zr	Y	Ce	In	Re	Be	Li	Pd	Pt
<0.001	0.66	0.413	1.39	<0.02	<1	<0.1	0.49	<2	2
<0.001	0.07	0.035	0.12	<0.02	2	<0.1	0.08	<2	2
<0.001	0.73	0.913	1.88	<0.02	<1	0.1	0.48	3	<1
<0.001	0.1	0.08	0.26	<0.02	<1	<0.1	0.24	<2	2
<0.001	0.58	0.299	1.06	<0.02	<1	<0.1	0.44	<2	2
<0.001	0.38	0.253	0.81	<0.02	<1	<0.1	0.37	<2	<1
<0.001	0.15	0.088	0.29	<0.02	1	<0.1	0.16	<2	<1
<0.001	0.29	0.22	0.67	<0.02	<1	<0.1	0.17	<2	<1
<0.001	0.15	0.252	0.64	<0.02	<1	<0.1	0.18	<2	1
<0.001	0.25	0.175	0.61	<0.02	<1	<0.1	0.17	<2	4
<0.001	0.35	0.23	0.8	<0.02	2	<0.1	0.28	4	2
<0.001	0.63	0.454	1.49	<0.02	<1	<0.1	0.39	3	3
<0.001	0.32	0.232	0.94	<0.02	<1	<0.1	0.33	<2	2
<0.001	0.15	0.071	0.26	<0.02	<1	<0.1	0.17	<2	4
<0.001	0.61	0.41	1.52	<0.02	<1	<0.1	0.34	<2	<1
<0.001	0.55	0.328	1.22	<0.02	<1	<0.1	0.38	<2	<1
<0.001	0.22	0.168	0.53	<0.02	<1	<0.1	0.17	3	3
<0.001	0.21	0.128	0.44	<0.02	3	<0.1	0.11	<2	3
<0.001	0.75	0.45	1.61	<0.02	<1	<0.1	0.49	5	<1
<0.001	0.3	0.194	0.63	<0.02	1	<0.1	0.27	<2	2
<0.001	0.14	0.09	0.3	<0.02	1	<0.1	0.25	<2	<1
<0.001	0.8	0.615	2.89	<0.02	<1	<0.1	0.48	<2	<1
<0.001	0.61	0.711	1.56	<0.02	<1	<0.1	0.44	3	1
<0.001	0.58	0.428	1.55	<0.02	<1	<0.1	0.31	<2	<1
0.002	0.5	0.494	1.35	<0.02	<1	<0.1	0.28	<2	<1
<0.001	0.11	0.072	0.25	<0.02	<1	<0.1	0.08	<2	2
<0.001	0.52	0.38	1.2	<0.02	<1	<0.1	0.37	<2	<1
<0.001	0.28	0.233	0.76	<0.02	<1	<0.1	0.2	<2	<1
<0.001	0.31	0.204	0.74	<0.02	<1	<0.1	0.24	<2	2
<0.001	0.39	0.324	0.92	<0.02	<1	<0.1	0.32	<2	1
<0.001	0.96	0.589	2.06	<0.02	<1	<0.1	0.65	4	<1
<0.001	0.29	0.145	0.57	<0.02	9	<0.1	0.24	<2	<1
<0.001	0.28	0.136	0.55	<0.02	6	<0.1	0.25	<2	<1
<0.001	0.32	0.178	0.71	<0.02	3	<0.1	0.62	<2	<1
<0.001	0.23	0.226	0.47	<0.02	5	<0.1	1.1	<2	<1
<0.001	0.12	0.079	0.26	<0.02	2	<0.1	0.36	<2	<1
<0.001	0.17	0.085	0.34	<0.02	10	<0.1	0.32	<2	<1
<0.001	0.11	0.091	0.23	<0.02	8	<0.1	0.13	<2	<1
<0.001	0.2	0.116	0.4	<0.02	6	<0.1	0.32	<2	2
<0.001	0.19	0.104	0.36	<0.02	11	<0.1	0.19	<2	2
<0.001	0.07	0.054	0.15	<0.02	4	<0.1	0.15	<2	<1
<0.001	0.21	0.176	0.51	<0.02	10	<0.1	0.33	<2	<1
<0.001	0.35	0.281	0.76	<0.02	16	<0.1	0.45	<2	<1
<0.001	0.16	0.079	0.3	<0.02	4	<0.1	0.29	<2	<1
<0.001	0.18	0.108	0.42	<0.02	5	<0.1	0.33	<2	2

Appendix 3.3 Regolith Carbonate data

				IDENT	Au	Au Dp1	Al	Ba	Ca	Cr	Cu	Fe	K
				UNITS	ppb	ppb	ppm	ppm	ppm	ppm	ppm	ppm	ppm
				SCHEME	AA10C	AA10C	IC3E	IC3E	IC3E	IC3E	IC3E	IC3E	IC3E
				DETECTIOI	1	1	10	5	10	2	2	100	10
RCA 28	547371	6448496	AGD 66		2	--	25100	220	244000	9	42	18900	3450
RCA 32	547482	6446991	AGD 66		1	--	21200	240	271000	8	17	9050	4300
RCA 33	548038	6446713	AGD 66		4	--	14300	800	269000	6	18	7050	3400
RCA 34	548568	6445594	AGD 66		2	--	26900	390	225000	9	45	15100	5400
RCA 35	549281	6445939	AGD 66		1	--	15300	470	294000	5	21	7400	3150
RCA 37	551756	6446089	AGD 66		2	--	21000	210	263000	8	26	11100	5550
RCA 38	552415	6446462	AGD 66		3	--	7900	390	290000	4	19	6050	1000
RCA 40	553330	6446960	AGD 66		4	--	34400	300	219000	13	28	16800	10000
RCA 42	554371	6447639	AGD 66		6	--	14900	230	295000	5	22	6800	2950
RCA 45	557150	6448975	AGD 66		3	--	12600	175	281000	30	45	6800	2050
RCA 50	556399	6453245	AGD 66		3	--	25000	330	260000	12	30	16100	10100
RCA 53	556411	6457362	WGS 84		5	--	31800	490	240000	13	19	15600	8250
RCA 55	557059	6457923	WGS 84		2	--	15300	340	266000	6	22	9550	5450
RCA 62	562628	6456456	WGS 84		2	--	23100	650	257000	4	32	11200	9300
RCA 63	563785	6456503	WGS 84		4	3	51000	2450		19	56	22500	15500
RCA 65	564359	6455996	WGS 84		5	--	8300	650	321000	4	24	4250	1950
RCA 67	564622	6455503	WGS 84		2	--	24300	650	235000	18	36	16000	5400
RCA 69	565187	6456059	WGS 84		<1	--	5400	1800	299000	2	25	3200	1250
RCA 71	565464	6455812	WGS 84		2	<1	10000	850	319000	3	19	5250	1450
RCA 96	554279	6453558	AGD 66		1	--	12800	290	310000	7	23	6650	3200
RCA 107	552278	6453179	AGD 66		5	--	9350	120	312000	2	18	5900	3050
RCA 108	552229	6453271	AGD 66		2	--	21500	280	267000	8	27	11700	7350
RCA 111	551186	6453710	AGD 66		2	--	14700	120	290000	3	26	9700	5200
RCA 119	548279	6453961	AGD 66		3	--	20300	230	289000	10	43	15100	7500
RCA 120	547670	6453410	AGD 66		<1	--	22800	240	225000	9	29	11800	8550
RCA 122	548704	6452747	AGD 66		<1	--	16700	300	291000	9	44	13500	5400
RCA 128	567510	6448983	AGD 66		<1	--	8500	175	323000	4	24	5400	1800
RCA 134	568885	6447553	AGD 66		4	--	16700	180	295000	11	30	8450	2150
RCA 142	564343	6455986	AGD 66		<1	--	7950	800	327000	4	23	3600	1450

Mg	Mn	Na	Nb	Ni	P	Pb	S	Ti	V	Zn	Ag	As	Bi
ppm	ppm	ppm	ppm	ppm	ppm	ppm	ppm	ppm	ppm	ppm	ppm	ppm	ppm
IC3E	IC3E	IC3E	IC3E	IC3E	IC3E	IC3E	IC3E	IC3E	IC3E	IC3E	IC3M	IC3M	IC3M
10	5	10	5	2	5	5	50	10	2	2	0.1	0.5	0.1
7200	270	2550	<5	14	200	8	450	1950	70	46	<0.1	2.5	<0.1
5500	115	4850	<5	10	190	6	550	1100	27	22	<0.1	4	<0.1
6900	76	1300	<5	8	130	6	800	700	23	24	0.2	4.5	0.3
6600	185	4600	<5	9	500	10	1450	1400	36	39	<0.1	2.5	0.1
7300	110	1950	<5	6	160	12	750	900	26	28	<0.1	3	<0.1
5850	110	3450	<5	10	230	6	550	1150	32	21	<0.1	3	<0.1
26400	170	1500	<5	6	80	6	450	600	26	14	<0.1	1	<0.1
10400	155	5100	<5	15	185	12	600	1700	48	19	<0.1	3	<0.1
6450	82	2600	<5	7	155	6	500	800	29	16	<0.1	3.5	<0.1
10100	125	3350	<5	16	1000	10	750	650	19	26	0.1	2.5	<0.1
12700	135	2550	<5	12	230	6	600	1250	44	25	0.1	6	<0.1
7200	115	850	<5	12	370	12	750	1500	31	40	<0.1	1.5	<0.1
12400	260	1150	<5	8	260	20	500	950	23	66	<0.1	2.5	<0.1
5100	175	1650	<5	4	500	72	800	850	18	80	<0.1	5	0.2
14300	140	1400	8	11	270	24	1200	1900	50	25	<0.1	5.5	0.6
4450	80	750	<5	5	500	<5	950	1000	10	19	<0.1	3	<0.1
8200	96	800	6	8	400	12	900	1350	32	45	<0.1	6	0.5
4850	54	650	<5	4	490	<5	1450	1300	9	13	<0.1	4	<0.1
3950	70	500	<5	<2	300	<5	1100	550	12	14	<0.1	2.5	<0.1
6000	165	1100	<5	7	480	30	550	750	15	44	<0.1	4	<0.1
4400	260	550	<5	<2	350	20	500	650	9	38	<0.1	2	<0.1
5550	220	1800	<5	7	400	26	500	1100	23	43	<0.1	3	0.2
3300	700	550	<5	4	600		550	1000	14		0.3	20.5	<0.1
7400	165	2450	<5	15	300	22	450	1050	39	46	0.1	3	<0.1
6550	94	3300	<5	8	220	10	450	1100	26	29	<0.1	3	<0.1
7100	250	900	<5	9	320	10	500	1100	40	34	0.3	0.5	<0.1
5050	92	1700	<5	4	300	6	650	600	15	16	<0.1	3.5	<0.1
6600	150	6100	<5	11	190	6	450	900	28	21	<0.1	3	<0.1
4550	72	750	<5	5	550	6	1200	800	9	18	0.2	4.5	0.1

Cd	Co	Cs	Ga	In	Mo	Rb	Sb	Se	Sn	Sr	Te	Th	Tl
ppm	ppm	ppm	ppm	ppm	ppm	ppm	ppm	ppm	ppm	ppm	ppm	ppm	ppm
IC3M	IC3M	IC3M	IC3M	IC3M	IC3M	IC3M	IC3M	IC3M	IC3M	IC3M	IC3M	IC3M	IC3M
0.1	0.2	0.1	0.1	0.05	0.1	0.1	0.5	0.5	0.1	0.1	0.2	0.02	0.1
0.4	9	0.9	6	<0.05	<0.1	14.5	<0.5	<0.5	1.1	350	<0.2	6	0.1
0.2	8.5	0.7	4.7	<0.05	0.2	14.5	<0.5	<0.5	1.1	550	<0.2	6	0.1
0.2	5	0.6	3.2	<0.05	0.3	14	<0.5	<0.5	0.6	600	<0.2	3	<0.1
0.5	6	1.1	6	<0.05	0.6	23.5	<0.5	<0.5	1	490	<0.2	6.5	0.2
0.4	5.5	0.7	3.6	<0.05	0.3	12.5	<0.5	<0.5	0.6	750	<0.2	3.4	0.1
0.2	9.5	1.1	5	<0.05	0.1	24.5	<0.5	<0.5	1.1	650	<0.2	4.7	0.2
0.4	6	0.3	1.9	<0.05	<0.1	4.8	<0.5	<0.5	0.4	850	<0.2	1.15	<0.1
0.2	9.5	1.2	9	<0.05	0.3	44	<0.5	<0.5	1.9	650	<0.2	9	0.3
0.2	7	0.7	3.6	<0.05	<0.1	12.5	<0.5	0.5	0.7	700	<0.2	3.1	0.1
0.3	9	0.3	3.3	<0.05	<0.1	8	<0.5	1	0.2	360	<0.2	3.3	<0.1
0.4	9	1	7.5	<0.05	<0.1	46.5	<0.5	0.5	1.4	650	<0.2	8	0.3
0.2	9	1.7	9.5	<0.05	<0.1	52	<0.5	<0.5	1.9	600	<0.2	12	0.6
1.2	9	0.5	4.7	<0.05	<0.1	27.5	<0.5	1	0.5	600	<0.2	6	0.2
0.4	5	0.7	6.5	<0.05	0.2	41.5	<0.5	1	1	470	<0.2	6.5	0.3
0.1	4.2	1	14	<0.05	0.8	56	<0.5	<0.5	1.9	340	<0.2	16.5	0.4
0.3	4.4	0.5	2.5	<0.05	0.1	8	<0.5	<0.5	0.4	390	<0.2	3	<0.1
0.2	4.5	0.5	8	<0.05	0.5	19.5	<0.5	1.5	1.1	470	<0.2	9	0.1
0.3	3.2	0.3	2	<0.05	<0.1	4.9	<0.5	2	0.3	460	<0.2	2.5	<0.1
0.2	3.1	0.3	3.9	<0.05	<0.1	6.5	<0.5	1.5	0.3	450	<0.2	2.4	<0.1
1.5	7	1.1	3.9	<0.05	<0.1	20	<0.5	0.5	0.2	430	<0.2	4	0.2
1.1	4.7	0.5	2.9	<0.05	<0.1	20	<0.5	1	0.2	440	<0.2	3.8	0.2
0.7	7.5	0.8	7	<0.05	<0.1	37.5	<0.5	1	0.4	430	<0.2	7.5	0.3
8.5	7.5	0.5	4.8	<0.05	0.2	31.5	<0.5	1	0.5	260	<0.2	7.5	0.3
0.7	10.5	0.8	6	<0.05	<0.1	32.5	<0.5	1	0.4	400	<0.2	8.5	0.2
0.6	4.5	0.8	6	<0.05	0.2	35.5	<0.5	0.5	1.1	500	<0.2	9	0.2
0.5	12.5	0.4	5	<0.05	<0.1	21.5	<0.5	<0.5	0.4	330	<0.2	4.5	0.1
0.5	7	0.4	2.6	<0.05	<0.1	8	<0.5	1.5	0.5	450	<0.2	2.8	<0.1
0.3	7.5	0.3	4.5	<0.05	0.1	9.5	<0.5	<0.5	0.7	310	<0.2	8	<0.1
0.4	4.3	0.4	2.3	<0.05	0.4	5.5	28	<0.5	0.4	440	<0.2	2.6	0.2

U	W	Y	Dy	Er	Eu	Gd	Ho	Lu	Pr	Tb	Tm	Yb	Sm
ppm	ppm	ppm	ppm	ppm	ppm	ppm	ppm	ppm	ppm	ppm	ppm	ppm	ppm
IC3M	IC3M	IC3M	IC3R	IC3R	IC3R	IC3R	IC3R	IC3R	IC3R	IC3R	IC3R	IC3R	IC3R
0.02	0.1	0.05	0.02	0.05	0.02	0.05	0.02	0.02	0.05	0.02	0.05	0.05	0.02
0.76	0.3	15	2.7	1.45	0.75	2.8	0.45	0.19	5	0.51	0.2	1.3	3.7
0.76	0.2	11.5	2.2	1.1	0.65	2.4	0.36	0.14	5	0.45	0.15	0.9	3.5
0.69	0.2	25.5	4.2	2.4	1.15	3.5	0.72	0.31	5	0.77	0.3	2	3.7
2.3	0.3	44	7	3.8	1.8	7.5	1.25	0.47	13.5	1.4	0.45	3.2	10
2	<0.1	35	6.5	3.4	1.7	6.5	1.05	0.43	10	1.25	0.4	3.1	8.5
0.95	0.2	11	2.1	1.15	0.64	2.2	0.34	0.15	4.6	0.43	0.15	1	3.3
1.1	<0.1	31.5	5	3.1	1.15	4.2	0.91	0.37	4.3	0.89	0.35	2.6	4.2
1.5	<0.1	14.5	3.1	1.45	0.93	3.6	0.48	0.19	7.5	0.64	0.15	1.25	5
0.88	0.3	11	2.2	1.05	0.65	2.3	0.36	0.13	4.2	0.44	0.15	0.85	3.2
0.51	<0.1	6.5	1.3	0.85	0.35	1.45	0.25	0.11	2.2	0.27	0.1	0.8	1.6
1.25	0.2	12.5	2.5	1.25	0.74	2.9	0.38	0.14	4.9	0.49	0.15	0.9	3.4
1.45	<0.1	11	2.4	1.35	0.72	3.1	0.39	0.14	6.5	0.51	0.15	1.05	4.1
1.35	0.1	19.5	3.5	2.2	0.71	3.6	0.62	0.23	5.5	0.66	0.25	1.75	4
2.5	0.2	23	4.1	2.8	0.88	4	0.77	0.32	5.5	0.79	0.35	2.3	4.3
2.9	1.9	11.5	2.5	1.55	0.89	2.7	0.41	0.18	6	0.5	0.2	1.3	2.8
0.9	0.3	7.5	1.4	0.9	0.38	1.45	0.23	0.1	2.3	0.28	0.1	0.7	1.55
0.99	0.2	6	1.2	0.75	0.43	1.55	0.21	0.1	2.8	0.27	0.1	0.6	1.75
0.8	0.4	12	1.75	1.15	0.75	2.2	0.35	0.13	2.8	0.35	0.1	0.8	1.55
0.48	<0.1	14	2	1.15	0.66	2.6	0.35	0.1	3.2	0.44	0.1	0.85	2.3
0.66	<0.1	12.5	2.2	1.25	0.7	2.8	0.36	0.14	5	0.51	0.15	0.95	3.4
0.87	<0.1	13	2.5	1.6	0.57	2.5	0.44	0.17	3.6	0.46	0.15	1.25	2.8
1.1	0.1	17.5	3.2	2.1	0.74	3	0.56	0.23	5.5	0.64	0.25	1.6	3.8
0.76	<0.1	14.5	3	1.7	0.57	3.4	0.49	0.18	5.5	0.62	0.2	1.5	4.2
0.85	<0.1	12	2.4	1.5	0.75	2.8	0.43	0.18	5.5	0.52	0.2	1.2	3.7
0.72	<0.1	12.5	2.3	1.4	0.71	2.7	0.36	0.2	5.5	0.47	0.15	1.2	3.8
0.46	<0.1	15	2.8	1.95	0.7	2.8	0.49	0.26	4.8	0.57	0.25	1.9	3.4
0.58	<0.1	22	3.1	2.1	0.73	3.1	0.61	0.23	4	0.61	0.25	1.65	2.9
0.72	<0.1	18	3.1	2	0.43	2.8	0.54	0.23	3.8	0.6	0.25	1.6	3.2
0.85	0.1	7.5	1.35	0.85	0.35	1.4	0.23	0.09	2	0.28	0.1	0.7	1.5

Nd	Ce	La											
ppm	ppm	ppm											
IC3R	IC3R	IC3R											
0.02	0.5	0.5											
19.5	30	23.5											
19.5	38.5	24											
21	24.5	26.5											
54	78	64											
42.5	66	50											
17.5	37.5	24.5											
19.5	14.5	20											
29	62	39.5											
17	30	22.5											
9	14.5	8.5											
18.5	32.5	19.5											
24	46	26	n.b. may have bed rock contamination										
22.5	39	23.5											
22.5	37	19.5											
22	41	21.5											
9.5	15.5	9.5											
11	20.5	11.5											
12	12.5	13											
14.5	9	16											
19.5	29	24.5											
14.5	25.5	16											
21	41.5	23.5											
22.5	36.5	24.5											
21.5	41	23											
21	41.5	24											
20	33.5	21.5											
16	19.5	18.5											
15.5	28	16	n.b. may have bed rock contamination										
8.5	15	9.5											